



**Synthesis, Deracemisation,
Photochemistry and Crystallisation
Studies in Organic, Organometallic and
Coordination Chemistry directed
towards Circularly Polarised Light and
Chiral Amplification**

**A thesis submitted to Cardiff University
for the degree of Philosophiae Doctor**

By

Merixell Casadesús i Puigneró

School of Chemistry

Cardiff University

February 2007

UMI Number: U584172

All rights reserved

INFORMATION TO ALL USERS

The quality of this reproduction is dependent upon the quality of the copy submitted.

In the unlikely event that the author did not send a complete manuscript and there are missing pages, these will be noted. Also, if material had to be removed, a note will indicate the deletion.



UMI U584172

Published by ProQuest LLC 2013. Copyright in the Dissertation held by the Author.
Microform Edition © ProQuest LLC.

All rights reserved. This work is protected against
unauthorized copying under Title 17, United States Code.



ProQuest LLC
789 East Eisenhower Parkway
P.O. Box 1346
Ann Arbor, MI 48106-1346

ABSTRACT

The work described in this thesis is based around attempts to find a system that could use the intrinsic chirality of circularly polarised light (CPL) to generate a small enantiomeric excess in photochemical reactions and couple it with crystallisation-induced chiral amplification to obtain a high enantiomeric excess. This type of system could provide a possible model for the origins of homochiral life on Earth. In order to study this possibility, synthetic and photochemical work has been carried out in the organic, inorganic and organometallic fields.

The synthesis of a new family of axially chiral benzylidenes and their enantiomeric resolution has been developed and the influence of CPL in the racemisation of the double bond has been studied.

The synthesis of a new family of Werner-type cobalt coordination complexes has been developed and their crystal packing studied, with special emphasis on the role of hydrogen bonding towards the crystal packing. The effect of CPL in the crystallisation pattern has also been investigated, along with a reinvestigation of polymorphism in a previously reported complex.

Finally, the synthesis of a new family of thioalkynyl derivatives has been developed with the subsequent products coordinated to dicobalt octacarbonyl. The displacement of a CO group and further coordination of the pendant sulphide to cobalt has been studied chemically and spectroscopically and the effect of CPL on the photochemistry of $\text{Co}_2(\text{CO})_6$ -alkyne compounds has been investigated. A new dechlorination reaction discovered during these studies is also discussed in this thesis.

ACKNOWLEDGEMENTS

Firstly, I would like to acknowledge Dr Coogan for giving me the opportunity not only to study a PhD, but also to experience living abroad, far from my family, friends and the Catalan culture. I would like to thank him for providing advice, ideas and support, both in and outside of the lab. Also, I would like to acknowledge and thank Sarah for her help with my English throughout the battle of writing up. Many times I wished I had not asked for her help, but deep inside I knew she did it in my best interests...

Almost four years of living in Cardiff has given me the opportunity to learn more about chemistry and also about life, and I would like to thank some of the people that contributed to make Cardiff a good place to live. Special thanks go to: Eli, Maria and Dimitris, for all the good (and not so good) moments; to the lab 1.86 and the rest of the chemistry team- Fabs, Lenni, Derek, Vanesa, Soraya, Richard, Manuel, Dirk, Frenchie, Dave, Deborha, Caterina, Antonio, Lino, Gracia, Anabel, Eugene, Nick, Andrea, Paula... Also thanks to the members of the Catalan team that have contributed to make my lunches a little bit more familiar: Eli, Guillem and Xavi.

I would also like to thank my family and my friends that are in Catalonia, they do not know much about the research that I have been doing, but nevertheless they have been very supportive at all times. Moltes gràcies!

Finally, many thanks to Anthony for all his support and his understanding, particularly during the final months of the writing up. My kindest thanks to him for encouraging me during the hardest moments, for showing me how to look at the good side of things, for his incredible patience and understanding, and for not getting tired of correcting my English again and again!

Many thanks also for those whom I might have forgotten.

ABBREVIATIONS

Å	Ångstrom
APCI	atmospheric pressure chemical ionization
app	apparently
approx	approximately
AT	asymmetric transformation of the second kind
<i>ax</i>	axial
bpy	bipyridine
bs	broad singlet
Bu	butyl
°C	degrees Celsius
<i>ca</i>	circa
conc.	concentrated
CPL	circularly polarised light
CSA	camphor sulphonic acid
CSR	chiral shift reagent
Cys	Cysteine
DCM	dichloromethane
d	doublet
dd	doublet of doublets
ddd	doublet of doublets of doublets
DIOP	2,2-dimethyl-4,5-bis(diphenylphosphinomethyl)-1,3-dioxalane
DMAP	dimethylaminopyridine
DMF	dimethylformamide
DMSO	dimethylsulphoxide
dppm	bisdiphenylphosphinmethane
dppmdo	bisdiphenylphosphinmethanedioxide
dquin	doublet of quintuplets
dt	doublet of triplets
EDCI	1-ethyl-3-(3-dimethylaminopropyl)-carbodiimide
EI/CI	electronic ionization / chemical ionization
<i>eq</i>	equatorial
ESI	electrospray ionization

esd	estimated standard deviation
FAB	fast atom bombardment
e.e.	enantiomeric excess
en	ethylenediamine
g	gram
GC	gas chromatography
h	hour
HPLC	high pressure liquid chromatography
Hz	hertz
IR	infrared
l-CPL	left-handed circularly polarised light
Leu	Leucine
m	multiplet
M	minus
MALDI	matrix-assisted laser desorption/impact
mg	milligram
MHz	megahertz
min	minute
mL	millilitre
mmol	millimol
m.p.	melting point
nm	nanometer
NMO	4-methylmorpholine-N-oxide
NMR	nuclear magnetic resonance
<i>o</i>	orto
ox	oxalate
<i>p</i>	para
P	plus
phen	phenanthroline
PK	Pauson-Khand
ppm	parts per million
<i>p</i> -TsOH	<i>para</i> -toluenesulphonic acid
py	pyridine
q	quartet
quin	quintuplet

r-CPL	right-handed circularly polarised light
RBF	round bottom flask
s	singlet
t	triplet
THF	tetrahydrofuran
TLC	thin layer chromatography
UV	ultraviolet

TABLE OF CONTENTS

CHAPTER 1: INTRODUCTION.....	1
1.1 Biohomochirality and the origins of life on Earth.....	1
1.2 The Murchison meteorite	3
1.3 Parity violation	4
1.4 Circularly polarised light (CPL).....	5
1.4.1 Asymmetric photolysis.....	7
1.4.2 Photoresolution.....	9
1.4.3 Asymmetric photosynthesis	11
1.5 Magnetochemical photochemistry	12
1.6 Amplification of chirality	13
1.6.1 Asymmetric autocatalysis	13
1.6.2 Crystallisation.....	15
1.7 Summary	18
1.8 Aims of the project	18
1.9 References.....	19
CHAPTER 2: SYNTHESIS AND CHIRALITY OF ALKYLIDENE DIOXANEDIONES.....	22
2.1 Introduction.....	22
2.1.1 Aims of the chapter	23
2.2 Syntheses of benzylidene malonate derivatives	25
2.2.1 Route <i>a</i>	27
2.2.2 Route <i>b</i>	29

2.3	Determination of enantiomeric excess (e.e.)	45
2.4	Deracemisation	45
2.4.1	Deracemisation <i>via</i> Michael addition.....	46
2.4.2	Optical activities for compounds 5-10	49
2.5	e.e. determination using Pt(0)-(S)-DIOP ethene	53
2.6	Studies with Circularly Polarised Light (CPL)	60
2.6.1	Attempted deracemisation of compounds 5-10 under the influence of CPL	62
2.7	Conclusions	63
2.8	References	63

CHAPTER 3: SYNTHESIS OF COBALT ETHYLENEDIAMINE COMPLEXES AND STUDIES ON THEIR CRYSTAL PACKING.. 66

3.1	Introduction	66
3.2	Complexes of type <i>cis</i>-[CoX(NH₃)(en)₂]X₂	68
3.2.1	<i>cis</i> -[CoBr(NH ₃)(en) ₂]Br ₂ (11)	69
3.2.2	<i>cis</i> -[CoI(NH ₃)(en) ₂]I ₃ (12).....	76
3.2.3	<i>trans</i> -[Co(NCS) ₂ (en) ₂](NCS) ₂ (13).....	82
3.2.4	<i>cis</i> -[CoF(NH ₃)(en) ₂]F ₂	84
3.3	Complexes of type <i>cis</i>-[Co(NO₂)₂(en)₂]X	85
3.3.1	<i>cis</i> -[Co(NO ₂) ₂ (en) ₂]Br (14)	85
3.3.2	<i>cis</i> -[Co(NO ₂) ₂ (en) ₂]Cl (16a)	86
3.3.3	<i>trans</i> -[Co(NO ₂) ₂ (en) ₂]Cl (16b)	86
3.4	Cobalt complexes that have tetrathionate (S₄O₆)²⁻ as a counterion	89
3.4.1	<i>cis</i> -[Co(NO ₂) ₂ (en) ₂]S ₄ O ₆ (17).....	90
3.4.2	<i>trans</i> -[CoCl ₂ (en) ₂]S ₄ O ₆ (18).....	95
3.4.3	<i>cis</i> -[CoCl(NH ₃)(en) ₂]S ₄ O ₆ (20).....	100
3.4.4	<i>cis</i> -[Co(ox)(en) ₂]S ₄ O ₆ (22).....	104

3.5	Optical studies	111
3.6	Summary	114
3.7	References.....	115

CHAPTER 4: SYNTHESIS AND OPTICAL STUDIES OF ALKYNYL THIOLS AND ORGANOCOBALT ALKYNYL THIOLS.....117

4.1	Introduction.....	117
4.2	Organic synthesis.....	119
4.3	Organometallic synthesis.....	128
4.4	Pauson-Khand reactions of alkynyl thiols	140
4.5	Synthesis of [Co(dppmdo)₃][CoCl₄]	144
4.6	CPL studies.....	149
4.7	Conclusions	151
4.8	References.....	152

CHAPTER 5: OPTICS AND EXPERIMENTAL DESCRIPTION..154

5.1	Optics	154
5.2	General	156
5.3	Synthesis of 3-(4-methoxyphenyl)-2-carboxy-2-propenoic acid 1.....	157
5.4	Synthesis of 3-(4-nitrophenyl)-2-carboxy-2-propenoic acid 2	157
5.5	Synthesis of 3-(2-nitrophenyl)-2-carboxy-2-propenoic acid 3	157

5.6	Synthesis of 2-methyl-2-(2-phenylethyl)-1,3-dioxane-4,6-dione 4.....	158
5.7	Synthesis of 5-(4-nitro-benzylidene)-2-methyl-2-(phenylethyl)-1,3-dioxane-4,6-dione 5.....	158
5.8	Synthesis of 5-(2-nitrobenzylidene)-2-methyl-2-(phenylethyl)-1,3-dioxane-4,6-dione 6.....	159
5.9	Synthesis of 5-(4-methoxybenzylidene)-2-methyl-2-(phenylethyl)-1,3-dioxane-4,6-dione 7.....	160
5.10	Synthesis of 5-benzylidene-2-methyl-2-phenylethyl-1,3-dioxane-4,6-dione 8.....	160
5.11	Synthesis of 5-isobutylidene-2-methyl-2-(2-phenylethyl)-1,3-dioxane-4,6-dione 9....	161
5.12	Synthesis of 5-benzylidene-2-phenyl-1,3-dioxane-4,6-dione 10.....	161
5.13	Deracemisation of 5-(4-nitro-benzylidene)-2-methyl-2-(phenylethyl)-1,3-dioxane-4,6-dione 5.....	161
5.14	Deracemisation of 5-(2-nitro-benzylidene)-2-methyl-2-(phenylethyl)-1,3-dioxane-4,6-dione 6.....	162
5.15	Deracemisation of 5-(4-methoxybenzylidene)-2-methyl-2-(phenylethyl)-1,3-dioxane-4,6-dione 7, using L-Cysteine	162
5.16	Synthesis of L-Leucine methyl ester hydrochloride	162
5.17	Deracemisation of 5-(4-methoxybenzylidene)-2-methyl-2-(phenylethyl)-1,3-dioxane-4,6-dione 7, using L-Leucine.....	163
5.18	Deracemisation of 5-benzylidene-2-phenyl-1,3-dioxane-4,6-dione 10 ...	163
5.19	General procedure for attempted deracemisation using Circularly Polarised Light.....	163
5.20	General procedure for coordination of Pt(0)-(S)-DIOP ethene to benzylidene malonates.....	164

5.21	Synthesis	of	bis(dihydroxobisethylenediaminecobalt(II))bisaquocobalt(III) disulphate pentahydrate $[(\text{H}_2\text{O})_2\text{Co}\{(\text{OH})_2\text{Co}(\text{en})_2\}_2](\text{SO}_4)_2 \cdot 5\text{H}_2\text{O}$	164
5.22	Synthesis of <i>cis</i> -bromoamminebis(ethylenediamine)cobalt(III) bromide (<i>cis</i> - $[\text{CoBr}(\text{NH}_3)(\text{en})_2]\text{Br}_2$)	11		165
5.23	Synthesis of <i>cis</i> -iodoamminebis(ethylenediamine)cobalt(III) triiodide (<i>cis</i> - $[\text{CoI}(\text{NH}_3)(\text{en})_2]\text{I}_3$)	12		165
5.24	Synthesis of <i>trans</i> -bis(isothiocyanato)bis(ethylenediamine)cobalt(III) thiocyanate (<i>trans</i> - $[\text{Co}(\text{NCS})_2(\text{en})_2]\text{NCS}$)	13		166
5.25	Synthesis of <i>cis</i> -bis(ethylenediamine)dinitrocobalt(III) bromide (<i>cis</i> - $[\text{Co}(\text{NO}_2)_2(\text{en})_2]\text{Br}$)	14		166
5.26	Synthesis of <i>cis</i> -bis(ethylenediamine)dichlorocobalt(III) chloride (<i>cis</i> - $[\text{CoCl}_2(\text{en})_2]\text{Cl}$)	15		167
5.27	Synthesis of <i>cis</i> -(bis(ethylenediamine)dinitrocobalt(III)) chloride (<i>cis</i> - $[\text{Co}(\text{NO}_2)_2(\text{en})_2]\text{Cl}$)	16		167
5.28	Synthesis of <i>cis</i> -bis[bis(ethylenediamine)dinitrocobalt(III)] tetrathionate (<i>cis</i> - $[\text{Co}(\text{NO}_2)_2(\text{en})_2]_2\text{S}_4\text{O}_6$)	17		168
5.29	Synthesis of <i>trans</i> -bis[bis(ethylenediamine)dichlorocobalt(III)] tetrathionate (<i>trans</i> - $[\text{CoCl}_2(\text{en})_2]_2\text{S}_4\text{O}_6$)	18		168
5.30	Synthesis of <i>cis</i> -chloroamminebis(ethylenediamine)cobalt(III) dichloride (<i>cis</i> - $[\text{CoCl}(\text{NH}_3)(\text{en})_2]\text{Cl}_2$)	19		169
5.31	Synthesis of <i>cis</i> -chloroamminebis(ethylenediamine)cobalt(III) tetrathionate (<i>cis</i> - $[\text{CoCl}(\text{NH}_3)(\text{en})_2]\text{S}_4\text{O}_6$)	20		169
5.32	Synthesis of bis-(ethylenediamine)oxalatocobalt(III) chloride $[\text{Co}(\text{ox})(\text{en})_2]\text{Cl} \cdot 4\text{H}_2\text{O}$	21		170
5.33	Synthesis of bis(bis-(ethylenediamine)oxalatocobalt(III)) tetrathionate $[\text{Co}(\text{ox})(\text{en})_2]_2\text{S}_4\text{O}_6$	22		170

5.34	Synthesis of (1R,2S,5R)-5-methyl-2-(1-methylethyl)cyclohexyl <i>p</i>-iodobenzoate 23	171
5.35	Synthesis of benzoic acid-4-(4-pentyne-1-ol)-(1R,2S,5R)-5-methyl-2-(1-methylethyl)cyclohexyl ester 24	172
5.36	Synthesis of benzoic acid-4-(4-pentyne-1-mesyl)-(1R,2S,5R)-5-methyl-2-(1-methylethyl)cyclohexyl ester 25.....	172
5.37	Synthesis of benzoic acid-4-(4-pentyne-1-thiophenyl)-(1R,2S,5R)-5-methyl-2-(1-methylethyl)cyclohexyl ester 26	173
5.38	Synthesis of benzoic acid-4-(4-pentyne-1-thiobenzyl)-(1R,2S,5R)-5-methyl-2-(1-methylethyl)cyclohexyl ester 27	174
5.39	Synthesis of benzoic acid-4-(4-pentyne-1-thiophenyl) 28	174
5.40	Synthesis of benzoic acid-4-(4-pentyne-1-thiophenyl)-methyl ester 29 .	175
5.41	Synthesis of dicobalthexacarbonyl bis(diphenylphosphino)methane (Co₂(CO)₆dppm).....	175
5.42	Synthesis of dicobalt hexacarbonyl benzoic acid-4-(4-pentyne-1-thiophenyl)-(1R,2S,5R)-5-methyl-2-(1-methylethyl)cyclohexyl ester 30.....	176
5.43	Synthesis of dicobalt tetracarbonyl bis-diphenylphosphinomethane benzoic acid-4-(4-pentyne-1-thiophenyl)-(1R,2S,5R)-5-methyl-2-(1-methylethyl)cyclohexyl ester 32.....	176
5.44	Synthesis of cobalt tris-diphenylphosphinomethane-dioxide cobalt tetrachloride ([Co(dppmdo)₃](CoCl₄)) 36	176
5.45	References.....	177

Chapter 1: INTRODUCTION

“All living organisms develop from germs,

That is to say, they owe their origins to other living beings.

But how did the first living things arise?

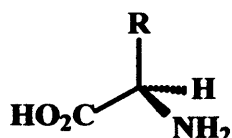
How did life originate on the Earth?”

A. I. Oparin (1924)

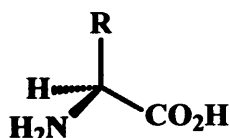
1.1 Biohomochirality and the origins of life on Earth

There has been evidence for the chiral nature of living beings on Earth for more than a century now, with Louis Pasteur being one of the pioneering scientists in the discovery of homochirality.^[1] Today, chirality is found in amino acids, proteins, DNA and RNA, thus demonstrating its universal nature in all known life forms. Living organisms are mainly constituted of just 22 different types of amino acids of which all but one (glycine, achiral) can exist as two enantiomeric forms (Scheme 1). However, it is remarkable that nature essentially uses only one of these forms: the L-conformation. Although the chemical and physical properties of D- and L-amino acids are extremely similar, only the L-amino acids were selected for polymerisation, peptide and protein formation on the primitive Earth. In this chemical evolutionary step, almost all D-amino acids were eliminated and all living organisms are now composed predominantly of L-amino acids. Nobody knows where, why or how nature selected L-amino acids, or whether the selection of L-amino acids has a

logical explanation or was through chance occurrence. However, it is clear that for the building blocks of life form, only one type of enantiomer could be selected because polymers which consist of mixed diastereoisomers are not able to fold into structures resembling modern proteins with the same efficiency as the enantiomeric homologues.^[2,3] Therefore, *homochirality is essential for life*.



D-amino acid



L-amino acid

Scheme 1 Enantiomeric forms of amino acids

The question of how life emerged on Earth raises a number of important and fundamental issues in natural philosophy. Humanity – specifically the scientific community – has been searching for answers for many decades. Many theories have been postulated, but none of them have been clearly proven. What is known is that life could not have originated from a racemic mixture, further, almost every reaction giving a homochiral product needs at some stage a chiral promoter (*e.g.* a chiral reactant, a chiral catalyst or a chiral auxiliary) that induces chirality. The only exception to this is in spontaneous resolution; a mixture of enantiomers naturally separates through the selective crystallisation of one of the enantiomers, with the other being left in solution. Thus both the solid and the solution exhibit optical activity. However, as the crystallisation occurs randomly, the sign of optical activity cannot be predicted.

At the time when organic compounds (which are the basis of life) were formed, the Earth had a reductive atmosphere composed of methane, ammonia, water and hydrogen instead of the present oxidative atmosphere of oxygen, carbon dioxide, nitrogen and water.^[4] In an attempt to reproduce these atmospheric conditions (the so-called *primordial soup*), Millet performed a reaction by mixing CH₄, NH₃, H₂O and H₂, and subjected this mixture to an electrical discharge (representing lightning) producing radicals.^[5] Amongst the many products formed were the amino acids glycine, α-alanine, β-alanine, aspartic acid and α-amino-n-butyric acid with no enantiomeric excess (as would be expected because there was no chiral inducer).

This experiment was crucial, as it proved that amino acids could be synthesised from simple organic molecules, but no enantiomeric excess could be obtained. Thus, an enantiomeric selection process was required at some stage in the origin or evolution of life on Earth, *i.e.* some kind of *absolute asymmetric induction*.

Three areas of physics have been shown to induce chirality in a racemic mixture: parity violation, circularly polarised light and magnetism. These will be discussed in sections 1.3, 1.4 and 1.5 respectively. A further hypothesis is that homochirality on Earth could also have been introduced by extraterrestrial material, *i.e.*, meteorites and comets. This possibility is discussed in the next section.

1.2 The Murchison meteorite

On September 28th 1969, a meteorite of considerable dimensions fell near Murchison, Victoria, Australia.* Several samples were collected and carefully examined to determine their composition.^[6] The amino acids glycine, alanine, valine, proline and glutamic acid were identified. The highest ratio of D-amino acids compared to L-amino acids was found in alanine which contained 50% of D-alanine. The lowest ratio of D:L was found in proline which contained 40% of D-proline. In all cases the percentage of L-amino acid was equal or superior to the percentage of D-amino acid. Further analysis of the stable-isotopes ¹³C, ¹⁵N and ²H indicated that the samples were genuinely extraterrestrial, with a very low degree of terrestrial contamination, as the amount of heavy-stable isotopes contained in the material was far higher than in terrestrial samples.^[7]

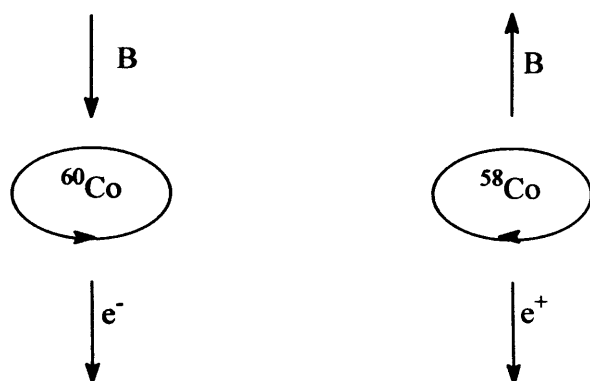
Amino acids have been detected in other meteorites, but Murchison has been the most thoroughly studied. Also, other meteorites (*e.g.* Murray) have contained non-racemic mixtures of amino acids, demonstrating that meteorites can carry a record of the organic chemical evolution of the early solar system. The Murchison and the Murray are meteorites of particular interest because they were found to contain six extraterrestrial α -methyl amino acids with a particularly large L-e.e.^[8] Thus, it is reasonable to assume that some asymmetric process influenced the formation or degradation of organic compounds in the prebiotic solar system, leaving observable enantiomeric excesses in the organic compounds of meteorites.

* Documented by *Rep. Centre for Shortlived Phenomena*, N° 779, Smithsonian Institute, Cambridge, Mass., 1969.

Comets have also been considered as possible sources of chiral material. In order to determine whether comets could indeed be the origin of chiral life on Earth the Rosetta Mission has been launched by the European Space Agency. In 2012 a robotical lander will detach from the orbiter of the Rosetta spacecraft (which began a 12 year journey in 2004) and set down on the surface of comet 46P/Wirtanen in order to separate and identify organic compounds present in the comet via *in situ* GC-MS.^[9]

1.3 Parity violation

In 1956 two Chinese-born physicists, Tsung-Dao Lee and Chen Ning Yang, proposed that parity is not always conserved in weak forces[†],^[10] for which they were awarded the Nobel Prize in Physics in 1957. In the same year, the hypothesis was conclusively proven by Wu and co-workers,^[11] who demonstrated that the electrons ejected together with antineutrinos from unstable cobalt nuclei (^{60}Co) in the process of β -decay are predominantly left-handed. When a strong magnetic field was applied to cobalt nuclei, then cooled to temperatures near absolute zero to reduce motion caused by heat, Wu *et al.* found that the atoms aligned and β -decay emission occurred in one of two directions: parallel or antiparallel to the field axis. If β -decay was a symmetric process, an equal number of electrons would be emitted in both directions. However, a larger number of electrons were ejected in one direction, thereby denoting a particular handedness (Scheme 2).

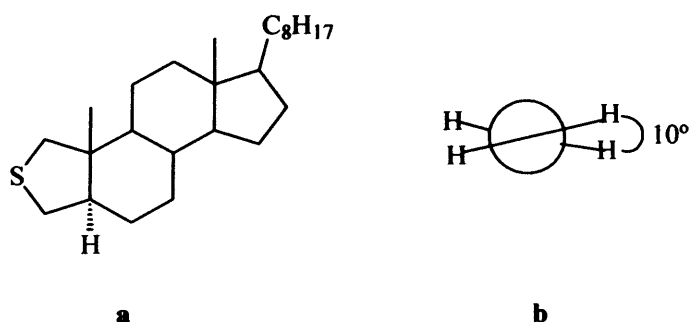


Scheme 2 Parity non-conservation in the weak interaction

An important consequence of parity violation is that all atoms are inherently chiral, therefore right-handed and left-handed enantiomers of molecules are not degenerate.

[†] Four fundamental forces are present in the universe: gravity, electromagnetism, strong and weak interactions.

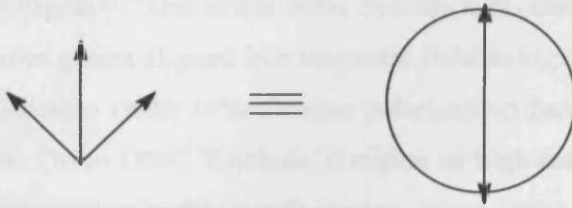
Nevertheless, this atomic electroweak energy difference is almost negligible, for example having values of $-2 \cdot 10^{-22}$ atomic units for a derivative of thiacholestane (**Scheme 3a**),^[12] or $+2 \cdot 10^{-20}$ for the chiral conformations of ethylene (**Scheme 3b**).^[13] Crystal structures of L- and D-alanine were resolved by single crystal neutron diffraction, finding no substantial difference between them at 60 K and 295 K,^[14] although theoretical calculations proved the amino acid L-alanine to be 10^{-14} Jmol⁻¹ more stable than the amino acid D-alanine.^[15] This difference corresponds to a preference of only 1 molecule in 10^{17} at room temperature.



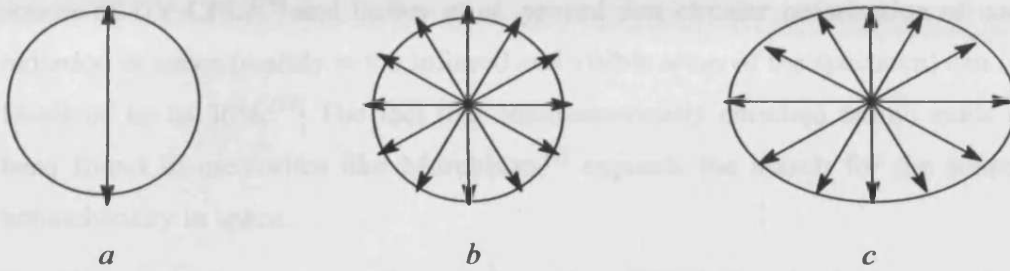
Scheme 3a) Molecular structure of thiacholestane derivative. **b)** Newman projection of chiral conformation for ethylene

1.4 Circularly polarised light (CPL)

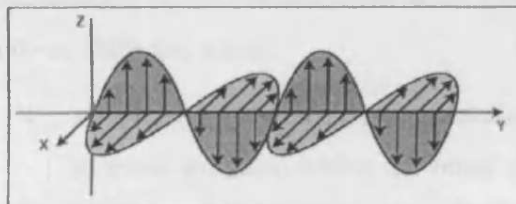
Ultraviolet circularly polarised light has been considered as a possible inducer of homochirality in organic molecules that absorb UV light. CPL is chiral, therefore when it interacts with a mixture of enantiomers it creates a diastereoisomeric relationship, favouring the preferential reaction of one of the enantiomers. From an optical point of view, linearly polarised light can be considered as the sum of two orthogonal components of equal wavelength, the sum of which always has the same direction (**Scheme 4**). CPL is formed when one component of linearly polarised light is retarded by a phase shift of $\lambda/4$ (using a wavelength retarder), leading to a helical shape of the sum of the two components (**Figure 1**). If a phase shift other than $\lambda/4$ is used, then the beam of light is elliptically polarised. When viewed along the propagation axes, linearly polarised light appears as a single line, circularly polarised light as a circle and elliptically polarised light as an ellipse (**Scheme 5**).



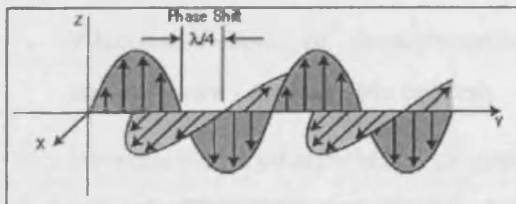
Scheme 4 Oscillating wave of linearly polarised light and view over the propagation axis



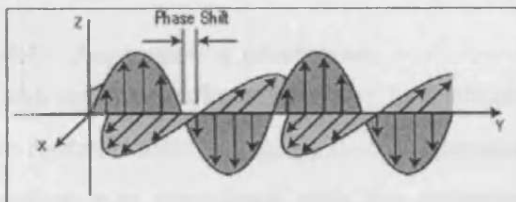
Scheme 5 View of different types of polarised light along the propagating axis. *a*) linearly polarised, *b*) circularly polarised, *c*) elliptically polarised.



Linearly Polarised Light



Circularly Polarised Light



Elliptically Polarised Light

Figure 1 Different types of polarised light: Linearly polarised, circularly polarised and elliptically polarised

Sunlight itself has an intrinsic, albeit tiny (approximately 1 ppm), circular polarisation due to the inclination of the solar magnetic axis on the ecliptic and to

sunspots.^[16] Out of the Solar System, CPL can be generated by the scattering of light from grains aligned in a magnetic field in high-mass star-forming regions. Such CPL radiation (with 17% circular polarisation) has been observed (in the IR domain) in the Orion OMC-1 nebula, a region of high-mass star formation.^[17] Due to high dust obscuration in this star formation, direct observation of UV light was not possible.

Circularly polarised synchrotron radiation emanating from one pole of an extremely rapidly rotating neutron star (or pulsar) has been suggested as another possible source of UV-CPL,^[18] and Bailey *et al.* proved that circular polarisation of cosmic radiation in space (mainly in the infrared and visible areas of the spectrum) can reach levels of up to 30%.^[19] The fact that enantiomerically enriched amino acids have been found in meteorites like Murchison,^[6] expands the search for the source of homochirality in space.

In order to obtain enantio-differentiation when CPL is involved, the enantiomers irradiated with CPL have to form a photo-stable product at a faster rate than racemisation in the photoexcited state. Enantioselective conversion can be achieved in three different ways:

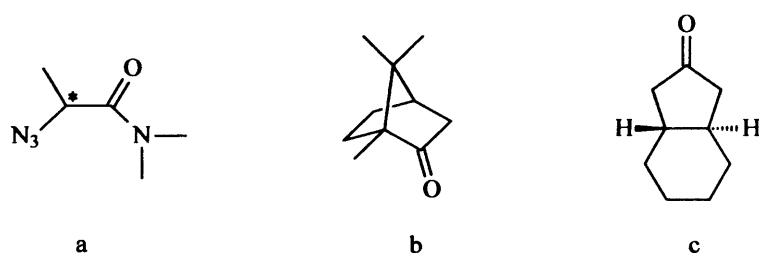
- *Asymmetric photolysis*, or photodestruction of one of the enantiomers in a racemic mixture, whilst the other remaining enantiomer is enriched, leading to an irreversible process
- *Photoresolution*, or deracemisation of photochemically interconvertible enantiomers - a reversible process
- *Asymmetric photosynthesis*, or enantioselective photochemical formation of an optically active compound from an achiral starting material

1.4.1 Asymmetric photolysis

Kuhn and co-workers were the first scientists to succeed in the *photodestruction* of the racemic dimethylamide α -azidopropionic acid (Scheme 6a).^[20] The final optical rotation was correlated with the anisotropy factor of the substrate derived from circular dichroism[‡] experiments. The Kuhn anisotropy factor (g) is the difference in adsorption of the two diastereoisomeric possible forms of one enantiomer with two

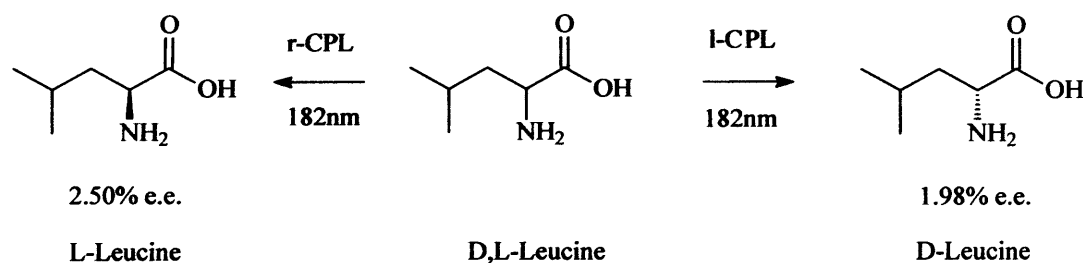
[‡] Circular dichroism can be defined as the difference in absorption of one enantiomer between left and right CPL. The work presented in this thesis is based in the difference of absorption of two enantiomers between either left or right CPL.

types of CPL, and it is expressed as ϵ_L for left-handed CPL and ϵ_R for right-handed CPL. $g = \Delta\epsilon/\epsilon$ and is typically in the order of 10^{-2} – 10^{-4} for simple chiral molecules, implying that the difference in the adsorption between left and right-handed CPL is only in the order of 1–0.01%.^[21] Kagan and co-workers reported optical purities of 20% for camphor (**Scheme 6b**) and 30% for *trans*-bicyclo[4.3.0]nonan-8-one (**Scheme 6c**), at 99% photodestruction of the racemates.^[22, 23]



Scheme 6 Compounds partially deracemised by asymmetric photolysis. **a**) dimethylamide α -azidopropionic; **b**) acid camphor and **c**) *trans*-bicyclo[4.3.0]nonan-8-one

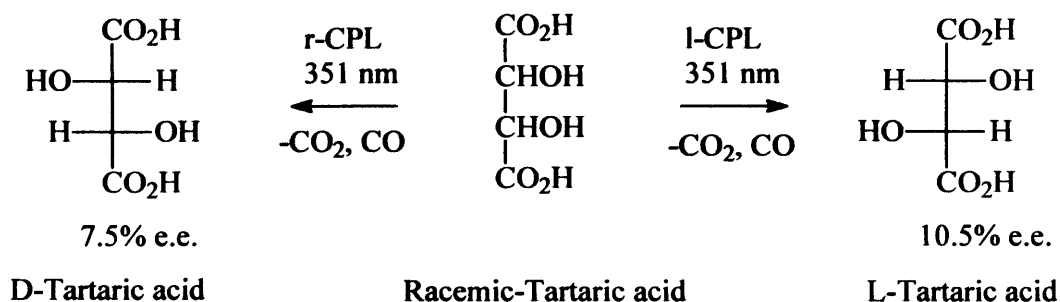
Bonner and co-workers photolysed leucine with laser induced UV-CPL, obtaining 1.98% e.e. for (R)-leucine when irradiated with r-CPL and 2.50% e.e. for (S)-leucine when irradiated with l-CPL (**Scheme 7**).^[24] This result is of great significance for the search as to how chiral life evolved as it is the first ever reported asymmetric photolysis of a prebiotic substrate.



Scheme 7 Asymmetric photolysis of leucine

Another example of asymmetric photolysis is the enantioenrichment of tartaric acid when irradiated with laser induced UV-CPL (**Scheme 8**).^[25] When a racemic sample of tartaric acid was irradiated (using a XeF laser beam) with r-CPL the resultant mixture was enriched in D-tartaric acid, presenting a maximum e.e. of 7.5%. Conversely, when a racemic sample of tartaric acid was irradiated with l-CPL the sample was enriched in L-tartaric acid with a maximum e.e. of 10.5%. According to the authors, the enantiodifferentiation proceeds through selective photodecomposition (*i.e.* decarboxylation) of the other enantiomer *via* two-photon absorption excitation, as judged from the gaseous products (CO_2 and CO). However,

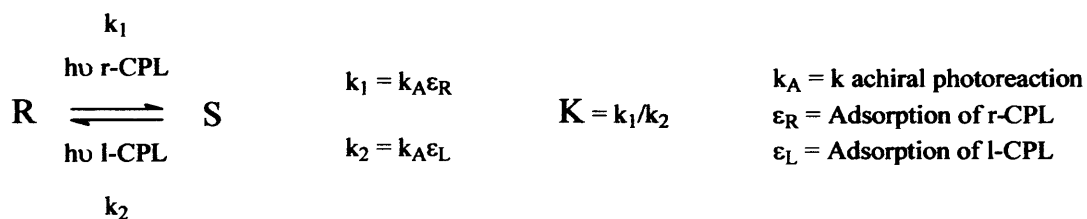
the origin of the difference of enantiomeric excesses observed is not explained. This is surprising because the diastereoisomeric relation between one enantiomer and one type of CPL should be the same as the diastereoisomeric relation between the other enantiomer and the opposite type of CPL, therefore the same degree of photolysis should be expected for both enantiomers.



Scheme 8 Asymmetric photolysis of tartaric acid

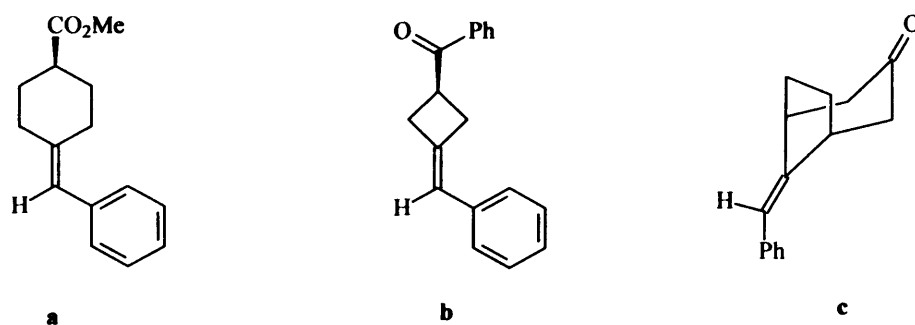
1.4.2 Photoresolution

The selectivity in a *photoresolution* process is governed by the anisotropy factor g . The enantiomeric excess in the photostationary state (ee_{PSS}) is defined as $ee_{\text{PSS}} = \Delta\epsilon/2\epsilon$ and for most compounds the value of g is around 1%, implying that the expected e.e. should be around 0.5%. However, there are some notable exceptions – chiral lanthanide complexes can show values of g up to 3%.^[26] Notice from **Scheme 9** that the equilibrium depends on the ratio $\epsilon_{\text{R}}/\epsilon_{\text{L}}$, which is always small, therefore the amount of enantiomeric excess obtained with CPL will always be small.



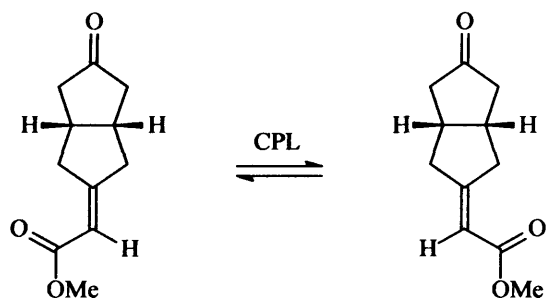
Scheme 9 General equation for photoequilibrium involving CPL

Schuster and co-workers studied a variety of axially chiral arylmethylenecycloalkanes in their search for a liquid crystal phototrigger based on CPL (**Scheme 10**).^[27]



Scheme 10 Axially chiral arylmethylenecycloalkanes studied by Schuster *et al.*

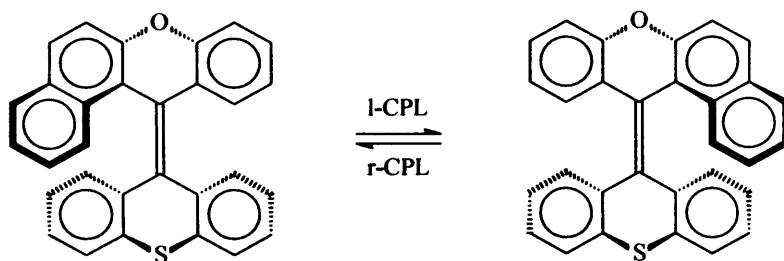
Irradiation of (*R*)-1-benzylidene-4-(methylester)cyclohexane (**Scheme 10a**) with CPL resulted in complete racemisation, and no decomposition was observed. Optically active *R*-[3-(phenylmethylene)cyclobutyl]-phenylmethanone (**Scheme 10b**) showed complete racemisation in one minute, but no successful photoresolution was described. Axially chiral bicyclo[3.2.1]octane-3-one (**Scheme 10c**) showed slow photoresolution, 47h of irradiation were necessary to reach the photostationary state, affording an e.e. of 1.6%. In 1995 Schuster and co-workers reported the first reversible photoderacemisation of an axially chiral bicyclic ketone using CPL (**Scheme 11**).^[28] The observed e.e. was 0.4%, and switching CPL to unpolarised light led to efficient photoracemisation.



Scheme 11 Reversible photoderacemisation of a rigid bicyclo[3.3.0]octanone with CPL

Feringa *et al.* searched for compounds that presented a selective interconversion of enantiomers by CPL without any photodestruction, had a high *g* factor, were thermally stable enantiomers and had a high quantum efficiency for photoracemisation.^{§ [29]} The best compound they found that met all the requirements was a helical-shaped alkene (**Scheme 12**), even though the maximum e.e. obtained was around 0.07%.

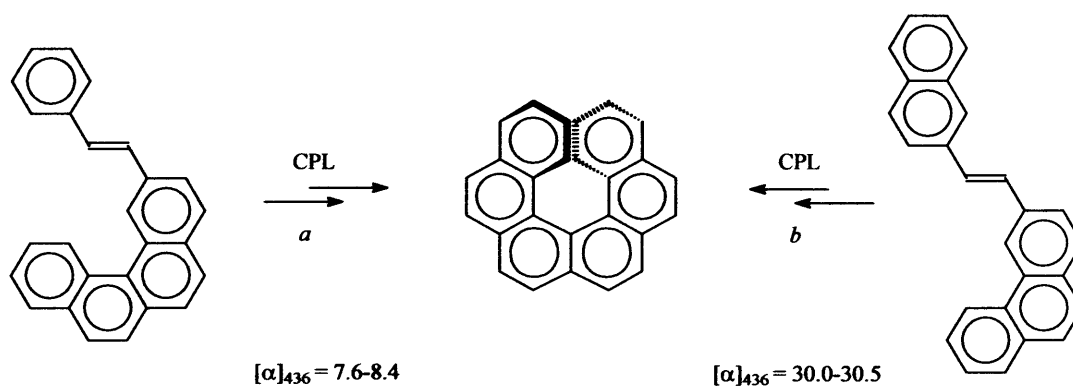
[§] The rate of photoresolution depends exponentially on the quantum efficiency



Scheme 12 Photochemical interconversion of right-handed and left-handed helical alkene

1.4.3 Asymmetric photosynthesis

The first attempt to perform an absolute asymmetric synthesis under CPL was the irradiation of an asymmetrically substituted triphenylmethyl radical, but no optical activity was observed.^[30] Helicenes are suitable for CPL-controlled asymmetric photosynthesis as they are formed by photochemical ring closure. Kagan and co-workers^[31] and also Calvin and co-workers^[32] independently succeeded in a CPL-induced enantioselective synthesis of helicenes, obtaining different values of optical activities depending on the route followed (**Scheme 13**). The reason for this may have been because the reaction went through a dihydrohelicene intermediate (different for both reactions), therefore one presented a higher value of g .



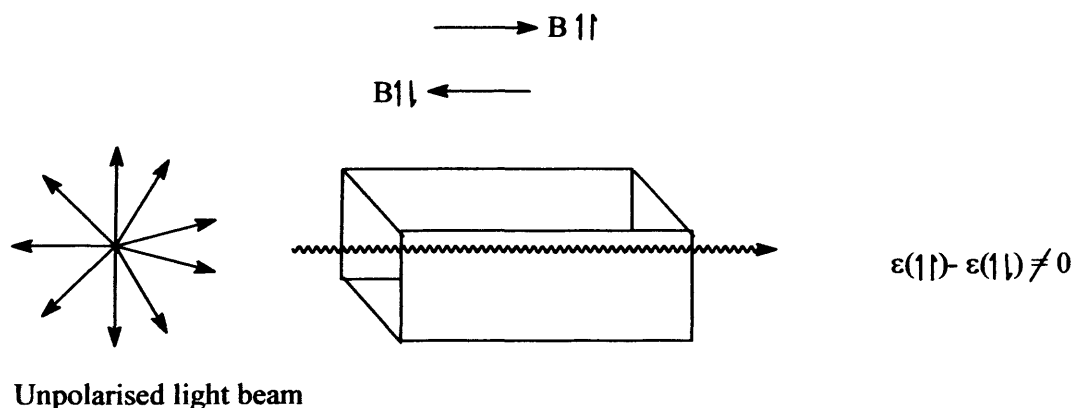
Scheme 13 Absolute asymmetric syntheses and optical activities achieved of hexalene using CPL performed by *a* Kagan and *b* Calvin

Asymmetric photosynthesis with UV-CPL is still a difficult task to achieve, the only example containing prebiotic compounds (*i.e.* amino acids) known to date is an experiment run by Meierhenrich and co-workers,^[33] in which they attempted to reproduce interstellar conditions by cooling the experiment atmosphere to 80 K and generating a high vacuum. Under these conditions, different mixtures of H₂O, CO, CO₂, CH₄, CH₃OH and NH₃ (interstellar ice analogues) were irradiated with UV-CPL, obtaining a mixture of proteinaceous and non-proteinaceous amino acids. The

enantiomeric excess was determined for the chiral amino acids showing 1% e.e., although systematic errors were estimated to be around 0.2%. The enantiomeric excess produced by asymmetric photosynthesis with UV-CPL therefore was very low, but the same experiment was performed under non-polarised light and resulted in a mixture of 16 amino acids (6 of them being protainaceous), of which none showed any photoresolution.^[34]

1.5 Magnetochemical photochemistry

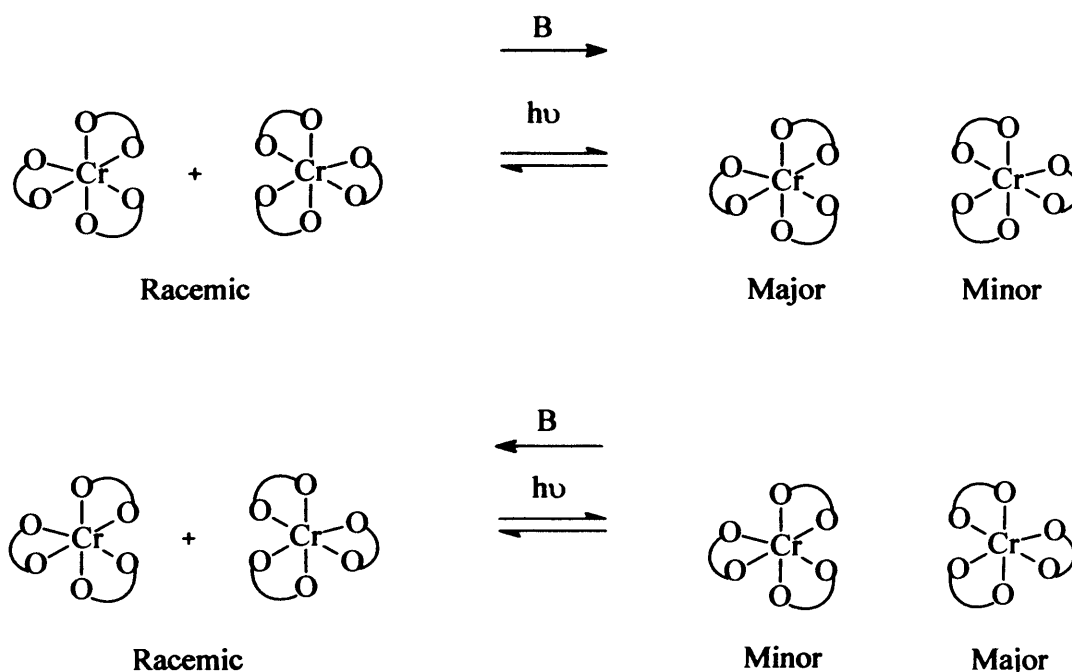
Along with parity violation and CPL, another possible inducer of homochirality considered by the scientific community is magnetism.^[35] This is based on the idea that light should be absorbed slightly differently by a solution of chiral molecules if the light beam travels parallel to an external magnetic field rather than if it travels antiparallel. Thus, the induction to homochirality should be completely independent of the polarisation state of the light beam, and should also work with unpolarised light (Scheme 14).



Scheme 14 Diagram of magnetochemical photochemistry

A suitable substrate to test this hypothesis was Cr(III)tris-oxalato, as it is an unstable complex in solution that spontaneously dissociates and re-associates. Thus, at equilibrium there are always equal concentrations of Λ - and Δ - enantiomers. A sample of Cr(III)tris-oxalato was irradiated with non-polarised UV, causing deracemisation to occur if an external magnetic field was applied parallel to the beam of light. However, when an external magnetic field was applied antiparallel to the beam of light the sample re-racemised. The e.e. values obtained were very small, around 0.01%, but consistent with the direction of the magnetic field. When the

external magnetic field was applied perpendicular to the beam of light, no e.e. was observed (Scheme 15).^[36]



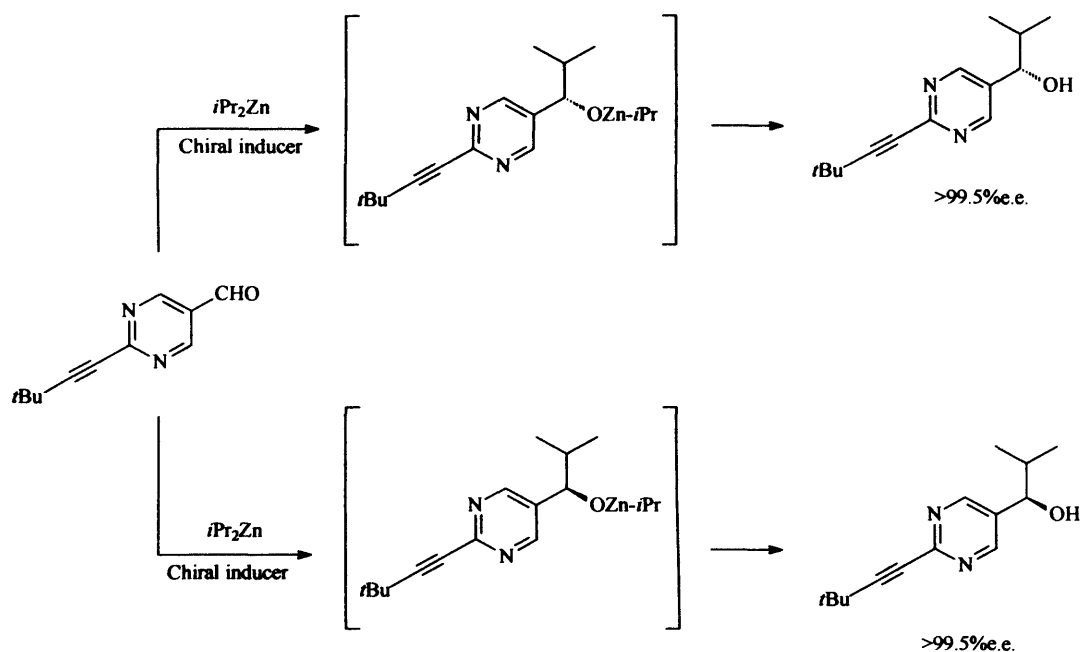
Scheme 15 Photochemical and magnetochiral reaction of tris-oxalato cobalt(III) complex

1.6 Amplification of chirality

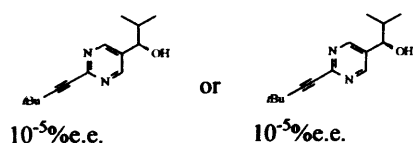
With the evidence that UV-CPL and other external forces can induce chirality in any sample that absorbs UV (even though the e.e.'s obtained are typically very low because of the small difference in absorption of the enantiomers), it seems that some mechanism that amplifies chirality must have been essential for the development of homochiral life on Earth. A chemical (asymmetric autocatalysis) and a physical (crystallisation) approach will be discussed next.

1.6.1 Asymmetric autocatalysis

Asymmetric autocatalysis can be defined as catalysis in which the chiral product acts as a chiral catalyst for its own production.^[37] For example, the addition of dialkylzinc species to aromatic aldehydes has been particularly closely examined in this respect, and various experiments concerning the autocatalysis of 2-alkynylpyrimidylalkanol have been performed (Scheme 16).



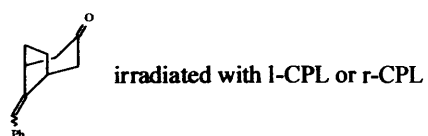
Chiral inducers:



$d\text{-NaClO}_3$ or $l\text{-NaClO}_3$

(P)-(+)-[6]helicene or (M)-(-)-[6]helicene

(P)-(+)-[5]helicene or (M)-(-)-[5]helicene



Scheme 16 Chiral autocatalysis of 2-alkynylpyrimidine-5-carbaldehyde with $i\text{Pr}_2\text{Zn}$ and different inducers

Diisopropyl zinc has been added to pyrimidyl aldehydes in the presence of a small amount of a chiral inducer. The chiral inducer not only consisted of small amounts of the chiral product, but also of an enantiomorphic inorganic ionic salt (NaClO_3),^[38] and chiral [5]- and [6]-helicenes.^[39] Another recent example, 2-alkynylpyrimidylalkanol with a chirality level of only $10^{-5}\% \text{ e.e.}$ (S or R configurations), automultiplies with significant amplification of chirality in the

addition of $i\text{Pr}_2\text{Zn}$ to 2-alkynylpyrimidine-5-carbaldehyde, producing itself with the corresponding configuration in almost enantiomerically pure form (>99.5% e.e.).^[40] In an attempt to induce chirality from a non chiral sample with the use of UV-CPL, Soai and co-workers studied the addition of $i\text{Pr}_2\text{Zn}$ to 2-alkynylpyrimidine-5-carbaldehyde in the presence of a series of chiral olefins that had been previously irradiated with UV-CPL.^[41] High e.e. was obtained in each reaction, proving a clear dependence between the enantiomer obtained and the chirality of CPL.

Concerning the origins of homochirality on Earth, it is very unlikely that the primordial soup contained much $i\text{Pr}_2\text{Zn}$, or any pyrimidyl carbaldehyde. Thus, a simpler autocatalysis example or another method of amplification of chirality is required to explain the formation of homochiral life. A physical approach was then considered, which is the symmetry breaking of the chirality through crystallisation, and is described in the next section.

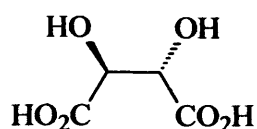
1.6.2 Crystallisation

A chemical approach to the amplification of chirality concerns asymmetric autocatalysis (Section 1.6.1), however a physical approach considers crystallisation. If a racemic compound can physically separate into both enantiomers during crystallisation (producing crystals of a single enantiomeric form), and if these crystal can seed the rest of the solution, the result is an enantiomeric solid. This method can only achieve 50% yield (but 100% e.e.), except in the ideal case when the solution is rapidly racemising and so the self-seeding effect of the initially formed crystals induces further crystallisation, until the entire sample forms crystals of a single enantiomer. This process of symmetry breaking is also known as *asymmetric transformation of the second kind (AT)*.^[42] The key process of AT is the secondary nucleation: the formation of new crystal nuclei in the vicinity of an existing “parent” crystal, which are dispersed by stirring.

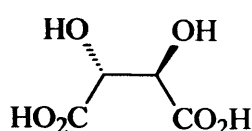
At the present time spontaneous chiral symmetry breaking in a stirred solution is a general phenomenon. It has been observed in crystallisation from both solution and melts. In reality, it occurs in all crystallisations of achiral molecules that crystallise in chiral forms, and in conglomerate crystallisation of chiral compounds that racemise rapidly compared to the rate of crystallisation. Of the 230 possible space groups, 65 are chiral, and it is worth noting that among the five most common space groups of

organic crystalline compounds** about 18% of crystals belong to two chiral space groups ($P2_12_12_1$ and $P2_1$).^[43, 44]

Louis Pasteur was the first scientist to realise that organic molecules can exist as mirror image enantiomers and this was also the first observation of conglomerate crystallisation. In 1848, he studied the chemistry of tartaric acid produced from wine residues, known to rotate polarised light in solution (it is optically active and dextrorotatory). Another acid, called racemic acid and discovered in 1820, was found to have the same molecular formula as tartaric acid ($C_4H_6O_6$), and also the same properties, except it did not rotate polarised light at all. Incomprehensibly, when tartaric acid was heated in water it slowly lost its optical activity without any apparent change in molecular structure. Pasteur observed that there were tiny differences in the crystals of the racemic acid, noticing that half of the crystals of the salt sodium ammonium racemate were actually the mirror image of the other half. Pasteur carefully separate the crystals in two piles, using a magnifying glass and tweezers, when they were dissolved separately in water, both were optically active: one solution rotated polarised light to the right (like the known tartrate), whilst the other rotated it to the left, obtaining the first levorotatory tartrate (Scheme 17). The optical activity was equal in each case, and when the solutions were combined they counteracted each other exactly to produce the typical optically inactive racemate. Pasteur then concluded that optical activity must be related to the fact that the crystals were mirror images. It is remarkable that sodium ammonium racemate only forms two types of crystals at temperatures below 26°C, above that, the two enantiomers form racemic crystals. So, if there had been a heat wave on the day that Pasteur had decided to work on sodium ammonium tartrate, he might not have made his original discovery at all.^[45]



D-Tartaric acid

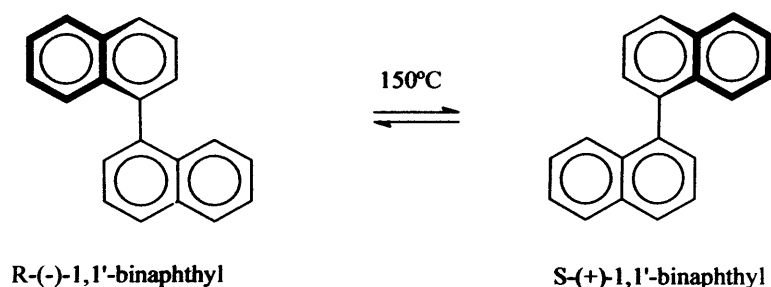


L-Tartaric acid

Scheme 17 Enantiomers of tartaric acid discovered by Louis Pasteur

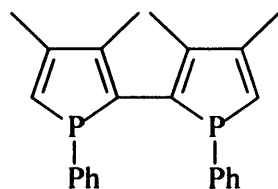
** Based on a survey of approximately 29000 crystal structure determinations

As mentioned in Section 1.6.1, NaClO_3 can resolve into enantiomers (which crystallise in a helical shape), although in this case the enantiomers are physically indistinguishable with the naked eye.^[38] Further, Kondepudi and co-workers reported chiral symmetry breaking in the stirred crystallisation of melted 1,1'-binaphthyl (Scheme 18). After melting at 150°C 1,1'-binaphthyl solidifies as a conglomerate of crystals, each consisting of either the (R)-(-) or (S)-(+)-enantiomer. Enantiomeric excesses up to 77% were obtained when the sample was stirred constantly, but the predominance of either (R)-(-) or (S)-(+)-enantiomer was random. The seeding effect was considerable, as unstirred samples produced much lower enantiomeric excess (20%). Kondepudi also studied the seeding effect of 1,1'-bi-2-naphthol – a compound isomorphous with 1,1'-binaphthyl but with a slightly higher melting point (208°C), observing a strong correlation between the chirality of the seeding enantiomer and the chirality of the product obtained.^[46]



Scheme 18 Melted 1,1'-binaphthyl can crystallise as conglomerate

Crystal symmetry breaking can also be combined with asymmetric catalysis, obtaining good results. For example, the phosphorilated ligand BIPHOS (1,1'-diphenyl-3,3',4,4'-tetramethyl-2,2'-biphosphole) (Scheme 19) combines axial chirality generated by the biphosphole framework with central chiralities of the phosphorous atoms. This implies the existence of six stereoisomers, corresponding to three pairs of enantiomers. BIPHOS crystallises as a conglomerate, and single crystals of a large size were used to obtain optically pure $[\text{PdCl}_2(\text{BIPHOS})]$, a catalyst used in asymmetric allylic substitution (obtaining e.e.'s up to 80%).^[47]



BIPHOS

Scheme 19 Ligand BIPHOS

Some substances known to be essential in living processes undergo conglomerate crystallisation (either as a neutral species or as a salt), for example asparagine, glutamic acid, histidine, methionine, proline, serine, threonine and valine,^[48] encouraging a theory that would combine amplification of chirality with generating tiny amounts of e.e. with CPL.

1.7 Summary

In summary, there are many theories about the origin of homochiral life on Earth, but none of them have been totally accepted. It has been demonstrated that homochirality is essential for the development of life and a small amount of e.e. has been detected in meteorites. It also seems that a method (either physical or chemical) that enhances the chirality of a sample is needed to achieve homochirality, as any of the physical interactions that would afford a chiral product (parity violation, CPL or magnetochirality) would only produce a small amount of e.e.

1.8 Aims of the project

Considering all the facts previously discussed, it is feasible to expect that a chiral crystalline molecule that can react under UV irradiation (either by racemisation around a double bond, by photolability of a metal or photolability of ligands) can generate a small amount of e.e., which can be rapidly increased if the molecule crystallises as a conglomerate. In addition, this could shine a new light on the origins of homochiral life on Earth. The work described in this thesis focuses on:

- *Crystalline axially chiral benzylidenes*; their synthesis, deracemisation and interaction with CPL
- *Photolabile cobalt (III) coordination compounds*; their synthesis, crystallisation studies, and interaction with CPL

- *Cobalt carbonyl organometallic complexes*; their synthesis, photochemistry and interaction with CPL

The chemistry of each of these families of compounds is introduced at the start of the relevant chapter.

1.9 References

- [1] L. Pasteur, *Comp. Rend. Paris* **1848**, 26, 535.
- [2] N. Fujii, *Origins of Life and Evolution of Biospheres* **2002**, 32, 103.
- [3] A. Brack, *Origins of Life and Evolution of Biospheres* **2002**, 32, 83.
- [4] A. I. Oparin, *The Origin of Life*, **1924**.
- [5] S. L. Miller, *Science* **1953**, 117, 528.
- [6] K. Kvenvolden, J. Lawless, K. Pering, E. Peterson, J. J. Flores, C. Ponnampereuma, I. R. Kaplan, C. Moore, *Nature* **1970**, 228, 923.
- [7] M. H. Engel, S. A. Macko, *Nature* **1997**, 389, 265.
- [8] S. Pizzarello, J. R. Cronin, *Geochim. et Cosmochim. Acta* **2000**, 64, 329.
- [9] W. H. P. Thiemann, U. Meierhenrich, J., *Origins of Life and Evolution of Biospheres* **2001**, 31, 199.
- [10] T. D. Lee, C. N. Yang, *Phys. Rev.* **1956**, 102, 290.
- [11] C.-S. Wu, E. Ambler, R. Hayward, D. Hoppes, R. P. Hudson, *Phys. Rev.* **1957**, 105, 1413.
- [12] R. A. Hegstrom, D. W. Rein, P. G. H. Sandars, *J. Chem. Phys.* **1980**, 73, 2329.
- [13] D. W. Rein, R. A. Hegstrom, P. G. H. Sandars, *Phys. Lett. A* **1979**, 71, 499.
- [14] C. C. Wilson, D. Myles, M. Ghosh, L. N. Johnson, W. Wang, *New J. Chem.* **2005**, 29, 1318.
- [15] S. Mason, G. Tranter, *Mol. Phys.* **1984**, 53, 1091.
- [16] J. C. Kemp, G. D. Henson, C. T. Steiner, E. R. Powell, *Nature* **1987**, 326, 270.
- [17] J. Bailey, *Science* **1998**, 281, 672.
- [18] J. Bailey, *Origins of Life and Evolution of Biospheres* **2001**, 31, 167.
- [19] J. H. Hough, J. Bailey, A. Chrysostomou, T. M. Gledhill, P. W. Lucas, T. M., S. Clark, J. Yates, F. Menard, *Adv. Space Res.* **2001**, 27, 313.
- [20] W. Kuhn, E. Braun, *Naturwissenschaften* **1929**, 17, 227.
- [21] J. Shao, P. Hänggi, *J. Chem. Phys.* **1997**, 107, 9935.

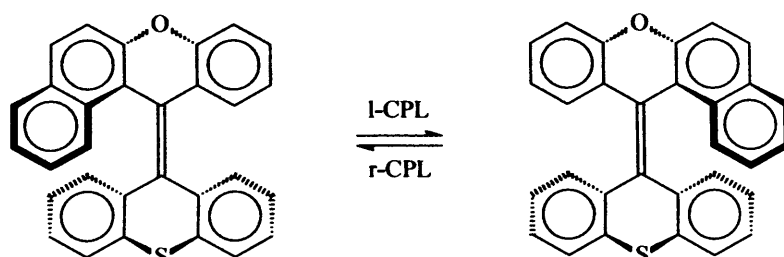
- [22] G. Balavoine, A. Moradpour, H. B. Kagan, *J. Am. Chem. Soc.* **1974**, *96*, 5152.
- [23] H. B. Kagan, J. C. Fiaud, *Top. Stereochem.* **1988**, *18*, 249.
- [24] J. J. Flores, W. A. Bonner, G. A. Massey, *J. Am. Chem. Soc.* **1977**, *99*, 3622.
- [25] Y. Shimizu, *J. Chem. Soc. Perkin Trans. 1* **1997**, 1275.
- [26] B. L. Feringa, R. A. van Delden, *Angew. Chem. Int. Ed.* **1999**, *38*, 3418.
- [27] R. P. Lemieux, G. B. Schuster, *J. Org. Chem.* **1993**, *58*, 100.
- [28] M. Suarez, G. B. Schuster, *J. Am. Chem. Soc.* **1995**, *117*, 6732.
- [29] N. P. Huck, W. F. Jager, B. de Lange, B. L. Feringa, *Science* **1996**, *273*, 1686.
- [30] G. Karagunis, G. Drikos, *Naturwissenschaften* **1933**, *21*, 607.
- [31] A. Moradpour, J. F. Nicoud, G. Balavoine, H. B. Kagan, G. Tsoucaris, *J. Am. Chem. Soc.* **1971**, *93*.
- [32] W. J. Bernstein, M. Calvin, O. Buchardt, *J. Am. Chem. Soc.* **1972**, *94*.
- [33] M. Nuevo, U. Meierhenrich, J., L. d'Hendecourt, G. M. Muñoz-Caro, E. Dartois, D. Deboffe, W. H. P. Thiemann, J. H. Bredehöft, L. Nahon, *Adv. Space Res.* **2005**, doi:10.1016/j.asr.2005.05.011.
- [34] G. M. Muñoz-Caro, U. Meierhenrich, J., W. A. Schutte, B. Barbier, A. Arcones-Segovia, H. Rosenbauer, W. H. P. Thiemann, A. Brack, J. M. Greenberg, *Nature* **2002**, *416*, 403.
- [35] L. D. Barron, *Nature* **2000**, *405*, 895.
- [36] G. L. J. A. Rikken, E. Raupach, *Nature* **2000**, *405*, 932.
- [37] K. Soai, T. Shibata, I. Sato, *Acc. Chem. Res.* **2000**, *33*, 382.
- [38] I. Sato, K. Kadowaki, K. Soai, *Angew. Chem. Int. Ed.* **2000**, *39*, 1510.
- [39] I. Sato, R. Yamashima, K. Kadowaki, J. Yamamoto, T. Shibata, K. Soai, *Angew. Chem. Int. Ed.* **2001**, *40*, 1096.
- [40] I. Sato, H. Urabe, S. Ishiguro, T. Shibata, K. Soai, *Angew. Chem. Int. Ed.* **2003**, *42*, 315.
- [41] I. Sato, R. Sugie, Y. Matsueda, Y. Furumura, K. Soai, *Angew. Chem. Int. Ed.* **2004**, *43*, 4490.
- [42] E. J. Ebbers, G. J. A. Ariaans, J. P. M. Houbiers, A. Bruggink, B. Zwanenburg, *Tetrahedron* **1998**, *53*, 9417.
- [43] T. Kawasaki, K. Jo, H. Igarashi, I. Sato, M. Nagano, H. Koshima, K. Soai, *Angew. Chem. Int. Ed.* **2005**, *44*, 2774.

- [44] M. Sakamoto, *Chem. Eur. J.* **1997**, *3*, 684.
- [45] D. Pye, *Polarised Light in Science and Nature*, Institute of Physics Publishing, Bristol and Philadelphia, **2001**.
- [46] D. K. Kondepudi, J. Laudadio, K. Asakura, *J. Am. Chem. Soc.* **1999**, *121*, 1448.
- [47] O. Tissot, M. Gouygou, F. Dallemer, J.-C. Daran, G. Balavoine, *Angew. Chem. Int. Ed.* **2001**, *40*, 1076.
- [48] I. Bernal, *Journal of Chemical Education* **1992**, *69*, 468.

Chapter 2: SYNTHESIS AND CHIRALITY OF ALKYLIDENE DIOXANEDIONES

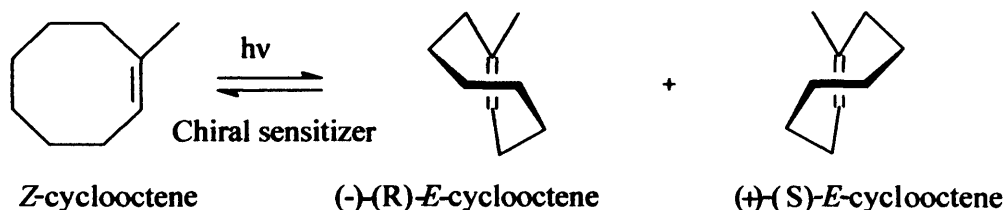
2.1 Introduction

This chapter discusses efforts to synthesise axially chiral organic molecules that were likely to be photoracemisable and expose them to circularly polarised light (CPL). Photoresolution of racemic axially chiral compounds in which the axis is an alkene, can be accomplished by irradiation with CPL. The potential use of r-CPL and l-CPL in photochemical reactions for the production of an excess of a particular enantiomer from a racemic substance was postulated as early as the 19th century by Le Bel and Van't Hoff.^[1, 2] This was first proved by Kuhn in 1929,^[3] and a range of compounds have been shown to undergo such photoreactions (See Section 1.4). For example, as discussed in Section 1.4.2, a helical alkene was found to selectively interconvert between enantiomers under CPL irradiation without observing any photodestruction, *i.e.*, without observing destruction of either of the enantiomers due to the effect of light (Scheme 1).^[4]



Scheme 1 Photochemical interconversion of a right-handed and a left-handed helical alkene

Photoresolution of alkenes has been achieved in the presence of a chiral sensitizer in the *E/Z* photoisomerisation of 1-methylcyclooctene (Scheme 2)^[5] reaching photostationary states *E/Z* ratios of 0.4 - 0.8:1 (Table 1).^{*[6]} The chiral sensitizer was based on (-)-menthyl benzenecarboxylate.



Scheme 2 Photoisomerisation of 1-methylcyclooctene

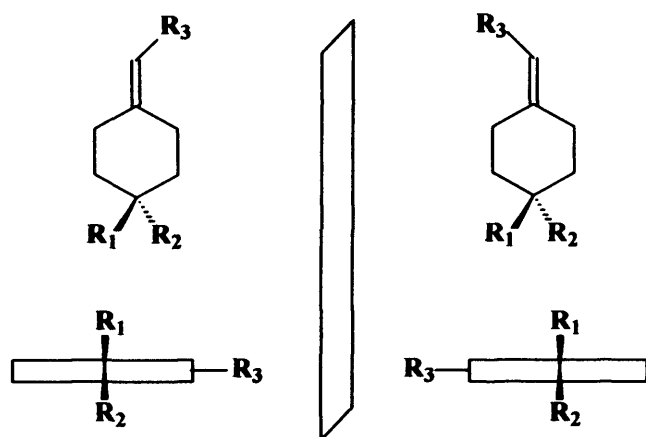
Sensitizer	<i>E/Z</i>	(+)-(E) e.e. (%)
Benzoate	0.165	3.2
Isophthalate	0.147	0.9
Terephthalate	0.050	5.0
Trimesate	0.065	0.0

Table 1 Sensitizers utilised in the photoisomerisation of cyclooctene and *E/Z* ratios obtained

2.1.1 Aims of the chapter

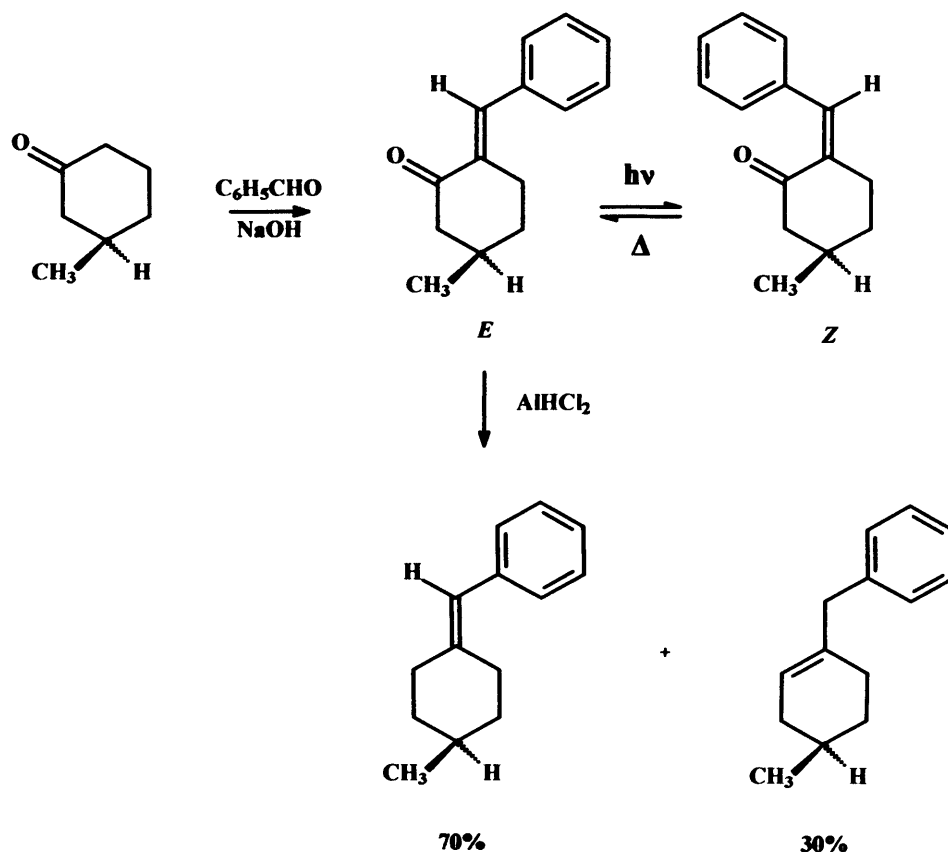
Target molecules for this chapter had to be photoracemisable and ideally, with a large $\Delta\epsilon$ (the difference in absorption of the two forms of CPL, see Section 1.4.1 for more information about Kuhn anisotropy), so that their e.e. could be affected by CPL. A family of molecules that fulfils both requirements are alkylidencycloalkanes. The chirality in these molecules can be visualised as an imaginary axis going along the ring and the alkene (Scheme 3). When $R_1 = R_2$ the molecules are not chiral as there is a plane of symmetry in the ring, but when R_1 and R_2 are different there is chirality along the axis (hence axial chirality), despite the high symmetry of the ring.

* Note that the presence of a chiral sensitizer does not require chiral light (or CPL), but shows that an interaction between non-chiral light and a chiral molecule can lead to enantiodifferentiation, in the same way that can do chiral light in presence of a non-chiral molecule.



Scheme 3 Axial chirality of alkylidenecycloalkanes, enantiomers with the mirror plane

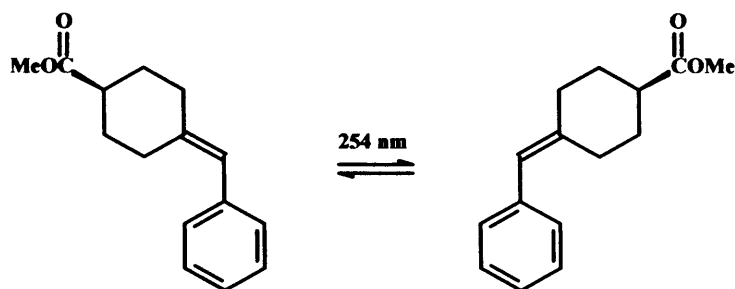
Alkylidenecycloalkenes were optically resolved for the first time in 1909,^[7, 8] when Perkin *et al.* successfully resolved 4-methylcyclohexylideneacetic acid. However, the absolute configuration of the compound was only assigned in 1966^[9] by Gerlach through correlation with (2R)-(-)-isoborneol. In the same year, Brewster and Privett converted the chiral (+)-3-methyl-cyclohexanone to the chiral (R)-(-)-2-benzylidene-5-methylcyclohexanone,^[10] showing that photochemical isomerisation of the condensation product led to the formation of two isomers with different thermal stability: isomer *E* was more stable than isomer *Z*. Further reduction of the ketone group in the *E* isomer afforded as a main product the *exo* (S)-(+)-1-benzylidene-4-methylcyclohexane, more conjugated and more stable than the *endo* product (**Scheme 4**).



Scheme 4 Synthesis of axially chiral (S)-(+)-1-benzylidene-4-methylcyclohexane and photochemical isomerisation of cyclohexanone (R)-3-methyl-cyclohexanone

2.2 Syntheses of benzylidene malonate derivatives

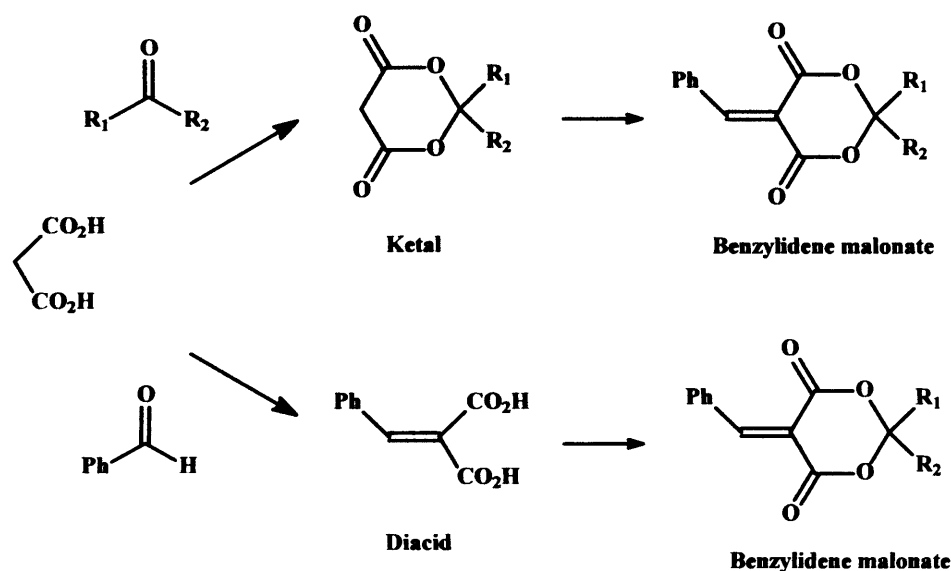
In 1997 Ebberts *et al.* reported that axially chiral methylene cycloalkenes were photoracemisable at wavelengths of 254 nm (**Scheme 5**),^[11] and these compounds were taken as a model to design a family of molecules that might be photoracemisable.



Scheme 5 Photoracemisable axially chiral methylene cycloalkene

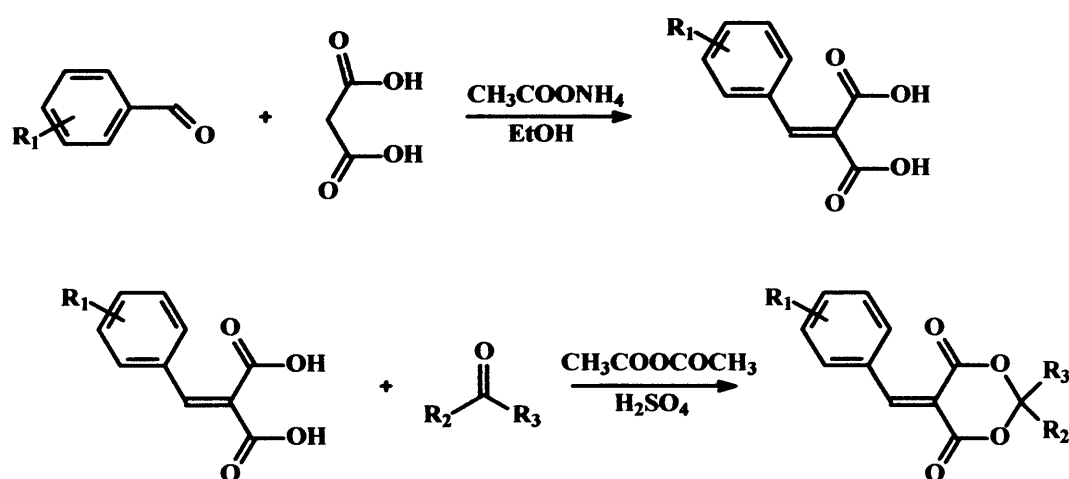
The target molecules chosen to commence the work on the synthesis of axially chiral alkylidenes were 5-benzylidene-2-R₁-2-R₂-1,3-dioxane-4,6-dione derivatives. These

compounds are very similar to methylene cycloalkenes and are synthesised from cheap and readily available starting materials: malonic acid, a ketone and an aromatic aldehyde (**Scheme 6**).

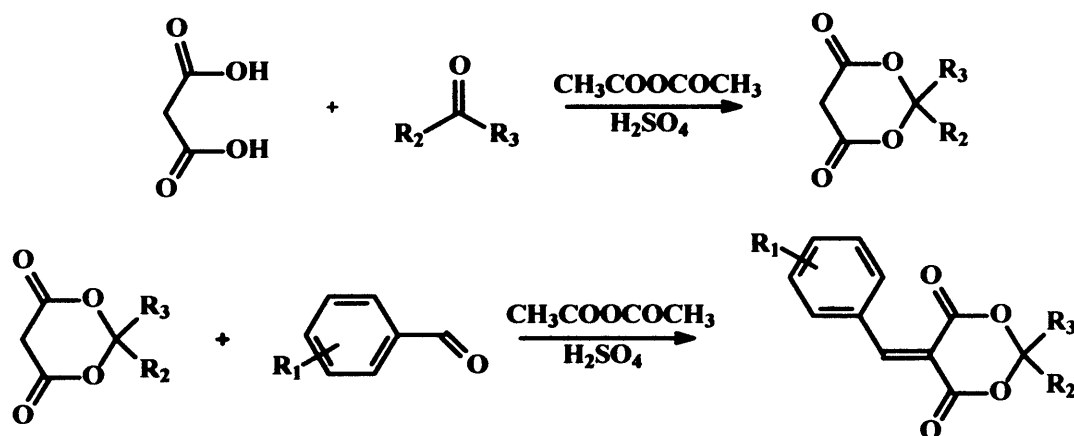


Scheme 6 Different approaches for the synthesis of benzylidene malonates

There are two different approaches to the target molecules, both of them using malonic acid as starting material, named route *a* and route *b*. Route *a* starts with a Knoevenagel reaction, followed by condensation of the α,β -unsaturated diacid with a ketone (**Scheme 7**). In route *b* malonic acid is condensed first with a ketone, to obtain a cyclic malonate ketal, followed by condensation with an aldehyde to afford an α,β -unsaturated malonate (**Scheme 8**).



Scheme 7 Route *a* for the synthesis of benzylidene malonates

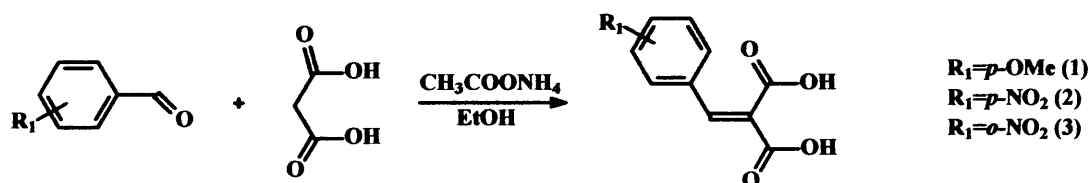


Scheme 8 Route *b* for the synthesis of benzylidene malonates

Route *a* was attempted first because the products of the reaction were expected to be carboxylic acids and therefore easy to purify by recrystallisation. In addition, route *b* was expected to lead to the formation of a ketal, which in acidic conditions and in the presence of water could reverse the equilibrium and hydrolyse.

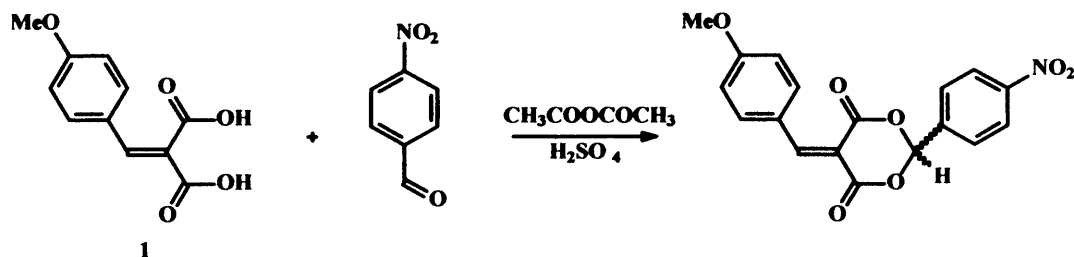
2.2.1 Route *a*

The first step of route *a* was the Knoevenagel condensation between malonic acid and an aldehyde. Diacids **1**, **2** and **3** were synthesised following procedures described in the literature (Scheme 9),^[12] affording yields of 45%, 43% and 48% respectively. **1**, **2** and **3** were identified by similarity of the ¹H-NMR spectrum described in the literature.^[12]



Scheme 9 Synthesis of diacids **1**, **2** and **3**

The second step of route *a* was the condensation of a diacid with an aldehyde or a ketone, obtaining the expected benzylidene malonate. The condensation of **1** with *p*-nitrobenzaldehyde to form the ketal was attempted following a literature procedure for the synthesis of cinnamylidene cinnamalmalonate, using sulphuric acid as catalyst and acetic anhydride as solvent (Scheme 10).^[13] The reaction became exothermic when sulphuric acid was added and the entire solution immediately became solid.



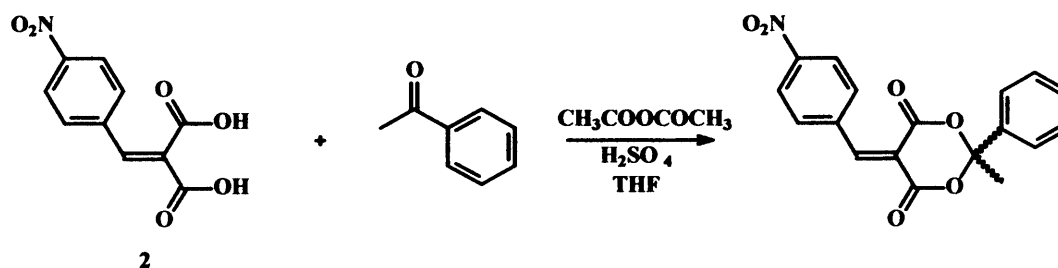
Scheme 10 Attempted of second step of route *a* with 1

The $^1\text{H-NMR}$ spectrum of the crude reaction mixture presented a sharp singlet at 2.1 ppm, probably acetic acid, and a triplet and a doublet at the aromatic zone (7.5 ppm and 8.2 ppm respectively), as well as the starting materials. Integration of the methoxy and aromatic group signals of the desired product showed a lower ratio of methoxy:aromatic than expected. The integration area for the methoxy peak (at 3.9 ppm) was approximately 5-10 % of the aromatic protons. This was not consistent with the desired product. After working-up the crude reaction mixture 46 % of diacid 1 was recovered from the mother liquors.

It is likely that the reaction did not work due to the presence of water, which might affect the ketal formed and reverse the equilibrium. The reaction was then attempted under different conditions, *i.e.*, use of a catalytic amount of acid (5 % *p*-TsOH), a Dean-Stark condenser and toluene as solvent. Due to the low solubility of 1 in toluene the reaction was left refluxing for 24 h. TLC showed three main species in the reaction mixture, two of which were starting materials (1 and *p*-nitrobenzaldehyde). The third species presented a R_f value in between the R_f values of the reactants. This indicated that the unknown product was more polar than 1 and less polar than *p*-nitrobenzaldehyde. In order to isolate the unknown product, the reaction mixture was dissolved in ethyl acetate and washed with 0.1 M NaOH. $^1\text{H-NMR}$ analysis of the isolated product proved that mainly *p*-nitrobenzaldehyde was present, instead of the expected condensation product. A third attempt to perform the reaction involved the condensation of 1 with *p*-nitrobenzaldehyde in the presence of CF_3COOH (used as the solvent). After two days stirring, TLC showed that the reaction mixture contained mainly starting materials.

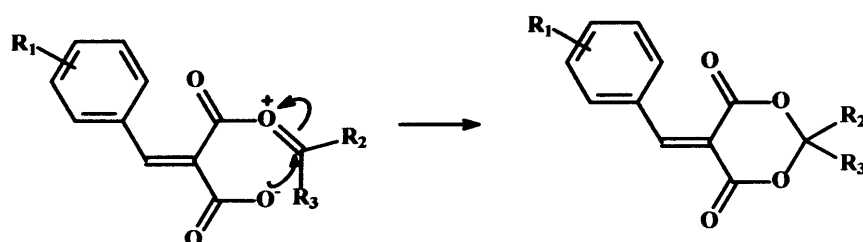
The condensation of 2 with acetophenone to form a ketal was attempted following a procedure similar to that described in the literature,^[13] using a mixture of acetic anhydride, sulphuric acid and THF (**Scheme 11**). However, even after stirring for

four days, the $^1\text{H-NMR}$ spectrum of the crude mixture indicated that essentially no reaction had taken place, with only starting materials present in solution.



Scheme 11 Attempt of second step of route *a* with 2

One possible explanation for the failure of the reaction despite the different synthetic conditions employed could be due to the high rigidity of the benzylidene malonic acid skeleton. The reaction was expected to proceed *via* an oxonium intermediate (in order to obtain the ring-closed product), followed by nucleophilic attack at the sp^2 carbon of the ketone (**Scheme 12**). Even though Baldwin's rules for closing a 6-Endo-Trig are favourable for this system,^[14] at that point flexibility around the malonate skeleton is essential, helping the carboxylate approach the sp^2 carbon.



Scheme 12 Oxonium cation intermediate, and key step for the ring formation

As neither compounds 1 and 2 had been successful in the second step of route *a*, compound 3 was not even attempted as 3 had a higher steric effect than 1 or 2, therefore it was assumed that the rigidity of the benzylidene malonic acid would be higher. Attention was then turned to route *b*.

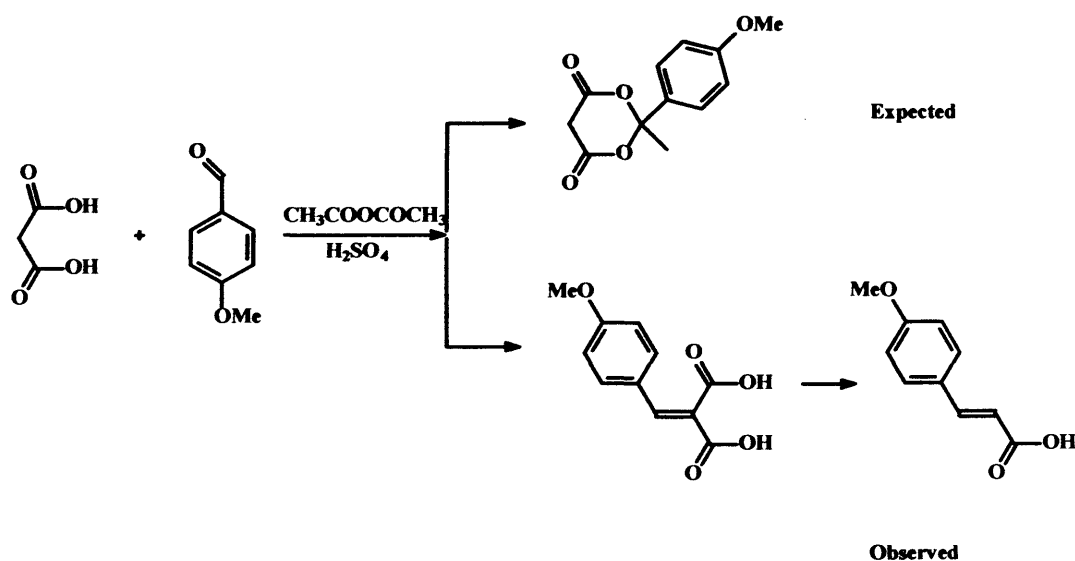
2.2.2 Route *b*

2.2.2.1 First step of route *b*

The first step of route *b* was based on the syntheses of cyclic malonate ketal and acetal derivatives. The first approach followed the method developed by Breitenstein *et al.*^[15] for the synthesis of similar malonates (*e.g.* 2-(4-methoxyphenyl)-1,3-dioxane-4,6-dione and 2-cyclohexyl-2-methyl-1,3-dioxane-4,6-dione **Scheme 13**).

Scheme 13 Reported malonates synthesised following route *b*

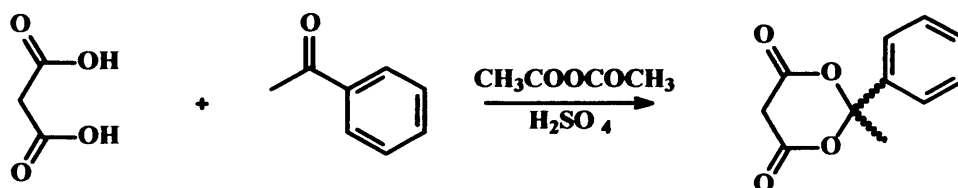
The reaction was attempted using malonic acid and *p*-anisaldehyde as reactants, sulphuric acid as catalyst and acetic anhydride as solvent. After three days a mixture of products was obtained, with none being identified as the desired product. The reaction was attempted again following a similar procedure outlined in a patent developed by Relenyi *et al.* for the synthesis of Meldrum's acid.^[16] The attempted reaction was performed with malonic acid and *p*-anisaldehyde (instead of acetone, the ketone used in the patent). However, the final product of the reaction (identified by ¹H-NMR spectroscopy) was a monoacid instead of the expected cyclic malonate ketal. One possible explanation is that an exothermic reaction occurred when acetic anhydride was added, which could have led to the formation of the diacid, followed by decarboxylation (Scheme 14).



Scheme 14 Expected product and possible explanation for the formation of the monoacid

The product of the reaction was unexpectedly colourful (bright violet) for the level of conjugation in the molecule, and ¹H-NMR spectrum showed very broad bands as if the product was paramagnetic. This could be explained in the hypothetical case where the reaction gave a radical by-product or if some transition-metal impurity (*e.g.* some traces from the spatula) was trapped in the product.

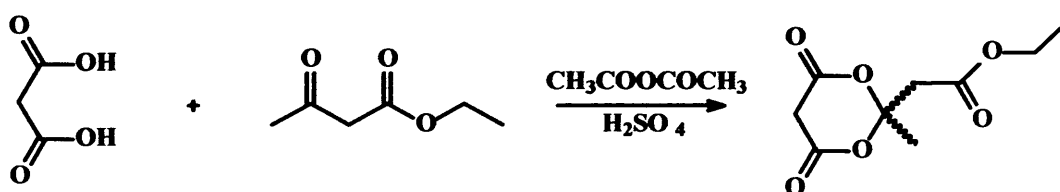
A second attempt was *via* the condensation of malonic acid with acetophenone (Scheme 15), which, being a ketone, is much less reactive than the aldehydes previously used. Also, the reaction conditions had to be changed due to the insolubility of malonic acid in acetophenone.



Scheme 15 Second attempt of first step of route *b*

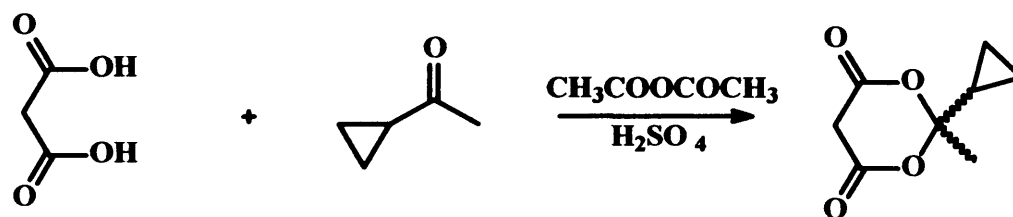
The product of the reaction, after extracting and recrystallising, was analysed by $^1\text{H-NMR}$ spectroscopy, but did not show any signals for the expected methyl protons. Further, the IR spectrum showed no carbonyl bands. Mass spectrometry indicated a molecular peak of 284.5 and taking the ratio of $(\text{M}+1)/\text{M}$ inferred that approximately seventeen carbon atoms were in the compound. However, this product has not been identified.

A third attempt using the approach in the patent for the synthesis of Meldrum's acid,^[16] but using malonic acid and ethyl acetoacetate (instead of acetone) (Scheme 16), with the expected ketal being a less conjugated product than the previous attempt and therefore the reaction might be quicker. After 48 h a $^1\text{H-NMR}$ spectrum again showed a mixture of products, unfortunately the required ketal was not identified.



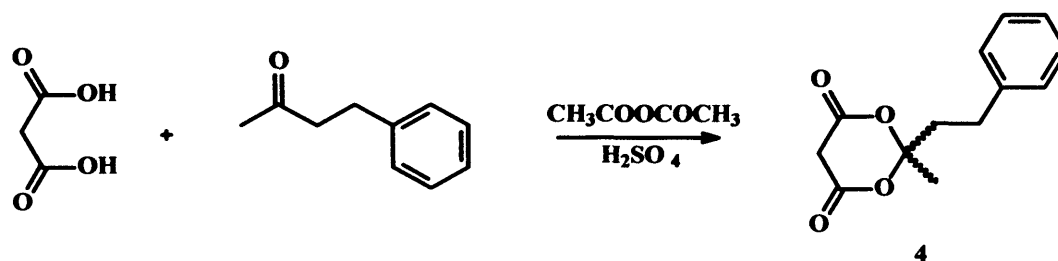
Scheme 16 Third attempt of first step of route *b*

Finally, the reaction was attempted using cyclopropylmethyl ketone; a ketone more similar to acetone than the previous ones used (Scheme 17). The $^1\text{H-NMR}$ spectrum again showed a mixture of products, none of which were the desired ketal, therefore the synthetic method and also the ketone were again changed.

Scheme 17 Last attempt of first step of route *b* with the conditions mentioned in the patent

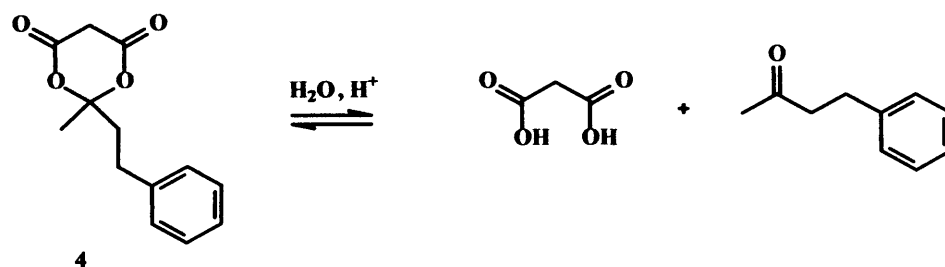
2.2.2.1.1 Synthesis of 2-methyl-2-(2-phenylethyl)-1,3-dioxane-4,6-dione (4)

A condensation with malonic acid and benzylacetone was performed, introducing some variations to the method described in the patent developed by Relenyi for the synthesis of Meldrum's acid (Scheme 18).^[16] Excess of malonic acid was removed by precipitation with DCM instead of diethyl ether (as described in the patent) and the crude product was identified by ¹H-NMR spectroscopy (Figure 1).



Scheme 18 Synthesis of 4

After leaving the product two days in solution, a crystalline solid formed and a sample analysed by ¹H-NMR presented signals characteristic of malonic acid. This led to the conclusion that the equilibrium between the ketal and the diacid could be reversed if the product was exposed to moisture from the air (Scheme 19). Hitherto the ketal had never been isolated under anaerobic conditions, even though the reaction had always been performed under nitrogen, so the next refinement was to perform the reaction under nitrogen and isolate the product by Schlenk techniques.



Scheme 19 Reversible equilibrium observed between 4 and starting materials

The crude product of the reaction was distilled under vacuum and from the residue **4** eventually crystallised in the Schlenk flask. Finally, **4** was purified by recrystallisation from ethyl acetate/petrol (**Figure 1**).

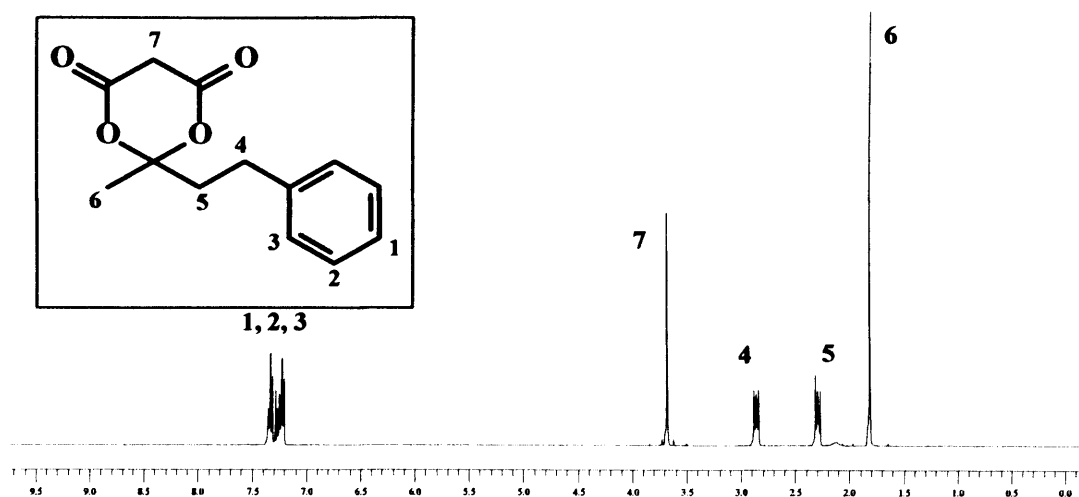


Figure 1 $^1\text{H-NMR}$ spectrum (400 MHz, CDCl_3) of **4**

A deuterated chloroform solution of **4** showed resonances at 2.3 ppm and 2.9 ppm corresponding to the proton groups of the ethylene chain shown in **Figure 2**. Each methylene group of the aliphatic chain was expected to show a triplet in a first order spectrum, however, the “crown” shape for the peaks at 2.3 ppm and 2.9 ppm (**Figure 2**) were not consistent with this. A simulation of the spectrum (using g-NMR v4.0)^[17] shows a geminal coupling constant of 12.0 Hz and vicinal coupling constants of 7.0 Hz and 8.6 Hz (**Figure 3**) as an AA'BB' system with diastereotopic protons. The non-first order spectrum is probably due to impaired free rotation of the ethyl chain, caused by the presence of the aromatic ring. This complex spectrum was disappointing as it had been hoped that diastereotopicity in these protons could be used to confirm chirality in the final products, or even be used to determine racemisation barriers by variable temperature NMR.

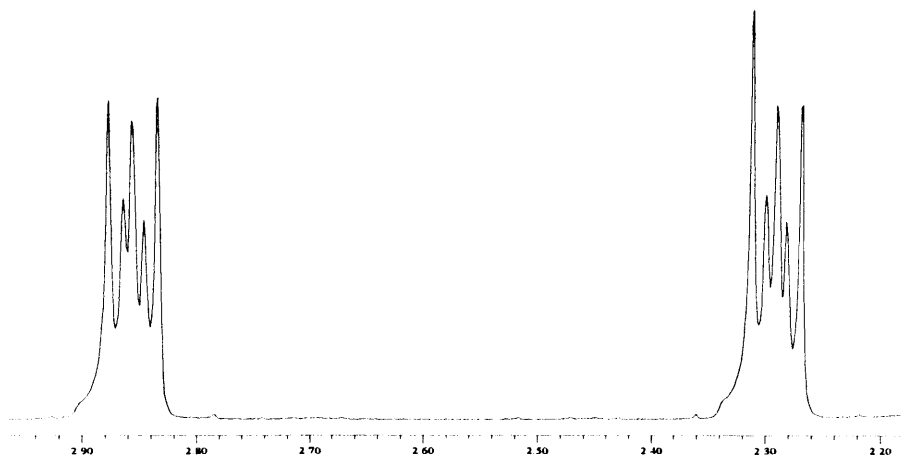


Figure 2 “Crown” peaks for the methylene groups of compound 4

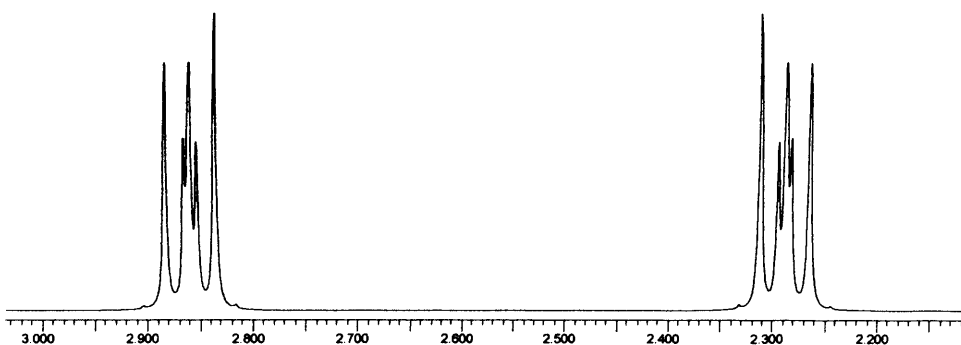


Figure 3 Simulation of “crown” peaks of compound 4

2.2.2.2 Second step of route *b*

The second step of route *b* consisted of a Knoevenagel condensation. The reaction was first attempted in ethanol, using the ketal **4**, a catalytic amount of ammonium acetate acting as a mild acid, and *p*-nitrobenzaldehyde. After two hours, a yellow solid precipitated from the solution. ¹H-NMR spectrum confirmed that the solid was the desired product **5**. Recrystallisation from ethanol afforded **5** analytically pure in 37 % yield, although this was later optimised to raise the yield to 90 %.

The structure of **5** was confirmed by the distinctive ¹H-NMR spectrum (Figure 4). The position of the olefinic proton (8.4 ppm) is higher than expected to the position estimated for a vinyl proton (8.1 ppm).^[18] This is probably because this proton is very electron deficient as it is positioned β to two carbonyl groups and also has a *p*-nitrobenzene group withdrawing electron density from the π-system, moving the chemical shift of the vinyl proton downfield. Again, a non-first order spin system was observed in the proton spectrum of the methylene groups of the aliphatic chain,

which can be explained as for the spin system discussed for compound 4. 5 was obtained as a racemic mixture because the reaction was performed in the absence of any chiral influence.

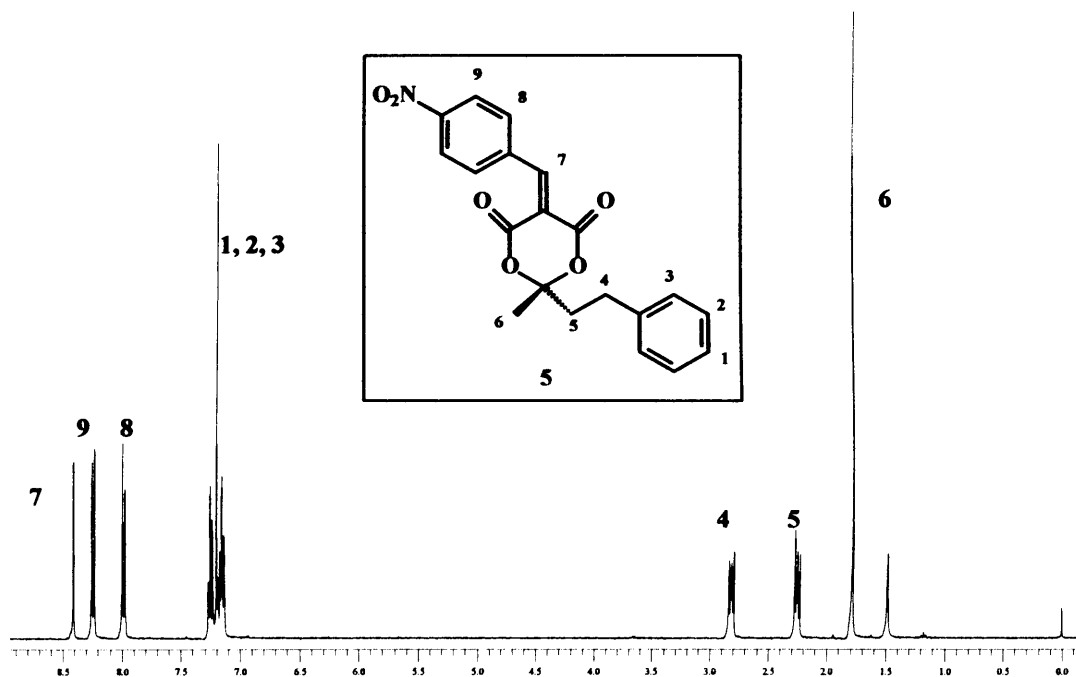
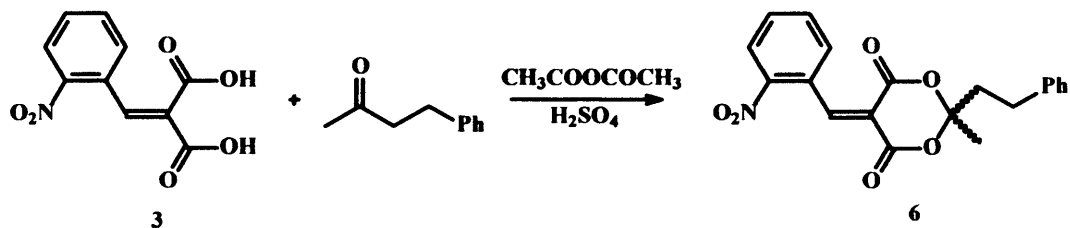


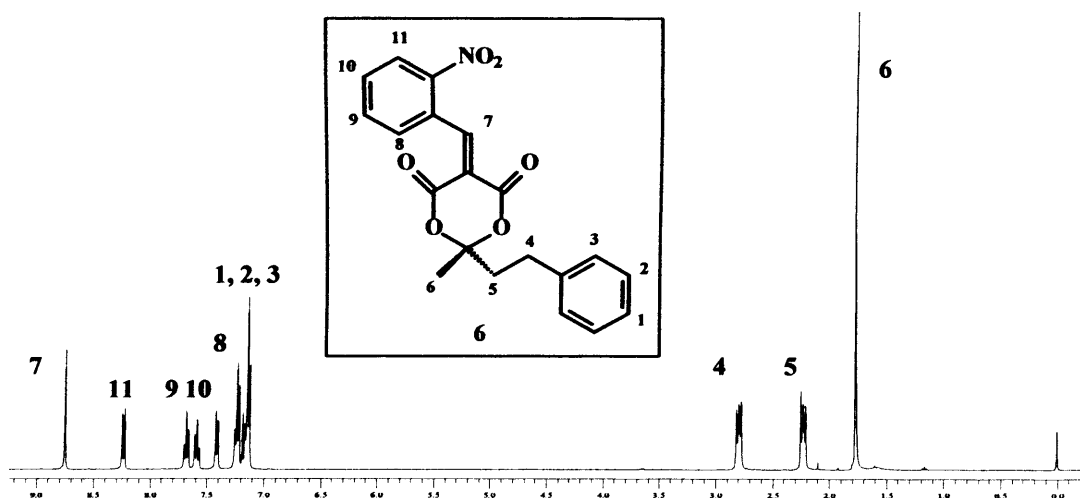
Figure 4 ¹H-NMR spectrum (400 MHz, CDCl₃) of 5

Subsequent to the successful synthesis of 5 and in order to study both electronic and steric effects of the aromatic ring on a benzylidene malonate family, the second step of route *b*, *i.e.*, the Knoevenagel condensation between the ketal 4 and an aldehyde, was attempted utilising *o*-nitrobenzaldehyde, benzaldehyde and *p*-methoxybenzaldehyde. In addition, a condensation reaction with an aliphatic ketone was attempted in order to compare the effect of aromatic groups with aliphatic chains.

The synthesis of 5-(2-nitro-benzylidene)-2-methyl-2-(phenylethyl)-1,3-dioxane-4,6-dione 6 was initially attempted following route *a*, utilizing the diacid 3 as reactant instead of malonic acid (Scheme 20). The product was extracted from the crude reaction mixture with cyclohexane, and then recrystallised from ethanol.

Scheme 20 The synthesis of **6** via route *a*

Following route *a*, the yield was very low (3.5 %), supporting the theory concerning the rigidity of the benzylidene malonate skeleton (See Section 2.2.1). However, following the procedure described for the formation of **5** (i.e. route *b*) afforded **6** in 66 % yield (Figure 5). This difference in yield observed depending on the route followed, is in total agreement with the rigidity of the malonate skeleton. The product was not always crystalline and was sometimes obtained as an oil.

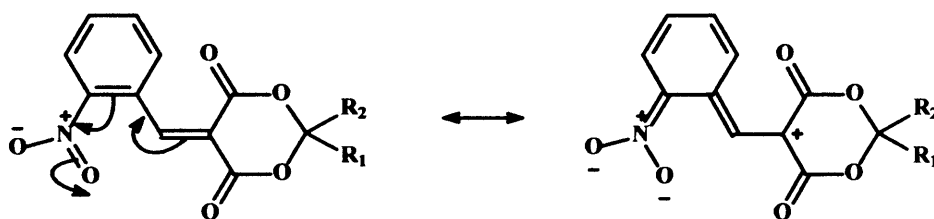
Figure 5 $^1\text{H-NMR}$ spectrum (400 MHz, CDCl_3) of **6**

Compound **6** was identified by $^1\text{H-NMR}$ spectroscopy of a deuterated solution of **6**. The second order nature of the methylene peaks was observed, also the singlet at 8.7 ppm attributed to the alkene proton was shifted downfield compared to the corresponding alkene proton in the *para* analogue **5** (Table 2), presumably, because of the proximity of the nitro group to the alkene, so the electron withdrawing effect was more acute. $^1\text{H-NMR}$ spectroscopy did not show any protic impurities regardless of the physical state of **6**. Mass spectroscopy showed a peak corresponding to the molecular ion (m/z 220) minus the nitrobenzylidene group (m/z 147), leaving a fragment presumably stabilised by the two carboxylate groups.

	5	6
H_8	8.00	7.42
H_{10}	-	7.60
H_9	8.25	7.68
H_{11}	-	8.24
H_7	8.40	8.76

Table 2 Relevant $^1\text{H-NMR}$ data for compounds 5 and 6

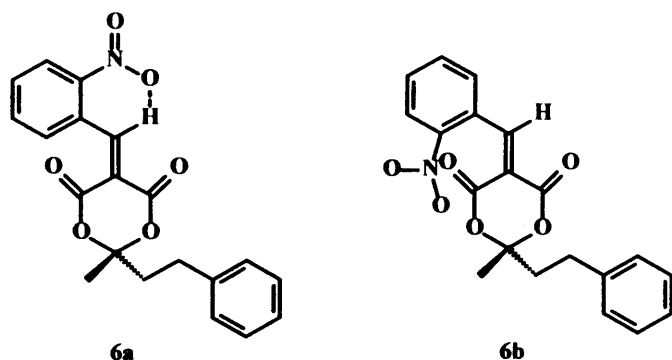
The free rotation along the single bond in the benzylidene malonate is probably restricted due to the *ortho* position of the nitro group. In addition, there is also a small contribution suggestive of a resonance form that can convert the single bond into a double bond (**Scheme 21**).



Scheme 21 Possible resonance form for 6

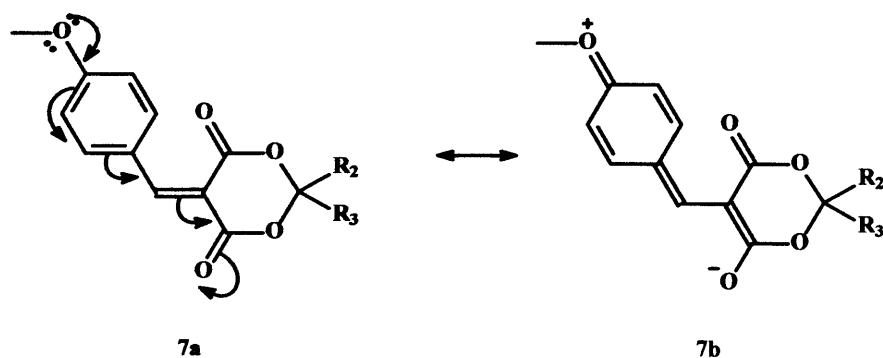
Due to partially double bond nature in the resonance form, the *o*-nitrophenyl ring is expected to be in the same plane as the malonate. Two possible conformations (**Scheme 22**), then, were expected, one conformation (the *s-trans* **6a**) being much more favourable (because of a possible six membered ring formed through $\text{C}(\text{sp}^2)\text{H}\cdots\text{O}$ hydrogen bonding – although not very common[†][19, 20]) than the other conformation (*s-cis* **6b**), which would imply seven atoms in the same plane without a ring closure.

[†] $\text{CH}\cdots\text{O}$ bonding is not commonly observed between proton of an sp^2 hybridised carbon belonging to an alkene and an heteroatom



Scheme 22 Two possible conformations for compound 6

The synthesis of 5-(4-methoxy-benzylidene)-2-methyl-2-(phenylethyl)-1,3-dioxane-4,6-dione **7** was carried out following the same procedure as the one used for the synthesis of **5**. The product of the reaction was a crystalline bright yellow solid. The colour of **7** is probably because of the “push-pull” nature of the substituents, polarising the system, *i.e.*, the conjugation of the system. Compound **7** contains an electron donating and an electron withdrawing group, which assists the movement of electrons towards the conformational resonance form (**7a** and **7b**) (**Scheme 23**). The high polarising effect of the charged resonance form (**7b**) explains the high crystallinity of **7**. This is in contrast to **5** and **6**, as they contain an electron withdrawing group (NO_2) and the movement of electrons is probably of less importance as the movement of electrons in compound **7** (**Scheme 21**).



Scheme 23 Resonance forms for compound **7**

The yield of the reaction was optimised up to 84 %. $^1\text{H-NMR}$ spectrum for **7** showed the expected singlet for the methoxy group at 3.8 ppm (**Figure 6**).

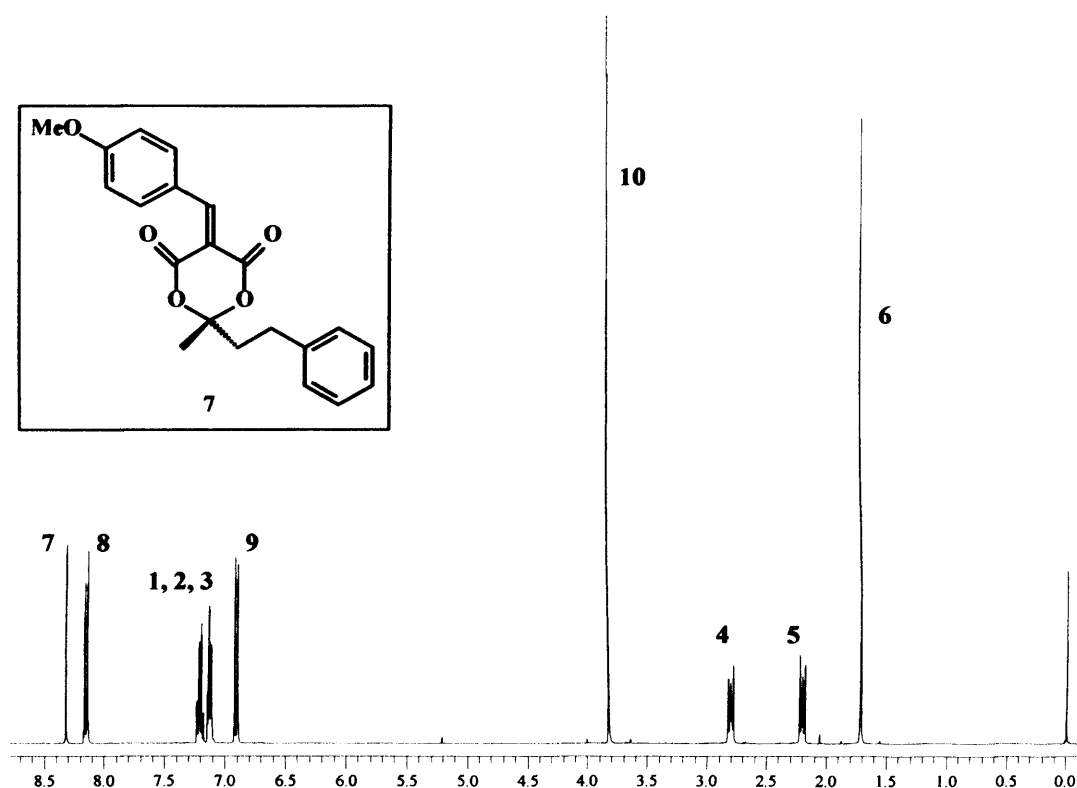


Figure 6 $^1\text{H-NMR}$ spectrum (400 MHz, CDCl_3) of 7

Mass spectrometric analysis of 7 showed that the molecule fragmented easily with peaks at m/z 105.1 (82 %), corresponding to the ethylbenzene group, and at m/z 91.1 (85 %) corresponding to the tropylium cation. In addition, a peak at m/z 148.1 (58 %) corresponding to 4-phenyl-2-butanone was observed. This susceptibility to fragmentation contrasts with compound 6, which fragmented to give 220 m/z (100 %) showing just the loss of the *o*-nitrobenzylidene group.

The different techniques used to analyse compounds 6 and 7 could explain the difference in the fragmentation pattern. 6 was analysed with APCI – chemical ionisation and 7 with EI – electronic ionisation. The substituents on the aromatic ring (6 – NO_2 , 7 – OMe) respond differently to these techniques and this would account for the interaction of the electronic effects observed.

As mentioned earlier in this section (see page 38), 7 was highly crystalline and single crystals suitable for X-ray diffraction were grown from an ethanol solution (Figure 7, Table 3). 7 crystallised in space group P21/a, which is an achiral space group. The structure consisted mainly of two planes perpendicular to each other (starting from the chiral centre). The lactone ring had an envelope shape, analogous to Meldrum's acid,^[21] with the methyl group occupying the pseudo-axial position and the 2-phenyl-

ethyl group occupying the pseudo-equatorial position (which is expected as it is more bulky).

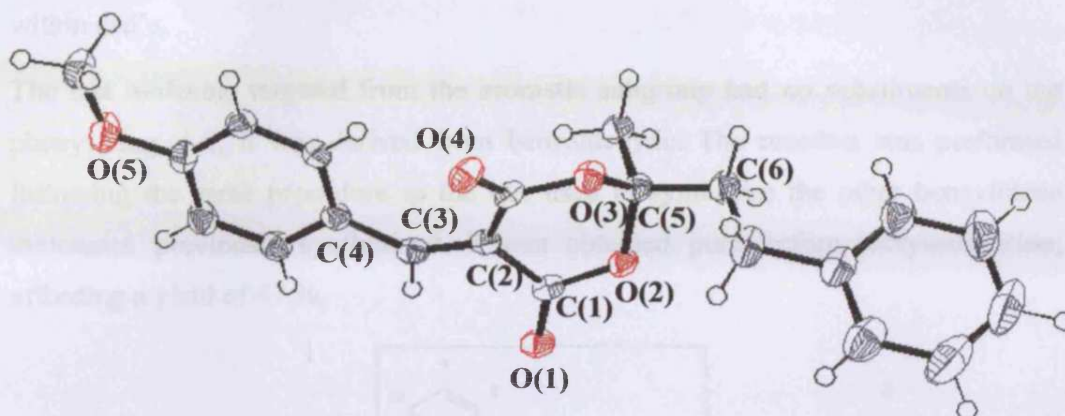


Figure 7 ORTEP^[22] view (50% probability) of crystal structure of compound 7

Empirical formula	C ₂₁ H ₂₀ O ₅
Crystal system	Monoclinic
Space group	P 21/a
Unit cell dimensions	a=9.6549(2) Å
	b=12.9703(3) Å
	c=14.7696(4) Å
	β=108.6430(10)°
Volume	1752.50(7) Å ³
Temperature	150(2)K
Final R indices [I>2σ(I)]	R1 = 0.0524, wR2 = 0.1052
R indices (all data)	R1 = 0.0899, wR2 = 0.1171

Table 3 Summary of data collection and processing parameters for compound 7

Bond	Distance (Å)
C(1)-C(2)	1.474(2)
C(2)-C(3)	1.359(2)
C(3)-C(4)	1.455(2)
C(5)-C(6)	1.513(2)

Table 4 Bond distances for compound 7

Similar to compound 6, there is a resonance form that would be favourable towards a plane containing the benzylidene and the malonate groups (Scheme 23). C-C distances in the crystal structure are summarised in Table 4, from which can be

appreciated that the bond C(2)-C(3) has more double bond character than the rest. Bonds C(1)-C(2) and C(3)-C(4) have also some double bond character, as they are shorter than bond C(5)-C(6) (single bond). These bond distances are not comparable within esd's.

The last molecule targeted from the aromatic subgroup had no substituents on the phenyl ring, *i.e.*, it was derived from benzaldehyde. The reaction was performed following the same procedure as the one used to synthesise the other benzylidene malonates previously synthesised. **8** was obtained pure before recrystallisation, affording a yield of 47 %.

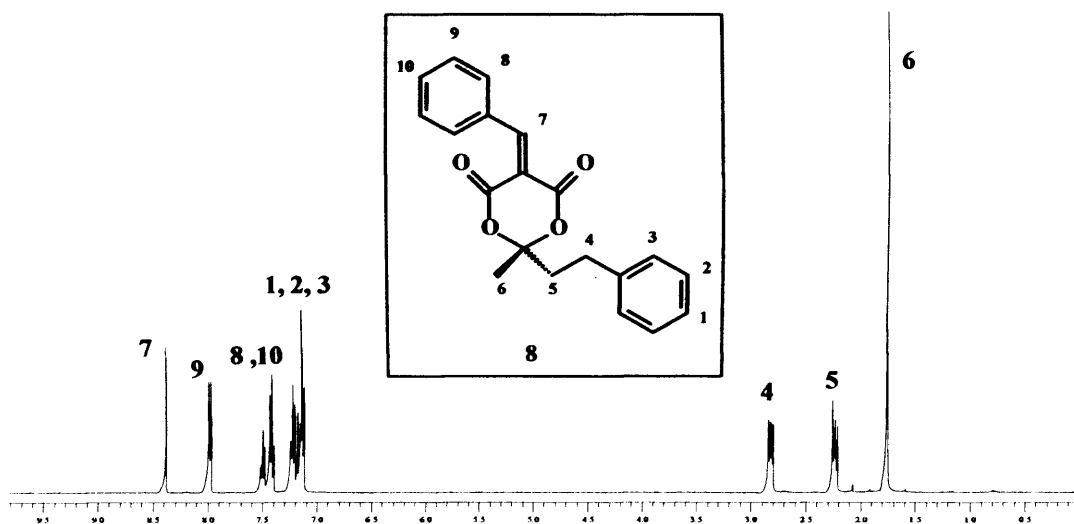


Figure 8 ¹H-NMR spectrum (400 MHz, CDCl₃) of **8**

The ¹H-NMR spectrum of **8** proved the proposed structure for the compound (Figure 8). The chemical shift for the olefinic proton on the ¹H-NMR spectrum was slightly lower than both *o*- and *p*-nitrophenyl analogues, but higher than the methoxyphenyl analogue (**7**) as would be expected given the electronwithdrawing effect of the substituent groups on the aromatic ring. The effect of the substituting groups on the olefinic proton is reported in Table 5.

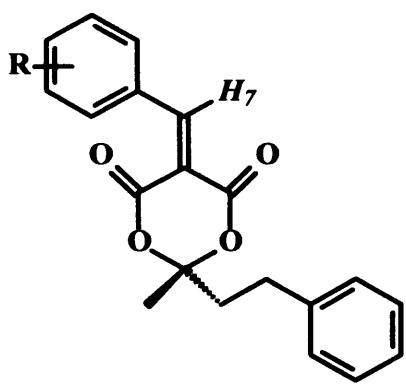
	<p>5</p> <p>(R = <i>p</i>-NO₂)</p>	<p>6</p> <p>(R = <i>o</i>-NO₂)</p>	<p>7</p> <p>(R = <i>o</i>-Me)</p>	<p>8</p> <p>(R = H)</p>
<i>H</i> ₇	8.40	8.76	8.35	8.39

Table 5 ¹H-NMR data for proton *H*₇ of compounds 5-8

Compounds 5-8 covered the range of electron donating, electron withdrawing and unsubstituted groups on the aromatic ring. In order to study also the effect of the conjugation of the aromatic ring to the alkene, one more compound containing an alkane (instead of an aromatic ring) was synthesised. The reaction was tried following route *b* and using 4 and isobutanal as starting materials.

The reaction time for the synthesis of 5-isobutylidene-2-methyl-2-(2-phenylethyl)-1,3-dioxane-4,6-dione **9** was longer than that required for compounds 5-8, presumably because the transition state of the last step of the reaction – *i.e.* the dehydration step – is less conjugated than for the benzylidene malonates, and therefore higher in energy than the transition states for compounds 5-8. The reaction was performed under the same conditions as the syntheses of 5-8, but also under dry nitrogen in order to avoid decomposition as the lower conjugation in the product could lead to hydrolysis. **9** was obtained in 50 % yield as a solid.

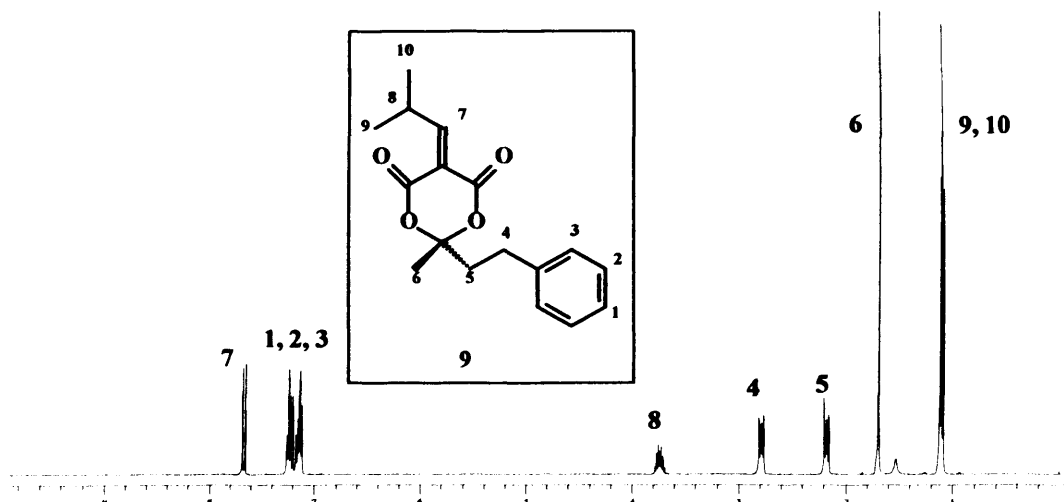


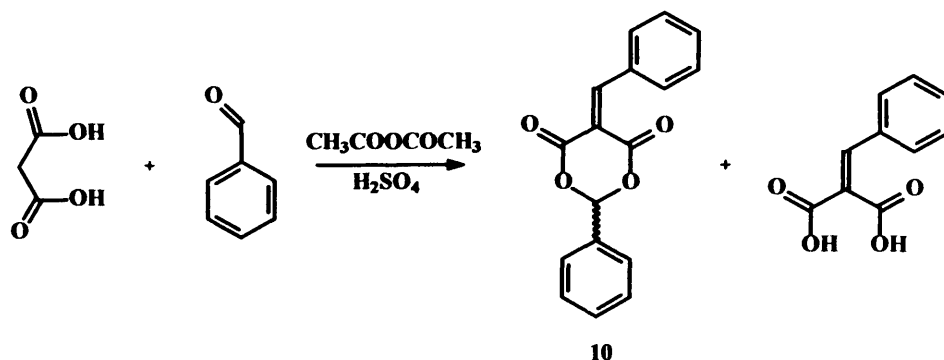
Figure 9 $^1\text{H-NMR}$ spectrum (400 MHz, CDCl_3) of **9**

The structure of **9** was confirmed by the distinctive $^1\text{H-NMR}$ spectrum (Figure 9). The chemical shift for the olefinic proton in the $^1\text{H-NMR}$ spectrum (7.7 ppm) is only affected by the two carbonyl groups conjugated to the double bond with no other groups present that could affect the chemical shift. This chemical shift is still high for an olefinic proton, which suggests that the main cause for the high chemical shift in the olefinic protons of compounds **5-9** observed is the conjugation with two adjacent carbonyl groups, and not the conjugation with the aromatic ring. In addition, for **9** the peak for the olefinic proton is a doublet, as it couples with the isopropyl proton.

2.2.2.3 Synthesis of 2-phenyl-1,3-dioxane-4,6-dione (**10**)

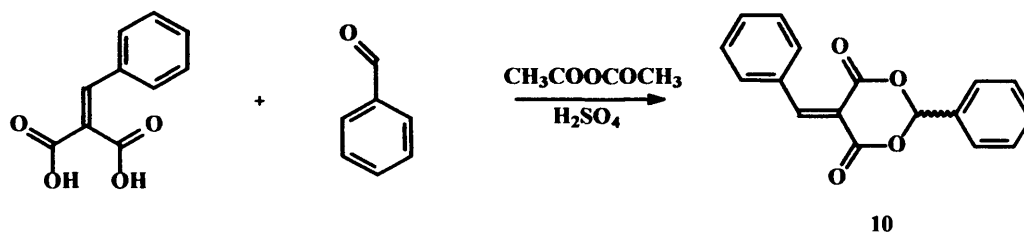
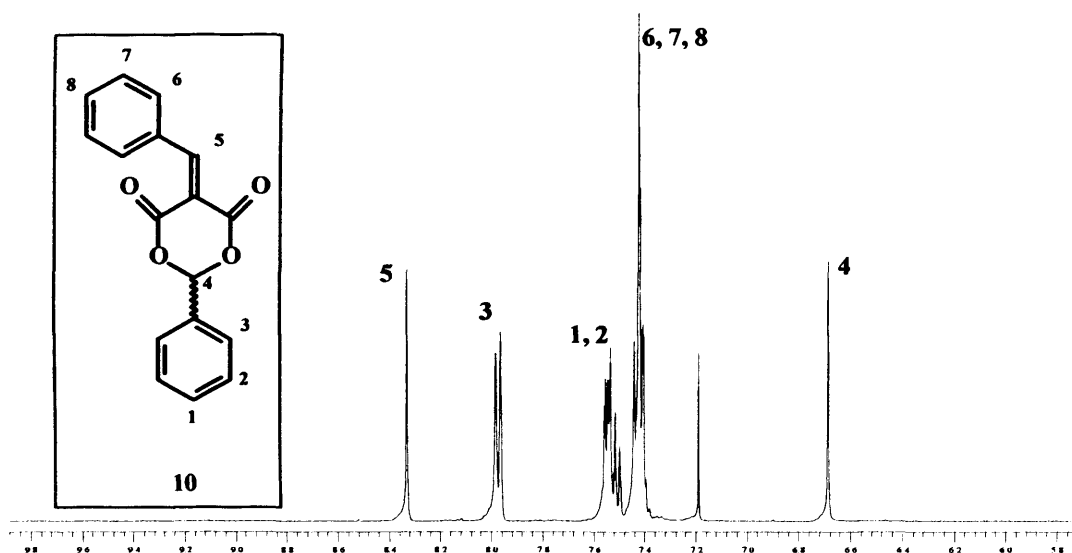
In order to obtain another “building block” (lactone ring) with a less bulky pseudo-chiral centre, the synthesis of another family of ketals was attempted, using an aldehyde instead of an acetone. Benzaldehyde was utilised in order to minimise any secondary aldol reactions. Initially, a condensation of malonic acid and benzaldehyde in a ratio 1:1 was attempted.

Unexpectedly, the product of the reaction was the double condensed 5-benzylidene-2-phenyl-1,3-dioxane-4,6-dione **10** (Scheme 24), although obtained in a very low yield (5%). The yield was presumably affected by the fact that the conditions of the reaction (acetic anhydride and sulphuric acid) were optimal for the formation of the ketal, rather than the Knoevenagel condensation. After carrying out the reaction with the corrected amounts of reactants, *i.e.*, two equivalents of aldehyde per equivalent of malonic acid, the yield was improved up to 21 %.



Scheme 24 Synthesis of 10

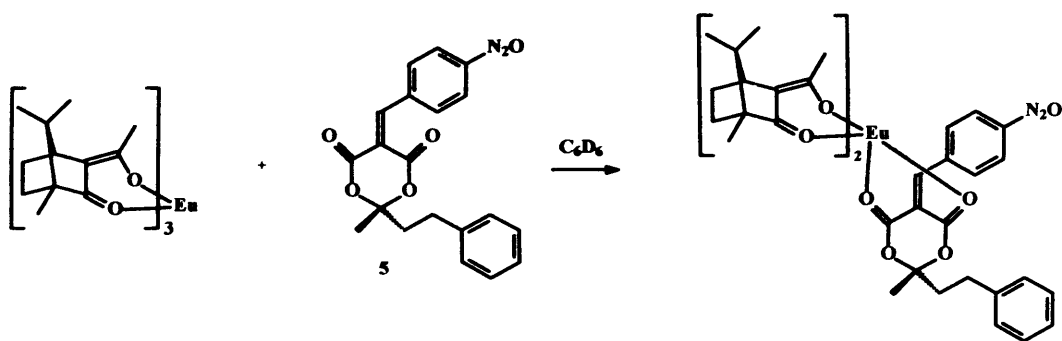
A major secondary product of the reaction was the diacid, which was not expected to be obtained under the reaction conditions. A further reaction of the diacid with benzaldehyde (following route *a*) afforded 10 in 38% yield as a solid (Scheme 25).

Scheme 25 Alternative route *a* to obtain compound 10Figure 10 $^1\text{H-NMR}$ spectrum (400 MHz, CDCl_3) of 10

The $^1\text{H-NMR}$ spectrum of 10 (Figure 10) proved the proposed structure as it showed all the peaks between the area of 6.5 and 8.5 ppm. No peaks were expected in the aliphatic area, and the non-aromatic hydrogen atoms could be easily identified as two singlets.

2.3 Determination of enantiomeric excess (e.e.)

Thus far, all the products synthesised were racemic because no chiral reactants were used. However, a method was needed that would enable the quantification of the enantiomeric excess for non-racemic samples. Samples of compounds **5**, **6**, **7** and **10** were analysed by HPLC using a chiral column, but all were retained in the column and therefore no e.e. could be quantified. An alternative method was then attempted, to form a coordination compound using compound **5** and the chiral shift reagent (CSR) Europium tris[3-(heptafluoropropylhydroxymethylene)-(+)-camphorate] (Scheme 26).



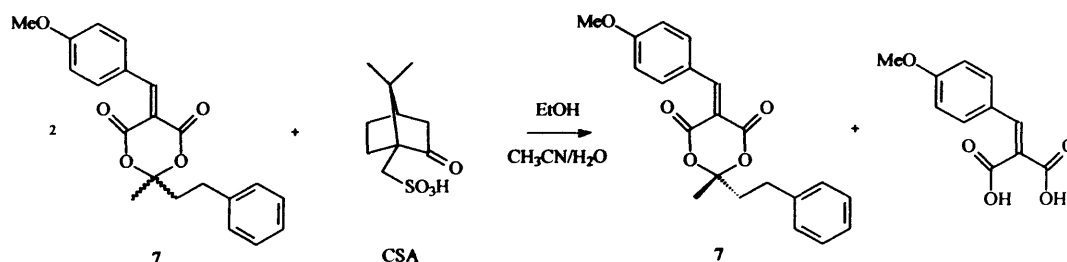
Scheme 26 Attempt of e.e. determination using a chiral shift reagent

Two diastereoisomers were expected to be formed with coordination of compound **5** to the chiral Eu complex through the oxygen of the carbonyl groups. The presence of two peaks for the proton at the double bond would confirm the formation of the diastereoisomers. The experiment was performed with different ratios of **5** and the CSR and different solvents ($CDCl_3$ and C_6D_6), but the spectra obtained presented very broad bands and a curvy baseline presumably because of the influence of Eu, which is relatively close to the protons, and the peaks correspondent to the diastereoisomers were not observed.

2.4 Deracemisation

Enantiomeric enrichment was then attempted by kinetic resolution, *i.e.*, reacting the mixture of enantiomers with a chiral reagent, D-(+)-camphorsulphonic acid (CSA). The aim was to hydrolyse the ketal (the chiral centre of the molecule) of only one of the enantiomers ideally, or hydrolyse the ketal of one enantiomer faster than the other enantiomer. This reaction was attempted with compound **7** in ethanol and an acetonitrile:water mixture (2:1) (Scheme 27). However, the amount of **7** hydrolysed

was negligible. This high stability to hydrolysis can be explained as a consequence of the high rigidity in the benzylidene malonate skeleton, which might have an influence on the acetal opening reaction opposite to the low rate of reaction for the formation of the product when diacid is used as starting material (Section 2.2.1).

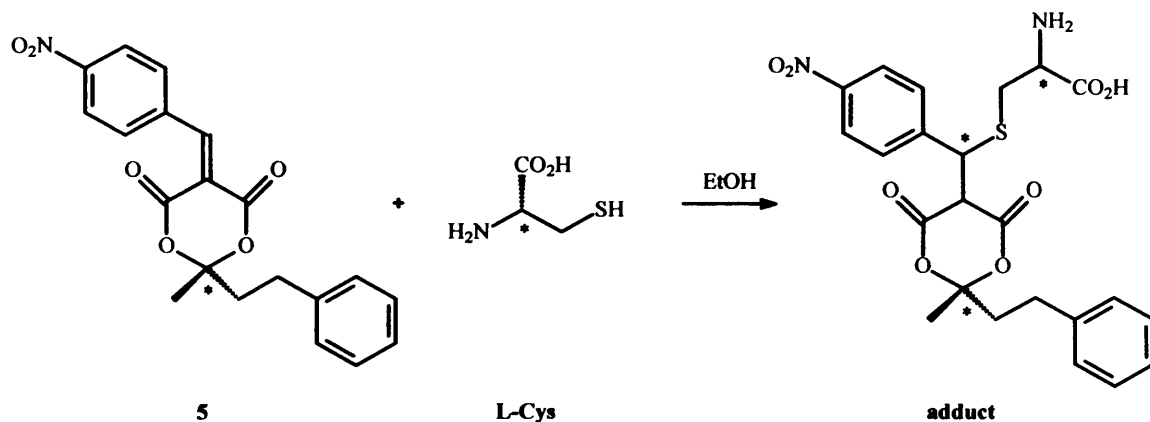


Scheme 27 Expected deracemisation using chiral reagent D-(+)-CSA

2.4.1 Deracemisation *via* Michael addition

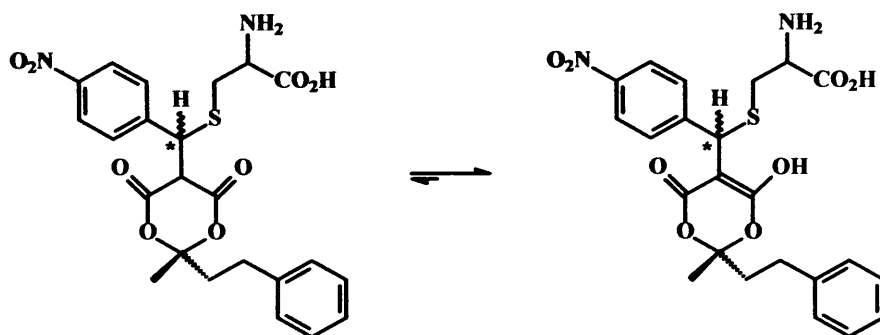
The next approach to deracemisation was through a reaction of the double bond with a chiral reagent. The alkene is electronic deficient because it is conjugated to two carbonyl groups, and thus a perfect candidate for a Michael addition. The nucleophile had to be chiral, and initially two amino acids (L-cysteine and L-leucine Me-ester) were selected. The main focus of the reaction was to recover the product that did not react *i.e.*, the least reactive enantiomer, as it would be partially or totally deracemised when isolated from the reaction mix. Thus, the reaction was attempted with only half an equivalent of the selected amino acid, expecting the reaction rate to be higher for the enantiomer that had the least hindered diastereoisomeric transition state, allowing kinetic resolution (The general procedure applied for deracemisation *via* Michael Addition is described in Scheme 28).

The product of the reaction would be an adduct that contains three chiral centres (Scheme 28). The chirality of the amino acid is already determined and presumably not be affected during the reaction, and therefore the predicted number of diastereoisomers is four. There are two possible products from the Michael addition: the kinetic (the first to be formed) and the thermodynamic (the most stable), however, it is not possible to predict their respective formation rates. In order to optimise formation of the kinetic product, short reaction times were necessary, as the appearance of the thermodynamic product would imply that the reaction had reached equilibrium and a kinetic resolution was required.



Scheme 28 Deracemisation of **5** using L-Cys as nucleophile *via* a Michael addition

The first attempt was performed with compound **5** and L-Cys (**Scheme 28**), as sulphur is typically a better nucleophile than nitrogen in Michael addition reactions. The reaction was performed in ethanol, even though neither of the reactants were very soluble, but a solvent that dissolved both reactants could not be found. The reaction was also performed at room temperature in order to avoid any thermal racemisation of the product. From the crude reaction mixture two main diastereoisomeric products of the Michael addition were obtained in the enol form and were distinguished by $^1\text{H-NMR}$ spectroscopy. The former alkene proton had shifted from 8.41 ppm to 5.50 ppm and 5.40 ppm in each diastereoisomer respectively. The fact that the peaks at 5.50 ppm and 5.40 ppm were singlets in the $^1\text{H-NMR}$ spectrum confirmed that they were not coupled to any other proton, therefore the two carbonyl groups were now an enol conjugated to a carbonyl (**Scheme 29**). A shift in the position of the aromatic protons from 8.3 ppm to 8.15 ppm, and from 8.10 ppm to 7.85 ppm was also observed (**Figure 11**).



Scheme 29 Tautomeric equilibrium of the adducts obtained after Michael addition

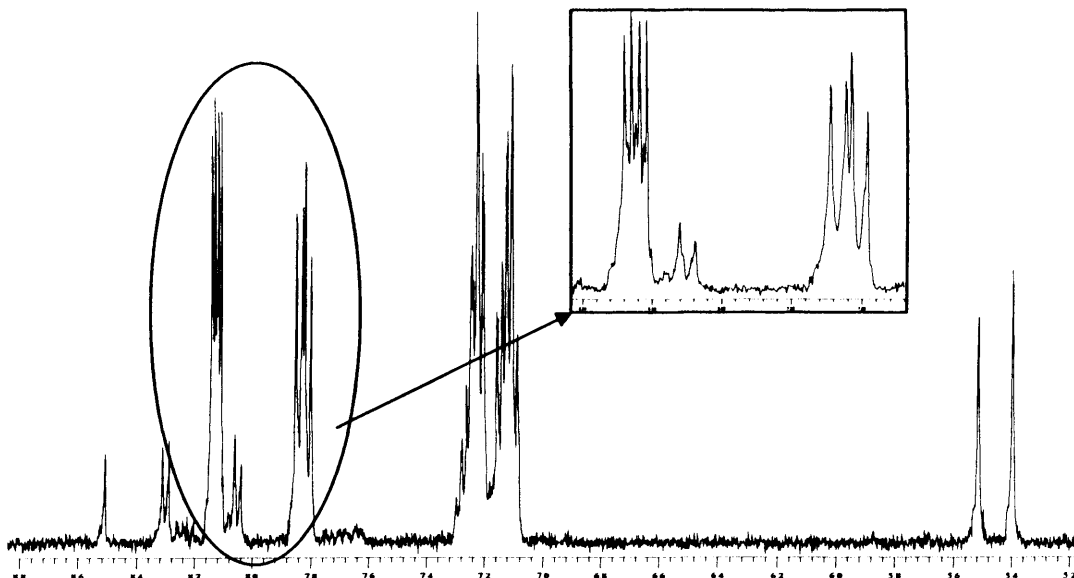


Figure 11 Part of the $^1\text{H-NMR}$ spectrum (400 MHz, CDCl_3) of the Michael addition adduct. By integrating the signals for the enolic proton, which is a singlet and is not overlapped with any other peak, would be possible to know the diastereoisomeric ratio of the reaction. Integration of the singlets at 5.40 ppm and 5.50 ppm allowed the isomer ratio to be calculated giving a ratio of 1.0:1.1. However, a very small ratio of diastereoisomers does not mean that the deracemisation was not successful. If the rate of *cis-trans* isomerisation of the alkenes was much slower than the rate of epimerisation of the adducts (because the proton of the new chiral centre is α - to a *p*-nitrobenzene group and a sulphur atom, making it relatively acidic), it could be possible that the starting material left in solution was enantiomerically enriched even though the observed ratio of product diastereoisomers is close to 1:1. The enantiomeric enrichment of both the solid and the mother liquid was measured in a polarimeter, obtaining an observed optical rotation. The optical rotation then is standardised to the specific rotation $[\alpha]_D$, defined as the observed optical rotation α_{obs} when light of 589 nm is used with a sample path length l measured in dm and a sample concentration c in g/100 mL, and multiplied by 100 (**Equation 1**).

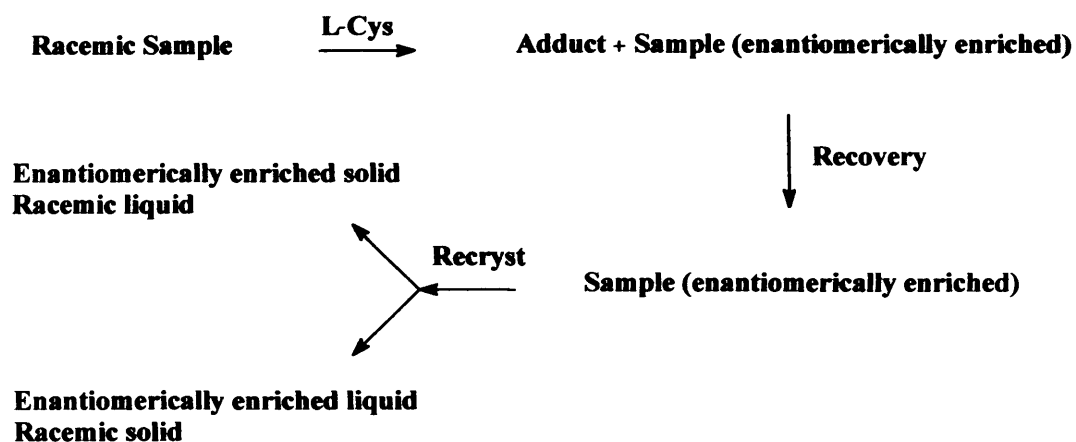
$$[\alpha]_D = \frac{\alpha_{\text{obs}}}{l \times c} \times 100$$

Equation 1 Standard optical rotation

When optical rotation is expressed in this standard way $[\alpha]_D$ is a physical constant characteristic of each optically active compound. Specific rotations of some organic molecules are summarised in **Table 6**.

Compound	$[\alpha]_D$ (°)
Camphor	+44.6
(S)-Glyceraldehyde	-8.7
L-alanine	+8.5
L-cysteine	+8.75

Table 6 Specific rotations of some organic compounds



Scheme 30 General procedure for deracemisation via Michael addition

As α_{obs} and $[\alpha]_D$ can be related to e.e., one method for e.e. determination was to find an $[\alpha]_D$ value for each compound 5-10 and then compare it to α_{obs} obtained in CPL experiments to determine the e.e. of the product.

2.4.2 Optical activities for compounds 5-10

To test the possibility that deracemisation occurred, unreacted 5 had to be recovered and its optical rotation measured. The sample could not be recrystallised using heating, nor could it be distilled because the heat might affect the optical purity of the alkene, therefore recovery of a pure sample of compound 5 was very difficult to achieve. The method used was to evaporate the solvent, dissolve the resultant solid in DCM (in order to precipitate both the adduct and any traces of L-Cys that had not reacted), filter, dry with MgSO_4 and collect 5 by evaporation. Even then, the product was still impure.

The reaction was repeated several times, and **5** was recovered pure from a small number of samples. When the optical rotation was measured, occasionally the observed optical activity had a value of $\approx 0^\circ$, implying that the deracemisation had not worked. However, on other occasions an optically active product was recovered implying that an unidentifiable key factor that was at work would determine whether the reaction would occur or not. Thus, the reaction was observed to work randomly, but whenever optical rotation was observed, it always had a negative value. Negative optical rotation was an indication that the deracemisation had succeeded, as the optical rotation measured could not be traces of L-Cys, because it has an optical activity of $+8.75^\circ$.

The deracemisation using L-Cys as nucleophile was also attempted on compounds **6-10**, with the same pattern being observed. In addition, all the samples were very difficult to recover pure, but whenever optical rotation was observed it always had a negative value.

The highest optical activity observed for compound **6** was of $[\alpha]_D -43.33^\circ$. At this stage, the e.e. of the product was unknown, as optical activity is a qualitative measure, given that the specific rotation is unknown. An attempt was made to recrystallise the sample, to see whether crystal packing phenomena could enhance the e.e. in the solid state, leaving the minor enantiomer in solution. After three consecutive recrystallisations, no alteration of the optical activity of filtrate or solid product was observed. This could mean either the sample was already 100 % enantiomerically pure, or the recrystallisation had no effect on the enantiomeric enrichment.

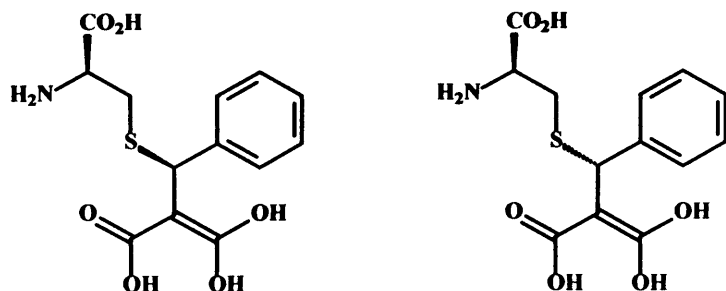
Compound **7** reacted slower with L-Cys than compounds **5**, **6** and **10**, probably because the resonance effect due to the methoxy group rendered the double bond less electrophilic than the alkene in **5** and **6**. Therefore, more time for this reaction was required and this probably enhanced the formation of the thermodynamic product. The reaction was attempted several times and no optical activity was observed. Eventually one sample displayed optical activity, and $^1\text{H-NMR}$ spectrum confirmed that the sample was pure, proving kinetic resolution had occurred. The average value of $[\alpha]_D$ was -4.2° . This value seemed very low, so assuming that this indicates a low e.e., attempts were made to deracemise **7** with L-leucine methyl ester in an effort to improve kinetic resolution. The reaction was performed several times and was

always found to be even slower than when L-Cys was employed, and no adduct formation could be observed. The L-Leu methyl ester was then discarded as a Michael addition nucleophile. The deracemisation of compound **10** was successful in the majority of attempts, probably because this is the compound with the least hindered double bond, and gave values of $[\alpha]_D$ up to -3.63° . Compound **10** was also recrystallised, in order to enhance the e.e., but no effect due to recrystallisation was observed on the $[\alpha]_D$.

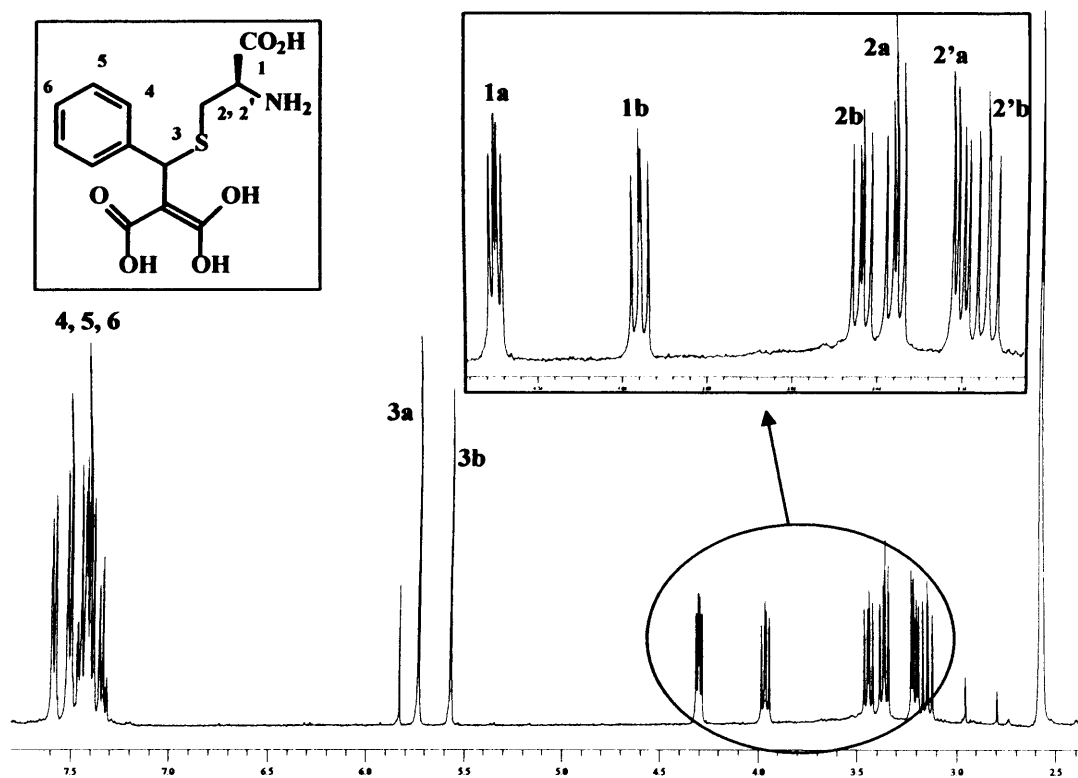
Compound	$[\alpha]_D$ ($^\circ$)
5	-3.4
6	-43.3
7	-4.2
8	0
9	0
10	-3.6

Table 7 Maximum optical activity observed for compounds **5 - 10**

Two diacids derived from the two possible adducts formed during the deracemisation of **10** were isolated in a mixture 1.0:1.2 (Scheme 31). The ketal underwent hydrolysis either during the reaction or the isolation process, as the reaction was performed in ethanol (which probably contained some water), and the isolation process involved an extraction with an aqueous phase. In addition, L-Cys contains two relatively acidic protons that could assist in the ketal ring opening. The corresponding peaks for each diastereoisomer were identified in the $^1\text{H-NMR}$ spectrum with the help of the coupling constants and integration, although it was not possible to assign these to each compound (Figure 12). This easy hydrolysis of the cyclic malonate esters after Michael addition is further support of the theory that rigidity of alkylidene malonates protects against hydrolysis, and prevents ring closure.



Scheme 31 Diastereoisomers of the diacids obtained after the Michael addition to 10

Figure 12 $^1\text{H-NMR}$ spectrum (400 MHz, CDCl_3) for mixture of diacids 10a and 10b

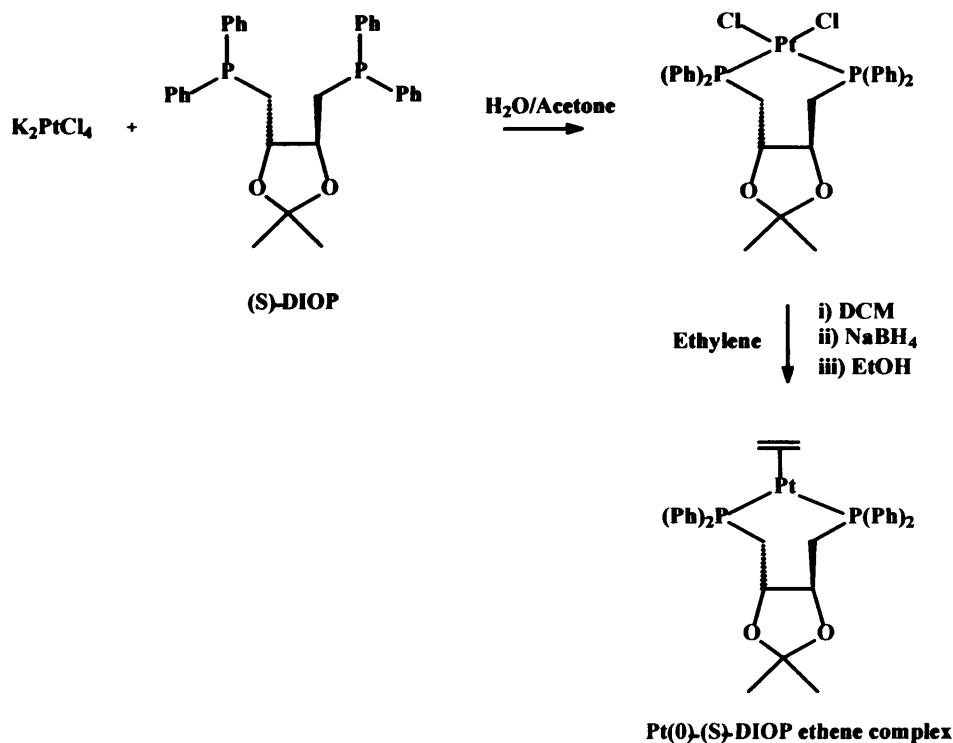
An attempt was made to deracemise compounds 8 and 9 with L-Cys, but the reactions were not successful. The non-reproducibility of all of the reactions could be due to the low solubility of the reactants in ethanol, or to the amount of water present in the solvent, which could have a major role on the speed of the reaction. The reaction was then performed in a biphasic system, $\text{H}_2\text{O}/\text{DCM}$, expecting complete dissolution of both reactants, allowing the reaction to take place at the interface between the two solvents at faster rate than in the previous attempts. This reaction rate was tested with compound 6 with rapid stirring, to allow as much contact as possible between the two phases. The phases were then separated and each solution

was evaporated and the resultant solid was analysed by $^1\text{H-NMR}$ spectroscopy. Unexpectedly, there was no evidence of reaction, and the amount of product identified in the aqueous layer was negligible. The optical activity of the benzylidene malonate was measured, however the value was 0° . The amounts of reactants recovered at the end of the reaction were weighed, and were consistent with the assumption that no reaction had occurred.

The same reaction in a biphasic system was then repeated but with the addition of the catalyst transfer agent $[\text{N}(n\text{-Bu})_4]\text{I}$, which could assist the movement of ions between phases, therefore improving the activity. This reaction was performed on compounds **6** and **10**, and the results showed that no enantiomeric enrichment was observed, nor the formation of the adduct. In summary, no repeatable protocol for deracemisation could be developed and no rationale for the factors involved could be proven. Thus, another method to measure e.e. was investigated.

2.5 e.e. determination using Pt(0)-(S)-DIOP ethene

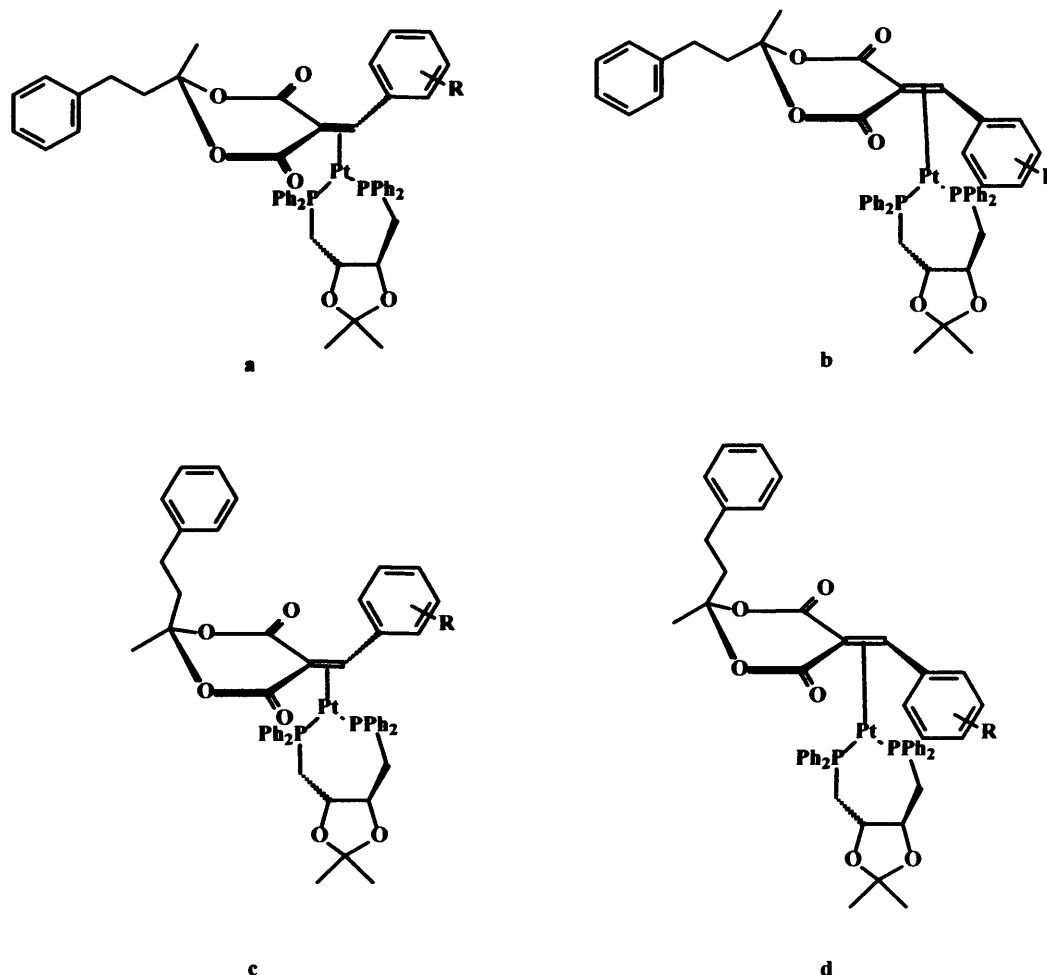
Another attempt to quantify enantiomeric excess was performed following a method developed by Parker and Taylor,^[23] using a Pt(0)-(S)-DIOP ethene complex synthesised according to the literature procedure (Scheme 32).^[23] Displacement of the ethene ligand by a chiral η^2 -donor (in excess) is the basis of the process, with the ratio of the resultant diastereoisomers being analysed by $^{31}\text{P-NMR}$ spectroscopy. The advantage of the method is that $^{31}\text{P-NMR}$ chemical shift dispersion is large, therefore the diastereoisomeric peaks can be easily integrated. The disadvantage is that the coupling between ^{31}P (spin 1/2) and Pt (33 % ^{195}Pt (spin 1/2)) could make spectra difficult to assign.



Scheme 32 Synthesis of Pt(0)-(S)-DIOP ethene complex

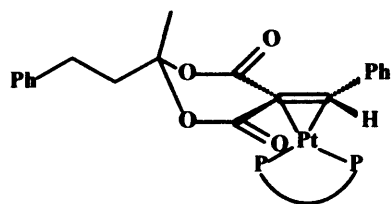
The Pt(0)-(S)-DIOP ethene complex contains two equivalent phosphorous nuclei due to the C_2 symmetry present in the molecule. However, when the ethene is substituted by a benzylidene malonate, the resultant product contains two non-equivalent phosphorous nuclei, each of which is expected to couple to 33 % of the platinum nuclei, with a large coupling constant (typically $J \approx 3500$ Hz), and to the other phosphorous atom, with a smaller coupling constant (typically $J \approx 60$ Hz)^[23]. Also for the non-spin active platinum, only coupling between the phosphorous nuclei is expected. Thus, the spectrum of Pt(0)-(S)-DIOP coordinated to any of the benzylidene malonates previously synthesised was expected to show two doublets of doublets with a large coupling constant (due to P-Pt coupling) and a small coupling constant (due to P-P coupling), and two doublets with a small coupling constant (due to P-P coupling) for each diastereoisomer.

The benzylidene malonates have an axially pseudo-chiral centre, therefore two enantiomers were present as a racemic mixture, also, considering that the platinum complex can be coordinated by either face of the double bond, the total number of expected diastereoisomers was four (**Scheme 33**).

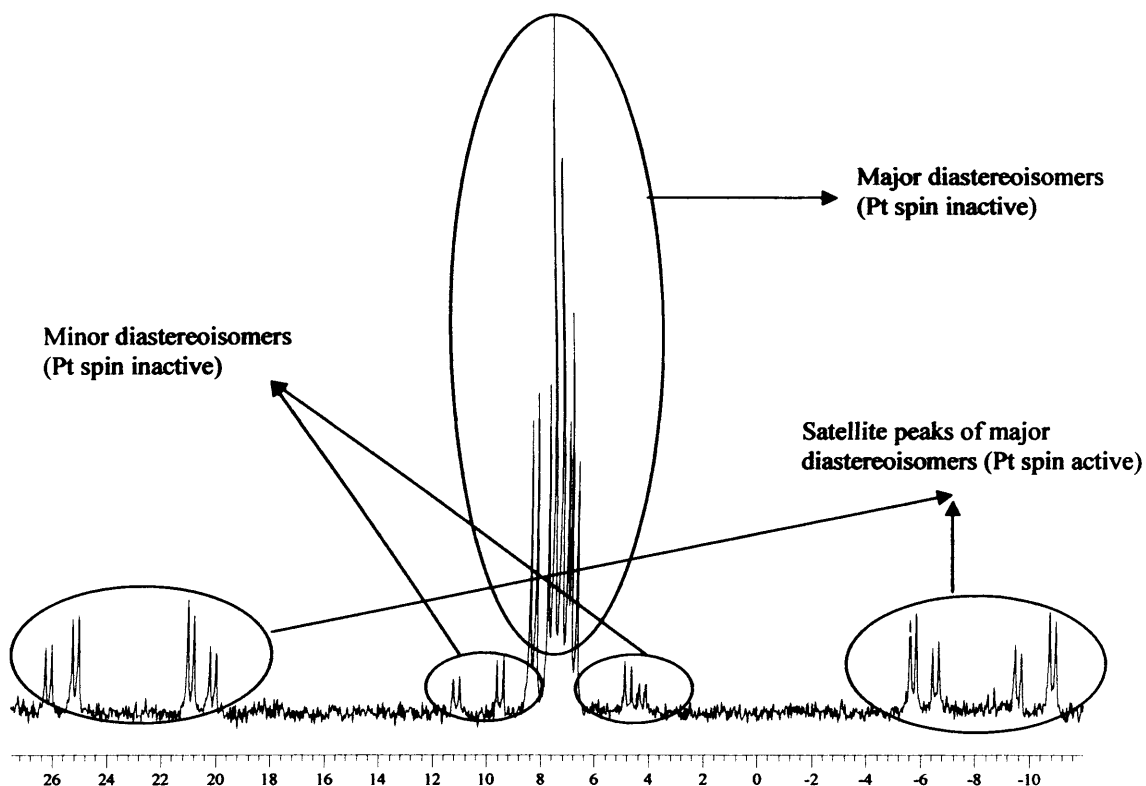


Scheme 33 Possible diastereoisomers after coordination of of Pt(0)-(S)-DIOP ethene complex with benzylidene malonates

The displacement reaction was performed on an NMR scale and followed by proton-decoupled ^{31}P -NMR spectroscopy. The reaction was first attempted on a sample of compound **5** which had not been previously deracemised. In the ^{31}P -NMR spectrum 32 peaks were observed (**Figure 13**), 16 being in the central region (centred at 7.5 ppm) and the other 16 were divided in two groups of what appeared to be doublets of doublets at around -8 ppm 23 ppm respectively. The group of peaks centred at 7.5 ppm corresponded to the complexes containing the non-active spin Pt, therefore the two doublets present in this group represented the signals from one diastereoisomer. Also, two major diastereoisomers were assigned within the central region of the spectrum with a ratio of 1:10 approximately.



Scheme 34 Pt-DIOP complex coordinated to the less hindered face of the double bond

Figure 13 ^{31}P -NMR spectrum of compound 5 coordinated to Pt-DIOP

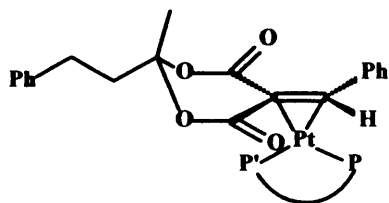
In order to assign the satellite peaks (spin active Pt), and therefore measure $^{\text{P-Pt}}J$ and $^{\text{P}'\text{-Pt}}J$, the central peaks with the non-active Pt were taken as reference. These assignments are summarised in Table 8.

Diastereoisomer	δ_{P} (ppm)	$\delta_{\text{P}'}$ (ppm)	$^{\text{P-Pt}}J$ (Hz)	$^{\text{P}'\text{-Pt}}J$ (Hz)	$^{\text{P}'\text{-P}}J$ (Hz)
major	7.62	7.12	27	3228	4362
minor	8.28	6.77	27	4326	3231

Table 8 ^{31}P -NMR data for the main diastereoisomers of the DIOP-Pt complex coordinated to 5

The coupling constants for P-Pt and P'-Pt had noticeably different values, which is assumed to be due to the *trans* influence.^[28, 29] As the platinum centre was expected

to have a square planar geometry, then the two phosphorous atoms would be *trans* to different groups, *i.e.*, one being *trans* to the carbon adjacent to the aromatic ring, and the other phosphorous being *trans* to the carbon next to the carbonyl groups (Scheme 35). The carbon adjacent to the carbonyl groups should have a more π -acidic nature than the carbon next to the aromatic ring. Thus, the *d* orbitals of platinum would back donate more electron density into the π^* orbitals of the carbon adjacent to the carbonyl groups. This would affect the phosphorous atom *trans* to this carbon, as the σ -bonding would also be affected, because the Pt-P bond would then have less *s* character. Therefore, there would be less interaction of the nuclear spins with the electrons in the Pt-P bond and the coupling would be smaller.



Scheme 35 P is *trans* to the carbon α to the carbonyl group and P' is *trans* to the carbon adjacent to the aromatic ring

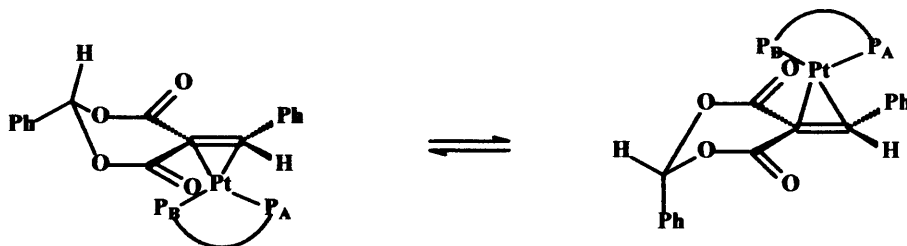
The value of $^{P-P'}J$ was much smaller (27 Hz) than the ones reported in the literature for similar complexes (from 59 Hz to 72 Hz). This could also be ascribed to the *trans* influence, for the same reason as stated above - one of the P-Pt bonds would be poorer in σ character and this could possibly affect the coupling between the two phosphorous atoms. The difference in coupling constants for the ^{P-Pt}J was unlikely to be linked to the P-Pt-P angle, as both phosphorous atoms were part of the same ligand, so they did not have free movement and the geometry was expected to be similar to literature values.^[23] The mass spectroscopy analysis (low resolution ES) confirmed that the product obtained was the expected one, showing a very similar theoretical and observed pattern for the isotope models $[M+H]^+$ and $[M+Na]^+$.

The difference in ratio between diastereoisomers was probably due to the coordination of the platinum complex to either of the two faces of the double bond. Assuming the malonate ring has an "envelope" type conformation (as found in most of the analogues),^[24-27] then the most bulky group would be in a *pseudo*-equatorial position and the least bulky group (methyl group) would be in a *pseudo*-axial position. This would protect one of the faces of the double bond, leaving the face with the ethylphenyl group the most available to platinum coordination. Thus, the

platinum complex was assumed to be coordinated mainly on the face with the ethylphenyl group (Scheme 34), *i.e.*, diastereoisomers **a** and **b** (Scheme 33).

A one to one ratio of signals derived from coordination of both enantiomers was expected for compound **5**, as little kinetic resolution was expected.^[23] Nevertheless, the major diastereoisomers were in a ratio of 1:1.2 (Figure 13), showing some kinetic resolution had occurred. However, this did not preclude use of this method for *e.e.* measurements. The spectrum obtained in Figure 13 was therefore used as a reference for when the same reaction was performed with deracemised **5**. In this way, any changes in the ratios would allow calculations of the *e.e.* to be carried out.

When the ligand substitution reaction was performed with compound **10**, a high degree of kinetic resolution was clearly seen, as just two doublets were observed in the ³¹P-NMR spectrum, at 10.88 ppm and 6.84 ppm. As compound **10** has just one bulky group this was expected to occupy the *pseudo*-equatorial position, with minimal contribution from the other possible conformer. Thus, more preference for coordination to only one side of the double bond was anticipated with a more marked degree of kinetic resolution (Scheme 36). Thus, the platinum complex would probably coordinate to the face opposite the one containing the axial group. The spectrum showed the presence of some Pt(0)-(S)-DIOP chloride (large singlet at 27.41 ppm), which interfered with the satellite peaks of platinum. Not all the product dissolved, so there was the possibility that one of the enantiomers crystallised when coordinated to Pt-DIOP, rather than showing kinetic resolution. As apparently almost all the Pt(0)-(S)-DIOP ethene preferentially coordinated to one of the enantiomers in a racemic mixture in solution, suggested that it was not a good candidate for the determination of the enantiomeric excess of compound **10**.



Scheme 36 Conformational equilibrium of coordinated Pt-DIOP to benzylidene malonate **10**

When the coordination reaction was performed with compound **6**, an extra challenge arose; the nitro group could be on either side of the double bond, increasing the

number of possible diastereoisomers to eight (implying a possible 96 peaks in the ^{31}P -NMR spectrum). Nevertheless, as discussed in Section 2.2.2.1, the *o*-nitro group was expected to be hydrogen bonded to the double bond proton, so the aromatic ring was likely to show hindered rotation, thereby reducing the number of possible diastereoisomers likely to form.

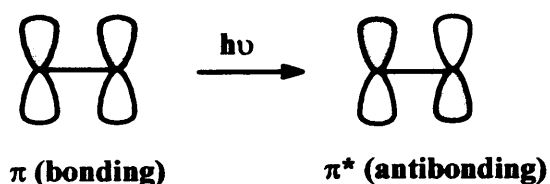
Analysis of the reaction mixture after attempted coordination revealed three groupings of signals. The central part of the ^{31}P -NMR spectrum centred at 8.82 ppm (*i.e.* non-Pt coupled) showed ten clear peaks, however an eleventh peak appeared to consist of two overlapping signals, judging by peak heights. This implied that only three of the eight possible diastereoisomers were observed. The rest of the spectrum was composed of two groups of sixteen peaks centred at 23.15 and -7.67, evidence that four diastereoisomers could be distinguished. The ratio between diastereoisomers was approximately 2:2:1:1. The same procedure applied to compound 5 in order to correlate the satellite peaks was also attempted for compound 6, but in this case no conclusions could be derived from the spectrum because of the similarity and overlap of the central area peaks.

The complexation of benzylidene malonates to Pt(0)-(S)-DIOP ethene was then tested for *e.e.* quantification, but there were hardly any deracemised alkylidene malonates available (they decompose with time and deracemisation was not reproducible, as discussed in Section 2.4). A sample of deracemised 6 was available, but only very low optical activity was recorded. As a test, 100 mg of partially deracemised compound 6 was coordinated to Pt(0)-(S)-DIOP ethene. Compound 6 had an optical rotation of $[\alpha]_{\text{D}} -2.63^\circ$ and after coordination to the platinum complex ^{31}P -NMR spectrum was acquired and the result was exactly the same as the spectrum for the racemic sample. It is possible that the enantiomeric excess was too small to be detected by any difference in the integration area.

In summary, the attempt of *e.e.* quantification using Pt(0)-(S)-DIOP ethene led to the formation of two new complexes, and showed some kinetic resolution in the complexation process. The conclusion was that this was not a good method to quantify the enantiomeric excess for any of the compounds attempted when the optical activity presented before coordination was small.

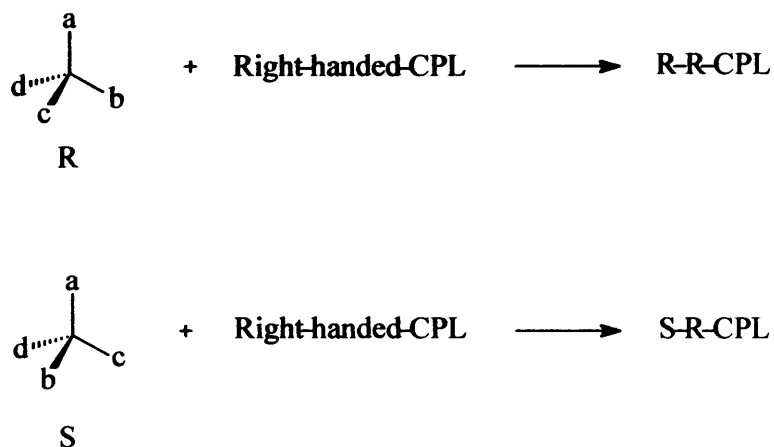
2.6 Studies with Circularly Polarised Light (CPL)

Irradiation of compounds **5-10** with UV light was expected to excite an electron from a π orbital to a π^* orbital transforming the double bond into a di-radical single bond (**Scheme 37**). Thus, the former double bond would have free rotation until the electron returned to the π orbital, allowing racemisation to occur.



Scheme 37 Transformation between π and π^* bonds

If the compound was irradiated with UV CPL then a slight increase in the proportion of one of the enantiomers was expected. CPL is chiral therefore a diastereoisomeric interaction would be expected from a mixture of different enantiomers depending on the polarisation of the CPL (**Scheme 38**). This would imply different transition states for the interaction of each enantiomer with CPL, which would have different energies, as discussed in **Section 1.4.1**. Therefore, one of the enantiomers would be expected to racemise faster than the other, giving an excess of the slower-reacting enantiomer. Or, stated in different terms, the enantiomer with the higher extinction coefficient for that form of CPL will be more efficiently excited, and thus racemise faster, giving an excess of the less-adsorbing enantiomer.



Scheme 38 Diastereoisomeric relation between R and S enantiomers and CPL

Prior to testing the effect of CPL on compounds **5-10**, the effect of UV irradiation was investigated on some deracemised benzylidene malonates. A sample of 217 mg

of **10** in 2.7 mL of DCM in a quartz cuvette that initially showed $[\alpha]_D -3.61^\circ$ was irradiated at 365 nm for 30 min, and the optical activity checked every 5 min. No changes in the optical rotation were observed, therefore the sample was then irradiated at 254 nm for another 30 min. As higher energy radiation would affect the double bond, a change in the optical activity was expected, but a reduction of 0.36° to $[\alpha]_D -3.25^\circ$ was observed, suggesting that photoracemisation of **10** at 365 nm and 254 nm is slow. The UV spectrum of **10** presented a minimum absorbance at 250 nm (with an extinction coefficient ϵ $1832 \text{ M}^{-1}\text{cm}^{-1}$), which explains why there was no re-racemisation at this wavelength. Also at 365 nm the absorbance was relatively low ($\epsilon = 3141 \text{ M}^{-1}\text{cm}^{-1}$). However, at 321 nm the absorbance presented a maximum with an extinction coefficient ϵ $19682 \text{ M}^{-1}\text{cm}^{-1}$. Therefore, the irradiation of compound **10** under a broad band of UV should be effective at racemisation.

An alternative test was carried out for compound **6**, that involved checking the sample for any racemisation at 365 nm. An initial $[\alpha]_D$ value of -10.0° was recorded, with no changes observed to the optical activity after irradiation with UV at 365 nm for one hour. Heating a sample of **6** at 60°C for 6 hours measuring any thermal racemisation, showed that the process was also unsuccessful. The sample was then subjected to broad-band irradiation (from 700 to 200 nm) for 20 h, as the UV spectrum for compound **6** presented low absorbance at 365 nm. Unfortunately, this led to decomposition. The racemisation was attempted again under broad-band irradiation, again with decomposition. The sample was then irradiated with UV (from 200 to 400 nm) and visible light (using an IR radiation blocking). No signs of decomposition were seen, although no observable racemisation that could be detected the polarimeter had occurred.

An alternative method discussed by Wyman *et al.* was reported to assist racemisation (and deracemisation with CPL) through the use of iodine.^[30] This method decreased the HOMO-LUMO gap, therefore assisting in the racemisation of the double bond. Two reactions were then performed with compound **6** in acetone (acetone can promote a *cis-trans* isomerisation by a biradical mechanism)^[31] and 20 % mol of iodine. The aim was to compare the reaction with a blank. Thus, both reaction vessels were covered in aluminium foil. One reaction was irradiated with the whole spectrum of UV-CPL, the other reaction was stirred in the dark. After 24 h, the

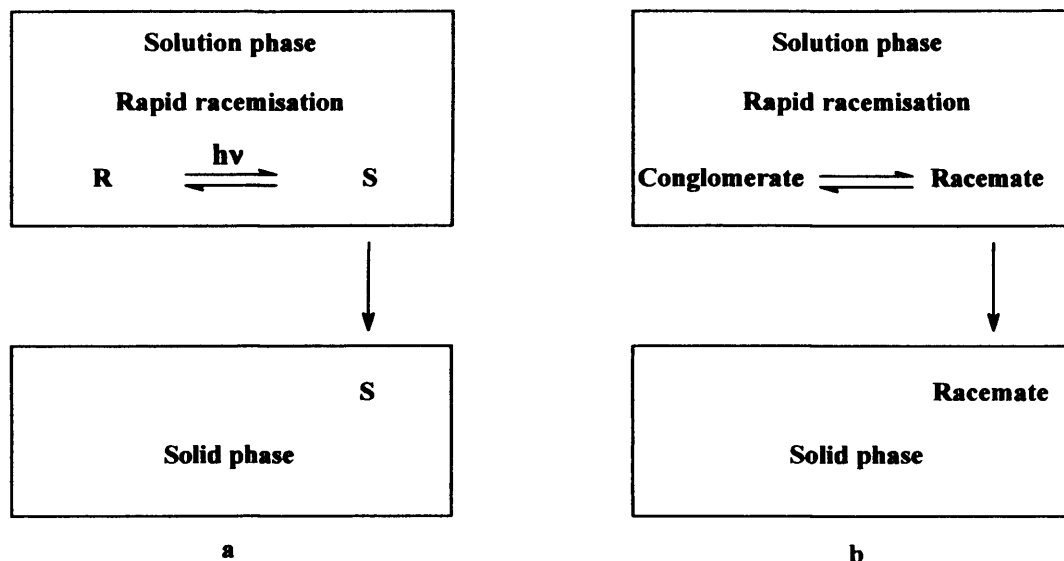
optical activity of both solutions was measured, but with no observable change in the $[\alpha]_D$ values for either sample.

2.6.1 Attempted deracemisation of compounds 5-10 under the influence of CPL

Although photoracemisation was problematical, it was felt that the interaction of these species with CPL should be studied, as only a small chiral influence is required, en theory, to obtain useful e.e.'s if an AT (*i.e.*, asymmetric transformation of the second kind) crystallisation can occur.^[32] Although only one crystal structure of these species had been obtained, and it was a racemate, it is known that CPL irradiation can influence the polymorphism of crystallisations^[33] and so it was still possible that AT behaviour could be observed.

The benzylidene malonate compounds 5-10 were then recrystallised whilst being irradiated with CPL. The recrystallisations were performed by dissolving a small amount of product (typically 100 mg) in a minimum amount of ethyl acetate. The mixture was then cooled in an ice bath under CPL until the solid precipitated.

Every compound was recrystallised twice, and after each recrystallisation the optical activity of both the mother liquor and the resultant solid was measured. The absence of optical activity in one of them did not prove the lack of optical activity in the other. Thus, if the solid obtained after recrystallisation had been seeded with the first molecule that crystallised (asymmetric transformation of the second kind, *AT*) then the mother liquor should contain mainly the other enantiomer, but CPL irradiation might have re-racemised the solution, and so therefore the optical activity of the solution would be zero. Conversely, if a racemate form (a crystal containing two enantiomers) was more crystalline than the conglomerate form (crystal containing one enantiomer) then the solid would have no optical activity, whereas the mother liquor would (Scheme 39).



Scheme 39 a) Asymmetric transformation of the second kind (AT) (conglomerate is in the solid phase). b) hypothetical case where a conglomerate is left in the solution phase

The recrystallisations were performed with compounds 5-10, and none of the recrystallised product showed any significant change in optical activity.

2.7 Conclusions

The synthesis of a new family of axially chiral benzylidene malonates was achieved. Their e.e. determination was attempted through different physical and chemical methods (HPLC, CSR, chiral reagents, Michael addition and Pt complexation). Deracemisation of several axially chiral benzylidene malonates was attempted under the effect of CPL, in order to obtain photoresolution. Unfortunately, no optical activity was observed for any of the compounds. This lack of optical activity does not imply the non-occurrence of deracemisation. There is the possibility that deracemisation occurred but in such a low degree that it was undetectable by the polarimeter. As mentioned in the introduction (**Section 1.4.2**) typical values of e.e. when samples have been irradiated with CPL are around 2 %.^[34]

2.8 References

- [1] J. A. Le Bel, *Bull. Soc. Chim. Fr.* **1874**, 22, 337.
- [2] J. H. Van't Hoff, *Arch. Neerl. Sci. Exactes Nat.* **1874**, 9, 445.
- [3] W. Kuhn, E. Braun, *Naturwissenschaften* **1929**, 17, 227.
- [4] N. P. Huck, W. F. Jager, B. de Lange, B. L. Feringa, *Science* **1996**, 273, 1686.

- [5] H. Rau, *Chem. Rev.* **1983**, *83*, 535.
- [6] H. Tsuneishi, T. Hakushi, A. Tai, Y. Inoue, *J. Chem. Soc. Perkin Trans. 2* **1995**, 2057.
- [7] W. H. Perkin, W. J. Pope, O. Wallach, *J. Chem. Soc.* **1909**, *95*, 1789.
- [8] W. H. Perkin, W. J. Pope, O. Wallach, *Justus Liebigs, Ann., Chem.* **1909**, *371*, 180.
- [9] H. Gerlach, *Helv. Chim. Acta* **1966**, *49*, 1291.
- [10] J. H. Brewster, J. E. Privett, *J. Am. Chem. Soc.* **1966**, *88*, 1419.
- [11] E. J. Ebberts, G. J. A. Ariaans, J. P. M. Houbiers, A. Bruggink, B. Zwanenburg, *Tetrahedron* **1997**, *53*, 9417.
- [12] C. Y. K. Tan, D. F. Weaver, *Tetrahedron* **2002**, *58*, 7449.
- [13] A. Michael, N. Weiner, *J. Am. Chem. Soc.* **1936**, *58*, 680.
- [14] J. E. Baldwin, *J. C. S. Chem. Comm.* **1976**, 734.
- [15] W. Breitenstein, F. Marki, S. Roggo, I. Wiesenberg, J. Pfeilschifter, P. Furet, E. Beriger, *European Journal of Medicinal Chemistry* **1994**, *29*, 649.
- [16] A. G. Relenyi, D. E. Wallick, J. D. Streit, US Patent 4614671 ed., USA, **1986**, p. 5.
- [17] P. H. M. Budzelaar, 4.0 ed. (Ed.: IvorySoft), Cherwell Scientific Publishing, **1998**.
- [18] E. Pretsch, T. Clerc, J. Seibl, W. Simon, *Tablas para la determinacion estructural por metodos espectroscopicos*, Ed. Springer Verlag, **1998**.
- [19] C. V. K. Sharma, G. R. Desiraju, *J. Chem. Soc. Perkin Trans. 2* **1994**, 2345.
- [20] G. R. Desiraju, T. Steiner, *The Weak Hydrogen Bond in Structural Chemistry and Biology*, Oxford University Press, Oxford, **1999**.
- [21] C. E. Pfluger, P. D. Boyle, *J. Chem. Soc. Perkin Trans. 2* **1985**, 1547.
- [22] L. J. Farrugia, *J. Appl. Cryst.* **1997**, *30*, 565.
- [23] D. Parker, R. J. Taylor, *Tetrahedron* **1988**, *44*, 2241.
- [24] A. J. Blake, H. McNab, L. C. Monahan, *J. Chem. Soc. Perkin Trans. 2* **1991**, 2003.
- [25] P. V. Bernhardt, R. Koch, D. W. J. Moloney, M. Shtaiwi, C. Wentrup, *J. Chem. Soc. Perkin Trans. 2* **2002**, 515.
- [26] R. M. Wilson, A. C. Hengge, A. Ataei, D. M. Ho, *J. Am. Chem. Soc.* **1991**, *113*, 7240.
- [27] M. K. Jeon, Y. Kim, *J. Chem. Soc. Perkin Trans. 1* **2000**, 3107.

Chapter 2: Synthesis and Chirality of Alkylidene Dioxanediones

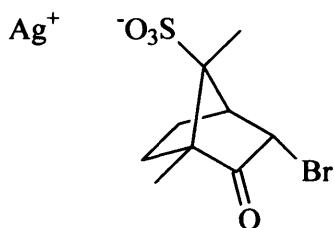
- [28] J. Mason, *Multinuclear NMR*, Plenum Press, New York, 1987.
- [29] D. W. Meek, T. J. Mazanec, *Acc. Chem. Res.* 1981, 14, 266.
- [30] G. M. Wyman, *Chem. Rev.* 1955, 55, 625.
- [31] R. A. Caldwell, *J. Am. Chem. Soc.* 1970, 92, 1439.
- [32] D. K. Kondepudi, J. Laudadio, K. Asakura, *J. Am. Chem. Soc.* 1999, 121, 1448.
- [33] B. A. Garetz, J. Matic, A. S. Myerson, *Physical Review Letters* 2002, 89, 4.
- [34] B. L. Feringa, R. A. van Delden, *Angewandte Chemie - International Edition* 1999, 38, 3418.

Chapter 3: SYNTHESIS OF COBALT ETHYLENEDIAMINE COMPLEXES AND STUDIES ON THEIR CRYSTAL PACKING

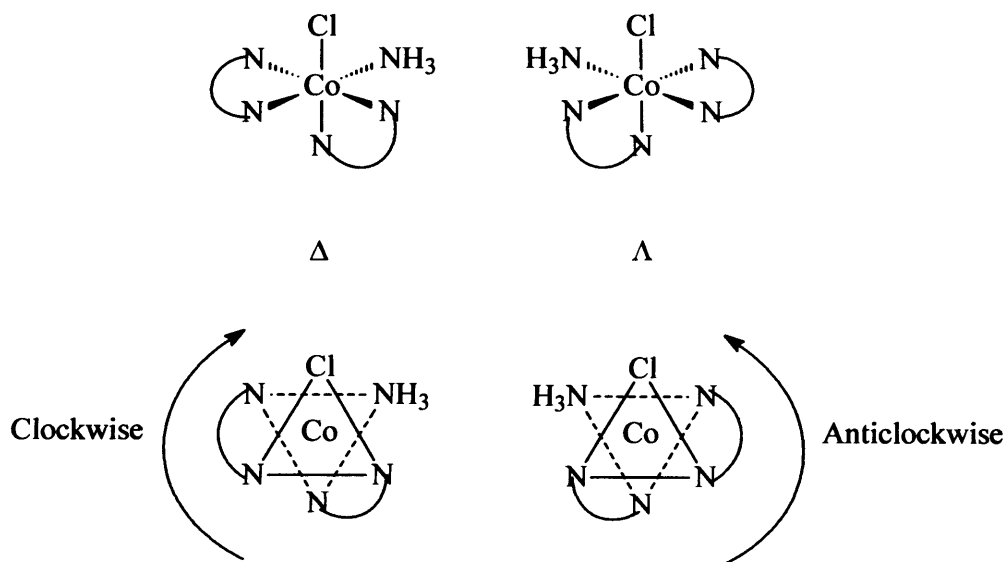
3.1 Introduction

Geometrically isomeric cobalt complexes were crucial for the development of coordination chemistry as it is understood today. Evidence for this is to be found in Alfred Werner's theory about isomerism among inorganic compounds which was developed studying octahedral cobalt complexes. In 1899, Alfred Werner considered for the first time the possibility of optical isomerism in an article on $[\text{Co}(\text{ox})(\text{en})_2]\text{X}$ (ox = oxalate, en = ethylenediamine).^[1] He and his students spent several years attempting to resolve various coordination compounds and finally, in 1911, Alfred Werner and his student Victor L. King, successfully resolved complexes of the type *cis*- $[\text{CoCl}(\text{NH}_3)\text{en}_2]\text{X}_2$, using a silver salt of (+)-3-bromocamphor-9-sulphonic acid (**Scheme 1**). The optical activity of the resolved complexes was measured with the improved Schmidt and Haensch (Landolt type) polarimeter.^[2] What was not known at that time is that certain complexes like *cis*- $[\text{CoBr}(\text{NH}_3)(\text{en})_2]\text{Br}$ and *cis*- $[\text{Co}(\text{NO}_2)_2(\text{en})_2]\text{X}$ (X = Cl, Br) can form conglomerate crystals, in what is now called *spontaneous resolution*. For the purposes of the project there is great interest in the crystallising form of the products, which can be in a *racemic* form (*i.e.*, both Δ and Λ enantiomers are present in the same crystal), or in a *conglomerate* form (*i.e.*, each crystal contains just one enantiomer, either Δ or Λ). Δ and Λ enantiomers are the

possible optical isomers observed in octahedral complexes involving bidentate ligands in a *cis* position. Their differentiation is shown in **Scheme 2**, if the ligands rotate clockwise then it is a Δ (delta) enantiomer and if the ligands rotate anticlockwise then it is a Λ (lambda) enantiomer.

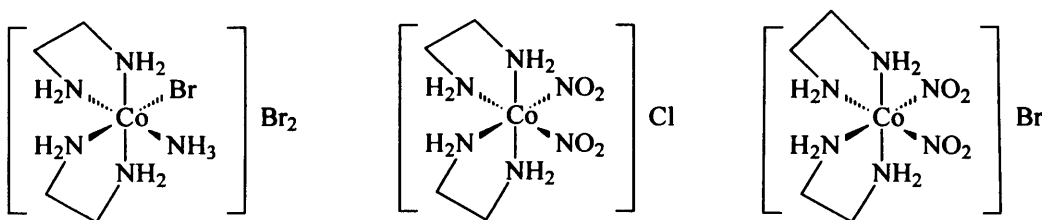


Scheme 1 (+)-3-bromocamphor-9-sulphonic acid silver salt

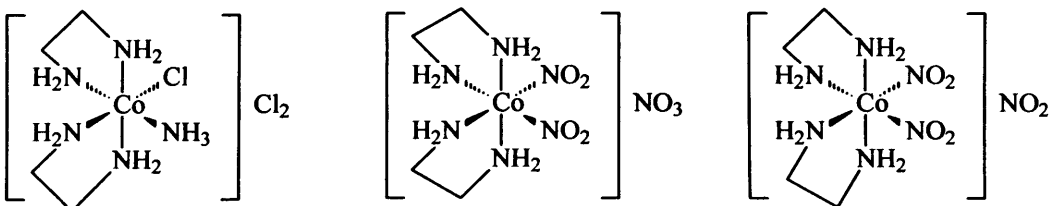


Scheme 2 Λ and Δ enantiomers for *cis*-[CoCl(NH₃)en₂]X₂

For the aim of this project cobalt complexes were studied that either are known to crystallise in a conglomerate form, or unknown compounds with the potential to crystallise as conglomerates. The known complexes that crystallised as conglomerates were taken from the literature (**Scheme 3**), all having a similar structure to Werner's coordination compounds. However, other complexes that appeared very similar are known to crystallise as a racemates (**Scheme 4**).



Scheme 3 Cobalt coordination compounds that crystallise as conglomerates



Scheme 4 Cobalt coordination complexes that crystallise as racemates

There is no complete and reliable theory that can predict the way that compounds crystallise, although it is known that the influence of hydrogen bonding between the nitrogen from the ethylenediamine and the counterion of another ion pair can affect the crystallisation packing. As an example, some complexes that have $[\text{NO}_2]^-$ in the first coordination sphere crystallise in a conglomerate form when a halide is acting as a counterion, however they crystallise in a racemate form when either $[\text{NO}_2]^-$ or $[\text{NO}_3]^-$ acts as a counterion,^[3] demonstrating the difference that hydrogen bonding can make to the crystal packing.

3.2 Complexes of type $cis\text{-}[\text{CoX}(\text{NH}_3)(\text{en})_2]\text{X}_2$

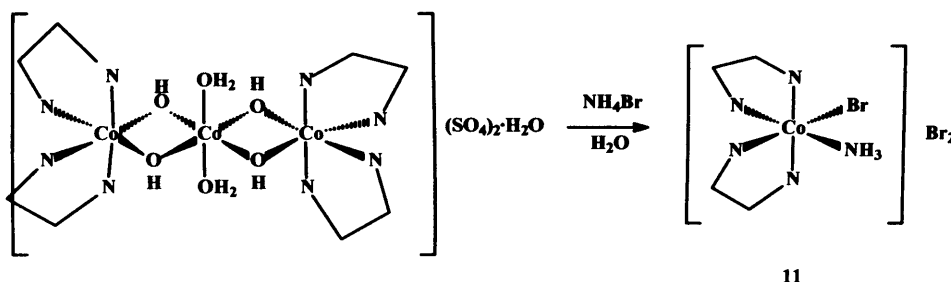
Octahedral cobalt complexes of the type $cis\text{-}[\text{CoX}(\text{NH}_3)(\text{en})_2]\text{X}_2^*$ are easy to synthesise from $[(\text{H}_2\text{O})_2\text{Co}\{(\text{OH})_2\text{Co}(\text{en})_2\}_2](\text{SO}_4)_2 \cdot 5\text{H}_2\text{O}$ and readily available ammonium halides or pseudohalides. These types of compounds were chosen a) because of the photolability of cobalt (III)^[4] and b) because the compounds are chiral, they can exist as Δ or Λ enantiomers. The successful synthesis and spontaneous resolution of $cis\text{-}[\text{CoBr}(\text{NH}_3)(\text{en})_2]\text{Br}_2$ (**11**) by Asakura *et al.*^[5] encouraged the attempt to synthesise $cis\text{-}[\text{CoX}(\text{NH}_3)(\text{en})_2]\text{X}_2$ ($\text{X} = \text{I}^-, \text{F}^-, \text{SCN}^-$) none of which have been reported before.

* Strictly the complexes mentioned in this chapter do not have an octahedral geometry, but they have been treated as so when examining molecular orbital theory for simplicity.

These complexes can potentially crystallise in a conglomerate form, similar to compound **11**. Even though the chloride analogue $cis\text{-}[\text{CoCl}(\text{NH}_3)(\text{en})_2]\text{Cl}_2$ was already known to crystallise in a racemic form,^[6] these compounds seemed good candidates for conglomerate crystallisation.

3.2.1 $cis\text{-}[\text{CoBr}(\text{NH}_3)(\text{en})_2]\text{Br}_2$ (**11**)

The synthesis was performed following a procedure similar to that described in the literature (**Scheme 5**).^[5] The mechanism of the reaction is not fully understood due to high insolubility of the starting material, but some spectroscopic studies support the idea that the reaction proceeds *via* an intermediate $[\text{Co}(\text{H}_2\text{O})(\text{OH})(\text{en})_2]^{2+}$, as this was identified by UV in the early stages of the reaction (approx $t = 1$ min) as the main product.^[7]



Scheme 5 Synthesis of **11**

11 has been reported to crystallise as a *racemate*,^[8] but it can also crystallise in a chiral space group when precipitated from an optically pure solution,^[9] *i.e.*, as it is already an homochiral solution then it must clearly generate homochiral crystals. However, **11** showed chiral symmetry breaking by chiral autocatalysis which implies conglomerate crystallisation^[5, 10-12] but has never been reported to crystallise in a chiral space group from a racemic mixture, even when the product of the reaction showed some optical activity.

Although compound **11** was synthesised for the first time in 1899, more recently **11** was shown to crystallise in a racemic form (denoted in this work as **11a**) by Bernal *et al.* in 1993.^[8] An alternative method to the synthesis of a presumed conglomerate form of **11** was developed later by Asakura *et al.* in 1995, based on the spontaneous resolution of **11** from solution (denoted as **11b**).^[5] The latter was the synthetic route chosen to reproduce the synthesis of **11** in this work, in the expectation that conglomerate crystals would be obtained. Suitable crystals for X-ray diffraction grew very easily; however, X-ray diffraction analysis revealed that a new polymorph

structure for **11** (denoted as **11c**) had been obtained (**Figure 1**). The product crystallised in a racemic form, in the space group P 21/n (**Table 1**).

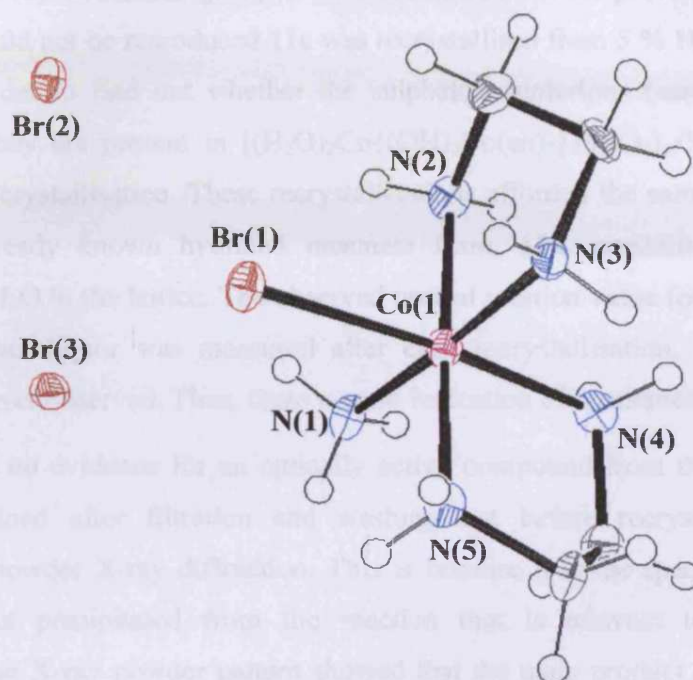


Figure 1 ORTEP view (50% probabilities) of **11c**

Empirical formula	C ₄ H ₁₉ Br ₃ CoN ₅
Crystal system	Monoclinic
Space group	P21/n
Unit cell dimensions	a=7.6301(2) Å
	b=12.3587(4) Å
	c=13.9682(5) Å
	β=98.5640(10)°
Volume	1302.49(7) Å ³
Temperature	150(2)K
Final R indices	R1=0.0547, wR2=0.0870
R indices (all data)	R1=0.0868, wR2=0.1015

Table 1 Summary of data collection and processing parameters for **11c**

When **11b** was synthesised in the work by Asakura *et al.*, the reaction was performed using various ratios of two of the starting materials ($[(\text{H}_2\text{O})_2\text{Co}\{(\text{OH})_2\text{Co}(\text{en})_2\}_2](\text{SO}_4)_2 \cdot 5\text{H}_2\text{O}:\text{H}_2\text{O}$), ranging from 0.189:1 to 0.377:1, with the best ratios for obtaining optical activity being 0.315:1 and 0.377:1.^[5] Thus, the reaction was performed at least once with all ratios and several times with the best ratios in order to try to reproduce the result. Recrystallised starting materials

from different commercial companies were used and the same polymorph (**11c**) was always obtained. Usually the product was recrystallised in 5 % HBr, and suitable crystals for X-ray diffraction grown from this solution. As the previous spontaneous resolution could not be reproduced **11c** was recrystallised from 5 % H₂SO₄ and 25 % H₂SO₄, in order to find out whether the sulphate counterions (assumed to be in solution as they are present in [(H₂O)₂Co{(OH)₂Co(en)₂}₂](SO₄)₂·5H₂O) had any effect on the crystallisation. These recrystallisations afforded the same product each time; the already known hydrated racemate form, **11a**, crystallising with one molecule of H₂O in the lattice. The observed optical rotation value for both the solid and the mother liquor was measured after each recrystallisation, but no optical activity was ever observed. Thus, there was no indication of spontaneous resolution.

As there was no evidence for an optically active compound from the reaction, the product obtained after filtration and washing but before recrystallisation was analysed by powder X-ray diffraction. This is because it is the space group of the initial product precipitated from the reaction that is relevant to spontaneous resolution. The X-ray powder pattern showed that the main product of the reaction was **11c**, with no traces of any other polymorph. Subsequently, the crude product of the reaction was analysed immediately after the reaction was finished, with the same result being obtained each time.^[13]

Data from the polymorphs **11a**, **11b** and **11c** is described in Table 2. **11c** presents bond distances within esd's of **11a** and **11b**. The relative conformation of the rings in **11c** is *cis*-[$\Delta(\delta\lambda)$ -CoBr(NH₃)(en)₂]Br₂ (the relevant torsional angles are N(2)-C(1)-C(2)-N(3) = -51.1° and N(4)-C(3)-C(4)-N(5) = +49.6°) (Table 3). Usually the expected configuration and conformation of the Co(en)₂ fragment is either $\Lambda(\delta\delta)$ or $\Delta(\lambda\lambda)$, which are the lowest energetic conformations for the cation,^[8] thus there must be hydrogen-bonding[†] or other packing forces such as Van der Waals interactions stabilising the non-favoured structure of **11c**.

[†] Hydrogen bonds described in this chapter have a maximum distance between heteroatoms of 3.500 Å, and an angle between 120° and 180°. The shorter the distance and the closer to 180° the angle, the stronger the hydrogen bond is.

Distance (Å)	11a (C2/c)	11b (P2 ₁ 2 ₁ 2 ₁)	11c (P2 ₁ /n)
Co(1)-Br(1)	2.403(1)	2.407(2)	2.408(10)
Co(1)-N(1)	1.960(6)	1.976(9)	1.966(5)
Co(1)-N(2)	1.977(6)	1.974(8)	1.952(5)
Co(1)-N(3)	1.951(6)	1.988(9)	1.953(4)
Co(1)-N(4)	1.961(6)	1.972(9)	1.967(5)
Co(1)-N(5)	1.984(6)	1.956(9)	1.951(5)

Table 2 Bond distances for different polymorphs of *cis*-[CoBr(NH₃)(en)₂]Br₂ (11)

Torsional atoms	Torsional angle (°)
N(2)-C(1)-C(2)-N(3)	-51.1
N(4)-C(3)-C(4)-N(5)	49.6

Table 3 Torsional angles for 11c

A centrosymmetric pair with Λ and Δ enantiomers (**Figure 2**) is created by hydrogen bonding between Br(1) and HN(2') from another molecule, and reciprocally between Br(1') and HN(2), with a distance of 3.476 Å, therefore helping racemic crystallisation. The hydrogen bond distances for 11c are listed in **Table 4**.

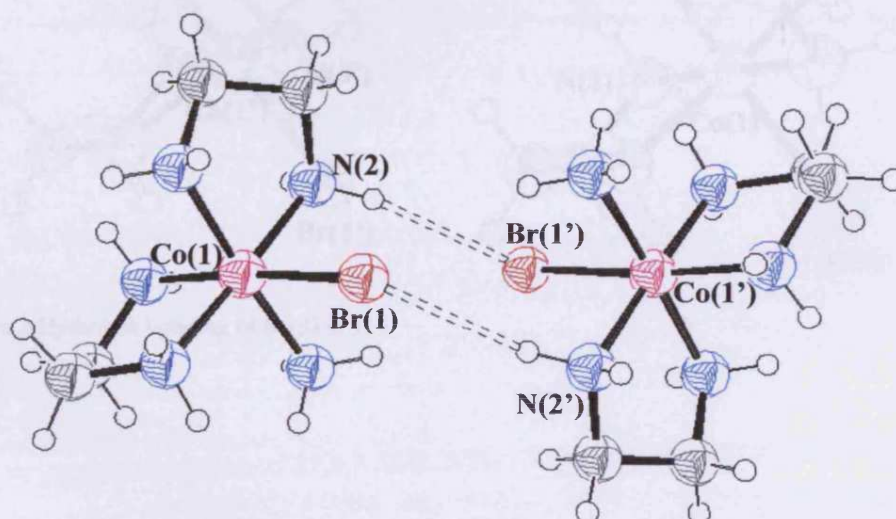


Figure 2 Centrosymmetric pair created by reciprocal hydrogen bonding between the Λ and Δ enantiomers for 11c

Hydrogen bonded atoms	Hydrogen bond length (Å)	Hydrogen bond angle (°)
N(5)···Br(3')	3.381	153.0
N(1)···Br(3')	3.407	168.2
N(1)···Br(2')	3.399	161.8
N(2)···Br(3)	3.303	167.1
N(2)···Br(1')	3.476	166.4
N(5)···Br(2)	3.400	169.9
N(4)···Br(2'')	3.462	162.4

Table 4 Hydrogen bonds for **11c**

Br(3) is connected to HN(2) of molecule 1 (3.303 Å) and at the same time is connected with HN(1') (3.407 Å) and HN(5') (3.381 Å) of molecule 2 (**Figure 3**). Br(2) is hydrogen bonded to three different molecules at the same time, with HN(5) (3.400 Å) from molecule 1, HN(1') (3.399 Å) from molecule 2 and HN(4'') (3.462 Å) from molecule 3 (**Figure 4**).

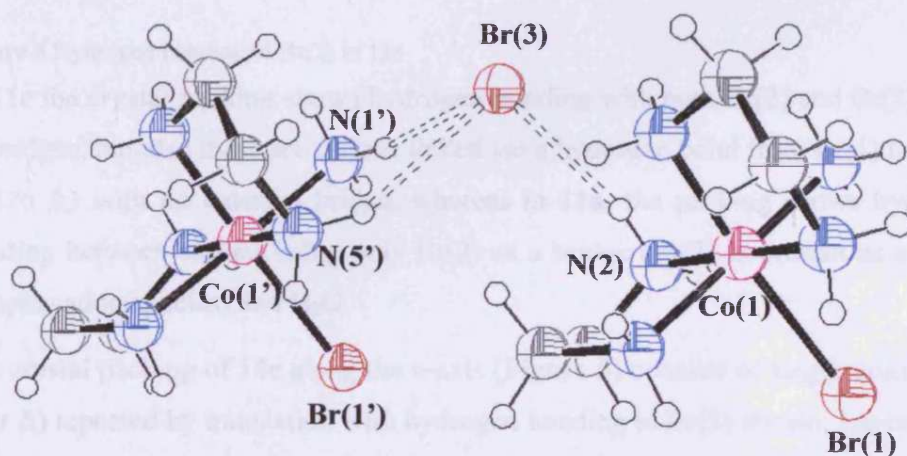


Figure 3 Hydrogen bonding of Br(3) in **11c**

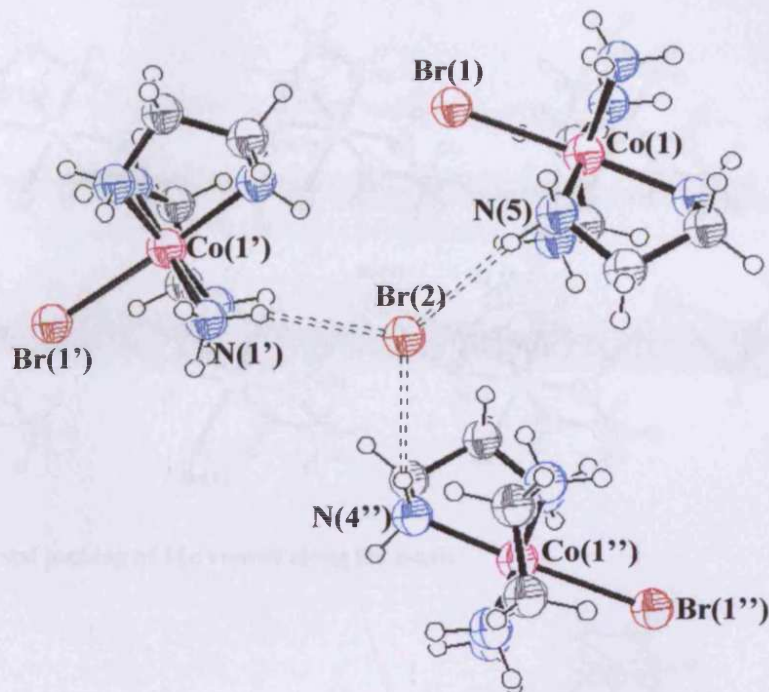


Figure 4 Hydrogen bonding of Br(2) in **11c**

In **11c** the crystal packing shows hydrogen-bonding with both Br(2) and Br(3) acting as bridges, but also there are cations linked *via* a hydrogen bond from Br(1) to HN(2) (3.476 Å) with no external bridge, whereas in **11a**, the packing shows hydrogen-bonding between cations using only Br(2) as a bridge (Br(3) is present as a charge compensating species) and H₂O.

The crystal packing of **11c** along the *a*-axis (**Figure 5**) consists of single units (either Λ or Δ) repeated by translation with hydrogen bonding to Br(3) shown. Layers of the opposite enantiomer are connected with hydrogen bonding to Br(2) shown. Along the *b*-axis (**Figure 6**) the Λ - Δ dimer is repeated by simple translation, with hydrogen bonding to Br(1) shown. Layers of dimers are connected with hydrogen bonding to Br(2) and Br(3) with a web type overall structure. Along the *c*-axis (**Figure 7**) single units (either Λ or Δ) are repeated by simple translation, connecting layers of the opposite enantiomer with hydrogen bonding to Br(2) shown.

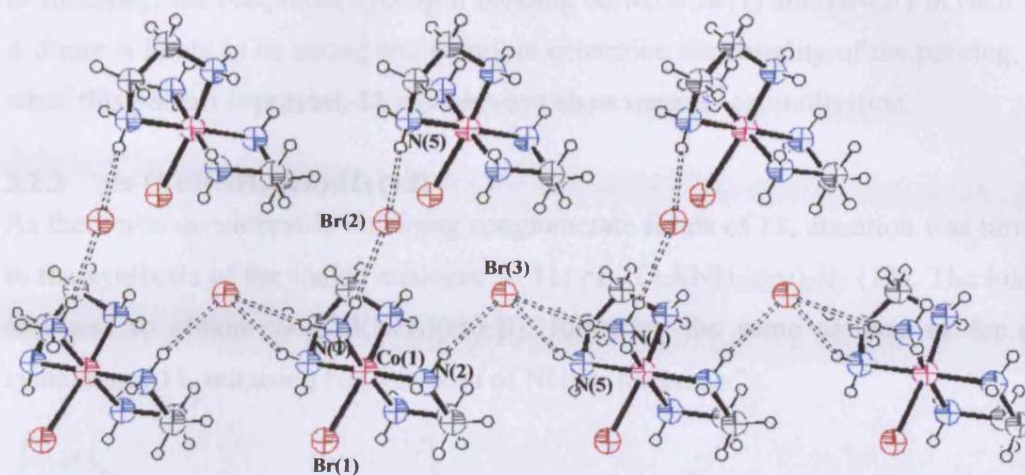


Figure 5 Crystal packing of 11c viewed along the a-axis

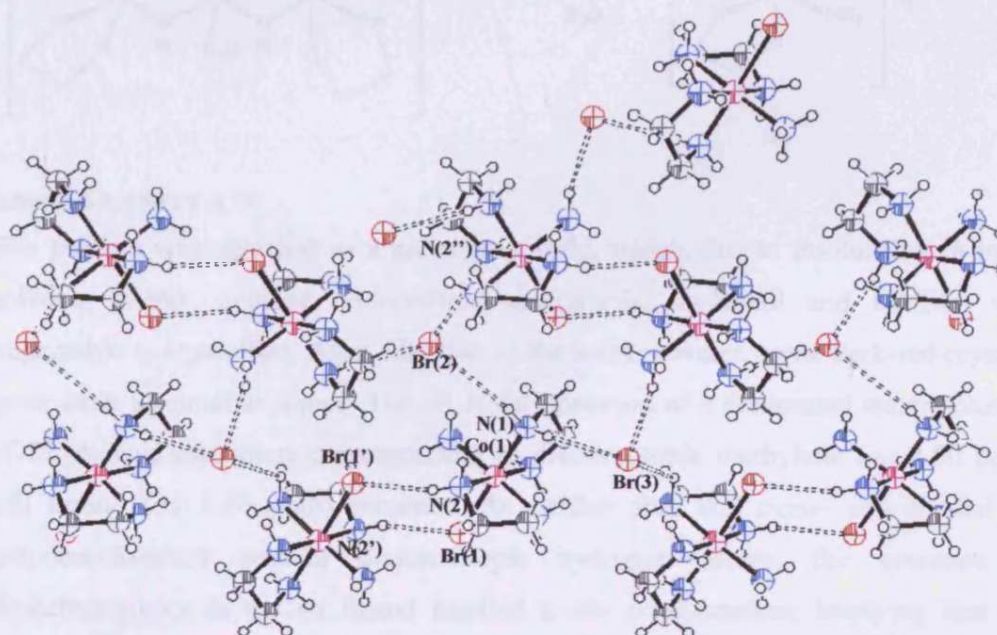


Figure 6 Crystal packing of 11c viewed along the b-axis

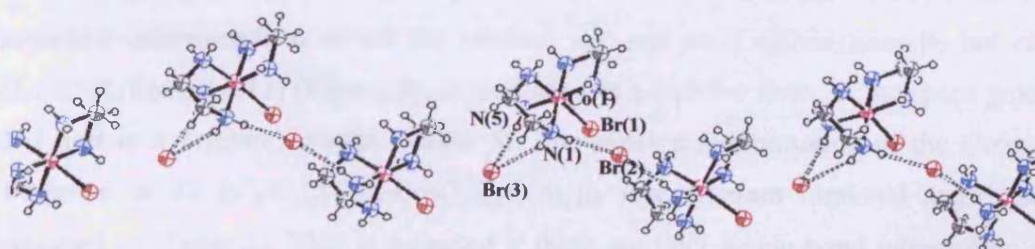
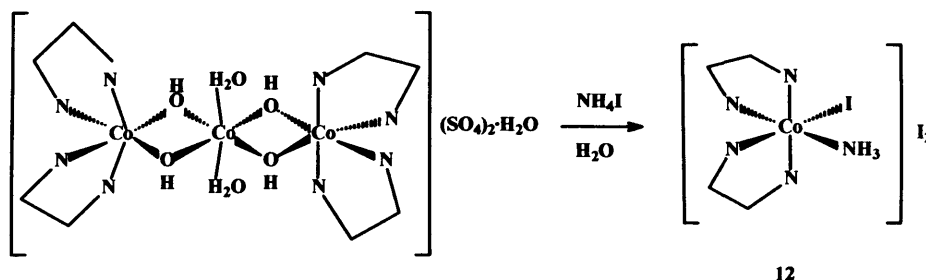


Figure 7 Crystal packing of 11c viewed along the c-axis

In summary, the reciprocal hydrogen bonding between Br(1) and HN(2') in each Λ - Δ dimer is likely to be strong and therefore determine the chirality of the packing, so when this pattern is present, **11** must always show racemic crystallisation.

3.2.2 *cis*-[CoI(NH₃)(en)₂]I₃ (**12**)

As there was no success in obtaining conglomerate forms of **11**, attention was turned to the synthesis of the iodide analogue to **11**; *cis*-[CoI(NH₃)(en)₂]I₂ (**12**). The initial aim was to obtain *cis*-[CoI(NH₃)(en)₂]I₂, following the same method as for the synthesis of **11**, but using NH₄I instead of NH₄Br (Scheme 7).



Scheme 6 Synthesis of **12**

The product was obtained as a green-grey solid, which, due to insolubility in polar solvents (water, acetone, chloroform, acetonitrile, methanol and DMSO) was impossible to crystallise. After filtration of the solid in water, some dark-red crystals grew from the mother liquor. The ¹H-NMR spectrum of a deuterated water solution of **12** showed multiplets corresponding to diastereotopic methylene (*ca* 2.50 ppm) and amine (*ca* 4.60 ppm) moieties. As neither free nor *trans*-coordinated en (ethylenediamine) contain diastereotopic hydrogen atoms, the presence of diastereotopicity in the en ligand implied a *cis*-conformation, implying that the desired product was obtained. IR spectroscopy seemed to confirm this, with two broad peaks at around 3100 cm⁻¹ which could indicate the presence of amines, both free and hydrogen bonded. Single crystal X-ray diffraction data was collected and the structure determined, to reveal the product was not *cis*-[CoI(NH₃)(en)₂]I₂ but *cis*-[CoI(NH₃)(en)₂]I₃ (**12**) (**Figure 8**), crystallising in a racemic form, in the space group P-1 and in a Triclinic system (**Table 5**). The relative conformation of the Co(en)₂ fragment in **12** is *cis*-[$\Lambda(\delta\delta)$ -CoI(NH₃)(en)₂]I₃ (the relevant torsional angles are reported on **Table 6**). This is expected if there are only single bond intramolecular interactions, as a $\delta\delta$ conformation (or $\lambda\lambda$) is more stable than a $\delta\lambda$.^[8] In contrast with product **11c**, **12** did not present any hydrogen bonding, therefore both Co(en) rings

had the same conformation. The conformation of the Co(en) fragments can be easily determined by the N(1)-N(2)-N(3)-N(4) torsional angles, a positive torsional angle designates a δ conformation, whereas a negative torsional angle indicates a λ conformation.

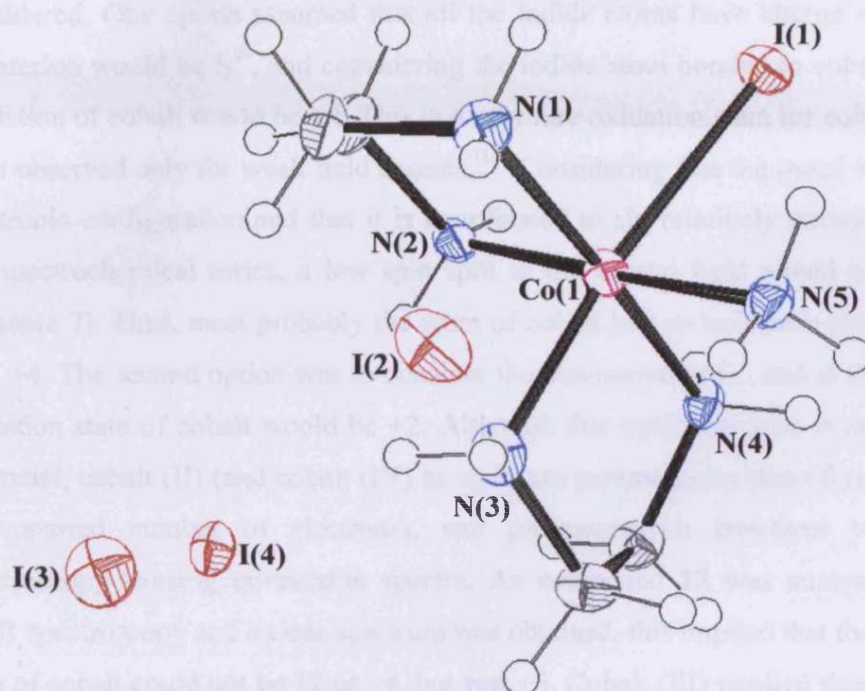


Figure 8 ORTEP view (50% probabilities) of 12

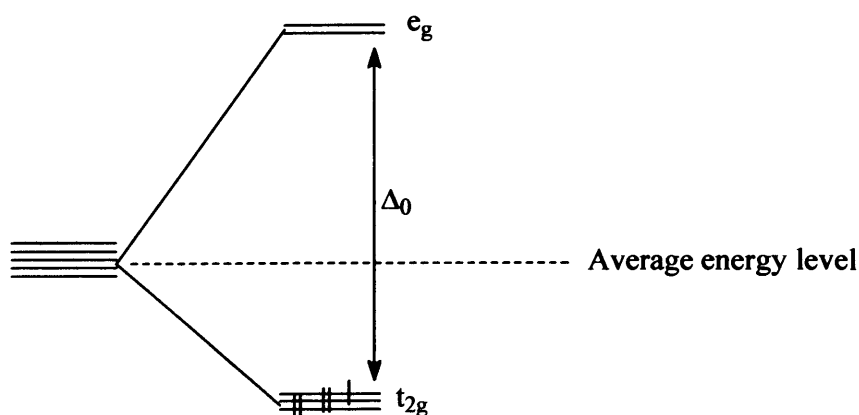
Empirical formula	$C_4H_{19}CoI_4N_5$
Crystal system	Triclinic
Space group	P-1
Unit cell dimensions	$a = 7.9760(2) \text{ \AA}$
	$b = 8.4940(2) \text{ \AA}$
	$c = 13.5110(5) \text{ \AA}$
	$\alpha = 93.6490(10)^\circ$
	$\beta = 104.4510(10)^\circ$
	$\gamma = 111.1420(10)^\circ$
Volume	$814.67(4) \text{ \AA}^3$
Temperature	150(2) K
Final R indices [$I > 2\sigma(I)$]	$R1 = 0.0449, wR2 = 0.1057$
R indices (all data)	$R1 = 0.0555, wR2 = 0.1124$

Table 5 Summary of data collection and processing parameters for 12

Torsional atoms	Torsional angle (°)
N(1)-C(1)-C(2)-N(2)	50.8
N(3)-C(3)-C(4)-N(4)	49.1

Table 6 Torsional angles for **12**

The oxidation state of the metal was difficult to assign, and initially two options were considered. One option assumed that all the iodide atoms have charge -1, thus the counterion would be I_3^{3-} , and considering the iodide atom bonded to cobalt the total oxidation of cobalt would be +4. This is a very rare oxidation state for cobalt and has been observed only for weak field ligands.^[14] Considering that the metal ion has a d^5 electronic configuration and that it is coordinated to six relatively strong ligands in the spectrochemical series, a low spin split in the crystal field would be expected (**Scheme 7**). Thus, most probably the atom of cobalt had an oxidation state different than +4. The second option was to consider the counterion as I_3^- , and in this case the oxidation state of cobalt would be +2. Although this oxidation state is common for the metal, cobalt (II) (and cobalt (IV) as well) are paramagnetic (therefore they have an unpaired number of electrons), and paramagnetism interferes with NMR spectroscopy causing unreadable spectra. As compound **12** was analysed by 1H -NMR spectroscopy and a clear spectrum was obtained, this implied that the oxidation state of cobalt could not be +2 or +4, but was +3. Cobalt (III) implied three atoms of I^- , and one atom of I neutral, and so to understand the nature of crystal packing in compound **12**, the crystal structure was expanded beyond the asymmetric unit.



Average energy
of metal ion in
spherical field

Metal ion in
octahedral field

Scheme 7 Crystal field splitting for octahedral low spin d^5 cobalt (IV)

Thus, when the crystal structure was expanded beyond the asymmetric unit, four atoms of iodide were linear (torsional angle of $+180^\circ$), describing the counterion as I_4^{2-} . Each asymmetric unit contains half of the I_4^{2-} group, along with one dicationic cobalt species and one isolated iodide atom (**Figure 9**). The non-symmetrical distances of I-I lengths (I(2)-I(3)-I(3')-I(2')) = 3.373 Å, 2.770 Å, 3.373 Å suggests that $I-I_2-I$ best describes the species rather than I_4^{2-} , and also suggests an inversion centre between I(3) and I(3'). Thus, considering the central I atoms to be a molecule of I_2 , it was concluded that the oxidation state of cobalt was +3. The I_2 bond distance is reported to be 2.715(6) Å,^[15] and the distance I(3)-I(3') is 2.779(1) therefore and considering esd's the central atoms of the I_4^{2-} unit can not be considered as a iodine molecule but they are very close to each other. The description of the counterion system is best seen in the unit cell, which contains two cationic units (described as unit 1 and unit 1', opposite enantiomers) and six iodine atoms, belonging to two I_4^{2-} units (**Figure 10**). Three iodine atoms belong to the unit 1, the other three iodine atoms belong to the unit 1'. The I(3) and I(3') atoms are bonded, hence showing that the unit I_4^{2-} is "shared" between to cationic units. When the crystal packing is expanded beyond the unit cell, four I_4^{2-} units are passing through four edges of the unit cell, although only two I_4^{2-} units are partially in the unit cell (**Figure 11**). I(4) is isolated as a one-off atom in the lattice, and does not show hydrogen bonding with any hydrogen atoms.

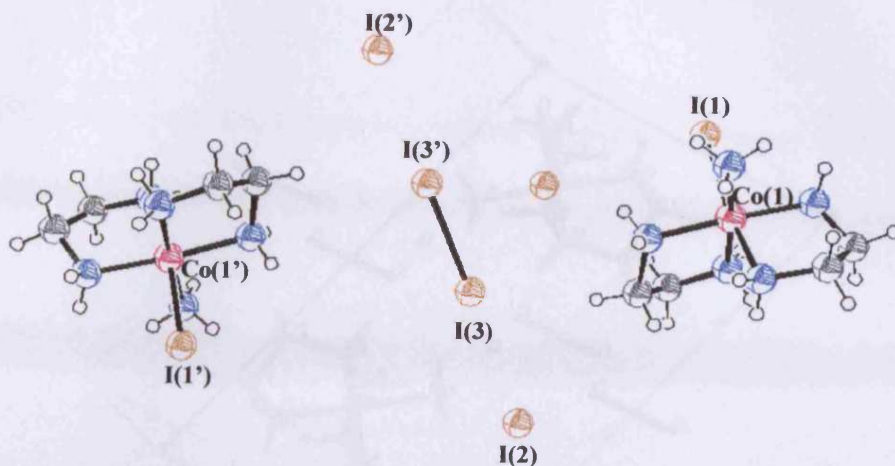


Figure 9 I_4^{2-} with two cationic units

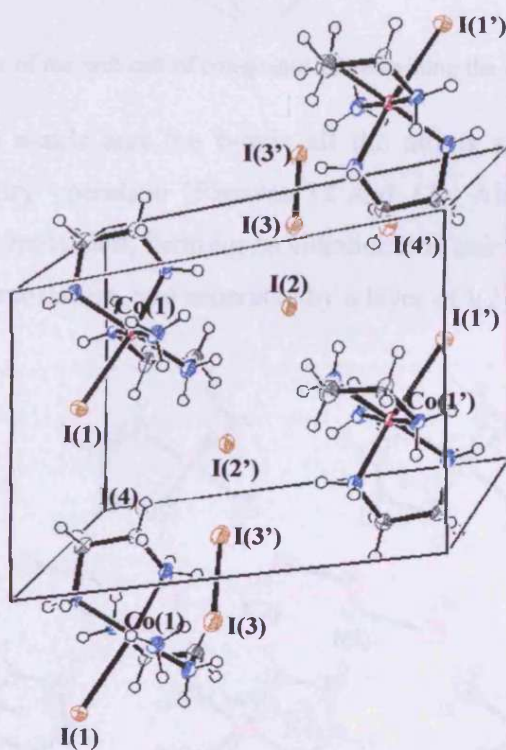


Figure 10 Unit cell of compound 12, containing two cationic units and one I_4^{2-} unit

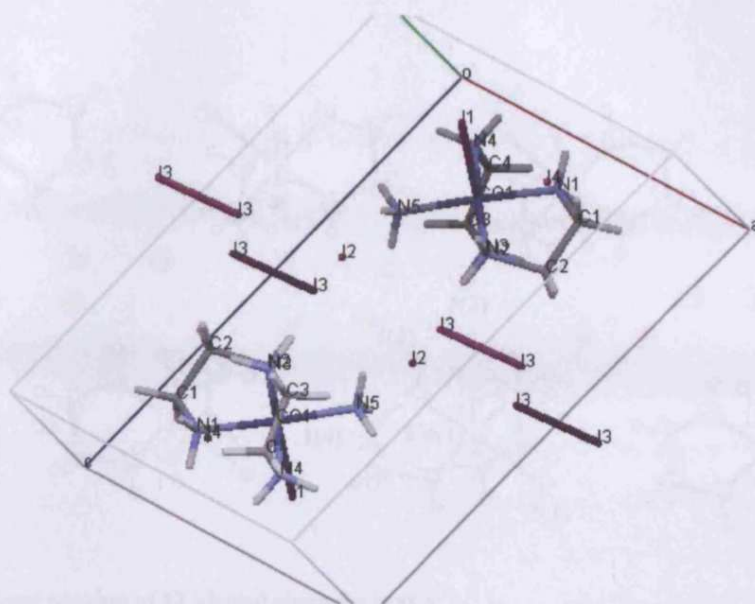


Figure 11 Mercury view of the unit cell of compound **12** containing the centre of the unit I_4^{2-} in each edge of the unit cell

Along the both the a-axis and the b-axis all the atoms are related by a simple translational symmetry operation (**Figures 12 and 13**). Along the c-axis cationic units are rotated and translated, forming an enantiomeric pair. This enantiomeric pair is then repeated by translation, and separated by a layer of $I(2)$ and $I(3)$ (**Figure 14**).

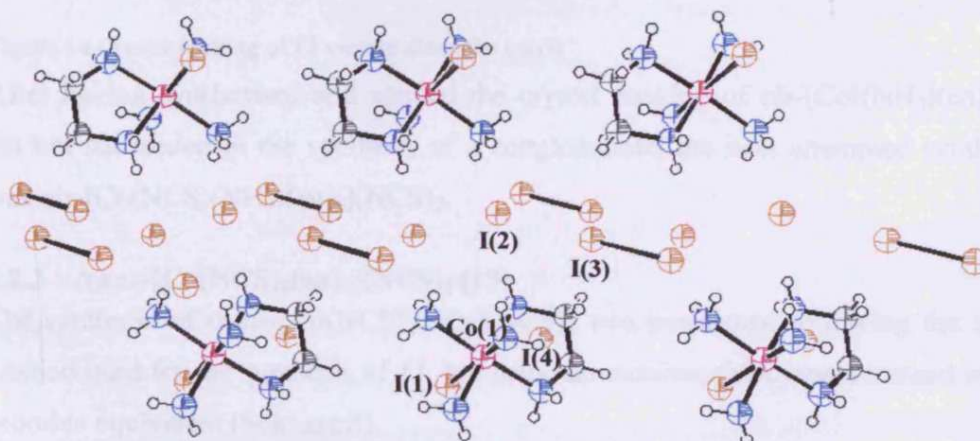


Figure 12 Crystal packing of **12** viewed along the a-axis

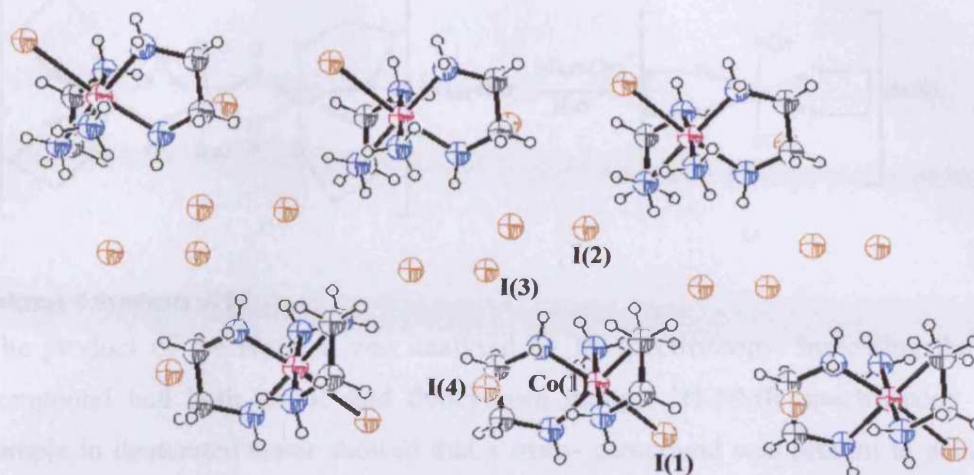


Figure 13 Crystal packing of 12 viewed along the b-axis

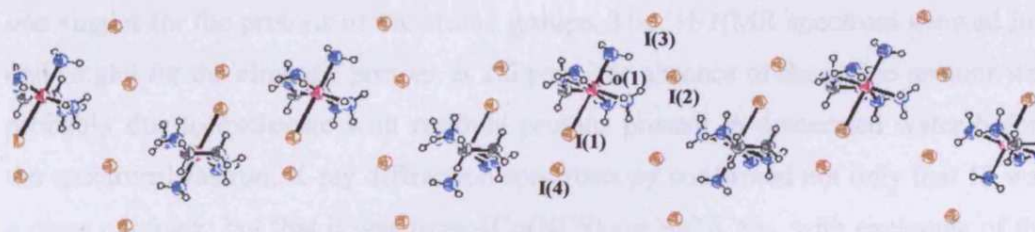
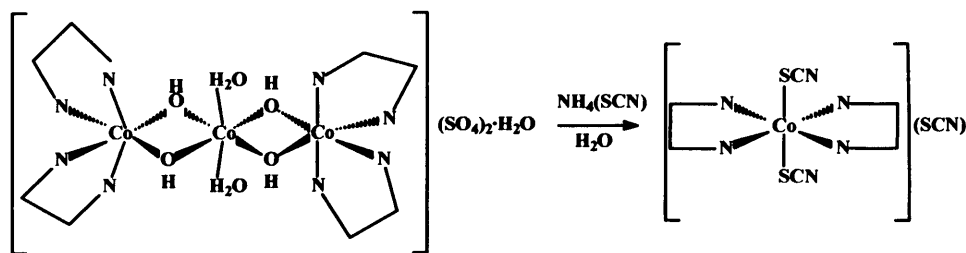


Figure 14 Crystal packing of 12 viewed along the c-axis

After having synthesised and studied the crystal packing of *cis*-[CoI(NH₃)(en)₂]₃, but not succeeded in the synthesis of a conglomerate, the next attempted synthesis was *cis*-[Co(NCS)(NH₃)(en)₂](NCS)₂.

3.2.3 *trans*-[Co(NCS)₂(en)₂](NCS)₂ (13)

The synthesis of *trans*-[Co(NCS)₂(en)₂](NCS)₂ was performed following the same method used for the synthesis of 11, but using ammonium thiocyanate instead of the bromine equivalent (Scheme 8).



13

Scheme 8 Synthesis of 13

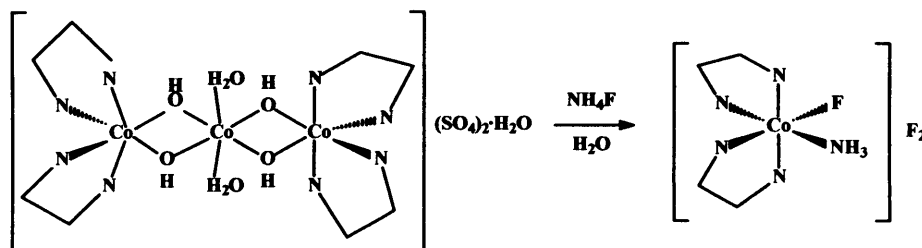
The product of the reaction was analysed by IR spectroscopy, indicating that the compound had both amino and thiocyanate groups. ¹H-NMR spectroscopy of a sample in deuterated water showed that a *trans*- compound was present in solution, as no diastereotopicity was observed. The presence of only two singlets in the ¹H-NMR spectrum is typical for *trans*- en compounds as all the aliphatic protons are chemically equivalent, showing just one singlet for all of the aliphatic protons and one singlet for the protons of the amine groups. The ¹H-NMR spectrum showed just one singlet for the aliphatic protons at 2.6 ppm, the absence of the amine protons was probably due to exchange with residual protons present in deuterated water before the spectrum was run. X-ray diffraction spectroscopy confirmed not only that 13 was a *trans* complex, but that it was *trans*-[Co(NCS)₂(en)₂](NCS)₂, with exchange of the expected ammine ligand for a thiocyanate ligand. Even though the compound is already known,^[16] the route by which it was synthesised was new. The synthesis of *trans*-[Co(NCS)₂(en)₂](NCS)₂ was unexpected, as the initial aim was to synthesise *cis*-[Co(NCS)(NH₃)(en)₂](NCS)₂ (thiocyanate analogue of 11).

Considering the synthetic route used, it was surprising that the product contained *trans*- coordinated en ligands. During the synthesis of 11 and 12 all the products had retained the initial *cis*- conformation of the starting material, so clearly this reaction either did not proceed *via* a the *cis*-[Co(H₂O)(OH)(en)₂]²⁺ intermediate,^[7] or, if it did, then not with a concerted mechanism. A non-concerted mechanism would leave a coordination vacancy, therefore the ligands could rearrange in the most stable isomer, with the more bulky ligands in the equatorial positions.

13 crystallises with two independent cations in the asymmetric unit, as previously reported.^[17] Hydrogen bonding is not present in the structure, and as it has a *trans*-conformation of the en ligands and high symmetry (a C₂ axis and a mirror plane) it is not chiral, therefore 13 is not a good candidate for the project.

3.2.4 *cis*-[CoF(NH₃)(en)₂]F₂

The attempted synthesis of *cis*-[CoF(NH₃)(en)₂]F₂ was performed using a method similar to that used for the bromine analogue (Scheme 9). The solid formed during the reaction appeared to be very hygroscopic gradually becoming an oil. Attempts at crystallising the oil with hot water or ethanol failed due to solubility problems.



Scheme 9 Attempted synthesis of *cis*-[CoF(NH₃)(en)₂]F₂

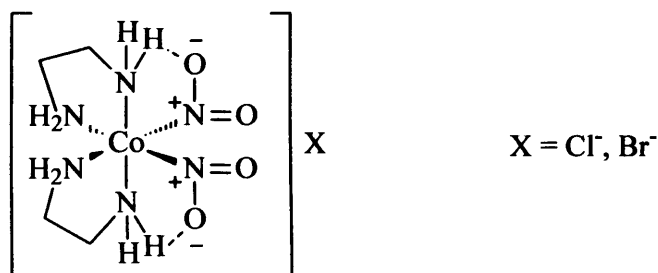
The oil was dissolved in deuterated water and ¹H-NMR spectroscopy revealed several broadened resonances suggestive of paramagnetic material present. This indicated that the sample contained some Co(II) (the starting material contained two Co(II) and one Co(III) atoms). The IR spectrum was recorded, and a broad band at 3216 cm⁻¹ indicated either the presence of NH₂ or H₂O. As a crystalline product was required for the CPL-crystallisation, further studies on *cis*-[CoF(NH₃)(en)₂]F₂ were abandoned.

In summary, compounds **11c**, **12** and **13** were synthesised. A new polymorph for compound **11** was found, and its crystal packing studied. It showed that hydrogen bonding plays an important role in the crystallisation pattern, even to the point of changing one of the Co(en) rings into the higher energy conformation. For novel compound **12** the crystal packing was also studied, observing no hydrogen bonding in the crystal packing, but an unusual system for the counterion I₄²⁻. The synthesis of **13** was achieved as an unexpected product, with its crystal structure being already discussed. The synthesis of *cis*-[CoF(NH₃)(en)₂]F₂ was also attempted, without success. None of the compound synthesised in this section crystallised as conglomerate, so synthesis of a different family of coordination compounds was attempted.

3.3 Complexes of type $cis\text{-}[\text{Co}(\text{NO}_2)_2(\text{en})_2]\text{X}$

After all the potential conglomerate complexes of the $cis\text{-}[\text{CoX}(\text{NH}_3)(\text{en})_2]\text{X}_2$ family were synthesised, the focus was turned to the $cis\text{-}[\text{Co}(\text{NO}_2)_2(\text{en})_2]\text{X}$ family, of which some complexes are known to crystallise as conglomerates.

Complexes of type $cis\text{-}[\text{Co}(\text{NO}_2)_2(\text{en})_2]\text{X}$ are easy to synthesise and some examples are also known to crystallise in a conglomerate form if the counterion is a halide. In these complexes intramolecular hydrogen bonding arranges packing as a conglomerate (**Scheme 10**).^[18] Crystallisation occurs in a racemic form when the counterion can potentially form stronger hydrogen bonding (intramolecular bonding is not strong enough to compete).^[19] Thus, packing induced chirality is determined by hydrogen bonding in the crystal lattice.^[20]

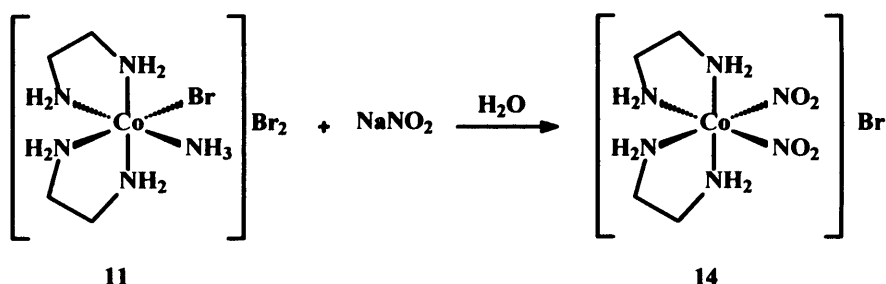


Scheme 10 Intramolecular hydrogen bonding that assists conglomerate crystallisation

Some compounds belonging to the family of $cis\text{-}[\text{Co}(\text{NO}_2)_2(\text{en})_2]\text{X}$ were synthesised, in order to examine the effect of different counterions having different hydrogen bonding capacity on crystal packing. Several compounds belonging to the $cis\text{-}[\text{Co}(\text{NO}_2)_2(\text{en})_2]\text{X}$ family of cobalt complexes were investigated.

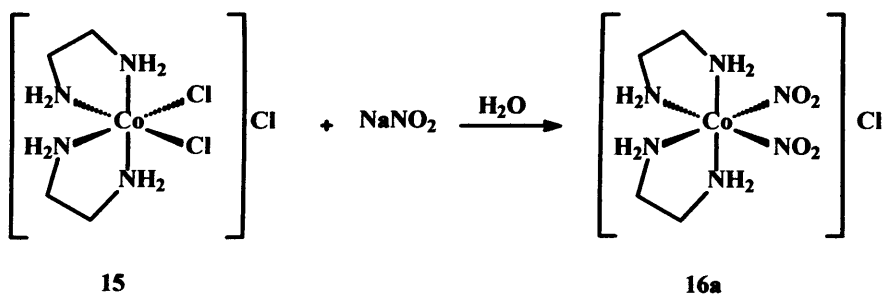
3.3.1 $cis\text{-}[\text{Co}(\text{NO}_2)_2(\text{en})_2]\text{Br}$ (14)

14 is a known compound that crystallises in a conglomerate form.^[19] It was obtained directly by dissolving compound **11** in water and adding a supersaturated solution of NaNO_2 (**Scheme 11**). Suitable crystals for X-ray spectroscopy were grown from water in a few days, and measurement of the unit cell dimensions confirmed the product as $cis\text{-}[\text{Co}(\text{NO}_2)_2(\text{en})_2]\text{Br}$, crystallising in a conglomerate form (space group $P2_1$).

Scheme 11 Synthesis of *cis*-[Co(NO₂)₂(en)₂]Br (**14**)

3.3.2 *cis*-[Co(NO₂)₂(en)₂]Cl (**16a**)

16a is a known compound and was obtained by the same procedure as **14** (Scheme 12), using *cis*-[CoCl₂(en)₂]Cl (**15**) as the starting material (synthesised by a procedure similar to that described in the literature).^[21] **16a** was analysed by ¹H-NMR, IR and mass spectrometry, and all the data obtained indicated the proposed structure. Suitable crystals for X-ray diffraction analysis grew from a water solution, and a measurement of the cell dimensions confirmed that **16a** was the expected compound (it also crystallised in a conglomerate form - Space group P2₁)^[22].

Scheme 12 Synthesis of *cis*-[Co(NO₂)₂(en)₂]Cl (**16a**)

3.3.3 *trans*-[Co(NO₂)₂(en)₂]Cl (**16b**)

The final step of the literature synthesis of *cis*-[CoCl₂(en)₂]Cl (**15**) which was followed^[21] involved an isomerisation from *trans*-[CoCl₂(en)₂]Cl to *cis*-[CoCl₂(en)₂]Cl. This isomerisation did not go to completion and therefore the starting material for the reaction to obtain **16a** contained some traces of *trans*-[CoCl₂(en)₂]Cl (seen by ¹H-NMR spectroscopy). These also reacted with NaNO₂ and led to the formation of *trans*-[Co(NO₂)₂(en)₂]Cl (**16b**).

X-ray crystallography was carried out on a single crystal of **16b** grown from water and analysis of the data revealed **16b** to be a distorted octahedral cobalt coordination compound, with a *trans*- conformation of the en ligands (Figure 15).

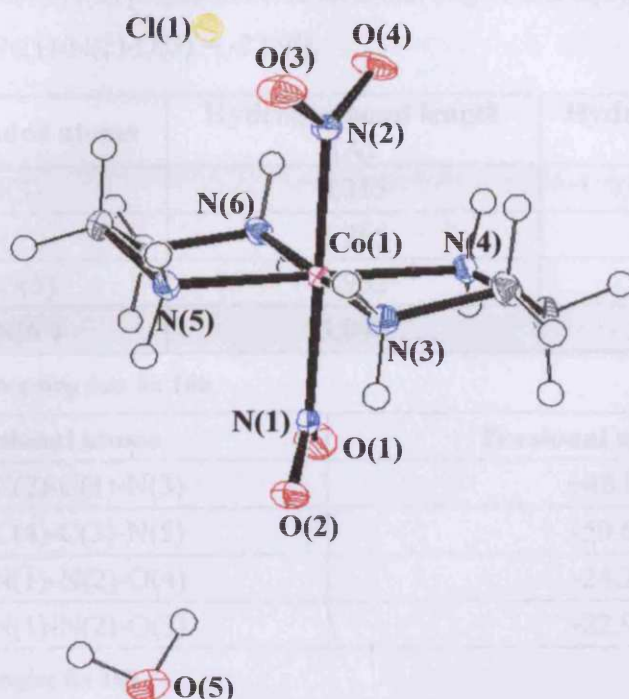


Figure 15 ORTEP view (50% probabilities) of 16b

Empirical formula	$C_4H_{18}ClCoN_6O_5$
Crystal system	Monoclinic
Space group	$P2_1/n$
Unit cell dimensions	$a = 7.2606(3) \text{ \AA}$
	$b = 11.9473(4) \text{ \AA}$
	$c = 14.0218(6) \text{ \AA}$
	$\beta = 95.7830(10)^\circ$
Volume	$1210.12(8) \text{ \AA}^3$
Temperature	150(2)K
Final R indices [$I > 2\sigma(I)$]	$R1 = 0.0345, wR2 = 0.0698$
R indices (all data)	$R1 = 0.0498, wR2 = 0.0761$

Table 7 Summary of data collection and processing parameters for 16b

Trans-[Co(NO₂)₂(en)₂]Cl crystallises in an achiral space group ($P2_1/n$) (Table 7) with one molecule of water in the lattice which affects its crystal packing in terms of hydrogen bonding. Hydrogen bonding data is summarised in Table 8. The torsional angles of the Co(en) ring are N(4)-C(2)-C(1)-N(3) = +48.8 ° and N(6)-C(4)-C(3)-N(5) = -50.6 ° (Table 9). The fact that the torsional angles of the Co(en) ring are not identical makes the molecule *pseudochiral* in the solid state (even though it has a *trans* disposition of the ligands it has two different conformers). The planes of the NO₂⁻ groups are perpendicular to the Co(en) rings although slightly twisted if viewed

from the N(1)-Co(1)-N(2) projection (the torsional angles are O(1)-N(1)-N(2)-O(4) = -24.2° and O(2)-N(1)-N(2)-O(3) = -22.9°).

Hydrogen bonded atoms	Hydrogen bond length (Å)	Hydrogen bond angle (°)
Cl \cdots HN(3)	3.315	149.25
Cl \cdots HN(5')	3.265	144.93
O(2) \cdots HO(5)	2.952	170.16
O(5) \cdots HN(6')	3.040	150.07

Table 8 Hydrogen bonding data for 16b

Torsional atoms	Torsional angle (°)
N(4)-C(2)-C(1)-N(3)	+48.8
N(6)-C(4)-C(3)-N(5)	-50.6
O(1)-N(1)-N(2)-O(4)	-24.2
O(2)-N(1)-N(2)-O(3)	-22.9

Table 9 Torsional angles for 16b

The smallest packing consists mainly of two conformers linked by reciprocal hydrogen bonding HN(3)-Cl-HN(5') and vice versa (3.315 Å, and 3.265 Å respectively). This hydrogen bonding seems to be responsible for the centrosymmetric packing, and therefore for an achiral space group (Figure 16).

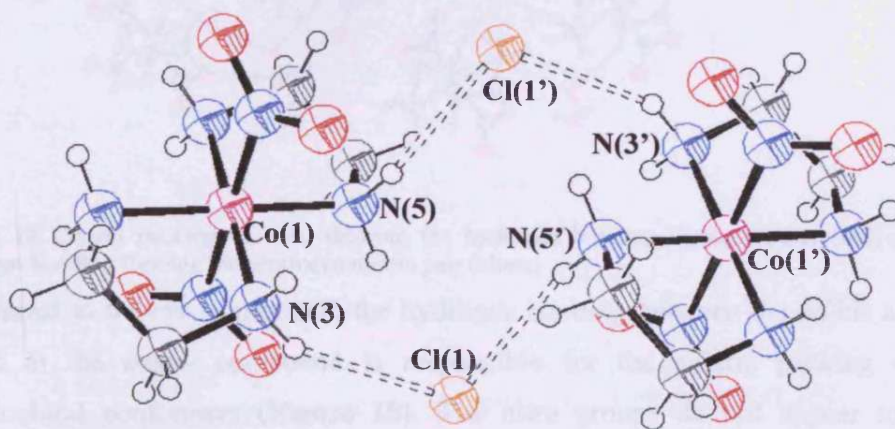


Figure 16 Centrosymmetric packing for *trans*-[Co(NO₂)₂(en)₂]Cl (16b)

Water is also acting as a bridge by hydrogen bonding cations of the same conformation, therefore transmitting chirality along the b-axis (Figure 17). O(2) belonging to the nitro group is hydrogen bonded to the water molecule (O(2)-HO(5) = 2.952 Å), and the water molecule is hydrogen bonded to the following cationic unit

(O(5)-HN(6') = 3.040 Å). The crystal packing of **16b**, therefore, is a combination of the centrosymmetric unit and the hydrogen bonding through water.

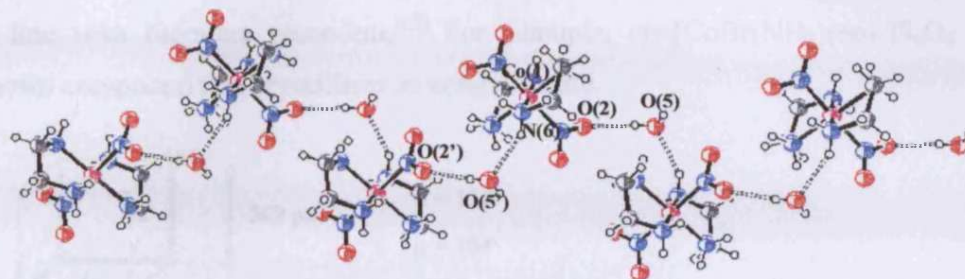


Figure 17 Hydrogen bonding of **16b** through water in the b-axis

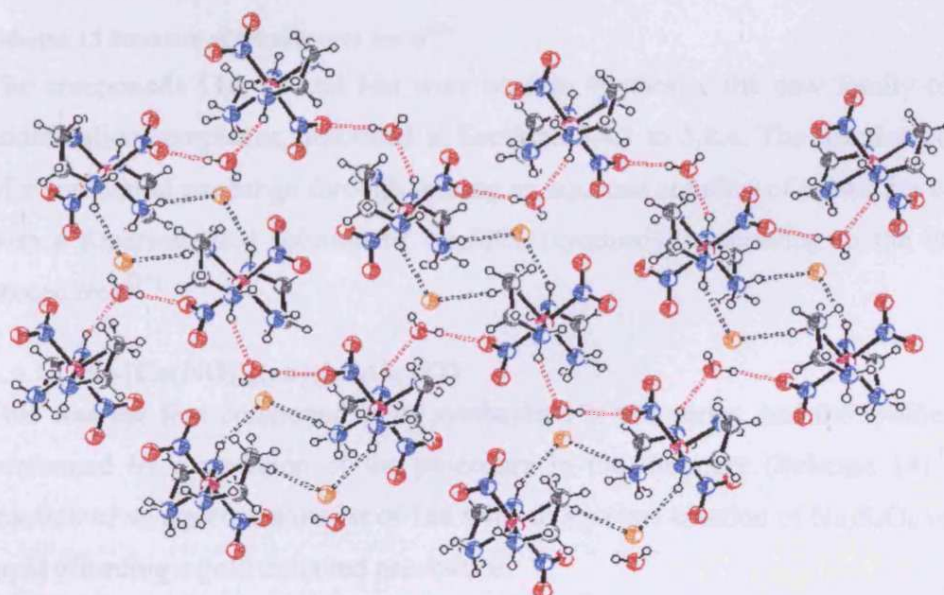


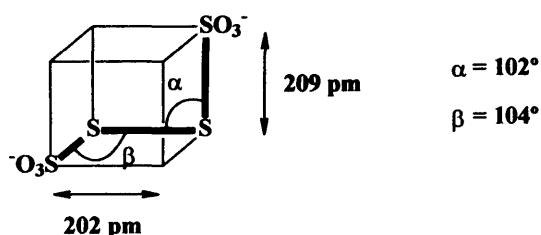
Figure 18 Crystal packing of **16b**, showing the hydrogen bonding through water (red) and the hydrogen bonding forming the centrosymmetric pair (black)

In contrast to the *cis*- compound, the hydrogen bonding between the halide and the cation in the *trans*- compound is responsible for the achiral packing of the pseudo-chiral conformers (Figure 18). The nitro groups do not appear to have intramolecular hydrogen bonding and therefore not assisting conglomerate crystallisation, which was the aim of this chapter.

3.4 Cobalt complexes that have tetrathionate (S_4O_6)²⁻ as a counterion

Considering the importance of hydrogen bonding in conglomerate crystallisation,^[3, 19, 22] tetrathionate was chosen as a counterion that, apart from being a potential

participant in hydrogen bonding, is axially chiral in the solid phase (although it has free rotation in the solution state) (Scheme 14)[†]. In this way the tetrathionate ion was expected to assist conglomerate crystallisation by acting as a pseudochiral auxiliary, in line with literature precedent.^[23] For example, *cis*-[CoBr(NH₃)(en)₂]S₄O₆ is a known compound that crystallises as conglomerate.

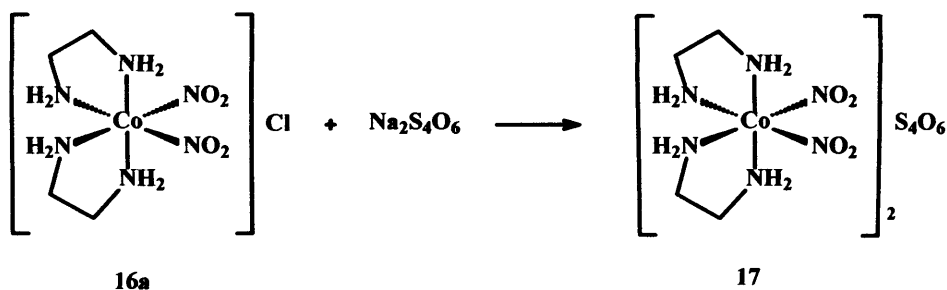


Scheme 13 Structure of tetrathionate anion^[23]

The compounds **11c**, **14** and **16a** were used to synthesise the new family of cobalt coordination complexes, described in Sections 3.4.1 to 3.4.4. The reaction consisted of a counterion exchange through mixing an aqueous solution of cobalt the complex with a supersaturated solution of Na₂S₄O₆ (synthesised according to the literature procedure).^[23]

3.4.1 *cis*-[Co(NO₂)₂(en)₂]S₄O₆ (**17**)

This was the first compound to be synthesised in this series, and the synthesis was performed by a variation of the procedure in the literature (Scheme 14).^[23] The reaction of an aqueous solution of **16a** with an aqueous solution of Na₂S₄O₆ was very rapid affording a gold coloured precipitate.



Scheme 14 Synthesis of *cis*-[Co(NO₂)₂(en)₂]S₄O₆ (**17**)

The ¹H-NMR spectrum of a solution of **17** in deuterated water showed diastereotopicity in the aliphatic region, typical for a *cis*- compound. From the IR

[†] The nomenclature for the tetrathionate counterion in this work will be P for positive torsional angle and M for negative torsional angle, in order to differentiate from (+) and (-) which are usually assigned to optical rotation.

spectrum a band was discerned for NH_2 at 3207 cm^{-1} and in the mass spectrum ions were observed at 495 m/z , corresponding to $([\text{Co}(\text{NO}_2)_2(\text{en})_2]\text{S}_4\text{O}_6)^-$, and at 271 and 225 m/z , corresponding to both the cation and the anion respectively. All of these data supported the predicted structure of the product, but did not define the crystalline behaviour. Therefore suitable crystals for X-ray structure determination were grown from water over a period of a few days. This confirmed that the product was **17** and allowed examination of the space group and packing in the solid state (Figure 19).

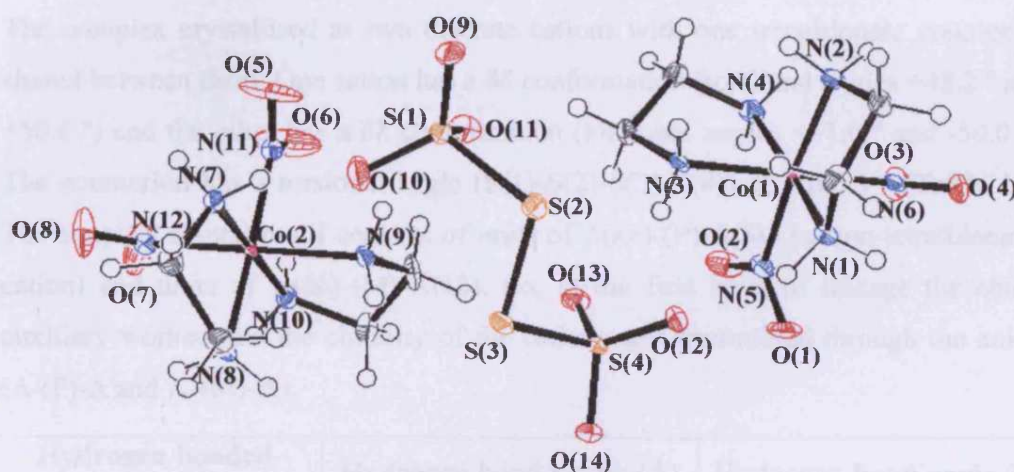


Figure 19 ORTEP view (50% probabilities) of **17**

Empirical formula	$\text{C}_8\text{H}_{32}\text{Co}_2\text{N}_{12}\text{O}_{14}\text{S}_4$
Crystal system	Monoclinic
Space group	$P2_1/n$
Unit cell dimensions	$a = 12.4425(2)\text{ \AA}$
	$b = 7.79690(10)\text{ \AA}$
	$c = 27.6488(5)\text{ \AA}$
	$\beta = 92.3300(10)^\circ$
Volume	$2680.07(7)\text{ \AA}^3$
Temperature	$150(2)\text{ K}$
Final R indices [$I > 2\sigma(I)$]	$R1 = 0.0452, wR2 = 0.1076$
R indices (all data)	$R1 = 0.0628, wR2 = 0.1165$

Table 10 Summary of data collection and processing parameters for **17**

Compound **17** crystallised in a racemic form in a monoclinic system with a space group $P2_1/a$ (Table 10). The chiral auxiliary did not assist in the expected conglomerate crystallisation, thus further study was required to determine what factors were affecting crystallisation. This information would help in predicting the

next step in the synthesis of complexes that have tetrathionate as a counterion and trying to control crystallisation.

Torsional atoms	Torsional angle (°)
N(1)-C(1)-C(2)-N(2)	+48.2
N(3)-C(3)-C(4)-N(4)	+50.6
N(9)-C(7)-C(8)-N(10)	+51.0
N(7)-C(5)-C(6)-N(8)	-50.0
S(1)-S(2)-S(3)-S(4)	+105.3

Table 11 Relevant torsional angles for 17

The complex crystallised as two discrete cations with one tetrathionate counterion shared between them. One cation has a $\delta\delta$ conformation (torsional angles +48.2 ° and +50.6 °) and the other has a $\delta\lambda$ conformation (torsional angles +51.0 ° and -50.0 °). The counterion has a torsional angle (S(1)-S(2)-S(3)-S(4)) of +105.3 ° (Table 11). The simplest crystal motif consists of units of $\Delta(\lambda\lambda)$ -(P)- $\Delta(\delta\lambda)$ (cation-tetrathionate-cation) and units of $\Lambda(\delta\delta)$ -(M)- $\Lambda(\lambda\delta)$. So, at the first level of linkage the chiral auxiliary worked and the chirality of the cations was transmitted through the anion (Δ -(P)- Δ and Λ -(M)- Λ).

Hydrogen bonded atoms	Hydrogen bond length (Å)	Hydrogen bond angle (°)
O(12)···HN(1)	2.947	153.7
O(13)···HN(3)	2.899	151.0
O(10)···HN(7)	2.914	157.3
O(11)···HN(9)	3.012	157.2
O(6)···HN(10)	2.785	120.5
O(12)···HN(2')	2.906	148.4
O(14)···HN(3')	2.975	171.4
O(1)···HN(4')	2.960	158.8
O(8)···HN(8')	3.009	157.6
O(9)···HN(8')	2.969	142.5
O(9)···HN(9')	2.995	144.0
O(5)···HN(10')	2.980	155.2

Table 12 Hydrogen bonding data for 17

On closer examination of the counterion (Figure 20) it was observed that all oxygen atoms were hydrogen bonded to at least one hydrogen atom of the en groups, if not two. The hydrogen bonding data for 17 is summarised in Table 12. One end of the counterion has two oxygen atoms attached to the same cation (O(11)-HN(9) (3.012

Å) and O(10)-HN(7) (2.914 Å)) and the other oxygen atom is attached to another cation at two different positions (O(9)-HN(8') (2.969 Å) and O(9)-HN(9') (2.995 Å)). The other end of the counterion is arranged conversely: two atoms of oxygen are linked to two different cations (O(14)-HN(3') (2.975 Å) and O(13)-HN(3) (2.899 Å)) and the other atom of oxygen is also linked to two different molecules simultaneously (O(12)-HN(2') (2.906 Å) and O(12)-HN(1) (2.947 Å)). In this case, the packing of the molecule itself was not centrosymmetric; therefore the chirality of the packing was not yet determined. Each molecule was hydrogen bonded to a second molecule (O(8)-HN(8') : 3.009 Å) and reciprocally NH(8)-O(8'). Thus the centrosymmetric pairing was favourable (each molecule was the enantiomer of the other) and this directed the packing towards an achiral space group (**Figure 21**).

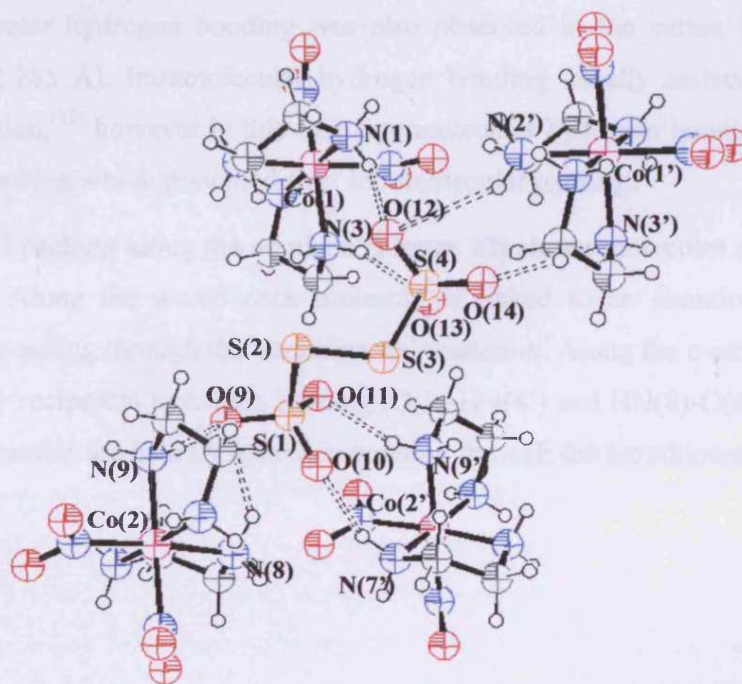


Figure 20 Hydrogen bonding of tetrathionate in compound 17

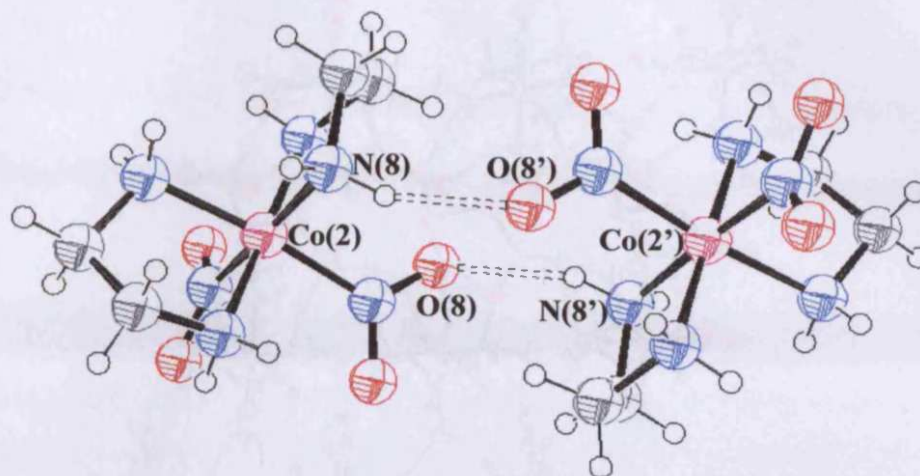


Figure 21 Centrosymmetric pair for **17**

Intramolecular hydrogen bonding was also observed in the cation between O(6)-HN(10) (2.785 Å). Intramolecular hydrogen bonding usually assists conglomerate crystallisation,^[19] however in this case intermolecular hydrogen bonding encouraged racemic packing which prevailed over intramolecular packing.

The crystal packing along the *ac* plane (**Figure 22**) shows molecules of **17** arranged in layers. Along the *a*-axis each molecule is linked to an enantiomeric one by hydrogen bonding through the tetrathionate counterion. Along the *c*-axis enantiomers are held by reciprocal hydrogen bonding (O(8)-HN(8') and HN(8)-O(8')). Along the *b*-axis molecules are held by hydrogen bonding through the tetrathionate.

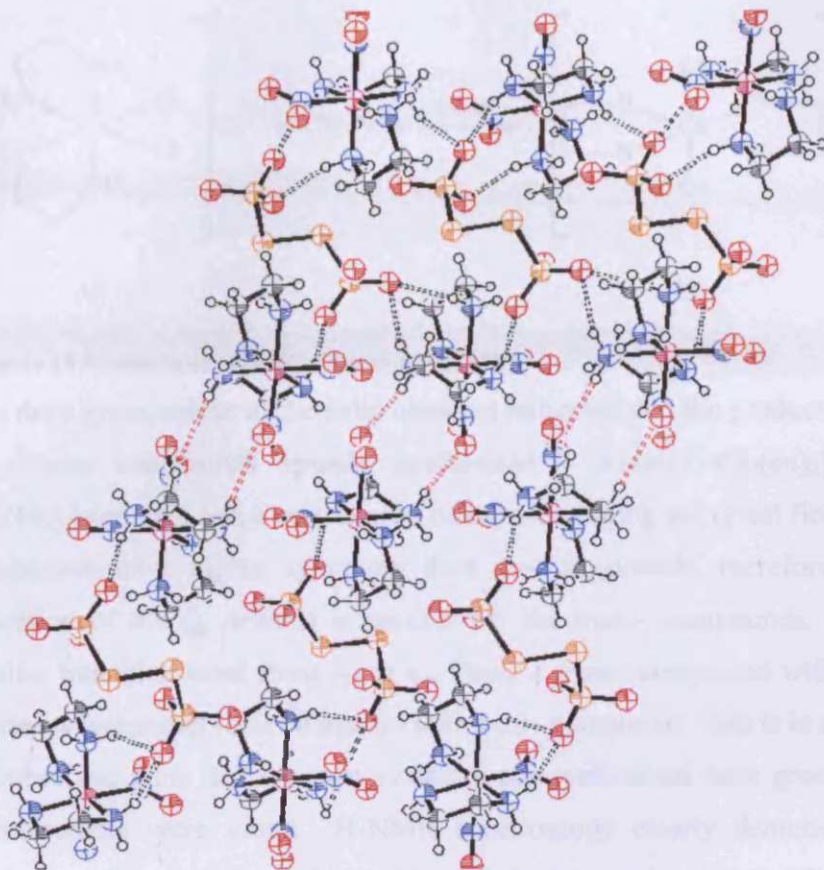
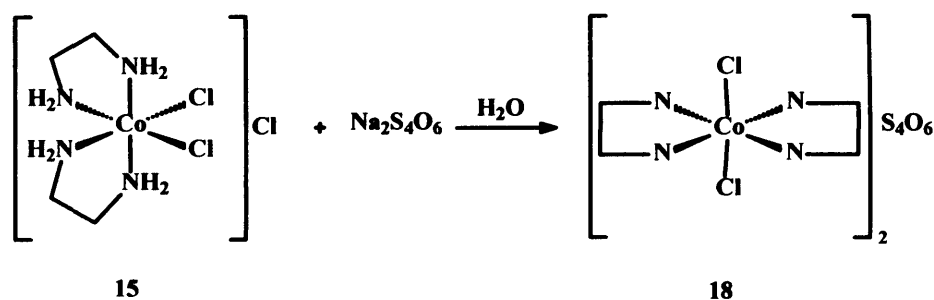


Figure 22 Crystal packing of **17** along the *ac* plane. Molecules are linked by hydrogen bonding with the tetrathionate counterion (black) along the *a* axis, and by hydrogen bonding through the cationic units (red) along the *c* axis

In summary, tetrathionate counterion was shown to have multiple hydrogen bonding to the cationic unit. The cationic unit also contained the nitro ligand, which showed some intramolecular hydrogen bonding, although this was not strong enough to direct the crystal packing towards a chiral space group. The nitro ligand also assisted to the formation of the centrosymmetric pair that determined the non-chiral space group for the crystal packing. **17** was not a good candidate to study the influence of CPL in the crystallisation packing, but showed that an excess of potential hydrogen bonding sites can lead to a higher probability of racemic crystallisation.

3.4.2 *trans*-[CoCl₂(en)₂]₂S₄O₆ (**18**)

Having studied the crystal packing of **17**, attention was turned to the synthesis and structural characterisation of *cis*-[CoCl₂(en)₂]₂S₄O₆, which had less hydrogen bonding potential. The reaction was first attempted following a method very similar to the one described in the literature for these kind of complexes, *i.e.*, mixing a solution of *cis*-[CoCl₂(en)₂]Cl with a solution of Na₂S₄O₆ (Scheme 15).^[23]



Scheme 15 Synthesis of *trans*-[CoCl₂(en)₂]₂S₄O₆ (**18**)

The deep green colour of the solid obtained indicated that the product might be *trans*, as similar compounds already synthesised – *trans*-[CoCl₂(en)₂]Cl and *trans*-[Co(NO₂)₂(en)₂]Cl had a very similar colour. According to crystal field theory, *trans*-compounds have higher symmetry than *cis*-compounds, therefore the tetragonal distortion of the t_{2g} orbitals is smaller for the *trans*-compounds. This leads to a smaller transition band from t_{2g} to e_g . Thus, a *trans*-compound will absorb light at shorter wavelengths (less energetic) than a *cis*-compound. This is in accordance with the observed facts that the *trans*-compounds synthesised were green and their *cis*-stereoisomers were violet. ¹H-NMR spectroscopy clearly demonstrated that the product was a *trans*-complex, with two singlets present: one at 2.9 ppm and the other at 5.2 ppm. IR spectrum showed the bands for NH₂ (approx. 3250 cm⁻¹) and SO (1226 cm⁻¹).

X-ray diffraction was performed on suitable single crystals (grown from a water solution of **18** over a period of a few days) confirming that the product of the reaction was *trans*-[CoCl₂(en)₂]₂S₄O₆ (**Figure 23**). The product crystallised in a space group P-1, in a triclinic crystal system (**Table 13**). Although the solid product had a *trans*-disposition of the en ligands, it isomerised to a *cis*-form when in solution. Thus, a change of colour (from green to dark violet) was observed over a few hours when the complex was dissolved in water. ¹H-NMR spectrum confirmed the *trans-cis* isomerisation, as some multiplets in the aliphatic zone appeared in a suitable chemical shift and with the correct multiplicity for a *cis*-complex. Nevertheless, upon removal of the solvents the ligands returned to a *trans*-disposition and the solid state product was always *trans*-. This was unexpected, as the starting material had a *cis*-disposition, therefore the *cis*-product was predicted, as had been the case with the previous complexes **11c**, **12**, **14** and **16a**. While in solution the material isomerised to the more stable *cis*-form and it was not possible

to obtain crystals other than *trans* – thus presenting an anomaly. It must be assumed that the *trans*- form is stabilised by packing forces (possibly the observed hydrogen bonds) and that isomerisation in solution is rapid enough to allow preferential conversion of *cis*- to *trans*- prior to crystallisation, even from a rapidly cooled solution. Although the mechanism of the isomerisation is not known, when **18** is in solution it presumably proceeds through a five coordinated intermediate that must allow the rearrangement of the ligands to the preferential disposition.^[24]

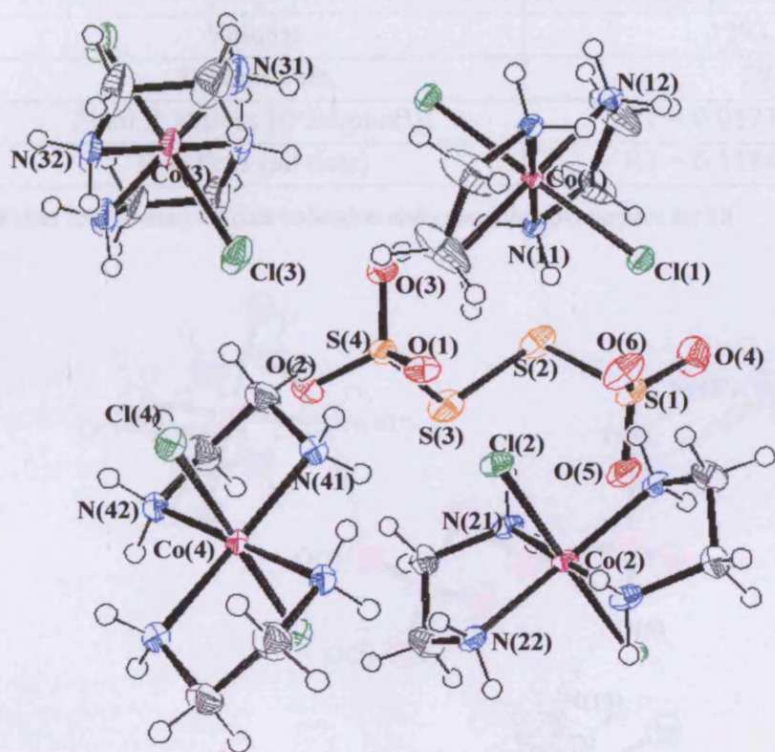


Figure 23 ORTEP view (50% probabilities) of **18**

Despite the apparent simplicity of the system, the unit cell is composed of four halves of conformationally differing cationic units. Each half of the cationic unit has a perfect symmetry inversion centre and a $\delta\lambda$ configuration of the Co(en) rings (Table 14), a requirement of the inversion centre.^[25] The torsional angle of the Co(en) ring for cation 1 is remarkably small in comparison with cations 2,3 and 4. The torsional angle of the tetrathionate is $+96.9^\circ$, which is also quite small compared to the free anion ($+104^\circ$). The tetrathionate counterion is hydrogen bonded only to cations 1 and 4 (Figure 24), and conversely to compound **17**, in compound **18** not all the oxygen atoms of tetrathionate are hydrogen bonded to the cation. The hydrogen bonding data for **18** is summarised in Table 15.

Empirical formula	$C_8H_{32}Cl_4Co_2N_8O_6S_4$
Crystal system	Triclinic
Space group	P-1
Unit cell dimensions	$a = 9.1266(2) \text{ \AA}$
	$b = 12.0312(3) \text{ \AA}$
	$c = 12.6384(4) \text{ \AA}$
	$\alpha = 79.7030(10)^\circ$
	$\beta = 87.0570(10)^\circ$
Volume	$\gamma = 71.353(2)^\circ$
	$1293.70(6) \text{ \AA}^3$
Temperature	293(2) K
Final R indices [$I > 2\sigma(I)$]	$R1 = 0.0577, wR2 = 0.1078$
R indices (all data)	$R1 = 0.1186, wR2 = 0.1267$

Table 13 Summary of data collection and processing parameters for 18

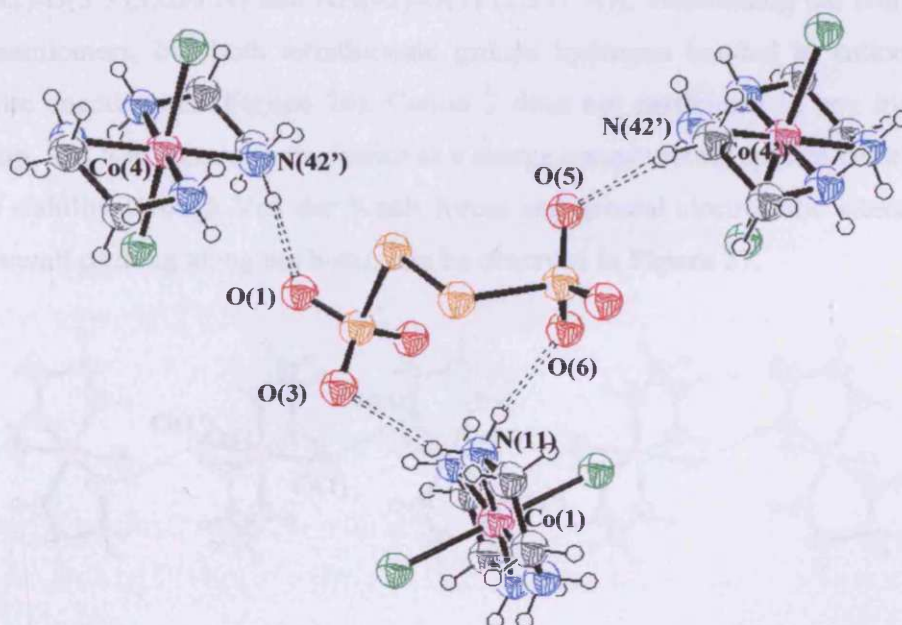


Figure 24 Hydrogen bonding of the tetrathionate counterion in 18

	Cation 1	Cation 2	Cation 3	Cation 4
Co-Cl (\AA)	2.2547	2.2451	2.2357	2.2627
Co-N (\AA)	1.940	1.956	1.959	1.932
Co-N' (\AA)	1.962	1.956	1.966	1.950
N-C-C-N ($^\circ$)	+20.0	+48.0	+48.2	+47.9
N'-C'-C'-N' ($^\circ$)	-20.0	-48.0	-48.2	-47.9

Table 14 Relevant bond lengths and torsional angles for cations of 18

Hydrogen bonded atoms	Hydrogen bond length (Å)	Hydrogen bond angle (°)
Cl(1)···HN(31)	3.259	168.9
O(1)···HN(42)	2.991	162.2
O(5)···HN(42')	3.039	165.9
O(6)···HN(11)	2.956	152.9
O(3)···HN(11)	3.026	155.3

Table 15 Hydrogen bonding data for **18**

Examining the packing, the c-axis is composed of alternate layers of cations 1 and 3, and cation 4. Along the b-axis cations 1 and 3 are linked by hydrogen bonding through the chlorine atom (Cl(1)-HN(31) (3.259 Å)) repeating units of the same enantiomer of cation 1-cation 3 by simple translation (**Figure 25**). Also along the b-axis cation 4 is linked by double hydrogen bonding to two tetrathionate anions (NH(42)-O(5') (3.039 Å) and NH(42)-O(1) (2.991 Å)), maintaining the chirality of the enantiomers, but both tetrathionate groups hydrogen bonded to cation 4 are opposite enantiomers (**Figure 26**). Cation 2 does not participate in any hydrogen bonding, and it is present in the lattice as a charge compensating species contributing to the stability through Van der Waals forces and general electrostatic interactions. The overall packing along the b-axis can be observed in **Figure 27**.

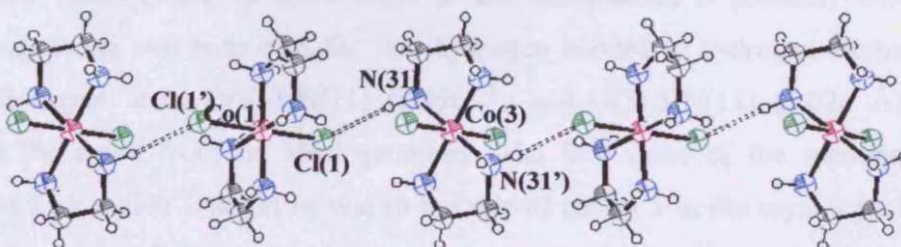


Figure 25 Hydrogen bonding of cations 1 and 3 through chloride along the b axis

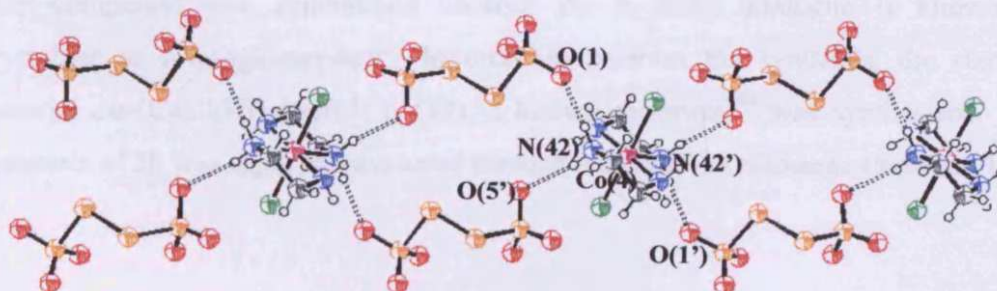


Figure 26 Hydrogen bonding of tetrathionate to cation 4 along the b-axis

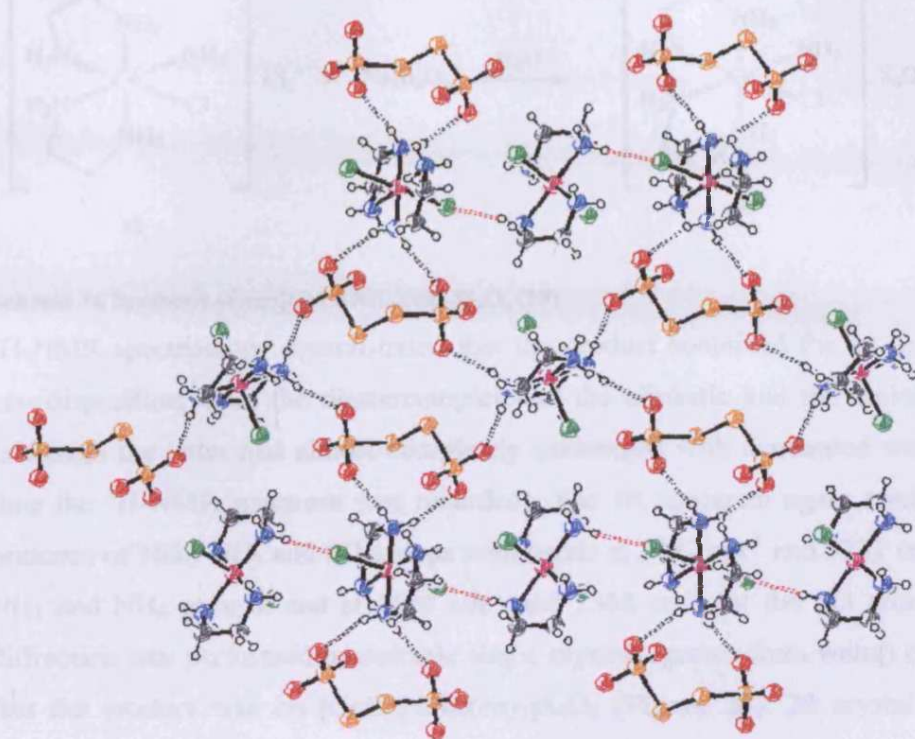
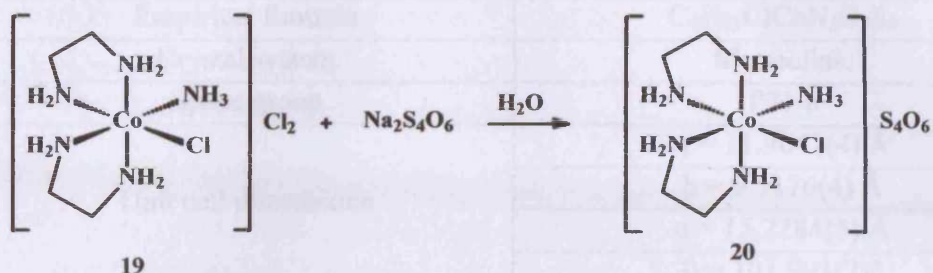


Figure 27 Packing of layers along the c-axis of cations 1 and 3 (red) and cation 4 (black) in **18**, extended along the b axis

The low value of the torsional angle of the tetrathionate is probably due to the packing, as the two ends of $S_4O_6^{2-}$ are hydrogen bonded to hydrogen atoms on the same nitrogen atom O(6)-HN(11) (2.956 Å) and O(3)-HN(11) (3.026 Å) which distort the anion from its ideal geometry. The low value of the torsional angle observed for cation 1 might be due to the role of cation 1 in the crystal packing, as the hydrogen bonding might add some tension to the Co(en) rings.

3.4.3 *cis*-[CoCl(NH₃)(en)₂]S₄O₆ (**20**)

This compound was synthesised because the bromine analogue is known to crystallise as a conglomerate.^[23] In order to perform the synthesis, the starting material *cis*-[CoCl(NH₃)(en)₂]Cl₂ (**19**), a known racemate,^[6] was synthesised. The synthesis of **20** was rapid and occurred through a counterion exchange (Scheme 16).



Scheme 16 Synthesis of *cis*-[CoCl(NH₃)(en)₂]S₄O₆ (20)

¹H-NMR spectroscopy demonstrated that the product contained the en ligands in a *cis*-disposition, from the diastereotopicity of the aliphatic and the aminic protons (although the latter had almost completely exchanged with deuterated water by the time the ¹H-NMR spectrum was recorded). The IR spectrum again confirmed the presence of NH₂, NH₃ and SO groups with bands at 3487 cm⁻¹ and 3237 cm⁻¹ for the NH₂ and NH₃ groups, and at 1629 cm⁻¹ and 1568 cm⁻¹ for the SO groups. X-ray diffraction was performed on suitable single crystals (grown from water) confirming that the product was *cis*-[CoCl(NH₃)(en)₂]S₄O₆ (Figure 28). 20 crystallised in a racemic form, with a monoclinic crystal system and space group P21/n (Table 16). It also crystallised with one molecule of water in the lattice, which was expected to affect the crystal packing.

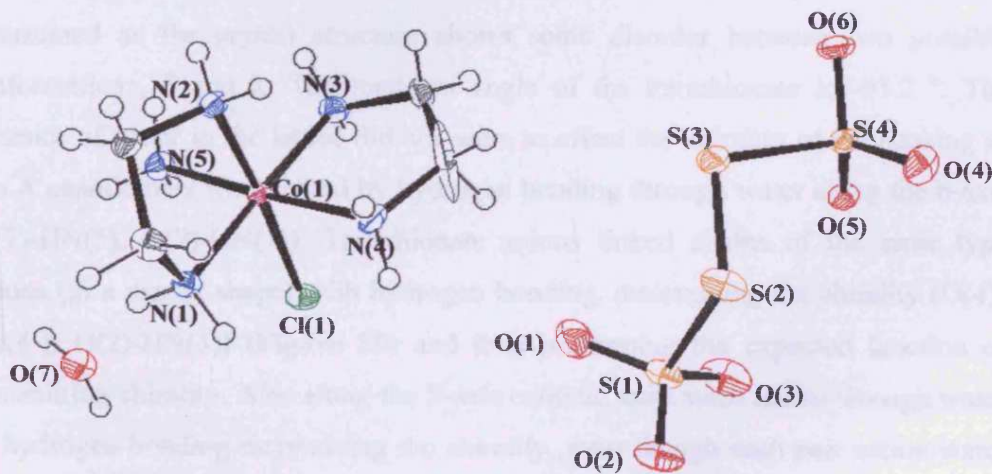


Figure 28 ORTEP view (50% probabilities) of 20

Empirical formula	C ₄ H ₂₁ ClCoN ₅ O ₇ S ₄
Crystal system	Monoclinic
Space group	P21/n
Unit cell dimensions	a = 11.9042(4) Å
	b = 9.5176(4) Å
	c = 15.2284(5) Å
	β = 101.993(2)°
Volume	1687.71(11) Å ³
Temperature	150(2)K
Final R indices [I>2σ(I)]	R1 = 0.0509, wR2 = 0.1204
R indices (all data)	R1 = 0.0725, wR2 = 0.1325

Table 16 Summary of data collection and processing parameters for 20

Hydrogen bond atoms	Hydrogen bond length (Å)	Hydrogen bond angle (°)
O(7)···HN(5')	3.038	158.1
O(7)···HN(1)	2.967	155.8
O(4)···HN(4')	2.936	149.9
O(2)···HN(3)	2.892	151.9
O(5)···HN(1'')	2.965	166.6

Table 17- Hydrogen bonding for 20

The configuration of one of the Co(en) rings was λ, but the other could not be determined as the crystal structure shows some disorder between two possible conformations, δ and λ. The torsional angle of the tetrathionate is -95.2°. The presence of water in the lattice did not seem to affect the chirality of the packing as two Λ enantiomers were linked by hydrogen bonding through water along the b-axis (O(7)-HN(5), O(7)-HN(1)). Tetrathionate anions linked chains of the same type cations (in a zigzag shape) with hydrogen bonding, maintaining the chirality (O(4)-HN(4'), O(2)-HN(3)) (Figure 29) and thus performing the expected function of transmitting chirality. Also along the b-axis cationic units were linked through water by hydrogen bonding maintaining the chirality, even though each pair cation-water was translated and rotated 180° compared to the previous pair. Thus, the molecule of water present in the lattice not only did not encourage racemic crystallisation, but also assisted the transmission of chirality along the b-axis (Figure 30). However, along the a-axis tetrathionate anions were hydrogen bonded through O(5) (O(5)-HN(1'')) to a mirror image layer, forming a centrosymmetric pair and therefore

determining the non-chiral symmetry of the space group (Figure 32). Data of hydrogen bonding is summarised in Table 17.

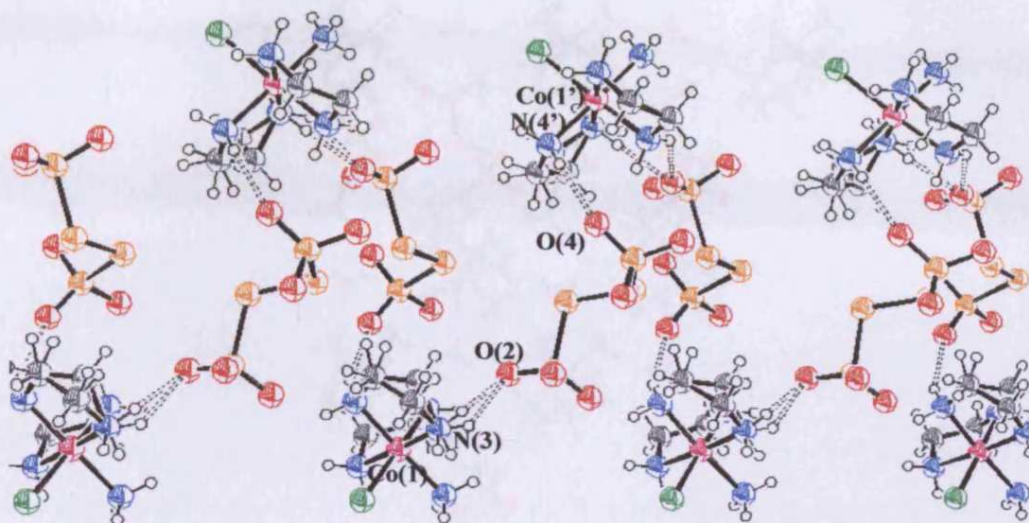


Figure 29 Zigzag chain of cationic units through tetrathionate counterions maintaining chirality along b-axis

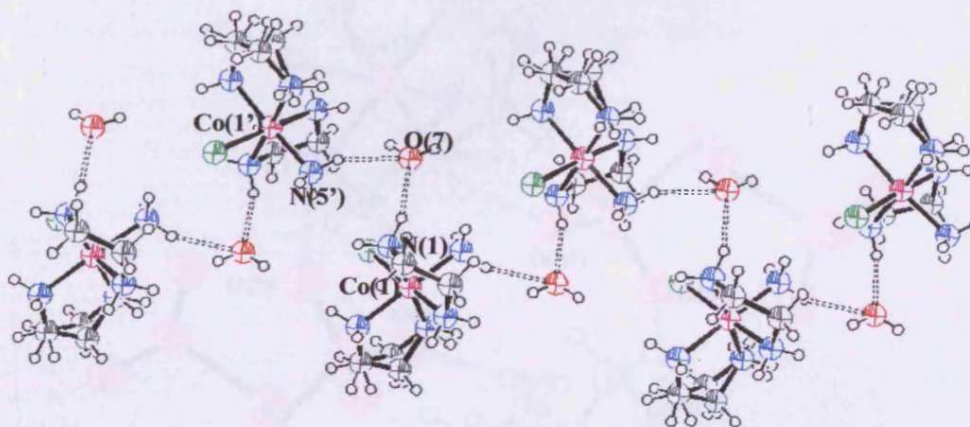


Figure 30 Zigzag chain of cationic units through water maintaining chirality along b-axis

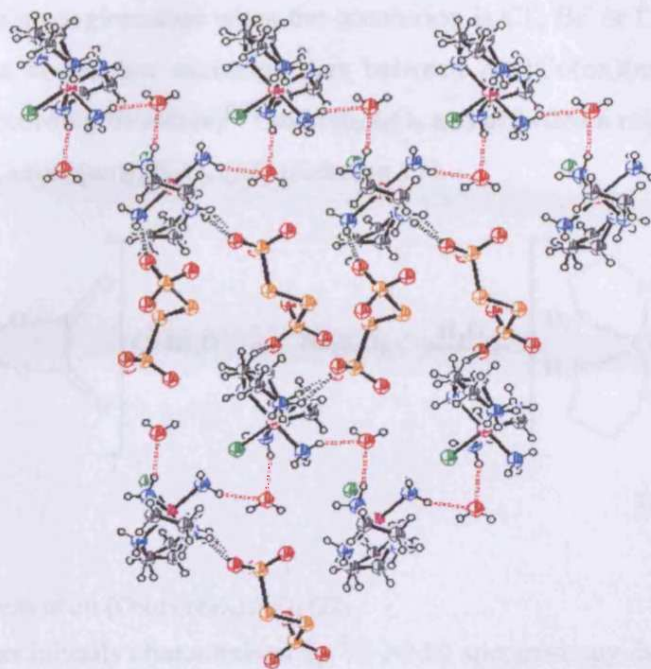


Figure 31 Crystal packing of 20 along the b-axis, with cationic units linked by hydrogen bonding water (red) and cationic units linked by tetrathionate counterions (black)

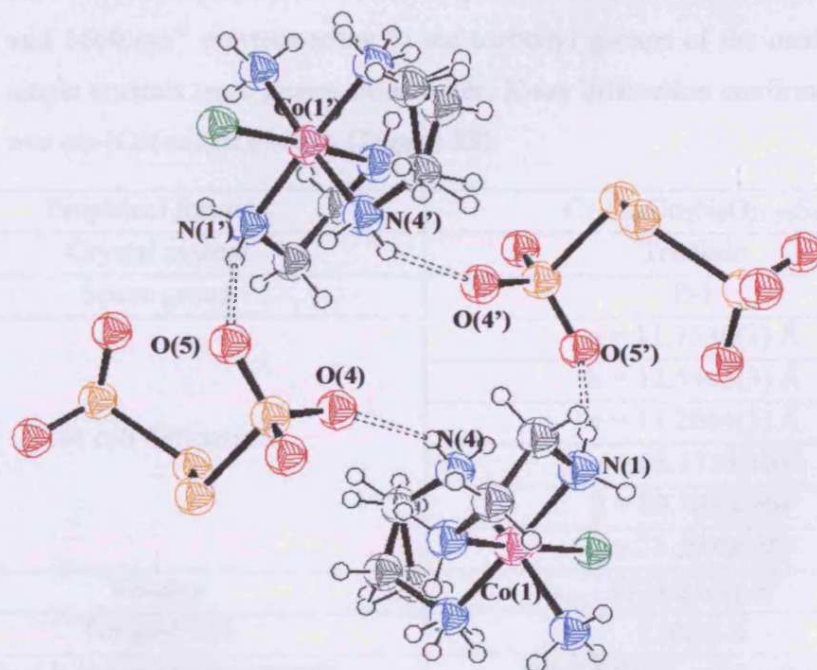
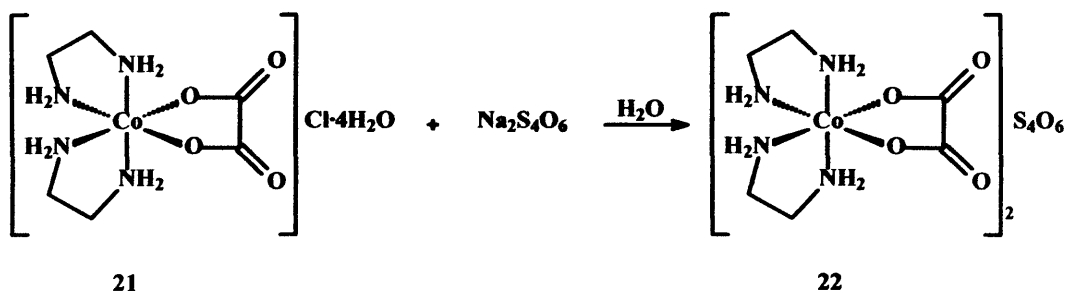


Figure 32 Centrosymmetric pair for 20

3.4.4 *cis*-[Co(ox)(en)₂]₂S₄O₆ (22)

The last complex synthesised in this series was a diethylenediamine monooxalate species chosen because of its potential to form multiple hydrogen bonding sites (higher than compound 20, but lower than compound 17), and which is also known

to crystallise as a conglomerate when the counterion is Cl^- , Br^- or I^- .^[26] The reaction, consisting of a counterion exchange was between *cis*- $[\text{Co}(\text{ox})(\text{en})_2]\text{Cl}\cdot 4\text{H}_2\text{O}$ (**21**) (synthesised according literature)^[27] and $\text{Na}_2\text{S}_4\text{O}_6$ and afforded a relatively high yield (75%) of *cis*- $[\text{Co}(\text{ox})(\text{en})_2]_2\text{S}_4\text{O}_6$ (**22**) (Scheme 17).



Scheme 17 Synthesis of *cis*- $[\text{Co}(\text{ox})(\text{en})_2]_2\text{S}_4\text{O}_6$ (**22**)

The product was initially characterised by $^1\text{H-NMR}$ spectroscopy due to the expected diastereotopicity of the aliphatic protons. The aminic protons were not observed in the spectrum due to deuterated water exchange. The IR spectrum showed two bands at 1700 and 1660 cm^{-1} corresponding to the carbonyl groups of the oxalate. When suitable single crystals were grown from water, X-ray diffraction confirmed that the product was *cis*- $[\text{Co}(\text{ox})(\text{en})_2]_2\text{S}_4\text{O}_6$ (**Figure 33**).

Empirical formula	$\text{C}_{12}\text{H}_{48}\text{Co}_2\text{N}_8\text{O}_{21.50}\text{S}_4$
Crystal system	Triclinic
Space group	P-1
Unit cell dimensions	$a = 11.7530(3)\text{ \AA}$
	$b = 12.5463(3)\text{ \AA}$
	$c = 13.2064(3)\text{ \AA}$
	$\alpha = 68.1750(10)^\circ$
	$\beta = 89.7030(10)^\circ$
Volume	$1721.21(7)\text{ \AA}^3$
Temperature	$150(2)\text{ K}$
Final R indices [$I > 2\sigma(I)$]	$R1 = 0.0565, wR2 = 0.1300$
R indices (all data)	$R1 = 0.0730, wR2 = 0.1376$

Table 18 Summary of data collection and processing parameters for **22**

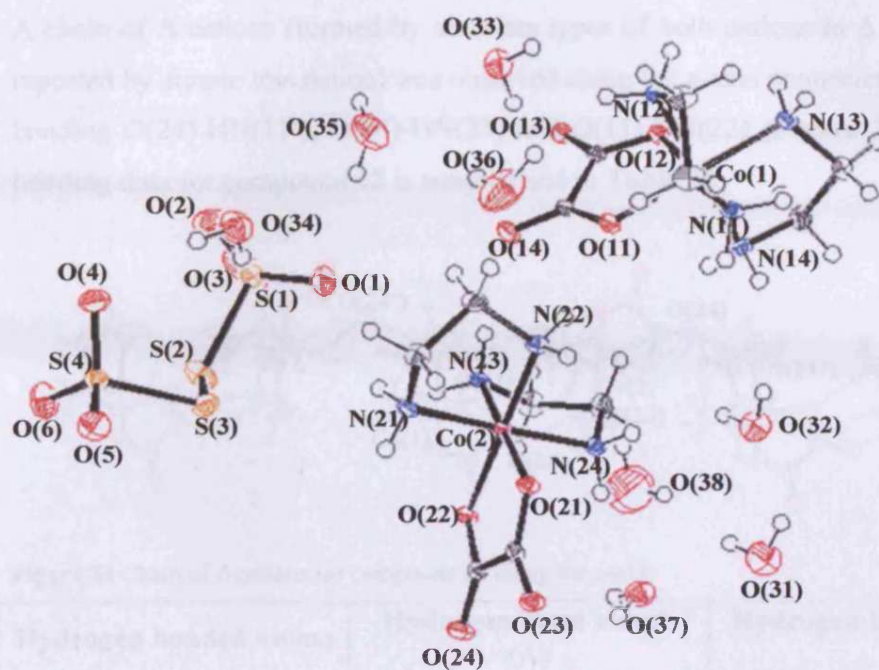


Figure 33 ORTEP view (50% probabilities) of 22

Torsional atoms	Torsional angle (°)
N(21)-C(25)-C(26)-N(22)	-52.4
N(24)-C(23)-C(24)-N(23)	+48.9
N(11)-C(15)-C(16)-N(12)	+48.7
N(14)-C(13)-C(14)-N(13)	-51.2
O(11)-C(11)-C(12)-O(12)	+3.9
O(21)-C(21)-C(22)-O(22)	+1.3
S(1)-S(2)-S(3)-S(4)	+100.1

Table 19- Torsional angles for 22

22 crystallised in a racemic form, space group P-1 and triclinic crystal system (Table 18). In the solid state 22 contained 15/2 molecules of water in the lattice which were probably responsible for the non-chiral space group. This is because there is a high probability that hydrogen bonding could break the pattern of the tetrathionate linkage. The complex consisted of two different $[\text{Co}(\text{ox})(\text{en})_2]^+$ units, each of which had a slightly different torsional angle (Table 19). Both cations had a $\delta\lambda$ configuration of the $\text{Co}(\text{en})$ rings, the lowest conformation for this cation,^[8] whereas the oxalate rings both had a δ configuration, even though the torsional angle was nearly 0°.

A chain of Δ cations (formed by alternate types of both cations in Δ configuration repeated by simple translation) was observed along the a-axis connected by hydrogen bonding O(24)-HN(11'), O(14)-HN(23) and O(11)-HN(22) (Figure 34). Hydrogen bonding data for compound 22 is summarised in Table 20.

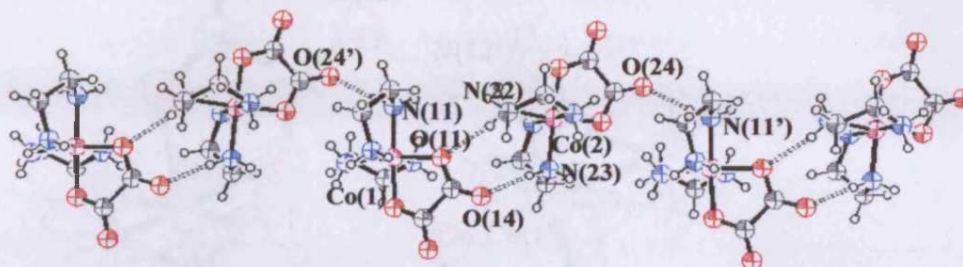


Figure 34 Chain of Δ cations for compound 22 along the a-axis

Hydrogen bonded atoms	Hydrogen bond length (Å)	Hydrogen bond angle (°)
O(1)···HO(35)	3.052	135.2
O(33)···HN(12)	3.052	173.2
O(24)···HN(11')	2.907	126.6
O(13)···HN(12')	3.016	164.2
O(13)···HN(23')	2.875	156.7
O(14)···HN(23)	2.941	171.5
O(23)···HN(11')	2.904	166.5
O(23)···HN(24')	3.002	173.1
O(11)···HN(22)	3.006	157.7
O(5)···HN(21)	2.908	137.9
O(37)···HN(24)	2.932	154.8
O(37)···HN(22')	3.117	155.4
O(6)···HO(31')	2.974	157.4
O(3)···HN(14)	2.880	151.9
O(35)···HO(38)	2.725	160.1
O(35)···HO(38')	2.885	159.0

Table 20- Hydrogen bonding for 22

The chirality was broken through one of the carbonyl groups belonging to cation 1 O(13), which was hydrogen bonded to HN(23') (cation 2) and HN(12') (cation 1), both cations of opposite chirality (Λ). A centrosymmetric pair is formed in the cationic unit 1 through O(13)-HN(12') and vice versa (Figure 35), another

centrosymmetric pair is formed by reciprocal hydrogen bonding in the cationic unit 2 between O(23)-HN(24') and NH(24)-O(37)-HN(22'), with a molecule of water acting as a bridge (Figure 36).

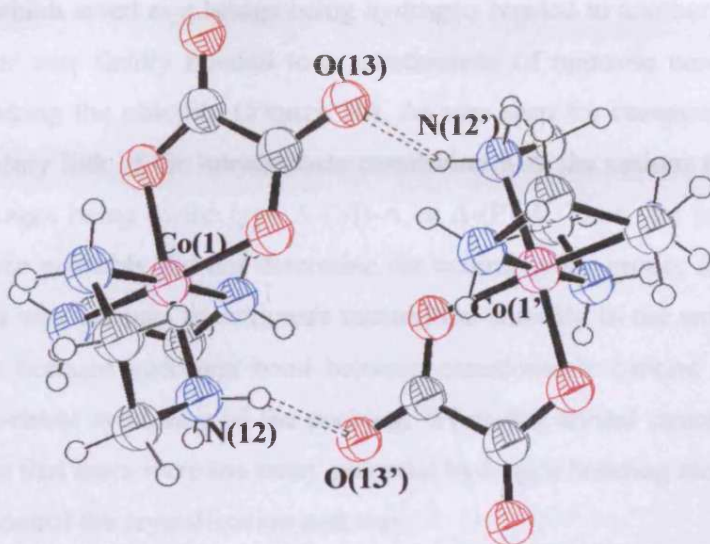


Figure 35 Centrosymmetric pair of cationic unit 1 of 22

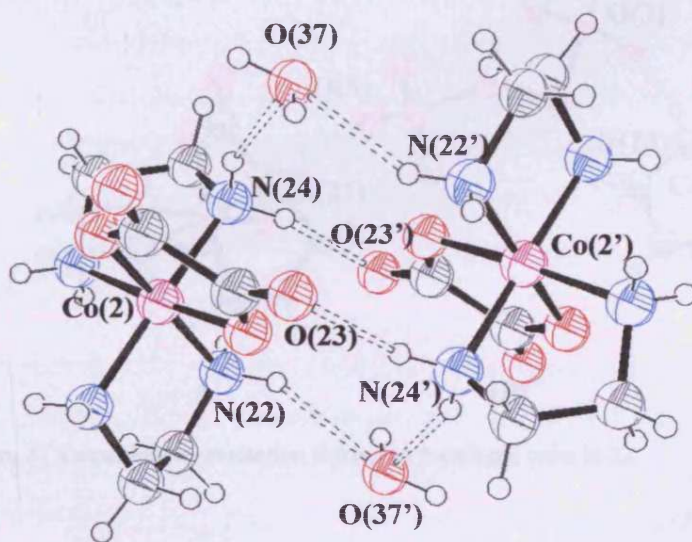


Figure 36 Second centrosymmetric pair of cationic unit 2 of 22 with a water molecule acting as bridge

Considering the effect of the counterion, there was a link of Δ -(P)- Δ , so again the chirality was transmitted along the tetrathionate in the first stage of packing as seen in the crystal packing for compounds 17, 18 and 20. This occurred despite the presence of a high number of solvent molecules in the lattice.

The tetrathionate counterion linked together two cations of the same configuration by hydrogen bonding (O(5)-HN(21) and O(3)-HN(14)), having a unit Δ -(P)- Δ (Figure 37). The tetrathionate anion was hydrogen bonded to three molecules of water, one of which acted as a bridge being hydrogen bonded to another molecule of water; the latter was finally bonded to a tetrathionate of opposite configuration, assisting in breaking the chirality (Figure 38). As was seen for compounds 17, 18 and 20, the primary link of the tetrathionate counterion with the cations transmits chirality, with linkages being of the type Λ -(M)- Λ or Δ -(P)- Δ . Thus, the presence of water in the lattice probably did not determine the achiral space group, as was initially thought. This was because tetrathionate transmitted chirality in the smallest packing unit and also because hydrogen bond between enantiomeric cations already established the non-chiral symmetry of the packing. When the crystal structure was solved, it was clear that there were too many potential hydrogen bonding atoms in the crystal lattice to control the crystallisation pathway.

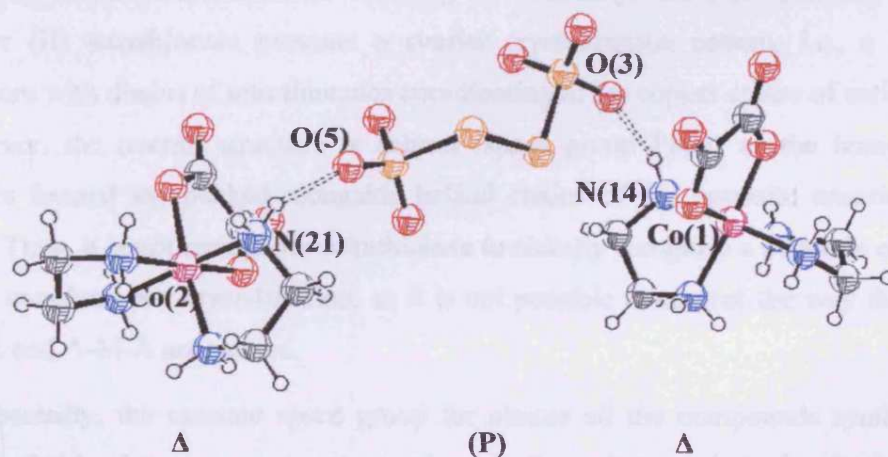


Figure 37 Tetrathionate counterion linking to Δ cationic units in 22

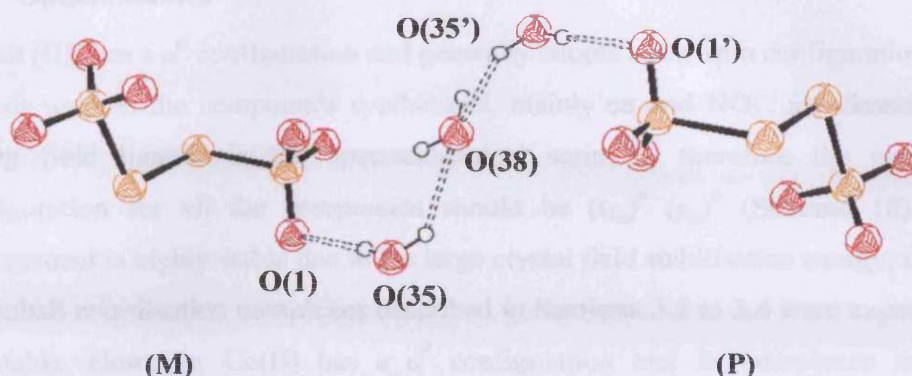


Figure 38 Hydrogen bonding between tetrathionate counterions through molecules of water in 22, breaking the chirality

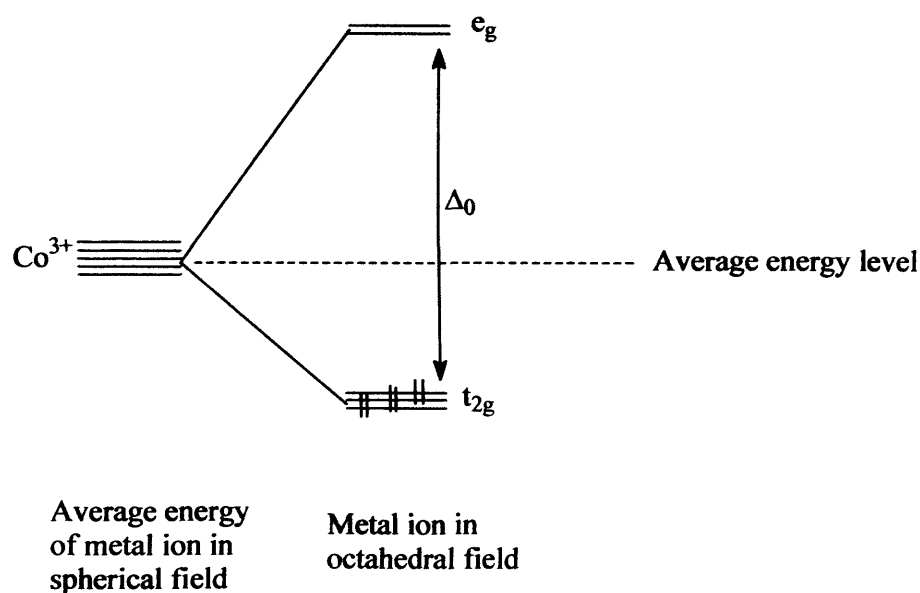
To summarise, the attempts to synthesise a conglomerate $\text{Co}(\text{en})_2$ complex failed, although certain hydrogen bonding patterns were identified amongst the complexes synthesised. The tetrathionate counterion transmitted chirality along one axis of the crystal packing, but its multiple hydrogen bonding sites were usually linked to opposite enantiomers therefore breaking the chirality. Bis-(1,10-phenanthroline) copper (II) tetrathionate presents a similar crystallisation pattern, i.e., a helical structure with chains of tetrathionates coordinating to the copper centre of cations.^[28] However, the overall structure is achiral (space group Pbcn) as the homochiral helices formed are packed alongside helical chains of the opposite enantiomeric form. Thus, it is not enough for tetrathionate to chirally recognise a cation in order to cause conglomerate crystallisation, as it is not possible to control the way the units $\Delta\text{-P-}\Delta$ and $\Lambda\text{-M-}\Lambda$ are packed.

Unexpectedly, the racemic space group for almost all the compounds synthesised was probably due to a centrosymmetric pair formed through hydrogen bonding between cations (via $(\text{en})\text{NH-halide/oxygen}$ hydrogen bond), as this was the smallest unit where symmetry breaking was observed. Thus, the potential of hydrogen bond acceptors within the cationic unit was undervalued, and this should be considered when designing a synthesis of a conglomerate.

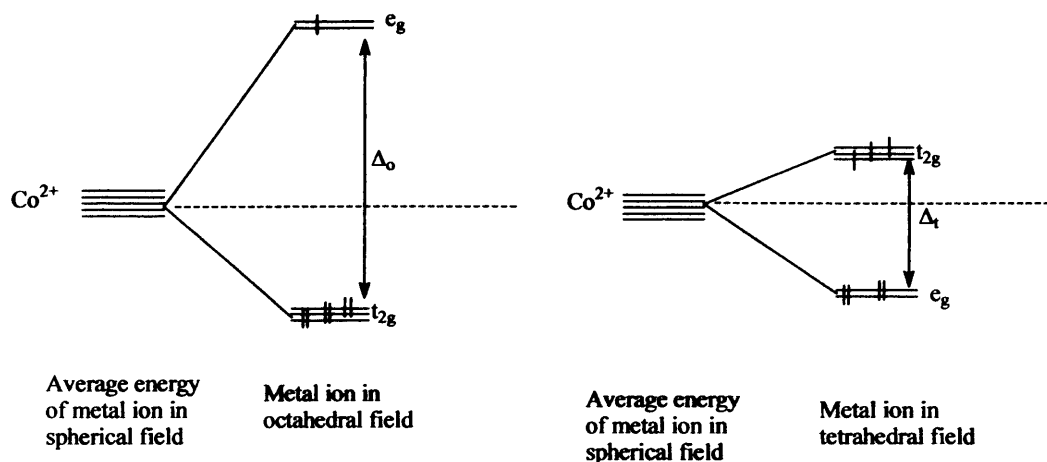
The next phase of the project was the search for any interaction between circularly polarised light and crystallisation patterns. Optical studies were thus performed on selected compounds studied in Sections 3.2 to 3.4.

3.5 Optical studies

Cobalt (III) has a d^6 configuration and generally adopts a low spin configuration. The ligands used in the compounds synthesised, mainly en and NO_2^- , are classified as strong field ligands in the spectrochemical series,^[29] therefore the electronic configuration for all the compounds should be $(t_{2g})^6 (e_g)^0$ (Scheme 18). This arrangement is highly stable due to the large crystal field stabilisation energy, thus all the cobalt coordination complexes described in Sections 3.2 to 3.4 were expected to be stable. However, Co(II) has a d^7 configuration and its complexes may be tetrahedral or octahedral, due to the small difference in stability in crystal field stabilization energy. When such a Co(II) complex is octahedral, its electronic configuration can be $(t_{2g})^6 (e_g)^1$ or $(t_{2g})^5 (e_g)^2$ and therefore is paramagnetic (Scheme 19).^[4] Although cobalt (III) complexes with amine ligands are known to be remarkably stable with respect to thermal substitution reactions, they can undergo photochemical reduction to give cobalt (II) species when irradiated with UV. Cobalt (II) complexes are known to be labile, due to the antibonding nature of the e_g unpaired electron. Thus, if a sample of a stable cobalt (III) coordination complex was irradiated with UV, a small amount of cobalt (III) would be expected to be reduced to cobalt (II). Due to the lability of cobalt (II) species, the coordination complex could easily racemise and therefore be oxidised by air to cobalt (III) as the opposite enantiomer.

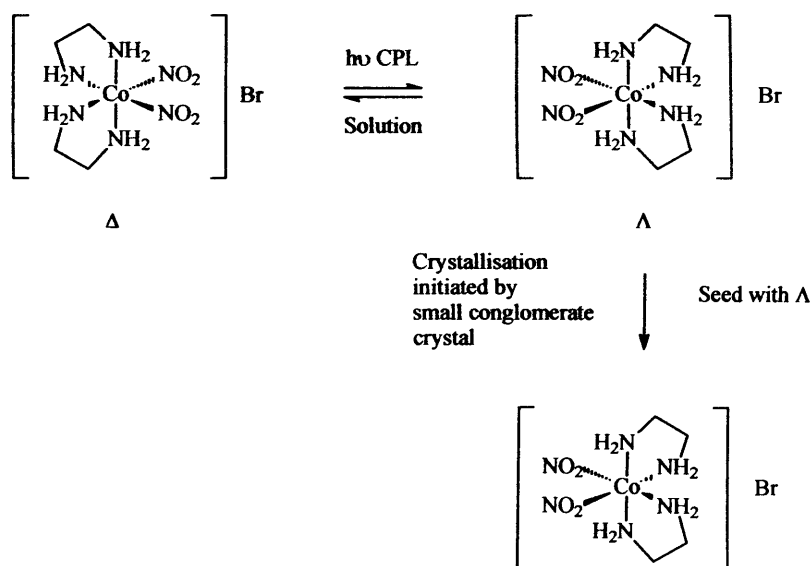


Scheme 18 Electronic arrangement for Co(III) d^6 in a strong octahedral field



Scheme 19 Possible electronic arrangement for Co(II) d^7 in a weak octahedral field and in a tetrahedral field

The aim of this chapter was to recrystallise compounds that crystallised as a conglomerate under CPL and stirring. In this way the first conglomerate crystal could seed the rest of the solution, and with the effect of CPL racemising the rest of the molecules left in solution, all the sample would end up being highly enantiomerically enriched (**Scheme 20**). Compounds **14**, **16b** and $cis-[CoBr(NH_3)(en)_2]S_4O_6$ were already known to crystallise as conglomerate, therefore they were the perfect candidates for the optical studies. Unfortunately, none the new compounds synthesised in this chapter crystallised as conglomerate, however their recrystallisation under CPL was attempted as it has been proved that CPL can affect the crystallisation pattern.^[30]



Scheme 20 Crystallisation of cobalt coordination compounds irradiated with CPL

Each compound was recrystallised under CPL twice. After a sample was recrystallised, both the solid and the mother liquor were tested for any optical activity.

Cis-[CoBr(NH₃)(en)₂]Br₂ (**11**) was reported to crystallise as a conglomerate,^[9] and some studies showed that a solution of **11** could be seeded and a good enantiomeric excess achieved.^[10-12] Even though each time the reaction was performed during this project a racemic polymorph was obtained (**11c**), the reaction was still carried out under UV-CPL irradiation. However, no sign of enantiomeric excess was detected in either the solid obtained or the mother liquor.

Compounds that crystallised as conglomerates (*cis*-[Co(NO₂)₂(en)₂]Br (**14**),^[19] *cis*-[Co(NO₂)₂(en)₂]Cl (**16a**)^[22] and *cis*-[CoBr(NH₃)(en)₂]S₄O₆^[23]) were recrystallised, initially without CPL, to examine the potential for any seeding effect. As no enantiomeric excess was detected, recrystallisation under CPL was performed. Optical activity was measured in both the solid obtained and the mother liquor, with no sign of any enantiomeric excess. *Cis*-[CoBr(NH₃)(en)₂]S₄O₆ decomposed when irradiated with CPL, so no effective recrystallisation could be performed.

The compounds which crystallised in a racemic form were also recrystallised under CPL. The compounds that contained tetrathionate as counterion (*cis*-[CoCl(NH₃)(en)₂]S₄O₆ (**20**), *trans*-[CoCl₂(en)₂]S₄O₆ (**18**) as well as the previously mentioned *cis*-[CoBr(NH₃)(en)₂]S₄O₆) decomposed when irradiated with CPL. There is some evidence that halides can sometimes aid in decomposition of these complexes by reducing cobalt (III) to cobalt (II) and eliminating the halide as a molecules of gas (X₂).^[31] Although many of the compounds irradiated contained halide ligands, only the ones that contained both halide and tetrathionate decomposed. This led to the conclusion that the presence of the tetrathionate and halide anions accelerated the rate of decomposition. This is probably because irradiation photooxidised sulphur, transferring an electron to cobalt. The cation then became much more labile without the stabilising presence of the sulphur moiety, therefore the chances of a halide being eliminated as X₂ were much higher. The tetrathionate anion and other sulphur anions are known to assist in oxidation of metals in aqueous solution by charge transfer upon irradiation with UV.^[32]

No evidence of optical activity was observed for the rest of compounds, probably because the crystallisation occurred faster than the seeding. It also could be possible that some e.e. was achieved but in such a small quantity that the optical activity was within the error of the polarimeter. In this case CPL might have had an effect on crystallisation of conglomerates, but the amplification of chirality (*i.e.* AT) failed. Another possible explanation for the lack of e.e. observed would be in the fact that racemisation between Λ and Δ enantiomers could be very fast, therefore by the time a sample was prepared and the optical rotation measured, the mixture could have reached the equilibrium in the presence of light.

3.6 Summary

The aim of this chapter was to synthesise cobalt complexes that crystallised as conglomerate. A new family of cobalt (III) coordination complexes was synthesised, with a variety of ligands and counterions. None of these complexes actually crystallised as conglomerate. The crystal packing for each compound was studied, focusing on the effect of hydrogen bonding upon the crystallisation pattern. It was found that although many potential hydrogen bonding sites in the tetrathionate might lead to racemic crystallisation, it was usually the hydrogen bonding between the cations that led to the formation of a centrosymmetric unit, and therefore to the smallest packing form that broke the chirality. The role assigned to the tetrathionate counterion as a chiral auxiliary in the solid state was found to work in terms of directing chirality between cations through hydrogen bonding. Unfortunately, this hydrogen bonding was not sufficient to overcome the hydrogen bonding observed between cations which caused the centrosymmetric pair.

All *cis*- compounds synthesised in this chapter were recrystallised under circularly polarised light irradiation to study the potential effect of CPL in the crystallisation pattern and any seeding effect during nucleation. No sign of enantiomeric excess was detected in the optical rotation upon recrystallisation, concluding that either CPL does not influence the equilibrium between Δ and Λ enantiomers, or if this is the case, the crystallisation rate of both enantiomers is similar, and faster than seeding. A third option would contemplate the possibility that racemisation in solution is so fast that by the time the solid was dissolved and optical rotation measured, any enantiomers in excess would have racemised due to the presence of light, although this is known not to be true in some cases (*e.g.* 11).^[5]

3.7 References

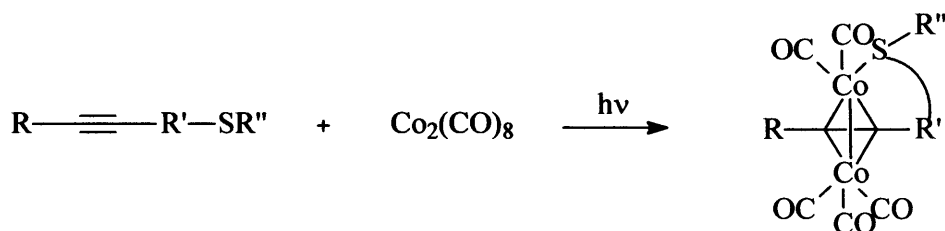
- [1] A. Werner, *Z. Anorg. Chem* **1899**, *21*, 145.
- [2] I. Bernal, G. B. Kauffman, *Journal of Chemical Education* **1987**, *64*, 604.
- [3] I. Bernal, J. Cetrullo, *Inorganica Chimica Acta* **1988**, *150*, 75.
- [4] V. Balzani, V. Carassiti, *Photochemistry of Coordination Compounds*, Academic Press, London and New York **1970**.
- [5] K. Asakura, K. Kobayashi, Y. Mizusawa, T. Ozawa, S. Osanai, S. Yoshikawa, *Physica D: Nonlinear Phenomena* **1995**, *84*, 72.
- [6] J. M. Harrowfield, B. W. Skelton, A. H. White, F. R. Wilner, *Aust. J. Chem.* **1986**, *39*, 339.
- [7] K. Asakura, k. inoue, S. Osanai, D. K. Kondepudi, *Journal of Coordination Chemistry* **1998**, *46*, 159.
- [8] I. Bernal, J. Cetrullo, W. G. Jackson, *Journal of Coordination Chemistry* **1993**, *28*, 89.
- [9] H. Nakagawa, S. Ohba, K. Asakura, T. Miura, A. Tanaka, S. Osanai, *Acta Crystallographica C* **1997**, *53*, 216.
- [10] D. K. K. R. M. Kouichi Asakura, *Chirality* **1998**, *10*, 343.
- [11] K. Asakura, A. Ikumo, K. Kurihara, S. Osanai, D. K. Kondepudi, *J. Phys. Chem. A* **2000**, *104*, 2689.
- [12] K. Asakura, K. Kobayashi, Y. Mizusawa, T. Ozawa, T. Miura, A. Tanaka, Y. kushibe, S. Osanai, *Recent Res. Devel in Pure and Applied Chem* **1997**, *1*, 123.
- [13] F. Guo, M. Casadesus, E. Y. Cheung, M. P. Coogan, K. D. M. Harris, *Chem. Commun.* **2006**, 1854.
- [14] F. A. Cotton, G. Wilkinson, C. A. Murillo, M. Bochmann, *Advanced Inorganic Chemistry*, John Wiley and Sons, **1999**.
- [15] F. v. Bolhuis, P. B. Koster, T. Migchelsen, *Acta Cryst.* **1967**, *23*, 90.
- [16] U. Thewalt, *Z. Naturforsch. Teil B* **1970**, *25*, 569.
- [17] Y. H. Liu, F. R. Fronczek, S. F. Watkins, *Acta Crystallographica C* **1995**, *51*, 1992.
- [18] I. Bernal, J. Myrczek, J. Cai, *Polyhedron* **1993**, *12*, 1149.
- [19] I. Bernal, J. Cetrullo, J. Myrczek, *Materials Chemistry and Physics* **1993**, *35*, 290.

- [20] R. G. Kostyanovsky, V. Y. Torbeev, K. A. Lyssenko, *Tetrahedron: Asymmetry* **2001**, *12*, 2721.
- [21] J. C. Bailar, Jr, *Inorganic Synthesis* **1946**, *2*, 222.
- [22] I. Bernal, *Inorganica Chimica Acta* **1985**, *96*, 99.
- [23] I. Bernal, J. Cetrullo, W. G. Jackson, *Inorg. Chem.* **1993**, *32*, 4098.
- [24] C. H. Langford, H. B. Gray, *Ligand substitution processes*, Benjamin, New York, **1966**.
- [25] I. Bernal, J. Cetrullo, *Inorganica Chimica Acta* **1986**, *122*, 213.
- [26] H. Chun, B. J. Salinas, I. Bernal, *European Journal of Inorganic Chemistry* **1999**, *1999*, 723.
- [27] I. Bernal, J. Myrczek, J. Cetrullo, S. S. Massoud, *Journal of Coordination Chemistry* **1993**, *30*, 29.
- [28] E. Freire, S. Baggio, R. Baggio, M. T. Garland, *Acta Crystallographica C* **1998**, *54*, 464.
- [29] R. Tsuchida, *Bulletin of the Chemical Society of Japan* **1938**, 388.
- [30] B. A. Garetz, J. Matic, A. S. Myerson, *Phys. Rev. Lett.* **2002**, *89*, 175501.
- [31] J. F. Endicott, M. Z. Hoffman, *J. Am. Chem. Soc.* **1965**, *87*, 3348.
- [32] G. H. Khoe, M. Zaw, P. S. Prasad, M. T. Emett, US patent 6884391 ed., USA, **2005**.

Chapter 4: SYNTHESIS AND OPTICAL STUDIES OF ALKYNYL THIOLS AND ORGANOCOBALT ALKYNYL THIOLS

4.1 Introduction

This chapter explores the design and synthesis of alkynes with pendant sulphides and their optical studies. The aim was to coordinate $\text{Co}_2(\text{CO})_8$ to the triple bond of those systems,^[1] and simultaneously coordinate the sulphide to one cobalt, displacing one CO ligand and forming an intrinsically chiral cyclic complex (Scheme 1). The influence of CPL in the coordination of the sulphur group to the cobalt would also be studied.

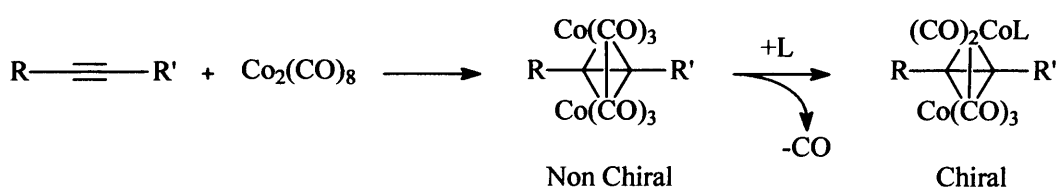


Scheme 1 Overall aim of Chapter 4

The initial approach was to synthesise a chiral alkyne containing a chiral centre in an easily hydrolysable group. In this way the chirality could easily be eliminated from the molecule at any time, leading to a much simpler and achiral alkyne. This would also provide an easy way to separate diastereoisomers that, after hydrolysis, would

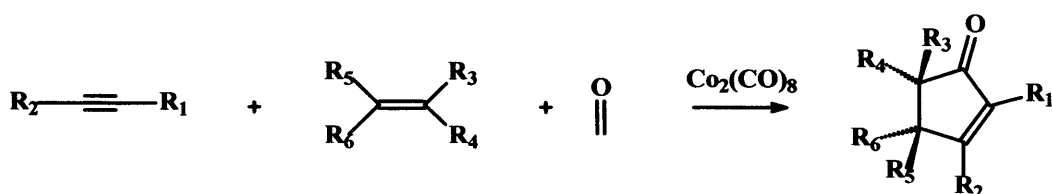
afford enantiomers of the cyclic complex allowing study of their optical properties (*i.e.*, photoracemisation and adsorption maxima).

When an achiral cobalt complex coordinates an achiral alkyne, the resultant molecule is also achiral. Once the organometallic complex was synthesised, an intramolecular reaction was expected to form two enantiomers as the plane of symmetry would be broken. The intramolecular reaction would be a coordination of sulphur to cobalt by displacing one CO ligand. Conversely, if the starting alkyne is chiral, then the intramolecular coordination of a pendant sulphur to the cobalt will produce two diastereoisomers having different chemical properties and therefore being possible to separate. So, in **Scheme 2** if R and R' are achiral, the final product will be a mixture of enantiomers. However, if either R or R' are chiral then the final product will be a mixture of diastereoisomers.



Scheme 2 Coordination of cobalt to an alkyne and subsequent substitution of CO for ligand L

The synthesis of a chiral alkynyl cobalt complex could be useful as a chiral controller in the Pauson-Khand reaction (reaction between an alkyne, alkene and CO in presence of $\text{Co}_2(\text{CO})_8$ to give a cyclopentenone in an overall [2+2+1] cycloaddition, **Scheme 3**).^[2] Camphor derived thiols have been proven to be good chiral controllers, with diastereoisomeric ratios of up to 98:2.^[3-5]



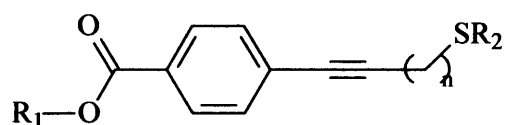
Scheme 3 Pauson-Khand reaction

The initial idea was to synthesise a chiral alkyne with a pendant sulphur that could coordinate to cobalt and displace one of the carbonyl ligands during a photochemical reaction. Study of the stability of the pair of diastereoisomers formed and their photochemical interconversion would allow the design of a system that allows photochemical interconversion of enantiomers. Finally, the reaction would be

performed on enantiomeric cyclic complexes derived from an achiral alkyne under irradiation with circularly polarised light (CPL) with a final mixture of enantiomers expected to be different from 1:1 due to the effect of CPL.

L-Menthyl was chosen to be incorporated into the target molecule as an ester as L-menthol is an alcohol which is readily available as an affordable single enantiomer. In addition, the chirality will be carried through the syntheses without racemisation and thus when sulphur coordinates to cobalt, two diastereoisomers must be formed. The diastereoisomers should be separable and as the ester can be hydrolysed, the two enantiomers will be recovered separately.

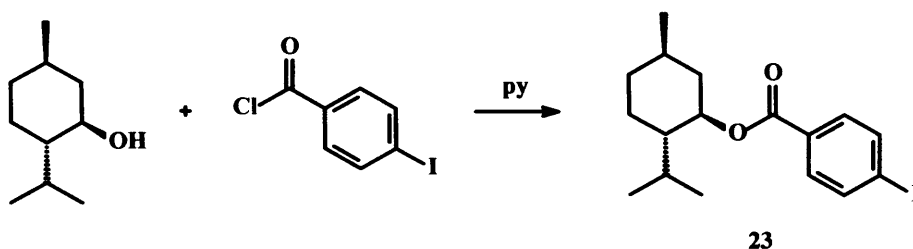
The target molecule was designed to contain a conjugated π system, to increase UV-vis absorbance and increase the chance of an e.e. being obtained when the reactions were performed under CPL. Thus in order to have a big chromophore, an aromatic ring, an ester carbonyl group and an alkyne were present and conjugated in the molecule (Scheme 4).



Scheme 4 Conjugated system of target molecules

4.2 Organic synthesis

The synthesis started with the formation of an ester using L-menthol (a chiral alcohol) and 4-iodobenzoyl chloride (Scheme 5).



Scheme 5 Synthesis of menthyl ester (23)

The reaction was performed in pyridine as solvent, enhancing the electrophilicity of 4-iodobenzoyl chloride, by replacing the chloride group with a better leaving group, but pyridine also enhances the nucleophilicity of the alcohol group. The product was obtained in a 74 % yield after eliminating the pyridinium salts and after removing

menthol by distilling the crude reaction mixture with a Kugelrohr glass oven. **23** (Figure 1) was identified by comparison to the $^1\text{H-NMR}$ description in the literature.^[6]

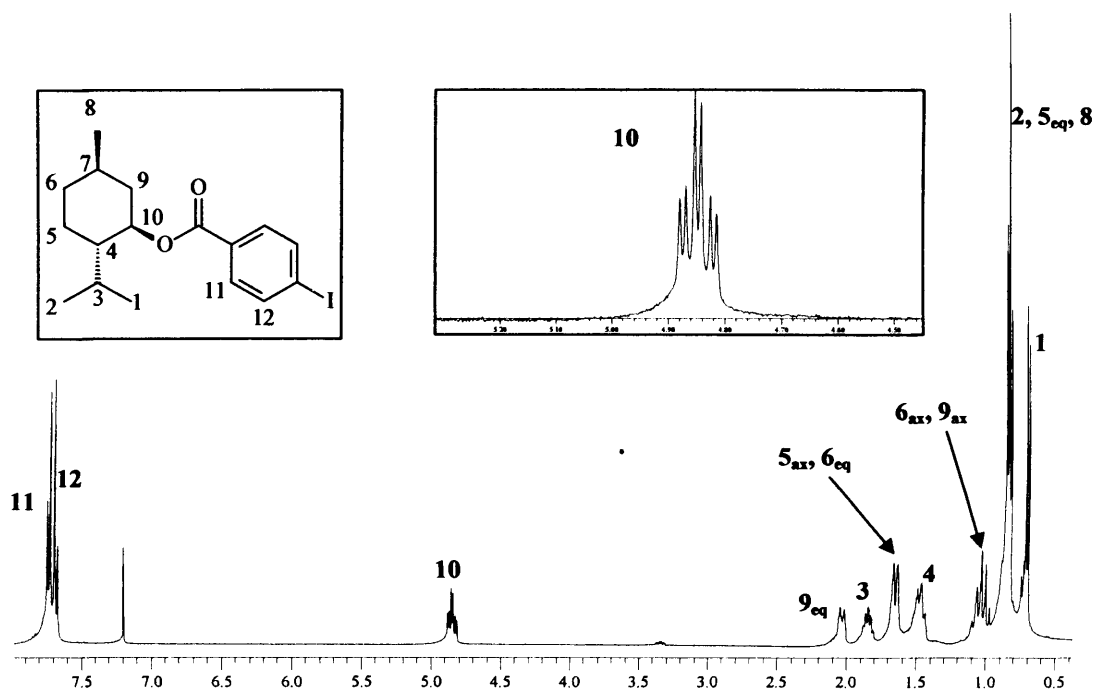
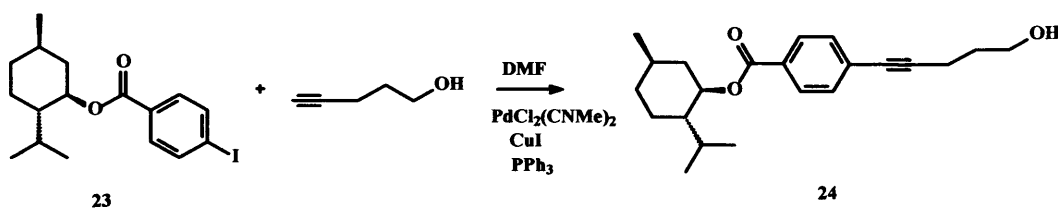


Figure 1 $^1\text{H-NMR}$ spectrum (400 MHz, CDCl_3) of **23**

The next step was the Sonogashira^[7] coupling between the aryl iodide **23** and pentynol forming a new C-C bond, initially using the typical catalysts: $\text{PdCl}_2(\text{NMe})_2$ (2 %), CuI (2 %) and PPh_3 (10 %) (Scheme 6).



Scheme 6 Synthesis of **24**

Aqueous work-up of the crude of the reaction was enough to afford pure **24** (Figure 2) in 96 % yield. Changes were observed in the $^1\text{H-NMR}$ spectrum (Table 1), which were taken as evidence of successful formation of **24**. The chemical shift of the aromatic protons (from 7.6 ppm to 7.4 ppm) and the appearance of two triplets and one multiplet (peaks of the methylene groups of the alkynol, each of them integrating an area equivalent to two protons), led to the conclusion that the product obtained was **24**. This displacement in the chemical shift of the aromatic protons H_{11} was in

accordance with the expected shifting for **24**, as the change of a halide for an sp hybridised carbon would increase the deshielding of H_{11} . M/z (EI/CI) of 343 was also consistent with the new product **24**, with the presence of $[M+H]^+$ and $[M+NH_3]^+$ peaks and observation of some typical fragmentations like the loss of the alcohol and the menthol groups. Also an accurate mass analysis of **24** supported the expected product, with a calculated mass for $[M+H]^+$ of 343.2268, and a measured value of 343.2270. Even though the product was obtained as an oil without chromatography or distillation, it was sufficiently pure to continue without any further purification.

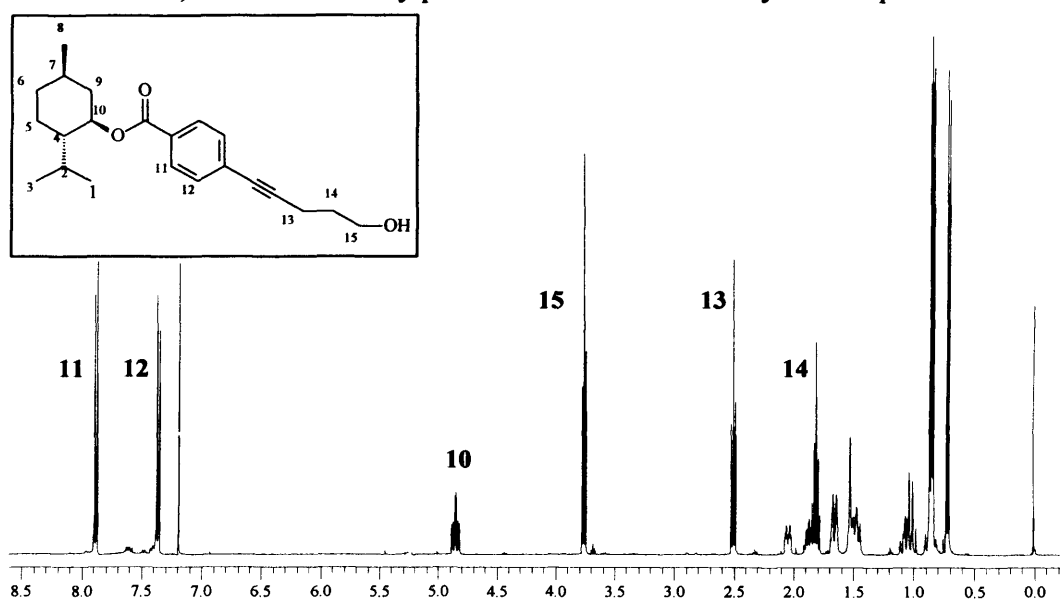


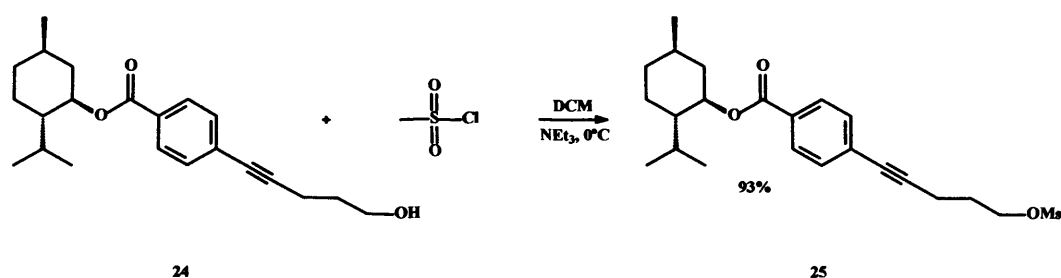
Figure 2 $^1\text{H-NMR}$ spectrum (400 MHz, CDCl_3) of **24**

	23	24
H_{14}	-	1.81 (quin, 2H, $^3J = 6.5$ Hz)
H_{13}	-	2.50 (t, 2H, $^3J = 6.5$ Hz)
H_{15}	-	3.76 (t, 2H, $^3J = 6.5$ Hz)
H_{12}	7.65 (d, 2H, $^3J = 8.3$ Hz)	7.41 (dd, 2H, $^3J = 8.5$ Hz, $^4J = 1.7$ Hz)
H_{11}	7.87 (d, 2H, $^3J = 8.3$ Hz)	7.89 (dd, 2H, $^3J = 8.5$ Hz, $^4J = 1.7$ Hz)

Table 1 Relevant $^1\text{H-NMR}$ data for compounds **23** and **24**

The following step was the conversion of the alcohol to a better leaving group. Initially this was attempted through a tosylation reaction. The reaction was attempted with an equimolar mixture of **24**, tosyl chloride and pyridine, and using DCM as solvent. After 48 hours refluxing, the reaction was just under a third of the way to

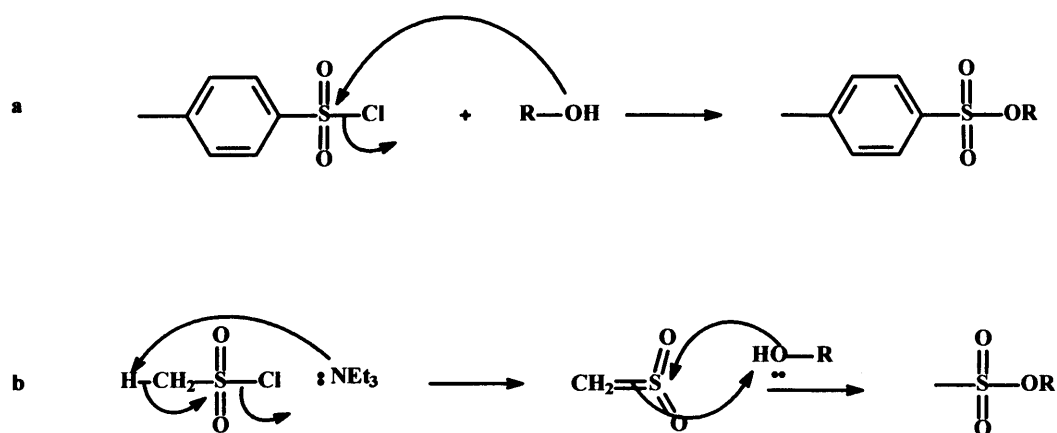
completion as judged by the $^1\text{H-NMR}$ spectrum. At this point a catalytic amount of 4-DMAP was added, expecting that it would increase the speed of the reaction, as DMAP acts as a nucleophilic acylation catalyst. However, the final residue (after performing aqueous work-up) of the reaction was a mixture 2:1 **25:24**. As it took 72 hours to get a conversion of 67 %, the tosylation reaction was replaced with a mesylation reaction (**Scheme 6**). In this way, the alcohol would be transformed into another sulfonate ester of similar characteristics to the tosylate but using a more reactive reagent, in the hope that the reaction would be quicker and would afford a higher yield.



Scheme 7 Synthesis of **25**

The reaction was performed using the alkynol **24** and mesyl chloride, with an excess of triethylamine and DCM as solvent. The reaction had gone to completion in just 2 hours when the reaction crude presented a mixture of the desired product **25** and triethylamine (seen by $^1\text{H-NMR}$ spectroscopy). A simple treatment with 0.1 M HCl removed the excess of NEt_3 affording **25** with 93 % yield.

There was a significant difference in the speed of reaction depending on the use of tosyl chloride or mesyl chloride. This may be explained by a difference of mechanism of the reactions: whilst in the tosylation (**Scheme 8.a**) there is a nucleophilic attack from the alcohol on the tosyl chloride, and displacement of the chloride ligand, in the case of the mesylate (**Scheme 8.b**) attack is from the sulfene (which has been synthesised in situ by reaction of mesyl chloride and triethylamine) to the alcohol from the alkynol.^[8]



Scheme 8 Mechanisms for a) tosylation and b) mesylation

Despite these two different reaction mechanisms, tosyl chloride is much bulkier than mesyl chloride and this fact may also have affected the rate of the reaction.

The product was identified by $^1\text{H-NMR}$ spectroscopy (**Figure 3**, **Table 2**) because of the appearance of a new singlet at 3.0 ppm (corresponding to the mesylate group), and also by the shift of the methylene peaks due to the change of an alcohol group for an electron-withdrawing mesylate group. The most significant shift of the methylene groups was H_{15} , which was shifted from 3.8 ppm to 4.4 ppm. The results from mass spectrometry confirmed the identity of the product, low resolution EI/CI showed the molecular peak at m/z 420.2, and the ionic peak at m/z 341.3, the latter being consistent with a fragmentation of part of the mesyl group (SO_2CH_3). Also high resolution Electrospray presented a measured mass of $[\text{M}+\text{NH}_4]^+$ of 438.2315, compared with the calculated mass for $[\text{M}+\text{NH}_4]^+$ of 438.2309.

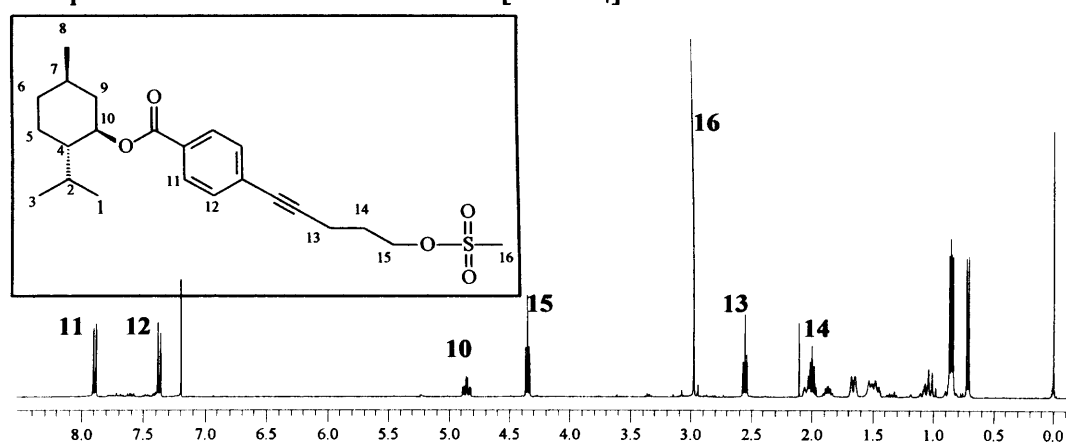
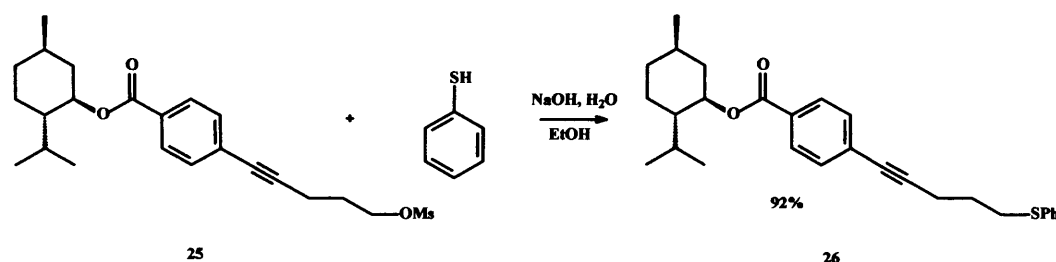


Figure 3 $^1\text{H-NMR}$ spectrum (400 MHz, CDCl_3) of **25**

	24	25
H_{14}	1.81 (quin, 2H, $^3J = 6.5$ Hz)	2.00 (quin, 2H, $^3J = 6.5$ Hz)
H_{13}	2.50 (t, 2H, $^3J = 6.5$ Hz)	2.55 (t, 2H, $^3J = 6.5$ Hz)
H_{16}	-	2.97 (s, 3H)
H_{15}	3.76 (t, 2H, $^3J = 6.5$ Hz)	4.35 (t, 2H, $^3J = 6.5$ Hz)

Table 2 Relevant $^1\text{H-NMR}$ data for compounds **24** and **25**

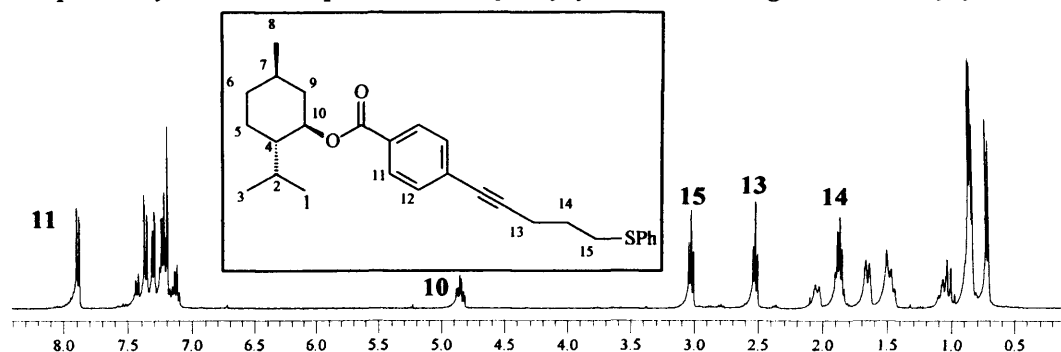
The last step was the synthesis of the alkynethiol, via an $\text{S}_{\text{N}}2$ displacement (**Scheme 9**). An extra step was required to dissolve thiophenol in basic water (which contained 1.1 equivalent of NaOH) before the mesylate was added. In this way the nucleophilicity of the thiol was enhanced and therefore when the mesylate was added no competition between thiophenol and water was expected.



Scheme 9 Synthesis of **26**

According to the integration of the $^1\text{H-NMR}$ spectrum the reaction was 95 % complete after 5 hours. The crude reaction mixture was worked up by adding NH_4Cl (in order to destroy unreacted NaOH). Evaporation of the solvent afforded 92 % yield of **26**, with no need for additional purification.

Product **26** was identified by $^1\text{H-NMR}$ spectroscopy (**Figure 4, Table 3**) from the disappearance of the methyl peak associated with the mesylate group (at 3.0 ppm). Also a shift upfield of the methylene groups was observed, particularly for the methylene group α to the sulphur (H_{15} , from 4.4 ppm to 3.0 ppm), reflecting the reduced electron density of the sulphur relative to the oxygen atom. The aromatic peaks showed an increase of the integration confirming the formation of the desired product.

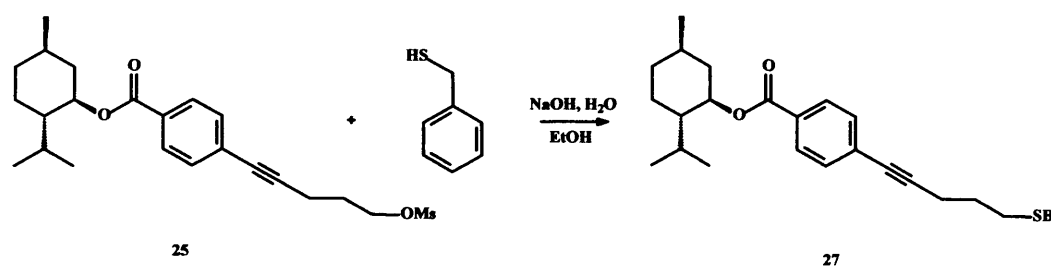
Figure 4 $^1\text{H-NMR}$ spectrum (400 MHz, CDCl_3) of **26**

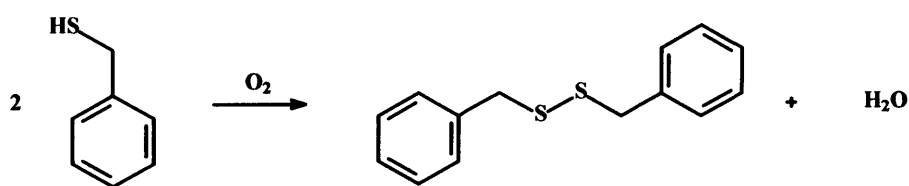
	25	26
H_{14}	2.00 (quin, 2H, $^3J = 6.5$ Hz)	1.86 (m, 2H)
H_{13}	2.55 (t, 2H, $^3J = 6.5$ Hz)	2.52 (t, 2H, $^3J = 6.9$ Hz)
H_{15}	4.35 (t, 2H, $^3J = 6.5$ Hz)	3.02 (t, 2H, $^3J = 7.2$ Hz)

Table 3 Relevant $^1\text{H-NMR}$ data for compounds **25** and **26**

Fragmentation of the molecule under EI/CI shows that the molecular peak of 434 is relatively stable to fragmentation, with an intensity of approx 70 % relative to approx 40 % intensity for $[\text{M}+\text{NH}_3]$ ion. The main peak of the spectrum is at m/z 279.1, corresponding with the loss of the mentholate group. High resolution mass spectroscopy also confirmed the accurate mass of the product: calculated for $[\text{M}+\text{H}]^+$ as 435.2352 and measured as 435.2354.

The synthesis of the alkyne benzylmercaptan (**27**) was performed following the same procedure to that as for the synthesis of **26** (Scheme 10). The crude reaction mixture after 48 hours (seen by $^1\text{H-NMR}$ spectroscopy) contained a mixture of mesylate (**25**) and at least one other product that did not correlate with any of the starting materials and which contained aromatic protons, as well as aliphatic ones. It is possible that with the presence of base and some oxygen a secondary reaction may have led to the formation of the disulphide compound (Scheme 11).

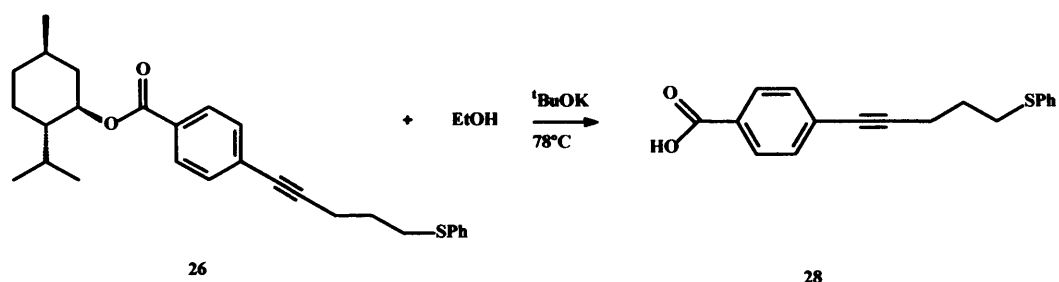
Scheme 10 Attempted synthesis of alkyne benzylmercaptan **27**



Scheme 11 Possible secondary reaction

This hypothesis would explain why the starting material **25** had not yet reacted, and the disappearance of the peak correspondent to benzyl mercaptan in the $^1\text{H-NMR}$ spectrum. It was then decided to add an extra equivalent of benzyl mercaptan to the crude reaction mixture, and let it react under nitrogen. The reaction then occurred, affording in the final crude reaction mixture a 1:1 ratio of **27**:disulphide. The product was purified by chromatography, using first petroleum ether as eluent. When all the disulphide had eluted, the polarity of the eluent was increased to a ratio of 10:1 (petrol:ethyl acetate). A third product of higher polarity eluted after the desired product, and $^1\text{H-NMR}$ spectroscopy indicated that it was menthol. Somehow the alkyne benzylmercaptan **27** had decomposed, either on or before the column. In order to explore whether the decomposition took place during the column, 2D TLC was performed. This showed one product out of the expected diagonal indicating that the decomposition was occurring on the column. Due to the problems encountered in attempts to purify and isolate the product, the reaction was abandoned.

In order to provide an achiral alkyne suitable for eventual CPL irradiation, it was decided to transesterify the chiral menthol ester to an ethyl ester (Scheme 12). The reaction was performed with ethanol as both reactant and solvent, and 10 % $^t\text{BuOK}$ to assist the formation of the ethanoate anion. When the crude reaction mixture was analysed by $^1\text{H-NMR}$ spectroscopy, only the peaks belonging to menthol were observed, the original alkyne peaks having disappeared. Also some solid appeared in the NMR tube, leading to the conclusion that during the reaction the menthol ester had been hydrolysed, but the new ester had not been formed, thus the main products of the reaction were menthol and the carboxylic acid **28**. Isolation of the insoluble solid in DCM and further $^1\text{H-NMR}$ spectroscopy analysis confirmed that the product was the carboxylic acid **28**. $^1\text{H-NMR}$ spectrum of a solution of **28** in deuterated water (Figure 5) showed only the peaks for methylene protons in the aliphatic area as well as aromatic protons corresponding to two phenyl groups in the area 7-9 ppm confirming hydrolysis of the ester.



Scheme 12 Synthesis of carboxylic acid 28

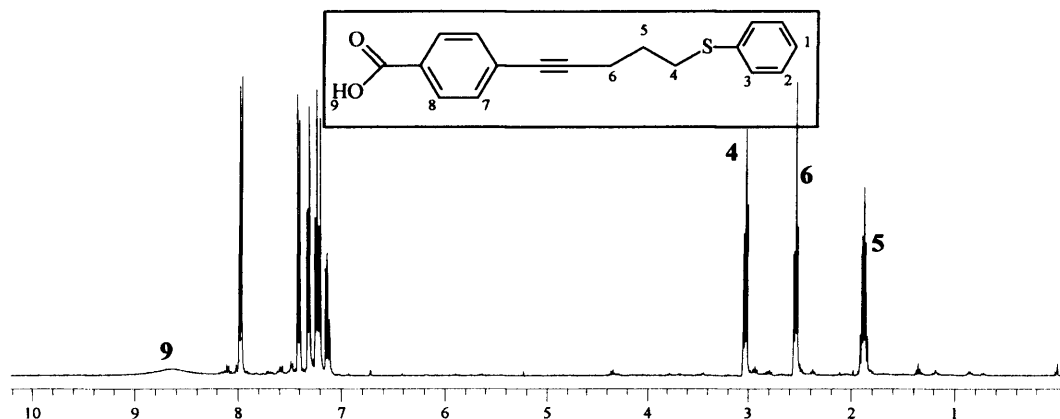
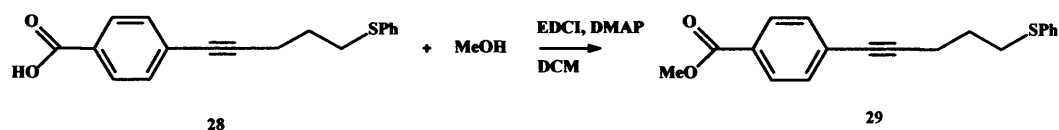


Figure 5 ¹H-NMR spectrum (400 MHz, D₂O) of 28

The yield of the reaction was not very high (24 %, probably because the solvent may have been wet), but it was high enough to proceed to the next step, *i.e.*, the esterification of the carboxylic acid with an achiral alcohol to give the achiral ester which had been expected from the attempted transesterification (Scheme 13). The esterification reaction was attempted following a method described in the literature, using stoichiometric amounts of EDCI and DMAP.^[9] The reaction was performed in DCM with methanol, in order to simplify the potential ¹H-NMR spectrum with respect to the number of peaks added to the aliphatic region.



Scheme 13 Synthesis of 29

The product obtained had oily consistency compared to the starting material 28, which was a solid, typical of converting an acid to an ester. The ¹H-NMR spectrum (Figure 6) showed the appearance of a singlet at 3.8 ppm belonging to the new methyl group, which had the appropriate integration compared to the rest of the spectrum. Accurate mass spectrum confirmed that the product obtained was as

expected, with a calculated mass (m/z) for the ion $[M+H]^+$ of 311.1100 and a measured mass of 311.1097.

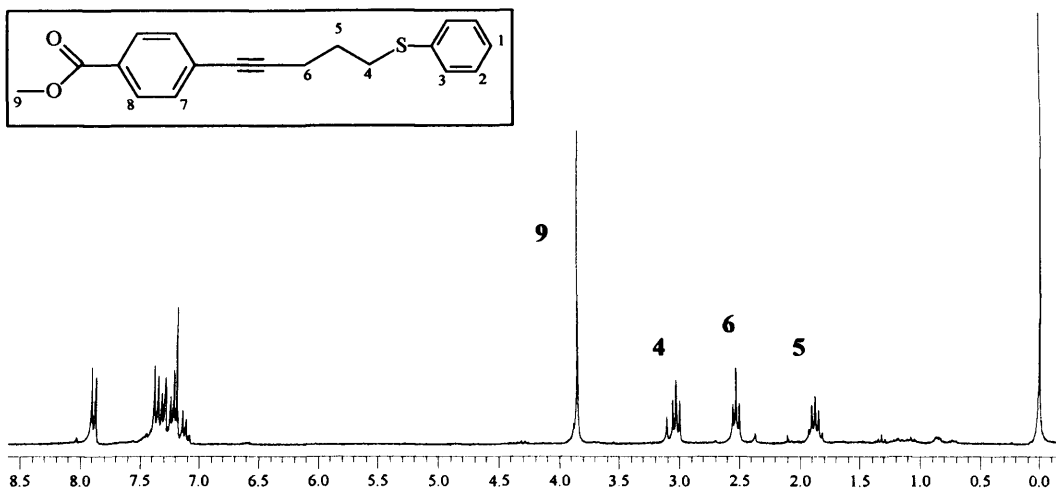


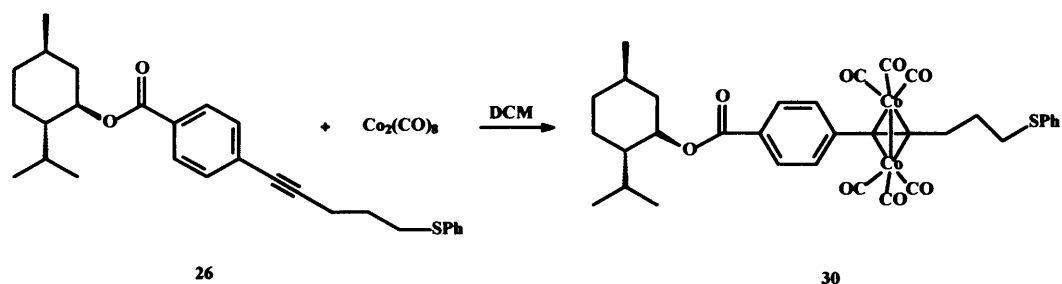
Figure 6 $^1\text{H-NMR}$ spectrum (400 MHz, CDCl_3) of **29**

Eventually the oil crystallised from a mixture of ethyl acetate and petrol to provide pure material in 48% yield.

4.3 Organometallic synthesis

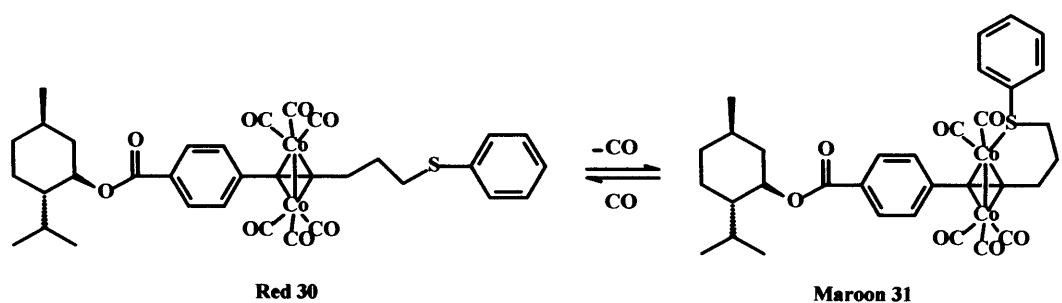
Once all the alkynethiols were synthesised, the next phase was the coordination of $\text{Co}_2(\text{CO})_8$ to the triple bonds.^[1] The first reaction attempted was performed under an inert atmosphere using **26** as alkyne source and degassed DCM as solvent to obtain the organometallic complex **30** (Scheme 14). When $\text{Co}_2(\text{CO})_8$ was added the mixture started bubbling indicating a gaseous release of CO. The reaction turned to a dark red colour, and was followed by TLC. When all the starting material had reacted a small sample of **30** dissolved in deuterated chloroform was analysed by $^1\text{H-NMR}$ spectroscopy. The spectrum presented highly noisy base line and no peaks, so no useful information could be extracted. The broadening of the baseline could be attributed to traces of paramagnetic Co^{2+} that were present in solution.*

* Although much care was taken in degassing all reactants and solvents, it is possible that a small amount of oxygen penetrated in the Schlenk flask, oxidising Co^0 to Co^{2+} .



Scheme 14 Synthesis of **30**

The crude reaction mixture was filtered through silica under nitrogen and then placed in the freezer for a few days, hoping that crystallisation would occur. After some days no crystals had grown and a black deposit was observed at the bottom of the Schlenk flask. The deposit indicated the presence of cobalt metal, showing the product was very unstable and decomposed very easily. TLC showed that apart from cobalt metal there were also two different products: the least polar, showing a bright red colour on the silica plate; and the most polar, indicated by a maroon colour. The presence of two coloured products (two products containing cobalt), may suggest that the coordination of the sulphur to the cobalt might have occurred during the cobalt coordination reaction (**Scheme 15**). In order to characterise the products obtained, a sample of the crude reaction mixture was separated by chromatography. The eluent was an initial mixture of petrol:ether 3:1, which was gradually increased to a 1:1 mixture. The first product eluted had a bright red colour (**30**), the second one had a maroon colour (**31**).



Scheme 15 Two possible products after the synthesis of **30**

¹H-NMR spectrum of a deuterated chloroform solution of **30** presented simply broad bands, and no multiplicity was observed. This could occur either because the product contained some traces of Co^{2+} (unlikely after purification by chromatography), or because of the rotation of the CO groups around the cobalt which at room temperature is likely to occur on the NMR timescales. The spectrum of **30** was

compared to the spectrum obtained for compound **26** (Figure 7, Table 4). A large shift downfield was observed for the methylene group α to the alkyne (from 2.5 ppm to 3.1 ppm). A smaller shift was observed also for the methylene β to the alkyne: the position of the protons shifted downfield (from 1.8 ppm to 1.9 ppm). This is typical and shows the electronic density change in the triple bond due to the coordination of the cobalt. Also, a downfield shift for the protons that are *ortho* to the alkyne was observed in the aromatic area (from 7.36 ppm to 7.42 ppm).

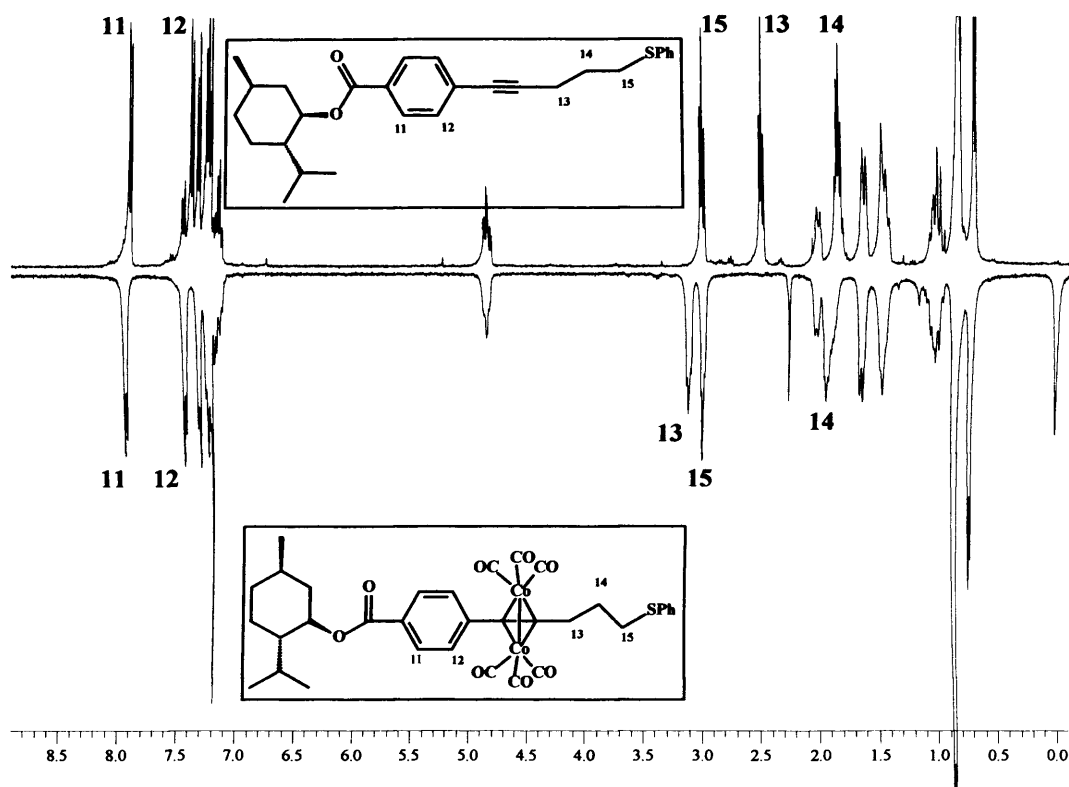


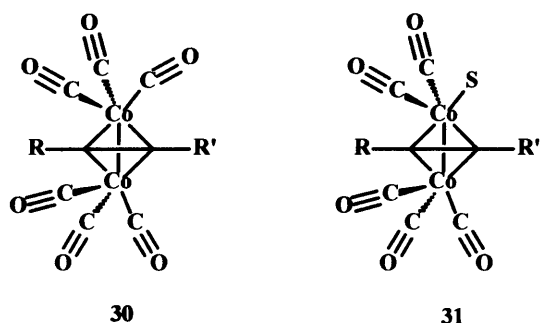
Figure 7 Comparison between $^1\text{H-NMR}$ spectra (400 MHz, CDCl_3) of compound **26** (top) and compound **30** (bottom)

	26	30
H_{14}	1.86	1.96
H_{13}	2.52	3.15
H_{15}	3.02	3.02
H_{12}	7.36	7.42
H_{11}	7.89	7.92

Table 4 Relevant $^1\text{H-NMR}$ data for compounds **26** and **30**

Although $^1\text{H-NMR}$ spectrum was concordant with compound **30**, it could not be definitely identified as **30** only by NMR spectroscopy, as cobalt can not be observed by $^1\text{H-NMR}$ spectroscopy. The $^1\text{H-NMR}$ spectrum was of high enough quality to ascertain that the metal had an oxidation state different from +2, and also that a mentholate group was part of the molecule. Mass spectrum analysis was performed by EI/CI and MALDI techniques. When analysed by EI/CI a theoretical isotope model for $[\text{M-2CO}]^+$ was concordant with the observed data. When analysed by MALDI (using DCTB as matrix) the theoretical model for $[\text{M-6CO+DCTB}]^+$ was also fully concordant with the observed data. Considering all these data it is not possible to conclude that **30** is the proposed product, but it is clear that the product contained two atoms of cobalt and at least four carbonyl groups. In the absence of a crystal structure these data were the best proof possible of the structure, along with IR, analysed below.

At this point, **31** was analysed and the results were compared to those obtained for **30**. After the compounds were separated by chromatography, the simplest analysis that could be performed was IR (Scheme 16). The data for the carbonyl groups obtained are summarised in Table 5.



Scheme 16 Carbonyl system for **30** and **31**

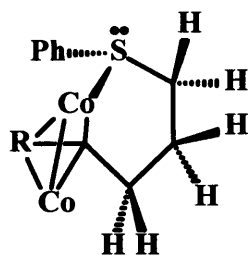
30 (red) cm^{-1}	31 (maroon) cm^{-1}
2090.7	2090.7
2054.4	2065.3
2028.5	2054.0
	2015.6
	1964.3

Table 5 IR data for carbonyl groups of compounds **30** and **31**

Compound **30** had higher symmetry due to six equal ligands around the cobalt, compared to compound **31**, thus less bands were expected in the IR spectrum. When

compound **30** was analysed by IR spectroscopy three bands were observed due to the CO stretching. Each CO group had a different environment, strongly influenced by the *trans* effect. Although the geometry around the cobalt is not perfectly octahedral, a difference of the *trans* ligands can influence the position of the bands for the CO groups in the IR spectrum. Thus, one CO ligand will be *pseudo-trans* to the other cobalt, and the other two will be *pseudo-trans* to an aromatic ring and an aliphatic chain. These different environments probably accounted for the difference in the position of the bands. Conversely, in compound **31** the symmetry has been broken by the presence of an atom of sulphur, thus presenting the molecule C_S symmetry and an expectation of five bands in the IR spectrum coinciding with the experimental data. **31** showed a different environment for each CO group. Two of the CO ligands from compound **31** were expected to have approximately the same environment as in compound **30**, *i.e.*, the two ligands that were *trans* to R and R', and were coordinated to the atom of cobalt which was adjacent to three CO ligands. The ligands were also expected to stretch at the same frequency as their homologues in compound **30**. This was observed in the IR spectrum. The average carbonyl frequency was lower for compound **31** (2038.0 cm^{-1}) than for compound **30** (2057.8 cm^{-1}), in accordance with the exchange from a carbonyl to a more electron-releasing ligand.^[3, 10] As sulphur is a less π -acidic donor than carbonyl, when the sulphur atom substituted a carbonyl group coordinated to cobalt, there was a larger amount of electronic density in the metal available for back-bonding to the rest of the carbonyl groups. This made them more electronically rich, and their triple bond character was diminished as it was more delocalised. Therefore, the stretching bands in the IR spectrum were shifted to a less energetic field.

$^1\text{H-NMR}$ spectra of **30** and **31** looked very similar, however, their comparison (Figure 8) shows some differences. In compound **31** one of the lone pairs of the sulphur atoms was coordinated to the cobalt, and thus the geometry around the sulphur was expected to be tetrahedral (Scheme 17). The protons of the methylene groups belonging to the new ring formed were therefore expected to show greater chemical shift differences than those due to menthol-induced diastereotopicity prior to ring formation.



Scheme 17 Tetrahedral disposition around the sulphur, with diastereoisotopic protons in the new ring formed

Around the region of 3 ppm, two peaks corresponding to the methylene protons for the two methylene groups of **30** (H_{13} and H_{15}) were split into four signals, although it was not possible to fully assign them. Also for the other methylene group of **30** (H_{14}) the appearance of another new peak at 1.4 ppm could indicate another case of diastereotopicity. In the aromatic region most of the peaks seem to be shifted downfield, which could be explained by the electronic enrichment around the Co-Co and Co-C bonds. Thus, **31** seems most likely to be the product of the coordination of sulphur on **30**, although at this point it is not absolutely proven.

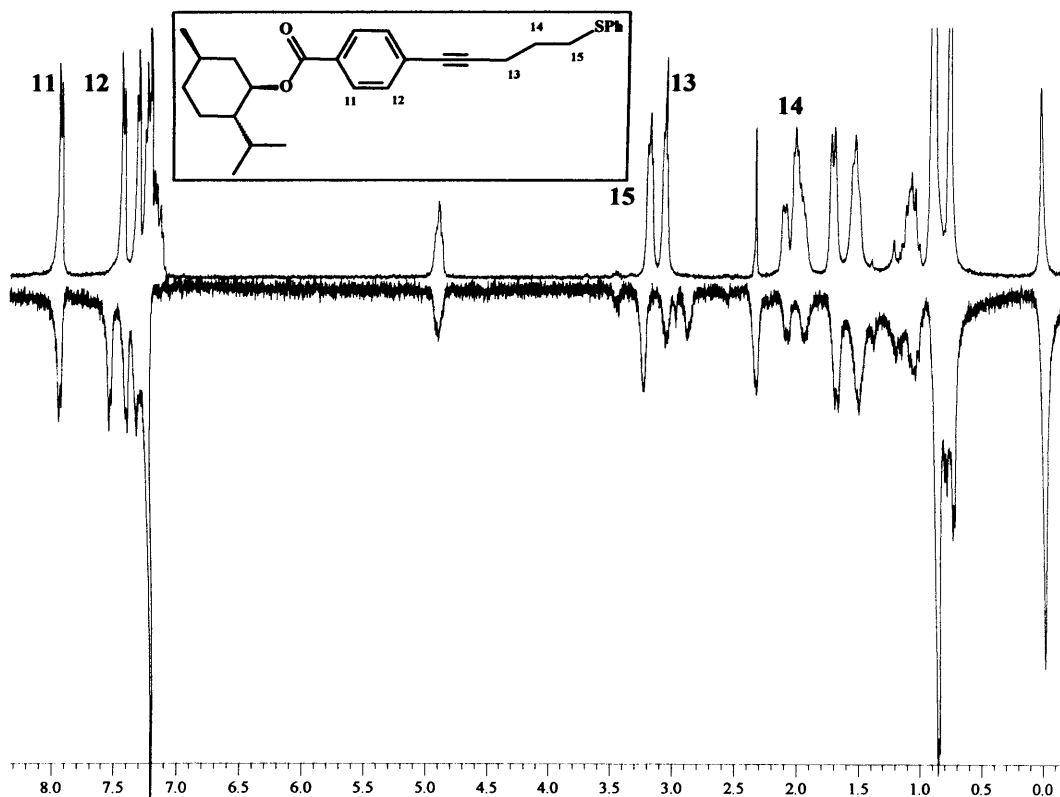


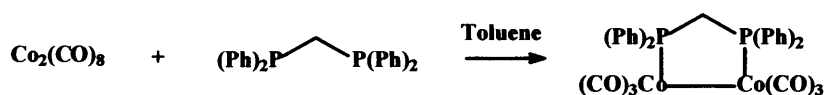
Figure 8 Comparison of $^1\text{H-NMR}$ spectra (400 MHz, CDCl_3) of **30** (top) and **31** (bottom)

In order to definitely prove the structures of **30** and **31**, an attempt was made to grow crystals from ether, from ether-octane and from toluene, with no success. **30** and

particularly **31** were very unstable and decomposed even when kept in the freezer under inert atmosphere.

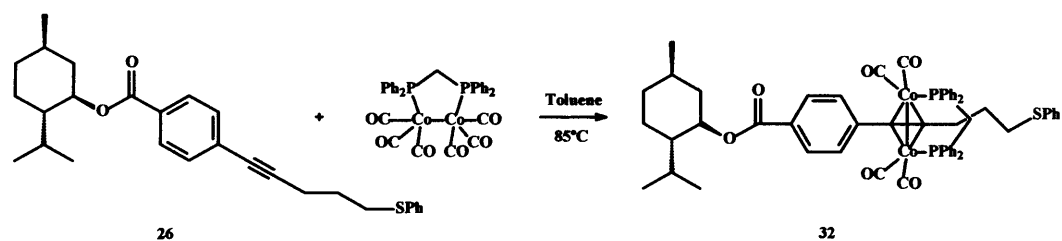
Due to the high levels of instability of **30** and **31**, it was decided to synthesise a homologous compound that contained an extra stabilising group – bisdiphenylphosphinomethane (dppm). There are many examples in the literature of dicobalthexacarbonyl alkyne complexes stabilised with dppm.^[11, 12]

The compound could possibly be synthesised in two different ways: **30** could react with dppm, or **29** could be coordinated to $\text{Co}_2(\text{CO})_6\text{dppm}$. The latter seemed more appropriate due to higher stability of starting material **29** and possibly of the cobalt complex. $\text{Co}_2(\text{CO})_6\text{dppm}$ was thus synthesised according to the method described in the literature^[12] and showed much higher stability than $\text{Co}_2(\text{CO})_8$ (Scheme 18).



Scheme 18 Synthesis of $\text{Co}_2(\text{CO})_6\text{dppm}$

The synthesis of **32** was then attempted under the same conditions as the synthesis of **30** (Scheme 19). ³¹P-NMR spectrum of a solution of **32** in deuterated chloroform showed a signal corresponding to $\text{Co}_2(\text{CO})_6\text{dppm}$ at 61.1 ppm, and another two signals at 38.4 ppm and 25.4 ppm. The peaks at 38.4 ppm and 61.1 ppm were of the same relative intensity. The peak at 25.4 ppm was of low intensity and it was assumed to be a by-product of the reaction. It seemed likely that the peak at 38.4 ppm was the desired product of the reaction. Thus, the reaction had gone to 50 % conversion and there was at least one secondary reaction that afforded a by-product that contained phosphorous. The reaction was reattempted using a 2:1 ratio of starting materials (**29**: $\text{Co}_2(\text{CO})_6\text{dppm}$). The product was a mixture of **32**, dppm-oxide and the impurity previously seen by ³¹P-NMR spectroscopy at 25.4 ppm.



Scheme 19 Synthesis of **32**

The reaction was then attempted in refluxing toluene to force the reaction to completion. The high temperature would assist in loss of CO, giving vacant coordination sites and allowing the alkyne coordination. After 1 hour ^{31}P -NMR spectrum showed just one peak at 38.2 ppm with no traces of starting material or other impurities. The ^1H -NMR spectrum of the product showed some similarity to starting material **26**, but it also showed the presence of some cobalt (II) in the sample, as the spectrum presented broad bands.

Comparing ^1H -NMR spectra of starting material **26** and product **32** (Figure 9) the appearance of more peaks can be observed. This was expected due to the diastereotopic protons of the methylene bridge of the dppm. Some of the methylene peaks of the pentyne chain had shifted downfield (as was observed in compounds **30** and **31**) and some of the aromatic protons had also shifted downfield.

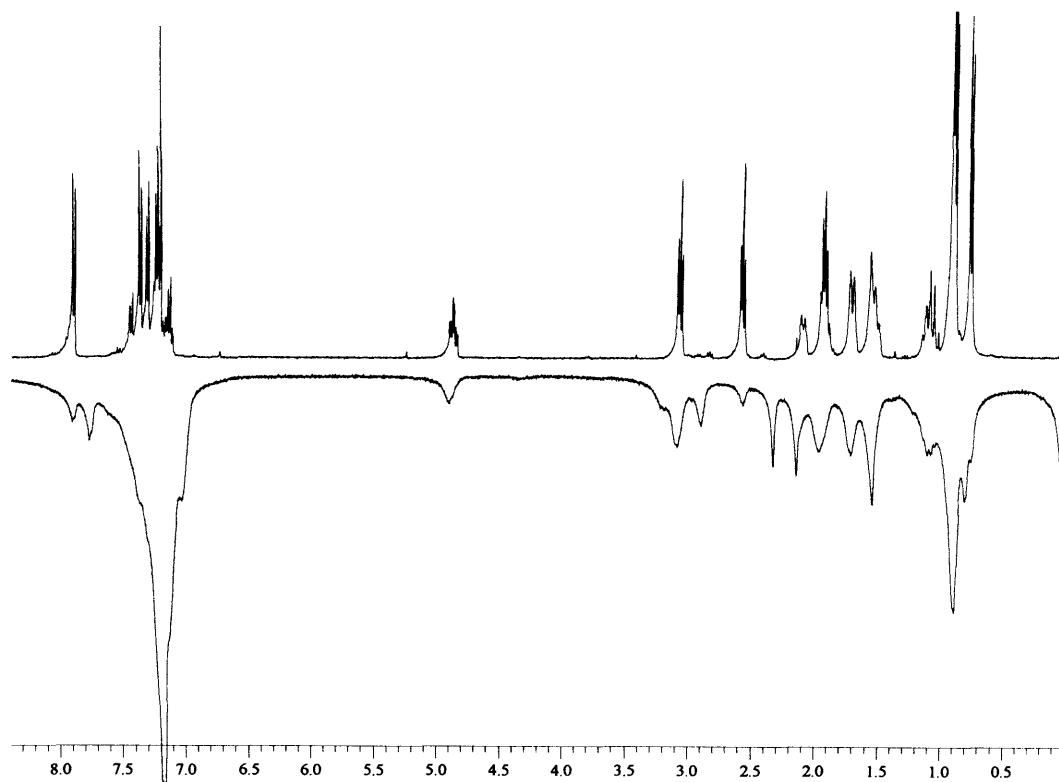


Figure 9 Comparison of ^1H -NMR spectra (400 MHz, CDCl_3) of **26** (top) and **32** (bottom)

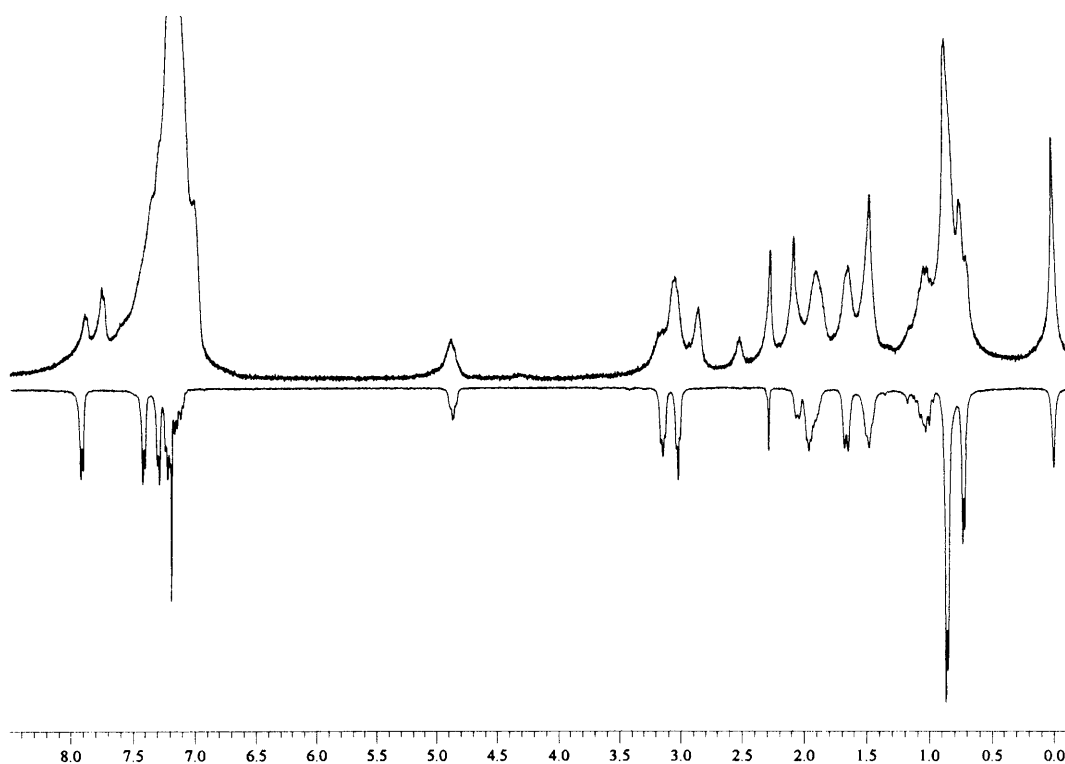


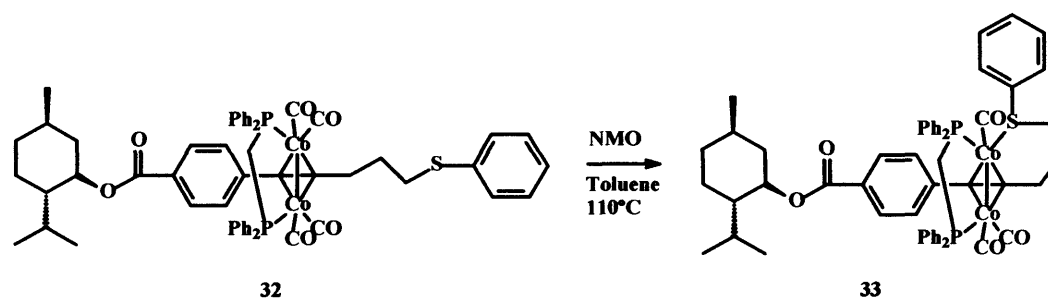
Figure 10 Comparison of ^1H -NMR spectra (400 MHz, CDCl_3) of **32** (top) and **30** (bottom)

The IR spectrum of **32** presented four bands at 2023, 1985, 1970 and 1954 cm^{-1} . Compared to compounds **30** and **31** (Table 6), IR bands for carbonyl groups of compound **32** have a lower triple bond character, probably due to the higher delocalisation of the electronic density between cobalt and carbonyls (as happened with compound **31**.) Mass spectrum of compound **32** correlated with a theoretical isotopic model of $[\text{M}-4\text{CO}]$, indicating the presence of four CO ligands. An attempt was made to grow suitable crystals for X-ray from DCM/methanol and from toluene, with no success. As happened for compounds **30** and **31**, no final proof (*e.g.* X-ray) was found to assure the structure of **32**, but all the data were in accordance with the proposed structure.

30 (cm^{-1})	31 (cm^{-1})	32 (cm^{-1})
2090.7	2090.7	2023
2054.4	2065.3	1985
2028.5	2054.0	1970
	2015.6	1954
	1964.3	

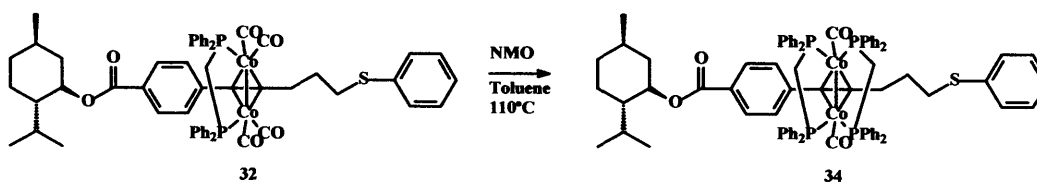
Table 6 IR data for carbonyl groups of compounds **30**, **31** and **32**

After the synthesis of **32** the following step was to attempt the coordination of the sulphur to one cobalt atom (**Scheme 20**). Electronically, this coordination reaction is not as favoured as the previous one (in which **31** was synthesised), because **32** has fewer CO ligands coordinated to metal. These remaining CO's are more strongly back-bonded to cobalt as can be seen by the IR frequencies, so it is more difficult to displace them. In order to assist the reaction, one equivalent of NMO was added (NMO is a tertiary amine N-oxide known to be useful in promoting the loss of a CO ligand from the metal, oxidised to CO₂).^[13, 14]



Scheme 20 Synthesis of **33**

After refluxing for one day TLC still showed one product, and ³¹P-NMR spectrum showed one single peak at 38.3 ppm. A small sample was purified by chromatography, starting with an eluent mixture of petrol:ether 3:1 and increasing the polarity to 1:1. Crystals of a purified sample grew very easily from ether and they were completely air stable. X-ray diffraction of crystals showed that the final product was not starting material **32**, or the expected chelated product **33**, but the incorporation of a second dppm ligand to the complex (**Figure 11**). Thus the reaction that took place was:



Scheme 21 Unexpected synthesis of **34**

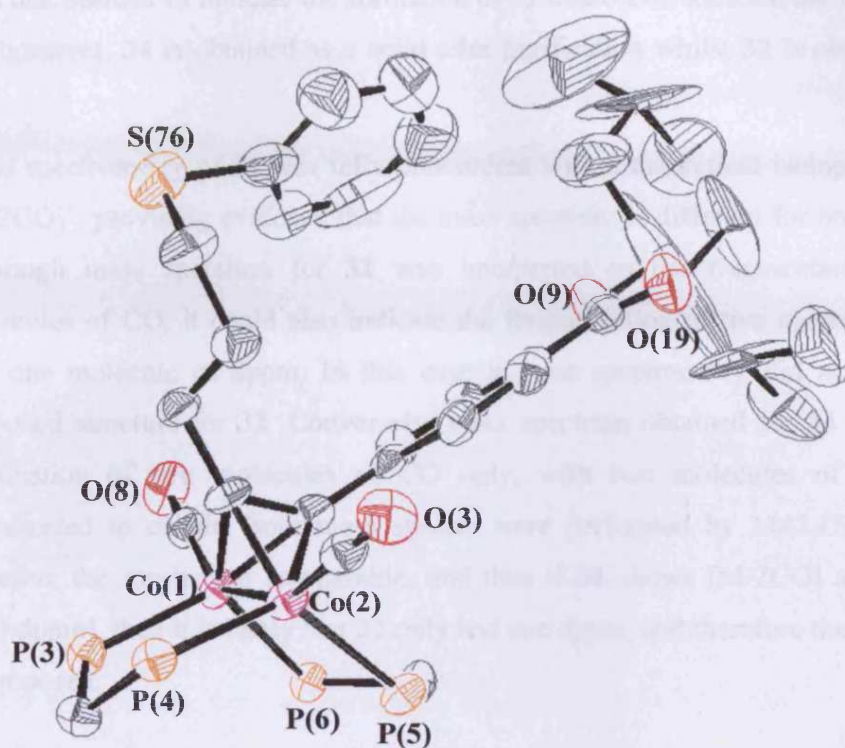


Figure 11 Ortep view (50% probabilities) of **34**. Phenyl rings have been omitted for more clarity. The achiral space group of the crystal, $C2/c$, is highly significant. This is an incoherent result as the molecule itself is chiral and, by definition, must crystallise in a chiral space group. All of the synthetic steps involved for the synthesis of **34** were revised, paying particular attention to any procedures in which the chirality of the mentholate group was affected. It was found that the chirality was transmitted all along the syntheses, therefore **34** had to be chiral. Although the R indices for the crystal structure are high (19%), the data suggested that the most suitable group was $C2/c$. One possible explanation for the achiral space group in a chiral molecule is the fact that the heaviest part of the molecule, the part that diffracted most strongly, contains the atoms of cobalt and phosphorous and this part is a relatively long way away from the chiral centres. Hence the cyclohexane region could not be solved properly (this area of the structure is disordered and some modelled bond-lengths are anomalous). In addition, the cyclohexane ring flipping would reduce the resolution of the structure, and even though the most bulky groups are probably in an equatorial position, some flipping is expected.

At this point it was questioned whether product **32** had indeed been synthesised, or whether the attempted synthesis of **32** gave as product the dibridged **34**. Some of the

data that seemed to indicate the formation of **32** could also indicate the formation of **34**, however, **34** is obtained as a solid after purification whilst **32** is obtained as an oil.

Mass spectrometry of **34** was fully concordant with a theoretical isotope model for $[M-2CO]^+$, providing evidence that the mass spectrum is different for both products. Although mass spectrum for **32** was interpreted as the fragmentation of four molecules of CO, it could also indicate the fragmentation of two molecules of CO and one molecule of dppm. In this case its mass spectrometry did not prove the proposed structure for **32**. Conversely, mass spectrum obtained for **34** showed the elimination of two molecules of CO only, with two molecules of dppm still coordinated to cobalt. Both mass spectra were performed by MALDI technique, therefore the results are comparable, and thus if **34** shows $[M-2CO]$ and not $[M-2CO-dppm]$, then it is likely that **32** only had one dppm, and therefore the structure is as proposed.

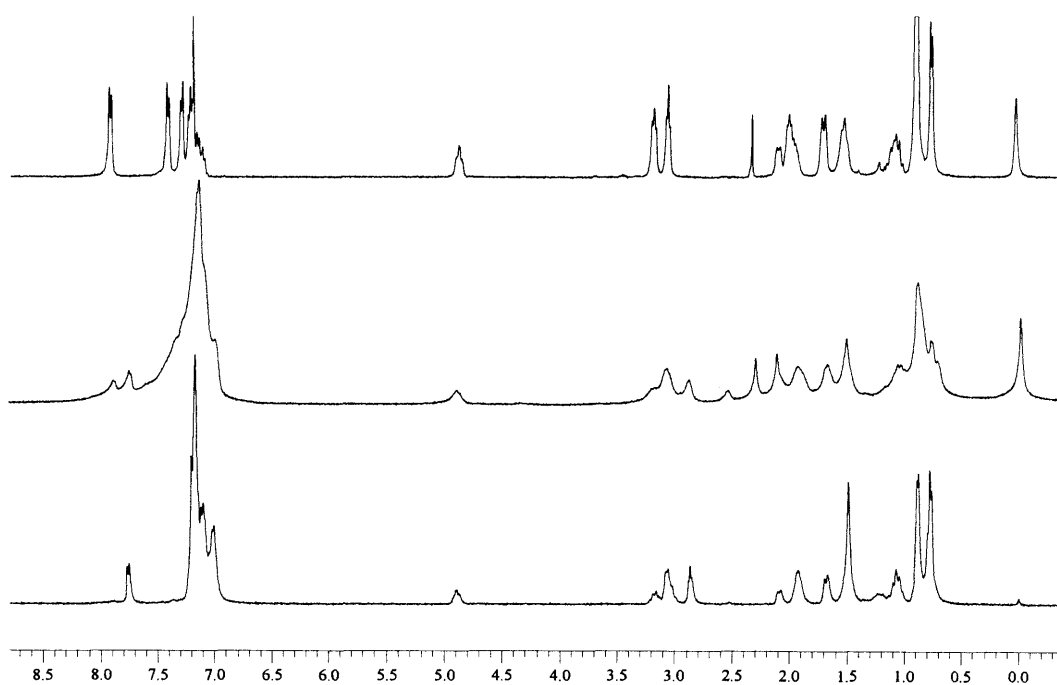


Figure 12 Triple comparison of $^1\text{H-NMR}$ spectra (400 MHz, CDCl_3) of **30** (top), **32** (middle) and **34** (bottom)

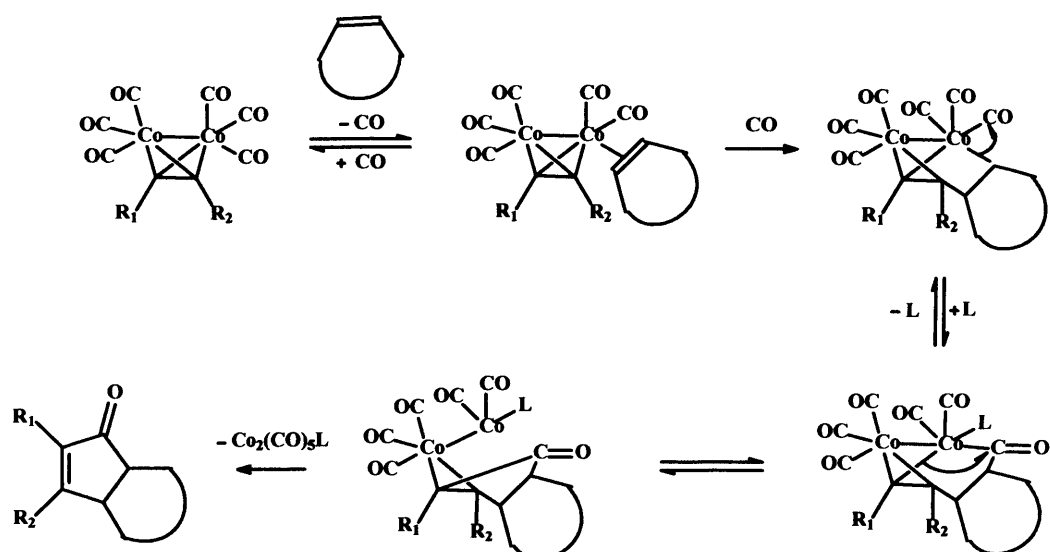
$^1\text{H-NMR}$ spectra for **32** and **34** also looked very different indicating it is unlikely that they belonged to the same compound (**Figure 12**). The fact that **34** contains two dppm ligands coordinated to the atom of cobalt explains why it was almost impossible (or at least very difficult) to coordinate the sulphur to the cobalt and

displace another carbonyl. As well as the big steric effect of two dppm groups (See X-ray structure **Figure 11**) the back-bonding from cobalt to the two remaining carbonyls is so strong that a more energy than the reaction conditions provided would be needed to remove the carbonyl groups. The formation of the bis-dppm complex **34** remains a mystery as no extra dppm was added, and thus presumably it is derived from decomposition of **32**.

4.4 Pauson-Khand reactions of alkynyl thiols

Discovered in 1973 by P.L. Pauson and I.U. Khand, the Pauson-Khand reaction^[2] has been shown to be a powerful synthetic tool in the synthesis of cyclopentenone derivatives. Even though the possibility of a catalytic mechanism was mentioned in the original publication,^[2] the reaction initially involved a stoichiometric amount of $\text{Co}_2(\text{CO})_8$. More recently, the Pauson-Khand reaction has been performed with catalytic amounts of $\text{Co}_2(\text{CO})_8$, using CO gas at high pressure and high temperatures,^[15] in the presence of phosphite ligands,^[16] under photochemical conditions,^[17] and even with heterogeneous catalysis.^[18]

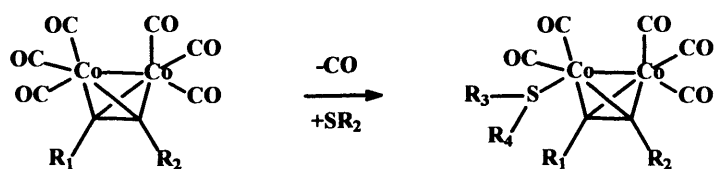
According to the first publication concerning the reaction, the bulkiest groups, derived from the appropriate monosubstituted acetylenes, are always found adjacent to the carbonyl group. Although there is no solid mechanistic data, a mechanism has been proposed based on regio- and stereochemical observations from many examples (**Scheme 22**).^[19] The coordination of the alkene to cobalt is believed to be the rate-determining and product-determining step of the reaction.



Scheme 22 Proposed mechanism for PK reaction

Although the Pauson-Khand reaction was proved to be a powerful tool for the synthesis of cyclopentenones, it also has some limitations. Regioselectivity of the alkenes is usually a problem. For an efficient conversion to product, a strained alkene is needed (with the exception of ethylene), and terminal alkynes are more effective than internal alkynes. In fact, trisubstituted alkenes are often unreactive. An intramolecular variation of the Pauson-Khand reaction was introduced in 1981 by Schore and Croudace, resulting in the formation of a bicyclic product from an acyclic substrate.^[20] The intramolecular Pauson-Khand reaction does not require a strained alkene and it also solves the regioselectivity problem.

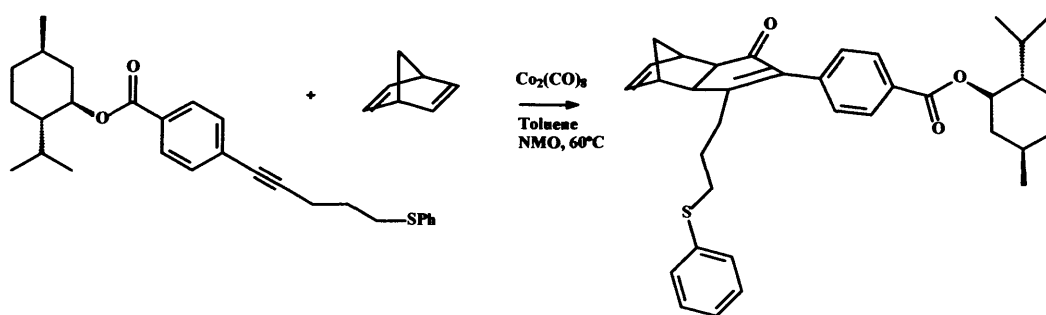
The use of a chiral cobalt complex can give diastereoselectivity when the alkene is a pro-chiral molecule, such as norbornene or norbornadiene.^[21] Some studies have also demonstrated good stereoselectivity with an alkyne dicobalt carbonyl complex containing a sulphide ligand bridge.^[3] Other examples demonstrated diastereoselectivity when a chiral alkyne containing a sulphite derivatives were used.^[22] In both cases, sulphur acted as a hemilabile ligand, displacing a carbonyl group bonded to cobalt, therefore generating a chiral dicobalt heptacarbonyl sulphide complex (**Scheme 23**).



Scheme 23 Chiral dicobalt heptacarbonyl sulphide

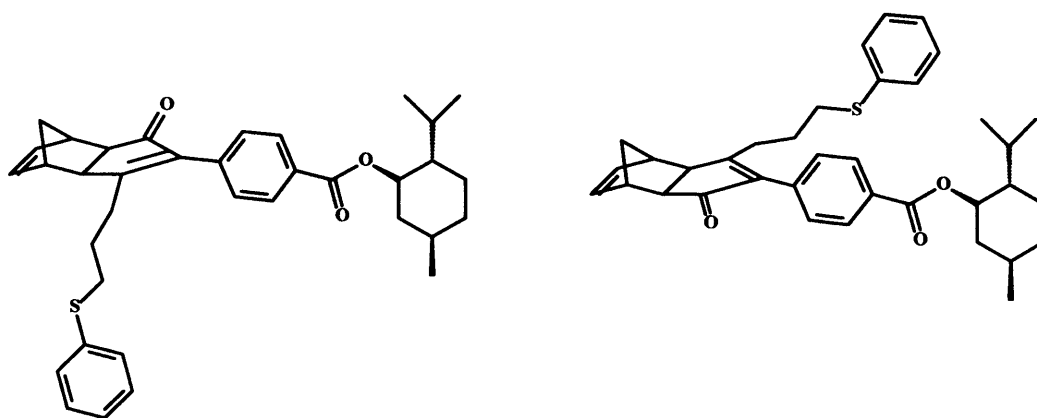
Even though this project was not focused on the efficiency of cobalt complexes for the Pauson-Khand reaction, compound **26** was tested in the Pauson-Khand reaction as it contained a sulphide that could coordinate to cobalt, displace a carbonyl group and form a new six-membered ring. The use of a pro-chiral alkene would lead to the formation of diastereoisomers, whilst the selectivity of regioisomers was expected to be null. The diastereoselectivity of the reaction would be determined by the configuration of the alkene.

The Pauson-Khand reaction was first attempted with **26**, dicobalt octacarbonyl and norbornadiene, which being a very strained alkene affords good yields in the Pauson-Khand reaction (**Scheme 24**). The reaction was followed by TLC, and after 24 hours with no sign of products, one equivalent of NMO was added and the mixture was heated at 60 °C. NMO was added in order to remove a CO ligand and allow coordination of the alkene – often the rate-determining step.



Scheme 24 Pauson-Khand reaction with compound **26**

After purification by chromatography, the $^1\text{H-NMR}$ spectrum of the main products of the reaction (**Figure 13**) showed the absence of the starting material (based on the non-appearance of the peak for the aromatic protons at 7.9 ppm) and the appearance of two doublets at 8.1 ppm. This led to the conclusion that the product of the reaction contained a mixture of two diastereoisomers (**Scheme 25**).



Scheme 25 Possible diastereoisomers from the PK reaction of **26**

Both diastereoisomers were observed in the $^1\text{H-NMR}$ spectrum (**Figure 13**) as two doublets at 8.0 ppm, corresponding to the signal for two protons belonging to the aromatic ring. Evidence is also found in a quartet of doublets at 4.9 ppm (probably overlapping two triplets of doublets) of what was usually observed as a triplet of doublets corresponding to the proton adjacent to the oxygen in the menthyl group (**Figure 14**).

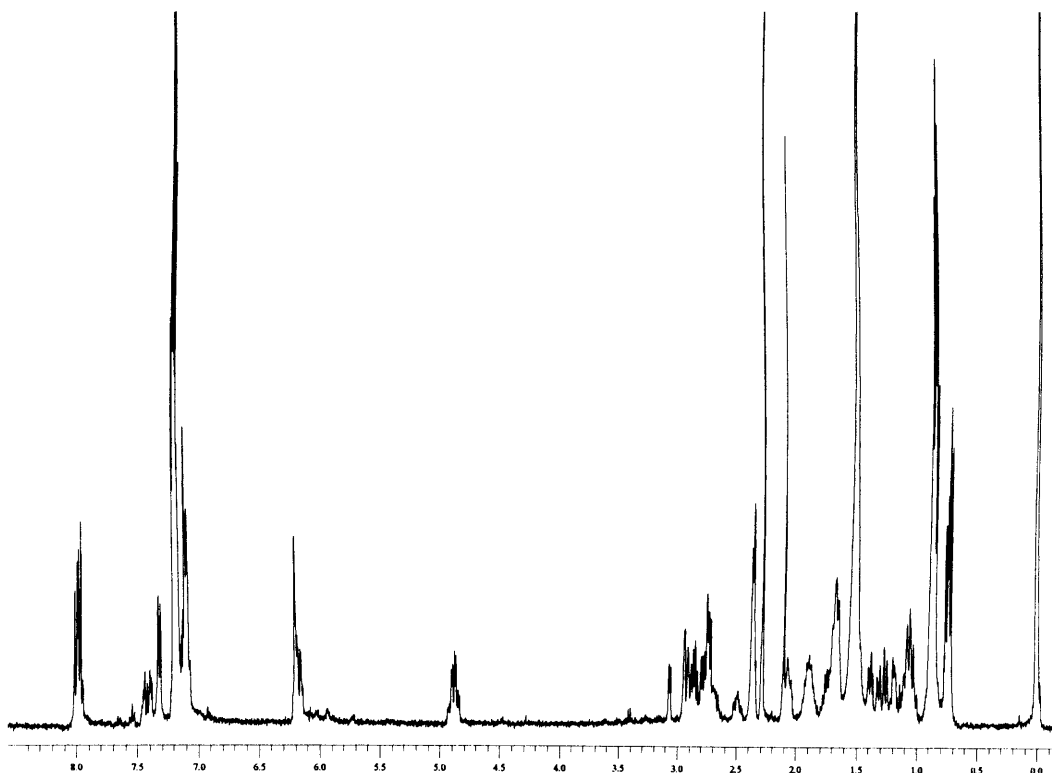


Figure 13 $^1\text{H-NMR}$ spectrum (400 MHz, CDCl_3) of the mixture of products after PK reaction

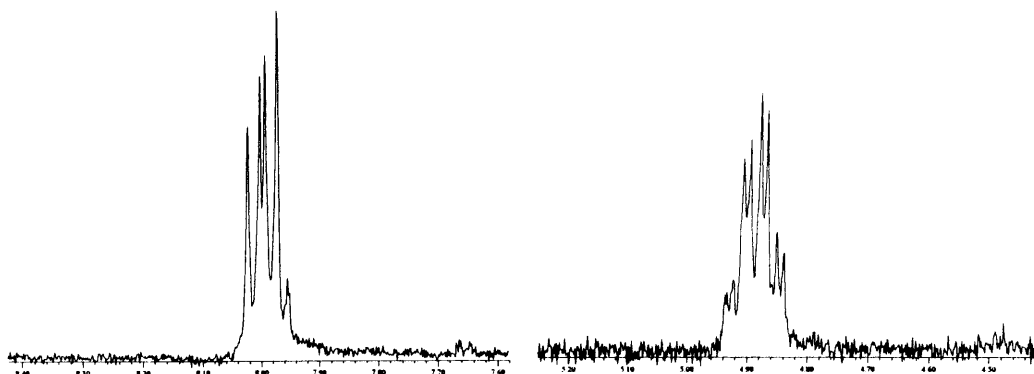


Figure 14 Amplification of ^1H -NMR spectrum (400 MHz, CDCl_3) for peaks at 8.0 and 4.9 ppm

The reaction also produced by-products that were observed by TLC, which were not isolated. ^{13}C -NMR spectrum of the mixture of diastereoisomers was too complicated to extract anymore useful information. As the reaction was just a test of compound **26** in the Pauson-Khand reaction, no further attempt to separate diastereoisomers or characterisation was performed on the products.

The Pauson-Khand reaction was then attempted with compound **26**, $\text{Co}_2(\text{CO})_6\text{dppm}$ and norbornadiene. The reaction was set up under the same conditions as the first attempt. After a few hours at 60 °C with no sign of any product, the temperature was raised to 100 °C ($\text{Co}_2(\text{CO})_6\text{dppm}$ was expected to be more stable than $\text{Co}_2(\text{CO})_8$) and one equivalent of NMO was added. After two days reacting under the new conditions, the only products of the reaction seen by TLC were a cobalt complex (identified by its red colour), **26** and norbornadiene. The reaction was then stopped and the products were analysed. The main product, after separating by chromatography, was the intermediate of the reaction **34**, a $\text{Co}_2(\text{CO})_2(\text{dppm})_2$ complex described in **Section 4.3**. In fact, the first time complex **34** was observed was during an attempt of the Pauson-Khand reaction. As the two remaining carbonyl groups were very strongly bonded to cobalt, they could not be displaced by sulphur, and due to this strong Co-CO bond, the next step in the reaction (the coordination of the alkene) could not be achieved. Thus, the reaction failed and no cyclopentenone derivatives were observed.

4.5 Synthesis of $[\text{Co}(\text{dppmdo})_3][\text{CoCl}_4]$

As has been mentioned previously in **Section 4.3**, during the synthesis of **32** an impurity was often observed in the ^{31}P -NMR spectrum around 25.4 ppm. It was not significant (never greater than 10 %), but appeared in almost every reaction and it

was initially attributed to dppm-oxide.^[23] Eventually some green-turquoise crystals suitable for X-ray diffraction crystallised in the NMR tube.

These characteristic crystals were first observed during the synthesis of **32** from **29**, but they also appeared in the NMR tube during the synthesis of $\text{Co}_2(\text{CO})_6\text{dppm}$. This led to the conclusion that the formation of the product was in some way linked to the reaction of $\text{Co}_2(\text{CO})_6\text{dppm}$ with CDCl_3 , and that there was no connection with the alkyne **29**. It is known that $\text{Co}_2(\text{CO})_8$ reacts with chloroform,^[24] but there is not any previously known example of reaction between $\text{Co}_2(\text{CO})_6\text{dppm}$ and chloroform. The X-ray crystal structure showed, unexpectedly, that the product of the reaction between $\text{Co}_2(\text{CO})_6\text{dppm}$ and CDCl_3 was a complex consisting of a cation of three dppm-dioxide ligands (dppmdo) coordinated to a Co^{2+} ($[\text{Co}(\text{dppmdo})_3]^{2+}$) and a counterion of $(\text{CoCl}_4)^{2-}$, as well as several molecules of chloroform in the crystallisation lattice (**Figure 15, Table 7**). Although the product is known and can also be synthesised from the reaction of dppmdo and cobalt chloride,^[25] it has never previously been structurally characterised.

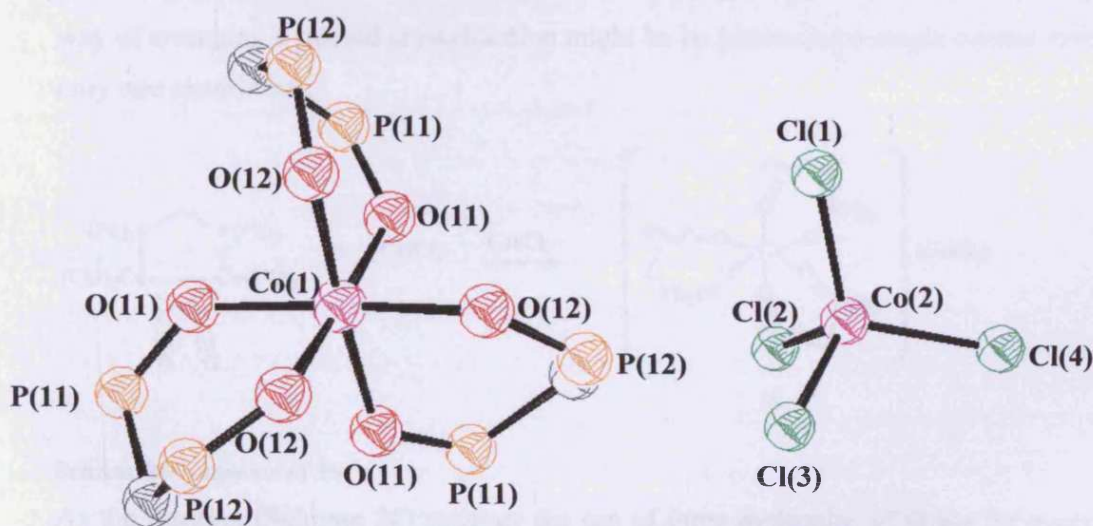
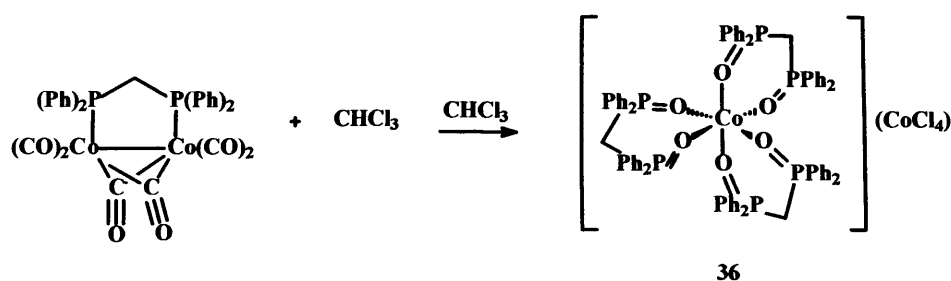


Figure 15 Ortep view (50% probabilities) of $[\text{Co}(\text{dppmdo})_3](\text{CoCl}_4)$ (**36**). Phenyl ring and chloroform molecules in the crystallisation lattice have been omitted for clarity

Empirical formula	C ₈₃ H ₇₄ Cl ₂₈ Co ₂ O ₆ P ₆
Crystal system	Cubic
Space group	P 21 3
Unit cell dimensions	a=21.8970(3) Å
	b=21.8970(3) Å
	c=21.8970(3) Å
	β=90.000(0)°
Volume	1302.49(7) Å ³
Temperature	150(2)K
Final R indices [I>2σ(I)]	R1=0.0780, wR2=0.1787
R indices (all data)	R1=0.0919, wR2=0.1872

Table 7 Summary of data collection and processing parameters for **36**

The geometry around the central atom of Co was perfectly octahedral. The product crystallised in a cubic crystal system with a chiral space group P213. No hydrogen bonding was observed in the crystal structure of **36**. Crystallization of **36** may occur as a conglomerate due to the bulkiness of the aromatic rings. In this case, the best way of arranging a packed crystallisation might be by producing a single crystal with only one enantiomer.



Scheme 26 Formation of **36**

As the reaction (**Scheme 26**) requires the use of three molecules of dppm for every two atoms of cobalt, and the starting material contains one molecule of dppm for every two atoms of cobalt, there is an excess of cobalt eliminated in an unknown form, different than the product. This was the likely cause of the low yield of the reaction.

The mechanism of the reaction is not fully understood, but it is clear that it needs oxygen to proceed (acting as oxidising agent). This was shown when two parallel reactions were set up, one of them using degassed chloroform and under anaerobic

conditions, the other using aerated chloroform and left open to the air. From the ^{31}P -NMR spectra it was deduced that in the absence of oxygen, the formation of **36** was halted. When oxygen was present, starting material $\text{Co}_2(\text{CO})_6\text{dppm}$ reacted to form **36** plus other products. After 48 hours the yield of the reaction had increased to 50 %, and after one week the reaction had gone to completion as indicated by ^{31}P -NMR spectroscopy.

An attempt was then made to synthesise **36** in an inert atmosphere to observe whether the atom of oxygen present in the phosphine oxide derived from air or from CO. After 24 hours of stirring at room temperature, ^{31}P -NMR spectrum indicated a yield of 33 % (**Figure 16.a**). The reaction was then heated at 60 °C in order to accelerate the rate. Unexpectedly, the mixture turned from brown to green-turquoise colour, and after a further 2 hours ^{31}P -NMR spectrum showed a mixture of starting material (60.9 ppm) and a new product (53.9 ppm), with no sign of **36** (**Figure 16.b**). The product ratio was 2:1 ($\text{Co}_2(\text{CO})_6\text{dppm}$:new product), as if **36** had reacted and formed the new product, but the starting material had not reacted. After a further 4 hours of stirring at 60 °C ^{31}P -NMR showed the disappearance of the starting material and the appearance of a new product at -5.1 ppm (**Figure 16.c**). The crude reaction mixture at this point contained a mixture of two unknown products containing phosphorous with a ratio of approx 1:1. When the reaction continued to be heated at 60 °C, eventually all the products containing phosphorous precipitated as a deep green solid. This solid was not soluble in any solvent and therefore no further studies were performed on the products. Judging by the position of the peaks in the ^{31}P -NMR spectra, the first unknown product could be an intermediate in which phosphorous is bonded to cobalt in a similar way to $\text{Co}_2(\text{CO})_6\text{dppm}$, the chemical shift is relatively similar (60.9 ppm v 53.9 ppm). The second unknown product (-5.1 ppm) seems more likely to be free phosphine. These speculations are based solely on the information extracted from the NMR spectra and there are no more data to corroborate this.

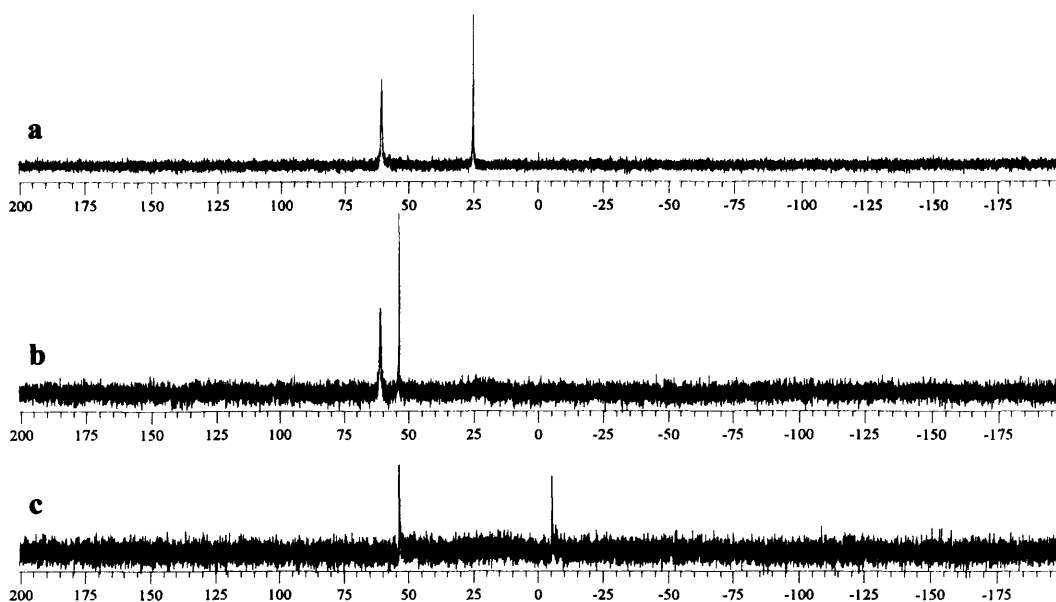


Figure 16 ^{31}P -NMR spectra (121 MHz, CDCl_3) of synthesis of **36** (a) after 24 hours stirring without heating, (b) 2 hours after heating and (c) 4 hours after heating

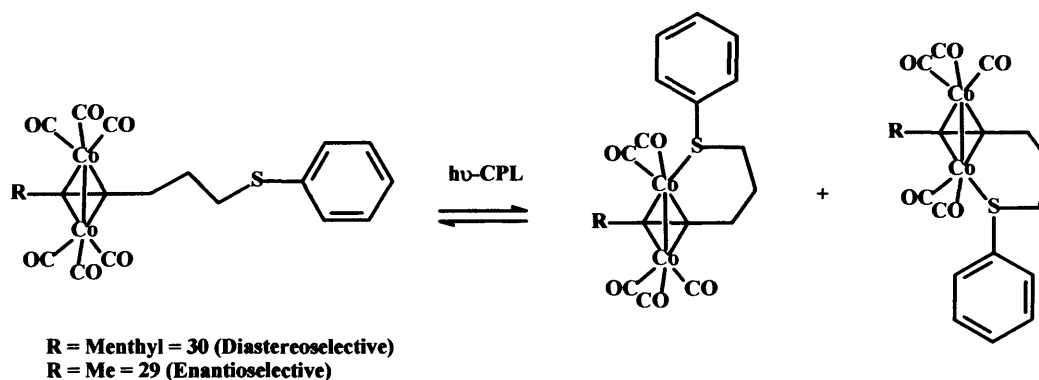
The oxidation state of the atoms of cobalt of compound **36** was not initially clear. Although the most common oxidation states of cobalt are Co(II) and Co(III) , Co(I) (known to be relatively unstable to disproportion to give Co^0 and Co(II)) has been reported to be stable in vitamin B12 and in complexes of ligands such as bipy and salen.^[26] Two options were considered when assigning the oxidation state to the atoms of cobalt: $\text{Co(I)} + \text{Co(III)}$ or $\text{Co(II)} + \text{Co(II)}$. Co(I) is a d^8 metal ion, and with this configuration a square planar geometry around the metal is most expected, thus it would need high field ligands. Looking at the crystal structure it is clear that neither the cation nor the anion has a square planar geometry around cobalt, so the option of $\text{Co(I)} + \text{Co(III)}$ was discarded. In the alternative option $\text{Co(II)} + \text{Co(II)}$, Co(II) contains seven electrons in its orbitals and is a paramagnetic metal ion. Although both ^1H -NMR and ^{31}P -NMR spectra gave sharp signals, which is unusual in the presence of a paramagnetic ion, it seems likely that the lack of a direct P-Co bond prevents line-broadening from being too great. Thus, the oxidation state of cobalt atoms in **36** was assigned as $\text{Co(II)} + \text{Co(II)}$.

As well as chloroform, the reaction was also attempted with dichloromethane as reactant (and solvent), again observing dechlorination and the formation of **36** by ^{31}P -NMR spectroscopy.

4.6 CPL studies

Photodissociation reactions are assumed to be the first step in most of the photoprocesses of all metal complexes (e.g. photoexchange, photosubstitution or photorearrangement).^[27] Thus, when a cobalt carbonyl species was irradiated under UV light, dissociation of a CO group was expected, followed by association of another group to the cobalt. The aim of the CPL studies in this chapter was the association of a sulphur group observed in Section 4.3, which would generate chiral complexes, and it was important to assess the levels of diastereoisomeric (or enantiomeric) excess in the products.

If an achiral molecule is used two enantiomers are formed when sulphur is coordinated to cobalt (Scheme 27). However, if a chiral molecule is used, after the coordination of sulphur, a mixture of diastereoisomers is obtained. Normally the enantiomers are formed in a 1:1 ratio. However, if CPL is used instead of non-polarised UV light, then one of the enantiomers is likely to be favoured because of the diastereoisomeric relationship of CPL and the enantiomers.



Scheme 27 Expected mixture of enantiomers/diastereoisomers after irradiation under CPL

Based on these principles, all the cobalt carbonyl compounds synthesised in this chapter were dissolved in toluene or DCM and irradiated under CPL. All the reactions were performed in duplicate and open to the air, the blank having no irradiation, the other irradiated. Thus, any effect of CPL on the products could be assessed by measuring the optical activity of the solutions. Two types of reactions were performed, one of them used chiral cobalt complexes, e.g. **30**, and the other type used achiral cobalt complexes, e.g. **29**. A reaction performed with chiral **30** would lead to diastereoisomers in the products, whilst **29** would lead to a mixture of enantiomers.

A sample of pure **30** in toluene was split in two flasks, one being stirred open to the air, the other was also exposed to the air, irradiated with CPL and stirred at the same speed as the previous one. Both of them were stirred for 15 min, then analysed by TLC, and in both cases some traces of **31** were observed, with no significant difference between them. Optical rotation was measured of diluted samples in toluene, but they had already decomposed and no useful data was obtained.

31 was not stable enough to carry out this procedure, as it decomposed after a few hours even under an inert atmosphere. This is probably because sulphur is a hemilabile ligand in this system and when it is not coordinated to cobalt, the metal has a vacancy in its coordination sphere, leading to the decomposition of the product.

The same procedure as described above was carried out on a sample of **32**, a chiral cobalt complex that would afford diastereoisomers. Optical activity was measured for both samples after stirring, showing an average observed optical activity value of +0.012 for the non-CPL and +0.015 for the CPL irradiated sample. **32** was very colourful and the polarimeter would not measure the optical activity, therefore the samples had to be diluted before the optical rotation measurements. The small difference in optical activity was attributed to experimental error rather than efficiency of CPL as a photochiral converter.

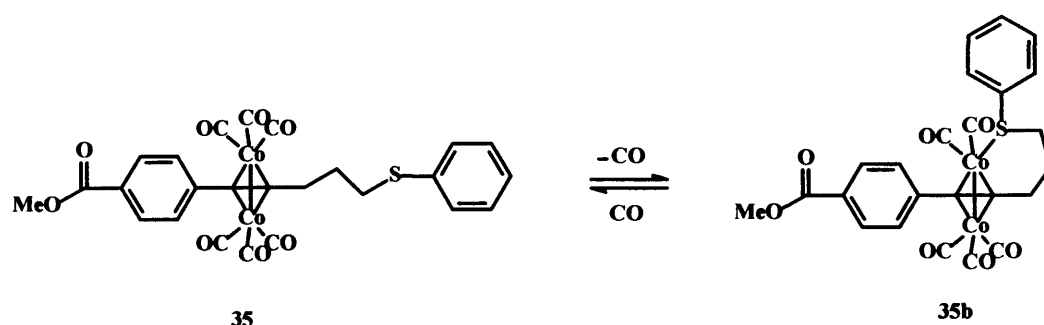
As optical studies performed on **30** and **32** did not provide evidence of any effect of CPL on the products, optical studies of **29** (an achiral cobalt complex) were carried out in a different manner. A reaction was designed to study the coordination of $\text{Co}_2(\text{CO})_8$ to the triple bond under irradiation with CPL. In this way CPL could affect all stages of the reaction, and would perhaps show some effect on the final product, even when irradiation of **30** with CPL had shown no significant effect (**Scheme 28**).



Scheme 28 Synthesis of **35**

The reaction was set up in a three neck RBF and a solution of **29** in DCM was degassed by the freeze-pump-thaw method. As irradiation with CPL was initiated, a stream of nitrogen was blown through the sample to try to avoid any ingress of oxygen. TLC analysis of the resultant mixture showed two different products, similar

to the mixture of products obtained after the synthesis of **30** (Section 4.3). By analogy with the synthesis of **30**, one complex contained non-coordinated sulphur, the other complex contained sulphur coordinated to cobalt. In this reaction the products had much lower R_f than **30** and **31**, most likely because **35** (and **35b**) (Scheme 29) were less polar.

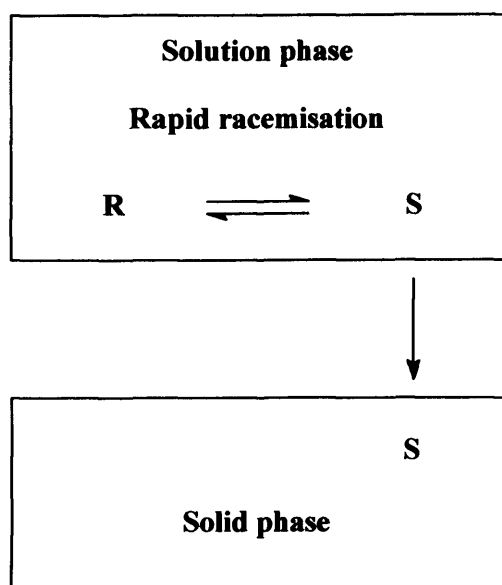


Scheme 29 Two possible products after the synthesis of **35**

Both products were separated and purified by chromatography and IR of **35** showed bands for carbonyl groups at 2090 cm^{-1} , 2053 cm^{-1} , 2021 cm^{-1} and 1958 cm^{-1} . These values are very similar to those obtained for compound **30**. **35b** is chiral due to the coordination of sulphur preferentially to one atom of cobalt after CPL irradiation. The average optical activity observed of **35b** is $+0.002$. This is considered an experimental error of the equipment, thus concluding irradiation with CPL had failed to induce a significant e.e. in this reaction.

4.7 Conclusions

The synthesis of chiral and achiral thioalkynyl derivatives was achieved. These molecules have a medium sized conjugated π system that can assist the absorption of UV-Vis light. The new compounds synthesised were coordinated to $\text{Co}_2(\text{CO})_8$ and to $\text{Co}_2(\text{CO})_6\text{dppm}$, with a mixture of products as a result. Sulphur was coordinated to cobalt displacing one CO ligand and forming a new six membered ring. Organometallic cobalt complexes synthesised in this part of the project were irradiated with CPL, observing no significant optical rotation for the achiral complexes.



Scheme 30 Preferential crystallisation of one enantiomer after irradiation with CPL

Crystallisation was an important part of the overall project (**Scheme 30**); and the irradiation of crystallising samples with CPL was expected to enhance the enantiomeric excess of the product. No crystalline organometallic cobalt complexes were achieved in the work described in this chapter, therefore the lack of optical activity after irradiation of the thioalkynyl cobalt complexes with CPL was attributed to the very low crystallinity of the complexes. The low values of optical activity observed were probably due to experimental error of the polarimeter, indicating no effect of CPL on the photochemistry of the thioalkynyl cobalt complexes studied.

4.8 References

- [1] N. Schore, S. D. Najdi, *J. Org. Chem.* **1987**, *52*, 5296.
- [2] I. U. Khand, G. R. Knox, P. L. Pauson, W. E. Watts, M. I. Foreman, *J. Chem. Soc. Perkin Trans. 1* **1973**, 977.
- [3] I. Marchueta, E. Montenegro, D. Panov, M. Poch, X. Verdaguer, A. Moyano, M. A. Pericas, A. Riera, *J. Org. Chem.* **2001**, *66*, 6400.
- [4] E. Montenegro, M. Poch, A. Moyano, M. A. Pericas, A. Riera, *Tetrahedron Lett.* **1998**, *39*, 335.
- [5] E. Montenegro, R. Echarri, C. Claver, S. Castillon, A. Moyano, M. A. Pericas, A. Riera, *Tetrahedron Asymmetry* **1996**, *7*, 3553.
- [6] N. Kamigata, A. Matsuhisa, H. Taka, T. Shimizu, *J. Chem. Soc. Perkin Trans. 1* **1995**, *7*, 821.

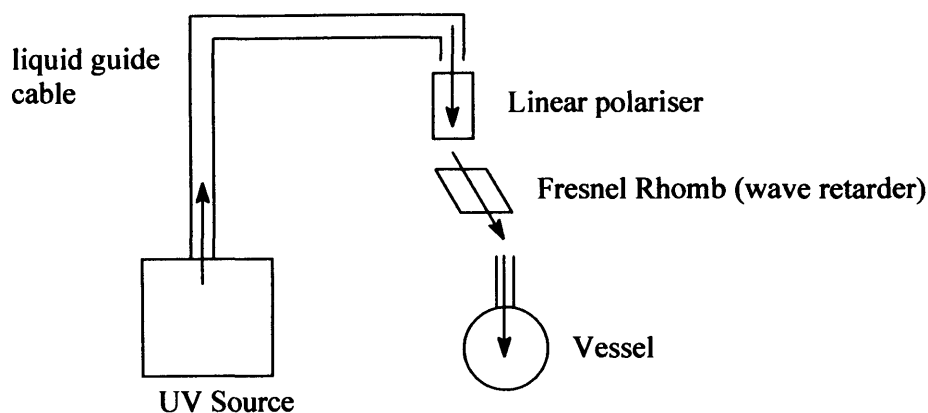
- [7] K. Sonogashira, Y. Tohda, N. Hagihara, *Tetrahedron Lett.* **1975**, 4467.
- [8] J. I. Morita, H. Nakatsuji, T. Misaki, Y. Tanabe, *Green Chem.* **2005**, 7, 711.
- [9] T. Fukuzaki, S. Kobayashi, T. Hibi, Y. Ikuma, J. Ishihara, N. Kanoh, A. Murai, *Organic letters* **2002**, 4, 2877.
- [10] X. Verdaguier, A. Moyano, M. A. Pericas, A. Riera, A. Alvarez-Lena, J. F. Piniella, *Organometallics* **1999**, 18, 4275.
- [11] T. J. Snaith, P. J. Low, R. Rosseau, H. Puschmann, J. A. K. Howard, *J. Chem. Soc. Dalton Trans.* **2001**, 292.
- [12] Y. C. Chang, J. C. Lee, F. E. Hong, *Organometallics* **2005**, 24, 5686.
- [13] S. L. Shreiber, S. Shambayati, W. E. Crowe, *Tetrahedron Lett.* **1990**, 31, 5289.
- [14] N. Jeong, Y. K. Chung, B. Y. Lee, S. H. Lee, S. E. Yoo, *Synlett* **1991**, 204.
- [15] V. Rautenstrauch, P. Megard, J. Conesa, W. Kuster, *Angew. Chem. Int. Ed.* **1990**, 29, 1413.
- [16] N. Jeong, S. H. Wang, Y. Lee, *J. Am. Chem. Soc.* **1994**, 116, 3159.
- [17] B. L. Pagenkopf, T. Livinghouse, *J. Am. Chem. Soc.* **1996**, 118, 2285.
- [18] S. W. Kim, S. U. Son, S. I. Lee, T. Hyeon, V. K. Chung, *J. Am. Chem. Soc.* **2000**, 122, 1550.
- [19] P. Magnus, L. M. Principe, *Tetrahedron Lett.* **1985**, 26, 4851.
- [20] N. Schore, M. C. Croudace, *J. Org. Chem.* **1981**, 46, 5436.
- [21] A. M. Hay, W. J. Kerr, G. G. Kirk, D. Middlemiss, *Organometallics* **1995**, 14, 4986.
- [22] J. Vazquez, S. Fonquerna, A. Moyano, M. A. Pericas, A. Riera, *Tetrahedron Asymmetry* **2001**, 12, 1837.
- [23] K. Moedritzer, L. Maier, L. C. D. Groenweghe, *Journal of Chemical and Engineering Data* **1962**, 7, 307.
- [24] G. Bor, L. Marko, B. Marko, *Chem. Ber.* **1962**, 95, 333.
- [25] F. Mani, M. Bacci, *Inorganica Chimica Acta* **1972**, 6, 487.
- [26] O. Buriez, E. Labbé, J. Périchon, *Journal of Electroanalytical Chemistry* **2006**, 593, 99.
- [27] V. Balzani, V. Carassiti, *Photochemistry of Coordination Compounds*, Academic Press, London and New York, **1970**.

Chapter 5: OPTICS AND EXPERIMENTAL

DESCRIPTION

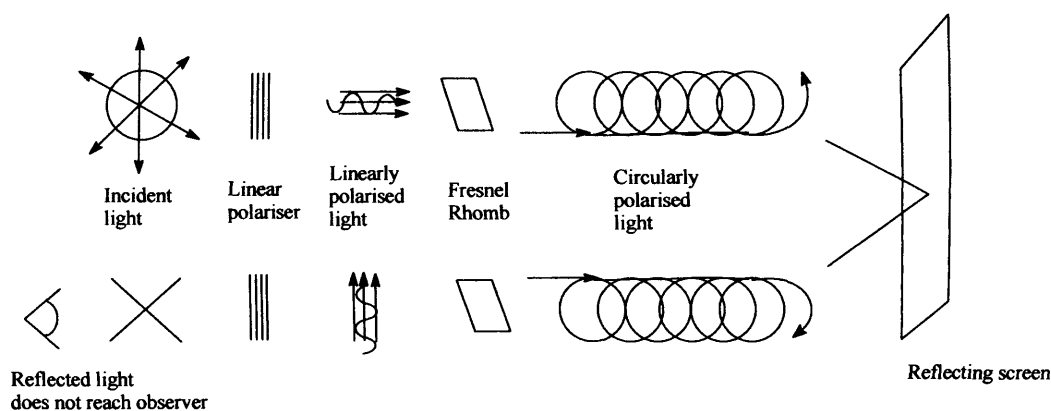
5.1 Optics

Right-handed circularly polarised light (r-CPL) was generated by passing a beam of light from a metal halide light source (Fiber-Lite MH100 Illuminator lamp, 100 W metal halide bulb, from Dolan-Jenner) through a liquid light guide cable, a linear polariser PS10 (from Halbo Optics, with a spectral range of 220-2800 nm) and a Fresnel Rhomb (a quarter wave retarder, from Halbo Optics, FRQ10-Si for spectral range 230-400 nm, FRQ10M-BK for spectral range 400-700 nm). These devices were positioned in the described order, vertically above the sample (**Scheme 1**). The Fresnel Rhomb was orientated at an angle of +45 ° (or -45 °, depending the type of CPL generated) to the plane of the incident linearly polarised beam, which penetrated the crude reaction mixture from the top of the container. The use of quartz glass vessels was found to be unnecessary because glass absorbs UV light and transmits visible light, so no reflection of CPL was observed, therefore standard Pyrex glass vessels were utilised. Left-handed circularly polarised light (l-CPL) was obtained by rotating the Fresnel Rhomb polariser by 90 °. Both l-CPL and r-CPL were focussed at the centre of the reaction vessel.



Scheme 1 Typical set up for reactions involving CPL

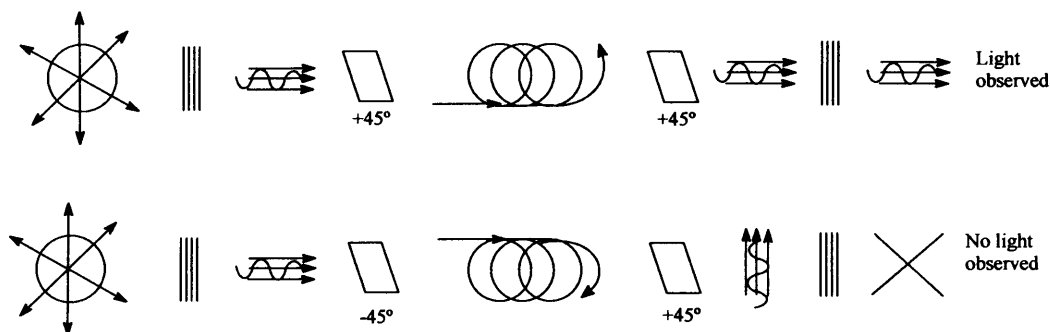
The efficiency of the Fresnel Rhomb was tested by applying the principle of the filter-screen reflection suppressors for display screens: when a beam of light passes through the filter it is first linearly polarised, then left-handed circularly polarised by retarding the incident beam of light by 45° , and thus reaching the computer screen as l-CPL. When the circularly polarised beam of light reaches the screen, it is reflected and reversed to r-CPL, then passes through a quarter wave retarder that retards the wavelength by a further 45° (in total 90° compared to the incident beam). The beam is then perpendicular to the original linear polariser and as a consequence, all the r-CPL is eliminated, minimising reflections from any external light (**Scheme 2**).



Scheme 2 Filter-screen reflection suppressor process

As a qualitative test, a filter-screen reflection suppressor (commercially available from 3M), which combines a linear polariser with a quarter wavelength plate retarder, producing l-CPL, was used, as well as the linear polariser and the Fresnel Rhomb. A beam of r-CPL was generated by a combination of a linear polariser and the Fresnel Rhomb orientated at $+45^\circ$ with respect to the linear polariser and

directed at the reverse of a filter-screen reflection suppressor. No light was observed passing through the filter, as the quarter wavelength plate retarder had changed the orientation of linear polarised light by 90° respect to the initial linear polarised light. Conversely, when the Fresnel rhomb was rotated by -45° , the beam was observed to pass through the reverse of the filter-screen reflection suppressor, no further changes were observed in the intensity of outgoing light (Scheme 3).



Scheme 3 Qualitative test to prove the efficiency of Fresnel Rhomb as a circular polariser

5.2 General

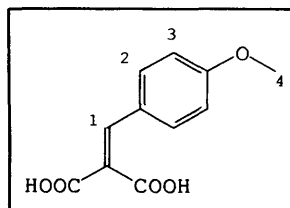
All starting materials, reagents and solvents were purchased from commercial suppliers and used as supplied unless otherwise stated. $^1\text{H-NMR}$ and $^{13}\text{C-NMR}$ spectra were recorded on a Bruker DPX 400 MHz at 400 MHz for proton and 160 MHz for carbon, or on a Bruker APX 250 at 250 MHz and 101 MHz respectively. $^{31}\text{P-NMR}$ spectra were recorded on a Jeol at 121 MHz. IR spectra were recorded on a Perkin Elmer 1600 FT IR as thin films or nujol mulls, UV spectra were recorded on a Jasco V-750 spectrophotometer and mass spectra were recorded on a VG Fisons Platform II or at the EPSRC national mass spectrometry service in Swansea (HRMS). Elemental analysis were performed by Warwick Analytical Services (University of Warwick). Optical activity was measured on a AA-1000 Polarimeter. $^{13}\text{C-NMR}$ and $^{31}\text{P-NMR}$ spectra were recorded proton decoupled. Residual protons from deuterated solvents were used as a reference for $^1\text{H-NMR}$ spectra. $^{31}\text{P-NMR}$ spectra were externally referenced by a program incorporated in Jeol. Chemically equivalent but magnetically inequivalent pairs of protons in 1,4 disubstituted aryls are reported as single signals with the mutual couplings recorded as 4J when observed. Protons signals for amine in ethylenediamine complexes often under-integrate or even are not seen due to exchange with deuterated solvent. Coupling constants of spectra recorded on a Bruker APX at 250 MHz are rounded to the

nearest half Hz unless otherwise stated, due to poor resolution. Mass spectra have been recorded as low resolution unless otherwise stated. Optical activities measured to determine e.e. achieved during the reaction are reported in **Chapters 2, 3 and 4**.

5.3 Synthesis of 3-(4-methoxyphenyl)-2-carboxy-2-propenoic acid 1

The synthesis of 3-(4-methoxyphenyl)-2-carboxy-2-propenoic acid **1** was performed following a procedure described in the literature.^[1] A mixture of *p*-anisaldehyde (9.0 mL, 55 mmol), malonic acid (11.44 g, 110 mmol) and ammonium acetate (0.04 g, 0.52 mmol) in EtOH (25 mL) was stirred under nitrogen at room temperature for 7 days. The solvent was then evaporated to dryness, the solid residue was dissolved in ethyl acetate, extracted with sodium hydroxide (0.1 M, 3 x 10 mL), precipitated with hydrochloric acid (1 M) and collected by filtration to afford

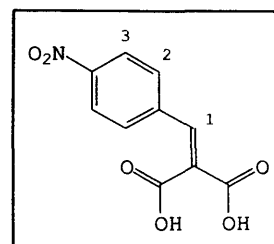
5.46 g (44.7 %) of **1**.^[1] ¹H NMR (400 MHz, CD₃OD) δ: 3.75 (s, 3H, *H*₄), 6.85 (dd, 2H, *H*₃, ³*J* = 7.1 Hz, ⁴*J* = 1.7 Hz), 7.45 (dd, 2H, *H*₂, ³*J* = 7.1 Hz, ⁴*J* = 1.7 Hz), 7.55 (s, 1H, *H*₁). m.p. 207-209 °C (lit.^[1] 204-205 °C).



5.4 Synthesis of 3-(4-nitrophenyl)-2-carboxy-2-propenoic acid 2

The synthesis of 3-(4-nitrophenyl)-2-carboxy-2-propenoic acid **2** was performed following a procedure similar to the one described in the literature.^[1] A mixture of *p*-nitrobenzaldehyde (2.02 g, 13.37 mmol), malonic acid (2.87 g, 27.57 mmol) and ammonium acetate (0.01 g, 0.13 mmol) in EtOH (25 mL) was stirred under nitrogen at room temperature for 14 days. The solvent was then evaporated to dryness, and the solid residue was dissolved in ethyl acetate. The product was

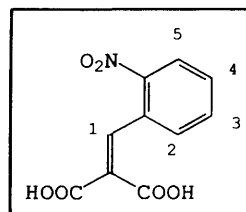
extracted with sodium hydroxide (0.1 M, 3 x 10 mL), precipitated with hydrochloric acid (1 M) and collected by filtration to afford 1.35 g (42.6 %) of **2**.^[1] ¹H NMR (400 MHz, CD₃OD) δ: 7.65 (s, 1H, *H*₁), 7.70 (d, 2H, *H*₃, ³*J* = 8.8 Hz), 8.2 (d, 2H, *H*₂, ³*J* = 8.8 Hz). m.p. 242-244 °C.



5.5 Synthesis of 3-(2-nitrophenyl)-2-carboxy-2-propenoic acid 3

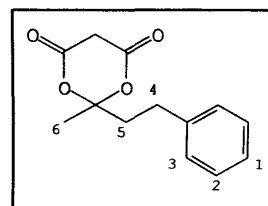
The synthesis of 3-(2-nitrophenyl)-2-carboxy-2-propenoic acid **3** was performed following a procedure similar to that described in the literature.^[1] A mixture of *o*-

nitrobenzaldehyde (14.70 g, 128 mmol), malonic acid (26.62 g, 256 mmol) and ammonium acetate (0.10 g, 1.3 mmol) in EtOH (40 mL) was stirred under nitrogen at room temperature for 5 days. The solvent was evaporated to dryness and the solid residue was dissolved in ethyl acetate. The product was extracted with sodium hydroxide (0.1 M, 3 x 10 mL), precipitated with hydrochloric acid (1 M) and collected by filtration to afford 14.7 g (48.3 %) of **3**.^[1] ¹H NMR (400 MHz, CD₃OD) δ : 7.80 (d, 1H, H_2 , $^3J = 8.0$ Hz), 7.90 (dd, 1H, H_4 , $^3J = 8.0$ Hz, $^2J = 7.0$ Hz), 8.00 (dd, 1H, H_3 , $^3J = 8.0$ Hz, $^2J = 7.0$ Hz), 8.40 (s, 1H, H_1), 8.50 (d, 1H, H_5 , $^3J = 8.0$ Hz). **m.p.** 151-154 °C.



5.6 Synthesis of 2-methyl-2-(2-phenylethyl)-1,3-dioxane-4,6-dione **4**

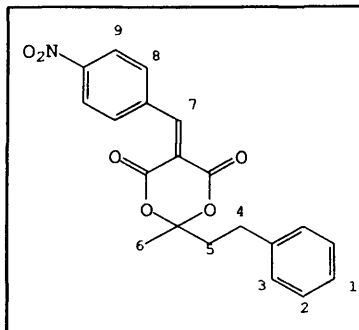
The synthesis of 2-methyl-2-(2-phenylethyl)-1,3-dioxane-4,6-dione **4** was performed following a similar procedure to that described in the literature.^[2] A mixture of 4-phenyl-2-butanone (45 mL, 300 mmol), malonic acid (20.8 g, 200 mmol) and conc. sulphuric acid (0.6 mL, 12 mmol) was added to a Schlenk flask, under nitrogen. The mixture was stirred for 15 min at room temperature then acetic anhydride (24 mL, 250 mmol) was added very slowly over a 30 min period and then stirred at room temperature for a further 18 h. The solvent was evaporated to dryness, and the remaining solid was dissolved in DCM, filtered and recrystallised from ethyl acetate and petrol to afford 5.39 g (11.5 %) of **4**. ¹H NMR (400 MHz, CDCl₃) δ : 1.75 (s, 3H, H_6), 2.29 (ddd, 2H, H_5 , $^2J = 12$ Hz, $^3J = 8.6$ Hz, $^3J = 7$ Hz), 2.86 (ddd, 2H, H_4 , $^2J = 12$ Hz, $^3J = 8.6$ Hz, $^3J = 7$ Hz), 3.60 (s, 2H, H_7), 7.10 (m, 3H, $H_{1,2}$), 7.25 (m, 2H, H_3). ¹³C-NMR (101 MHz, CDCl₃) δ : 26.53, 29.46, 36.64, 42.59, 107.64, 126.91, 128.69, 129.13, 140.12, 163.27. **m.p.**: 85-87 °C. λ_{\max} (ϵ): 257.7 nm (402 M⁻¹cm⁻¹), 207.5 nm (7722 M⁻¹cm⁻¹). ν_{\max} (cm⁻¹): 1781 (CO), 1744 (CO). **Accurate m/z** (EI) Calculated: 234.0892; Measured: 234.0889



5.7 Synthesis of 5-(4-nitro-benzylidene)-2-methyl-2-(phenylethyl)-1,3-dioxane-4,6-dione **5**

A mixture of *p*-nitrobenzaldehyde (0.75 g, 5 mmol), **4** (1 g, 4.3 mmol) and ammonium acetate (0.003 g, 0.004 mmol) in EtOH (10 mL) was stirred under nitrogen at room temperature for 3 h. A yellow solid was then collected by filtration

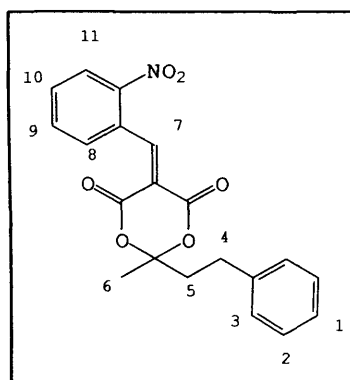
and recrystallised from EtOH, to afford 0.59 g (37 %) of **5**. $^1\text{H NMR}$ (400 MHz, CDCl_3) δ : 1.75 (s, 3H, H_6), 2.20 (m, 2H, H_5), 2.75 (m, 2H, H_4), 7.15 (m, 3H, $H_{1,2}$), 7.20 (m, 2H, H_3), 8.00 (d, 2H, H_8 , $^3J = 7.0$ Hz), 8.25 (dd, 2H, H_9 , $^3J = 7.0$ Hz, $^4J = 1.8$ Hz), 8.40 (s, 1H, H_7). $^{13}\text{C-NMR}$ (101 MHz, CDCl_3) δ : 26.97, 29.59, 42.66, 106.69, 118.78, 123.98, 126.91, 128.72, 129.14, 133.52, 137.80, 140.21, 149.92, 155.13, 159.29, 162.55. **m.p.** 146-149 °C. ν_{max} (cm^{-1}): 1729 (CO), 1529 (NO_2), 1350 (NO_2). λ_{max} (ϵ): 306.2 nm (13567 $\text{M}^{-1}\text{cm}^{-1}$), 268.5 nm (12000 $\text{M}^{-1}\text{cm}^{-1}$), 200.7 nm (28131 $\text{M}^{-1}\text{cm}^{-1}$). $\text{C}_{20}\text{H}_{17}\text{NO}_6$ requires C 65.39, H 4.66, N 3.81; found C 65.22, H 4.64, N 3.78. **m/z** (EI) 367.



5.8 Synthesis of 5-(2-nitrobenzylidene)-2-methyl-2-(phenylethyl)-1,3-dioxane-4,6-dione **6**

A mixture of *o*-nitrobenzaldehyde (0.76 g, 5 mmol), **4** (1.0 g, 4.3 mmol) and ammonium acetate (0.003 g, 0.004 mmol) in EtOH (6 mL) was stirred under nitrogen at room temperature for 18 h. A yellow solid was then collected by filtration and recrystallised from EtOH, to afford 1.03 g (66 %) of **6**. $^1\text{H NMR}$ (400 MHz, CDCl_3)

δ : 1.75 (s, 3H, H_6), 2.22 (m, 2H, H_5), 2.83 (m, 2H, H_4), 7.15 (m, 3H, $H_{1,2}$), 7.24 (dd, 2H, H_3 , $^3J = 7.1$ Hz, $^4J = 1.8$ Hz), 7.42 (d, 1H, H_8 , $^3J = 7.7$ Hz), 7.60 (m, 1H, H_{10}), 7.68 (m, 1H, H_9), 8.24 (dd, 2H, H_{11} , $^3J = 8.2$ Hz, $^4J = 1.1$ Hz), 8.76 (s, 1H, H_7). $^{13}\text{C NMR}$ (101 MHz, CDCl_3) δ : 27.02, 29.57, 42.63, 106.83, 118.04, 125.28, 126.82, 128.74, 129.08, 130.27, 130.67, 131.34, 134.25, 140.35, 146.69, 156.46, 159.36, 161.919. **m.p.**



89-91 °C. ν_{max} (cm^{-1}): 1777 (CO), 1743 (CO), 1531 (NO_2), 1336 (NO_2). λ_{max} (ϵ): 310.8 nm (5869 $\text{M}^{-1}\text{cm}^{-1}$), 251.8 nm (16645 $\text{M}^{-1}\text{cm}^{-1}$), 202.5 nm (29496 $\text{M}^{-1}\text{cm}^{-1}$). $\text{C}_{20}\text{H}_{17}\text{NO}_6$ requires C 65.39, H 4.66, N 3.81; found C 65.12, H 4.64, N 3.72. **m/z** (APCI) 368 (M+1), 266 (M-102), 220 (M-148).

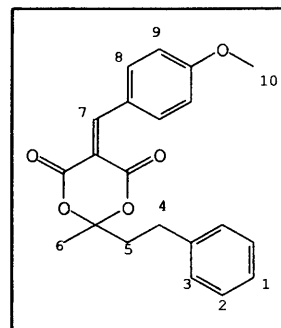
5.9 Synthesis of 5-(4-methoxybenzylidene)-2-methyl-2-(phenylethyl)-1,3-dioxane-4,6-dione 7

A mixture of *p*-anisaldehyde (1.12 mL, 10 mmol), 4 (2 g, 8.6 mmol) and ammonium acetate (0.006 g, 0.008 mmol) in EtOH (10 mL) was stirred under nitrogen at room temperature for 24 h. A bright yellow solid was then collected by filtration and recrystallised from EtOH to afford 2.00 g (66 %) of 7. ¹H

NMR (400 MHz, CDCl₃) δ: 1.68 (s, 3H, H₆), 2.22 (m, 2H, H₅), 2.80 (m, 2H, H₄), 3.83 (s, 3H, H₁₀), 6.93 (dd, 2H, H₉, ³J = 7.1 Hz, ⁴J = 1.8 Hz), 7.18 (m, 3H, H_{1,2}), 7.22 (m, 2H, H₃), 8.17 (dd, 2H, H₈, ³J = 7.1 Hz, ⁴J = 1.8 Hz), 8.35 (s, 1H, H₇).

¹³C-NMR (101 MHz, CDCl₃) δ: 26.52, 29.62, 42.51, 56.13, 105.54, 111.04, 114.81, 125.13, 126.70, 128.76, 129.04,

138.20, 140.69, 158.61, 160.88, 164.53, 165.14. **m.p.:** 91-93 °C. **v_{max}** (cm⁻¹): 1722 (CO). **λ_{max}** (ε): 365.9 nm (30178 M⁻¹cm⁻¹), 243.4 nm (9084 M⁻¹cm⁻¹), 206.9 nm (19110 M⁻¹cm⁻¹). **C₂₁H₂₀O₅** requires C 71.58, H 5.72; found C 71.41, H 5.61. **m/z** (EI) 352.2. **X-ray:** C₂₁H₂₀O₅; temperature 150(2)K; crystal system Monoclinic; space group P 21/a; a=9.6549(2), b=12.9703(3), c=14.7696(4) Å, β=108.6430(10)°; final R indices [I>2σ(I)] R1 = 0.0524, wR2 = 0.1052; R indices (all data) R1 = 0.0899, wR2 = 0.1171.



5.10 Synthesis of 5-benzylidene-2-methyl-2-phenylethyl-1,3-dioxane-4,6-dione 8

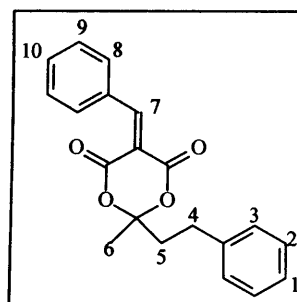
A mixture of 4 (0.47 g, 2 mmol), benzaldehyde (0.24 mL, 2.4 mmol) and ammonium acetate (1.5 mg, 0.002 mmol) in EtOH (10 mL) was stirred at room temperature for 18 h. A white solid was collected by filtration and washed with cold EtOH, to afford 0.276 g (43 %) of 8. ¹H NMR (400 MHz, CDCl₃) δ: 1.75

(s, 3H, H₆), 2.23 (m, 2H, H₅), 2.82 (m, 2H, H₄), 7.15 (m, 3H, H_{1,2}), 7.23 (t, 2H, H₃, ³J = 6.5 Hz), 7.42 (t, 2H, H₈, ³J = 7.0 Hz), 7.51 (t, 1H, H₁₀, ³J = 7.0 Hz, ⁴J = 1.8 Hz), 7.99 (d, 2H, H₉, ²J = 7.72 Hz), 8.39 (s, 1H, H₇).

¹³C NMR (101 MHz, CDCl₃) δ: 26.68, 29.61, 42.57, 105.97, 115.06, 126.78, 128.75, 129.08, 129.18, 132.06, 134.13, 134.22,

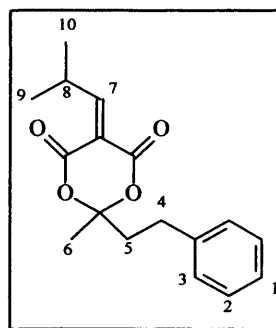
140.52, 158.83, 160.13, 163.72. **m.p.** 107-109 °C. **m/z** (EI/CI MS) 173.9, 91.1, 43.2.

v_{max} (cm⁻¹): 1737 (CO). **C₂₀H₁₈O₄** requires C 74.52, H 5.63, N 0.00; found C 74.31, H 5.69, N 0.07.



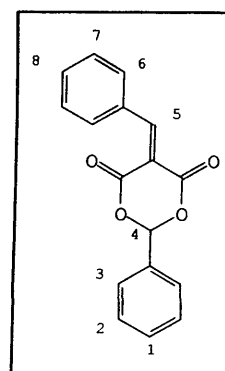
5.11 Synthesis of 5-isobutylidene-2-methyl-2-(2-phenylethyl)-1,3-dioxane-4,6-dione **9**

A mixture of isobutanal (0.91 mL, 10 mmol), **4** (0.94 g, 4.00 mmol) and ammonium acetate (0.003 g, 0.004 mmol) was dissolved in EtOH (10 mL) and stirred under nitrogen at room temperature for 18 h. A white solid was collected by filtration and recrystallised from EtOH to afford 0.56 g (50 %) of **9**. $^1\text{H-NMR}$ (250 MHz, CDCl_3) δ : 1.08 (d, 3H, H_9 , $^3J = 6.6$ Hz), 1.11 (d, 3H, H_{10} , $^3J = 6.6$ Hz), 1.67 (s, 3H, H_6), 2.15 (m, 2H, H_5), 2.78 (m, 2H, H_4), 3.71 (dh, 1H, H_8 , $^3J = 10.6$ Hz, $^3J = 6.6$ Hz), 7.10 (m, 3H, $H_{1,2}$), 7.20 (m, 1H, H_3), 7.65 (d, 1H, H_7 , $^2J = 10.6$ Hz). $^{13}\text{C-NMR}$ (101 MHz, CDCl_3) δ : 21.54, 21.86, 26.78, 29.52, 30.01, 42.57, 106.19, 116.55, 126.77, 128.71, 129.06, 140.50, 160.03, 162.55, 174.38. m.p.: 79-81 °C. ν_{max} (cm^{-1}): 1731 (CO). m/z (ES) 288.2 (M). $\text{C}_{17}\text{H}_{20}\text{O}_4$ requires C 70.83, H 6.91, N 0.00; found C 70.29, H 6.97, N 0.09.



5.12 Synthesis of 5-benzylidene-2-phenyl-1,3-dioxane-4,6-dione **10**

A mixture of benzaldehyde (11.4 mL, 112.5 mmol), malonic acid (10.4 g, 100 mmol) and conc. sulphuric acid (0.30 mL, 6 mmol) was stirred at 0 °C for 15 min. Acetic anhydride (12 mL, 125 mmol) was then added very slowly over a period of 30 min and the mixture was then stirred at room temperature for 18 h. A white solid was collected by filtration and recrystallised from ethyl acetate and petrol to afford 2.26 g (21 %) of **10**. $^1\text{H NMR}$ (400 MHz, CDCl_3) δ : 6.70 (s, 1H, H_4), 7.40 (m, 5H, $H_{6,7,8}$), 7.50 (m, 3H, $H_{1,2}$), 7.95 (dd, 2H, H_3 , $^3J = 8.0$ Hz, $^4J = 1.4$ Hz), 8.30 (s, 1H, H_5). $^{13}\text{C-NMR}$ (101 MHz) δ : 97.11, 116.1, 126.85, 129.30 (x2), 131.16, 131.85, 133.26, 134.11, 134.56, 159.58, 161.25, 164.55. m.p. 146-148 °C. λ_{max} (ϵ): 320.8 nm ($19682 \text{ M}^{-1}\text{cm}^{-1}$), 226.1 nm ($9611 \text{ M}^{-1}\text{cm}^{-1}$), 203.1 nm ($24631 \text{ M}^{-1}\text{cm}^{-1}$). m/z (ES) 280.2 (M).



5.13 Deracemisation of 5-(4-nitro-benzylidene)-2-methyl-2-(phenylethyl)-1,3-dioxane-4,6-dione **5**

A mixture of 5-(4-nitro-benzylidene)-2-methyl-2-(phenylethyl)-1,3-dioxane-4,6-dione **5** (0.80 g, 2.18 mmol) and L-Cysteine (0.132 g, 1.09 mmol) in EtOH (20 mL)

was stirred at room temperature for 18 h. The solvent was then evaporated and the solid residue was dissolved in DCM (200 mL) and filtered. The product was collected as the filtrate, by evaporation of the DCM, and its purity was confirmed by ¹H-NMR. **5** (100 mg) was then dissolved in DCM (2.7 mL) and its optical activity was measured in the polarimeter. See Section 2.6 for results. Adduct formed: *m/z* (Accurate Mass): 489.1326 (Calculated for M+H⁺), 489.1324 (Measured).

5.14 Deracemisation of 5-(2-nitro-benzylidene)-2-methyl-2-(phenylethyl)-1,3-dioxane-4,6-dione **6**

A mixture of 5-(2-nitro-benzylidene)-2-methyl-2-(phenylethyl)-1,3-dioxane-4,6-dione **6** (0.13 g, 0.35 mmol) and L-Cysteine (0.022 g, 0.18 mmol) in EtOH (10 mL) was stirred at room temperature for 18 h. The solvent was evaporated and the residue was dissolved in DCM and filtered. The product was collected as the filtrate, by evaporation of DCM and its purity checked by ¹H-NMR. **6** (80 mg) was then dissolved in DCM (2.7 mL) and the optical activity was measured in the polarimeter.

5.15 Deracemisation of 5-(4-methoxybenzylidene)-2-methyl-2-(phenylethyl)-1,3-dioxane-4,6-dione **7, using L-Cysteine**

A mixture of 5-(4-methoxybenzylidene)-2-methyl-2-(phenylethyl)-1,3-dioxane-4,6-dione **7** (0.335 g, 0.95 mmol) and L-Cysteine (0.058 g, 0.48 mmol) in EtOH (15 mL) was stirred at room temperature for 18 h. The solvent was then evaporated until dryness, and the residue was dissolved in DCM. The precipitate was separated by filtration, the product was collected after evaporation of DCM and its purity was confirmed by ¹H-NMR. **7** (80 mg) was then dissolved in DCM (2.7 mL) and the optical activity was measured in the polarimeter.

5.16 Synthesis of L-Leucine methyl ester hydrochloride

Thionyl chloride (3 mL, 41.3 mmol) was added very slowly to a solution of MeOH (25 mL) at 0 °C under nitrogen. The mixture was stirred for 15 min and L-Leucine (5.02 g, 38.3 mmol) was then added and the reaction was heated at reflux for 48 h. MeOH and thionyl chloride were evaporated under reduced pressure and the product was collected as a white solid as the hydrochloride salt (4.8 g, 69 %). ¹H NMR (250 MHz, CDCl₃) δ: 0.79 (d, 6H, ³J = 5.9 Hz), 1.75 (m, 3H), 3.61 (s, 3H), 4.90 (m, 1H), 8.61 (bs, 3H).

5.17 Deracemisation of 5-(4-methoxybenzylidene)-2-methyl-2-(phenylethyl)-1,3-dioxane-4,6-dione **7**, using L-Leucine

L-Leucine methyl ester hydrochloride (0.543 g (3 mmol)), was dissolved in aqueous NaHCO₃ (25 mL) and immediately extracted with DCM (10 mL). The solution was dried with MgSO₄ and then **7** (0.74 g, 2.1 mmol) and triethylamine (excess) were added and the mixture was then stirred for 5 days. The solvent was evaporated to dryness, and the residue was dissolved in DCM. A solid precipitated and was separated by filtration, the product was collected as the filtrate after evaporation of DCM and its purity was confirmed by ¹H-NMR. **7** (80 mg) was then dissolved in DCM (2.7 mL) and the optical activity was measured in the polarimeter.

5.18 Deracemisation of 5-benzylidene-2-phenyl-1,3-dioxane-4,6-dione **10**

A mixture of 5-benzylidene-2-phenyl-1,3-dioxane-4,6-dione **10** (0.28 g, 1 mmol) and L-Cysteine (0.06 g, 0.5 mmol) in EtOH (10 mL) was stirred at room temperature for 18 h. The solvent was then evaporated to dryness and the residue was dissolved in DCM. The precipitate was separated by filtration and the product was collected after evaporation of DCM. Its purity was confirmed by ¹H-NMR. **7** (80 mg) was then dissolved in DCM (2.7 mL) and the optical activity was measured in the polarimeter. Adduct: *m/z* (Accurate Mass): 400.0860 (Calculated for M-H⁺), 400.0864 (Measured). A white solid by-product (Section 2.5.1) contained an inseparable mixture of diastereoisomeric acids derived from hydrolysis of the adducts. **10a** (55 %): ¹H NMR (400 MHz, CDCl₃) δ: 3.20 (dd, 1H, ²*J* = 10.2 Hz, ³*J* = 4.5 Hz), 3.36 (dd, 1H, ²*J* = 10.2 Hz, ³*J* = 7.1 Hz), 4.30 (dd, 1H, ³*J* = 4.5 Hz, ³*J* = 7.0 Hz), 5.73 (s, 1H), 7.39 (m, 3H), 7.51 (d, 2H, ³*J* = 7.3 Hz). **10b** (45 %): ¹H NMR (400 MHz, CDCl₃) δ: 3.13 (dd, 1H, ²*J* = 9.9 Hz, ³*J* = 9.0 Hz), 3.42 (dd, 1H, ²*J* = 10.0 Hz, ³*J* = 7.1 Hz), 3.96 (dd, 1H, ³*J* = 8.7 Hz, ³*J* = 7.2 Hz), 5.58 (s, 1H), 7.39 (m, 3H), 7.58 (d, 2H, ³*J* = 8.2 Hz).

5.19 General procedure for attempted deracemisation using Circularly Polarised Light

A small sample of benzylidene malonate (*ca* 100 mg) was dissolved in the minimum amount of hot acetonitrile (*ca* 1.5 mL). The mixture was then stirred at a constant speed of 600 rev/min and boiled for 2 min. CPL was then turned on and the oil bath was replaced by an ice bath. The mixture was left to crystallise for 15min, then

filtered. The optical activity was measured for both the mother liquor and the solid by diluting the solutions to 2.7 mL (max capacity of quartz cell).

5.20 General procedure for coordination of Pt(0)-(S)-DIOP ethene to benzylidene malonates

Pt(0)-(S)-DIOP ethene (40 mg, 0.055 mmol)^[4] was dissolved in C₆D₆ (0.7 mL). An excess of benzylidene malonate was then added to the solution and the mixture was vigorously agitated for 2 min and the ³¹P-NMR spectrum was recorded immediately. Low solubility of the complexes derived from **7** and **10** meant that no ¹⁹⁵Pt satellites were observed. Conformational isomerism (hindered rotation around the C-C bond between the alkene and the 2-nitrophenyl group) is assumed to lead to the doubling of the peaks for **6**. Compound **5**: ³¹P-NMR (121 MHz, C₆D₆) δ: 7.12 (J_{PP} = 27 Hz, J_{PP} = 4326 Hz), 7.62 (J_{PP} = 27 Hz, J_{PT} = 3228 Hz), 8.28 (J_{PP} = 27 Hz, J_{PT} = 4326 Hz), 6.77 (J_{PP} = 27 Hz, J_{PT} = 3231 Hz). *m/z* (ES). Theoretical isotope model [M+H]⁺ 1060.3 (62 %), 1061.3 (100 %), 1062.3 (97 %), 1063.3 (42 %), 1064.3 (25 %), 1065.3 (10 %); Observed data 1060.3 (30 %), 1061.3 (73 %), 1062.4 (100 %), 1063.5 (27 %), 1064.5 (10 %). Theoretical isotope model [M+Na]⁺ 1082.2 (62 %), 1083.2 (100 %), 1084.2 (98 %), 1085.3 (41 %), 1086.3 (25 %), 1087.3 (10 %); Observed data 1082.3 (27 %), 1083.2 (85 %), 1084.4 (62 %), 1085.3 (20 %). Compound **6**: ³¹P-NMR (121 MHz, C₆D₆) δ: 8.52 (J = 29.6 Hz), 8.05 (J = 29.6 Hz), 7.50 (J = 26.7 Hz), 7.05 (J = 29.6 Hz), 6.80 (J = 29.6 Hz), 5.24 (J = 29.6 Hz). Compound **7**: ³¹P-NMR (121 MHz, C₆D₆) δ: 9.72 (J = 35.5 Hz), 8.42 (J = 35.5 Hz). Compound **8**: ³¹P-NMR (121 MHz, C₆D₆) δ: 10.22 (J = 35.5 Hz), 9.32 (J = 35.5 Hz), 8.39 (J = 35.5 Hz), 7.99 (J = 32.5 Hz), 7.24 (J = 35.5 Hz), 5.29 (J = 35.5 Hz). Compound **10** ³¹P-NMR (121 MHz, C₆D₆) δ: 10.89 (J = 32.6 Hz) 6.84 (J = 32.6 Hz).

5.21 Synthesis of bis(dihydroxobisethylenediaminecobalt(II))bisaquocobalt(III) disulphate pentahydrate ((H₂O)₂Co{(OH)₂Co(en)₂}₂)(SO₄)₂·5H₂O)

This synthesis was performed following a similar procedure to that described in the literature:^[5] A mixture of CoSO₄·7H₂O (300 mL, 450 mmol) in a 10 % solution of ethylenediamine in H₂O (300 mL) was stirred at room temperature for 4 h, allowed to settle for 1 h and then filtered. The mother liquor was left to crystallise for 18 h before filtering, to afford 20.71 g (22.9 %) of [(H₂O)₂Co{(OH)₂Co(en)₂}₂](SO₄)₂·5H₂O.^[1] *v*_{max} (cm⁻¹): 3416 (OH), 3247 (OH), 3116 (OH).

5.22 Synthesis of *cis*-bromoamminebis(ethylenediamine)cobalt(III) bromide (*cis*-[CoBr(NH₃)(en)₂]Br₂) 11

This synthesis was performed following a similar procedure to that described in the literature:^[6] NH₄Br (6.86 g, 70 mmol) was added to a solution of [(H₂O)₂Co{(OH)₂Co(en)₂}₂](SO₄)₂·5H₂O (2.56 g, 3.19 mmol) in H₂O (6.8 mL). The mixture was stirred at room temperature for 1 min, followed by stirring at 50 °C for 5 min. Immediately after stirring had finished, the mixture was cooled in an ice bath for 1 h. The product was recrystallised from 5 % HBr to afford 1.58 g (57 %) of dark violet crystals *cis*-[CoBr(NH₃)(en)₂]Br₂ 11.^[7] ¹H-NMR (400 MHz, D₂O) δ: 2.22 (m, 2H, CH₂), 2.49 (m, CH₂, 4H), 2.71 (m, 2H, CH₂), 3.16 (s, 3H, NH₃), 4.00 (s, 1H, NH), 4.07 (s, 1H, NH), 4.29 (s, 1H, NH), 4.51 (s, 1H, NH), 4.88 (s, 1H, NH), 4.98 (s, 2H, NH), 5.18 (s, 1H, NH). ¹³C-NMR (101 MHz, D₂O) δ: 44.70; 45.05; 45.17; 45.33; 45.46. **m.p.**: 225-227 °C. **m/z** (ES): Theoretical isotope model for C₄H₁₆Br₂CoN₄: 336.9 (51.3 %); 338.9 (100 %); 340.9 (48.6 %), observed data: 336.9 (47.3 %); 339.0 (100 %); 341.0 (47.3 %). **v_{max}** (cm⁻¹): 3413 (NH), 3217 (NH). **λ_{max}** (ε): 542.4 nm (85 M⁻¹cm⁻¹). **X-ray**: C₄H₁₉Br₃CoN₅, *M* = 435.90, red block, 0.20 × 0.20 × 0.15 mm³, monoclinic, space group *P*2₁/*n* (No. 14), *a* = 7.6301(2), *b* = 12.3587(4), *c* = 13.9682(5) Å, β = 98.5640(10)°, *V* = 1302.49(7) Å³, *Z* = 4, *D_c* = 2.223 g/cm³, *F*₀₀₀ = 840, KappaCCD, MoKα radiation, λ = 0.71073 Å, *T* = 150(2)K, 2θ_{max} = 55.0°, 11930 reflections collected, 2910 unique (*R*_{int} = 0.0950). Final *Goof* = 1.038, *RI* = 0.0457, *wR2* = 0.0870, *R* indices based on 2035 reflections with *I* > 2σ(*I*) (refinement on *F*²), 119 parameters, 0 restraints. μ = 10.492 mm⁻¹.

5.23 Synthesis of *cis*-iodoamminebis(ethylenediamine)cobalt(III) triiodide (*cis*-[CoI(NH₃)(en)₂]I₃) 12

This synthesis was performed following a similar procedure to that described in the literature for 11:^[6] NH₄I (10.15 g, 70 mmol) was added to a solution of [(H₂O)₂Co{(OH)₂Co(en)₂}₂](SO₄)₂·5H₂O (2.56 g, 3.19 mmol) in H₂O (6.8 mL). The mixture was stirred at room temperature for 1 min, followed by stirring at 50°C for 5 min. Immediately after stirring had finished, the mixture was cooled in an ice bath for 1 h. After filtration of a green-grey solid, the mother liquid was left to crystallize. After several days of crystallization the solution was filtered and washed with cold H₂O to afford 0.184 g (16.4 %) of dark red *cis*-[CoI(NH₃)(en)₂]I₃ 12. ¹H-NMR (400

MHz, D₂O) δ : 2.40 (m, 2H, CH₂), 2.73 (m, 4H, CH₂), 2.99 (m, 2H, CH₂), 4.57 (s, 0.1H, NH₂), 4.90 (s, 0.1H, NH₂), 5.24 (s, 0.1H, NH₂). **m.p.**: decomposes at 206 °C. ν_{\max} (cm⁻¹): 3182 (NH), 3096 (NH). λ_{\max} (ϵ): 364.5 nm (1510 M⁻¹cm⁻¹), 286.5 nm (21913 M⁻¹cm⁻¹). **C₄H₁₉N₅CoI₄** requires C 6.83, H 2.72, N 9.63; found C 6.78, H 2.62, N 9.95. **X-ray**: C₄H₁₉CoI₄N₅, $M = 703.77$, black block, 0.20 × 0.20 × 0.20 mm³, triclinic, space group *P*-1 (No. 2), $a = 7.9760(2)$, $b = 8.4940(2)$, $c = 13.5110(5)$ Å, $\alpha = 93.6490(10)$, $\beta = 104.4510(10)$, $\gamma = 111.1420(10)^\circ$, $V = 814.67(4)$ Å³, $Z = 2$, $D_c = 2.869$ g/cm³, $F_{000} = 634$, MoK α radiation, $\lambda = 0.71073$ Å, $T = 293(2)$ K, $2\theta_{\max} = 55.0^\circ$, 14911 reflections collected, 3711 unique ($R_{\text{int}} = 0.1265$). Final $Goof = 0.887$, $RI = 0.0445$, $wR2 = 0.1224$, R indices based on 3149 reflections with $I > 2\sigma(I)$ (refinement on F^2), 140 parameters, 0 restraints. $\mu = 8.614$ mm⁻¹.

5.24 Synthesis of *trans*-bis(isothiocyanato)bis(ethylenediamine)cobalt(III) thiocyanate (*trans*-[Co(NCS)₂(en)₂]₂NCS) 13

This synthesis was carried out using a variation on the method described in the literature for 11.^[6] NH₄SCN (5.30 g, 70 mmol) was added to a solution of [(H₂O)₂Co{(OH)₂Co(en)₂}₂](SO₄)₂·5H₂O (2.56 g, 3.19 mmol) in H₂O (6.8 mL). The mixture was stirred at room temperature for 1 min, followed by stirring at 50 °C for 5 min. After that the mixture was cooled in an ice bath for 2 h and then left to crystallise overnight. The solid was collected by filtration to afford 0.179 g (8 %) of *trans*-[Co(NCS)₂(en)₂]₂NCS 13.^[8] ¹H-NMR (400 MHz, D₂O) δ : 2.59 (s, 8H, CH₂). ¹³C-NMR (101 MHz, D₂O) δ : 45.43; 45.72; 141.23. **m.p.**: 226-228 °C. ν_{\max} (cm⁻¹): 3216 (NH), 2107 (CN). λ_{\max} (ϵ): 514.0 nm (87 M⁻¹cm⁻¹), 315.5 nm (839 M⁻¹cm⁻¹).

5.25 Synthesis of *cis*-bis(ethylenediamine)dinitrocobalt(III) bromide (*cis*-[Co(NO₂)₂(en)₂]₂Br) 14

The synthesis was performed using a procedure similar to that described in the literature.^[9, 10] NaNO₂ (0.85 g, 10 mmol) was dissolved in H₂O (2 mL) at 50 °C. The mixture was stirred until all material had dissolved and then *cis*-[CoBr(NH₃)(en)₂]₂Br₂ (0.87 g, 2 mmol) was added. The mixture was stirred at 50 °C for 1 h, followed by cooling in an ice-bath. An orange-yellow solid was collected by filtration to afford 0.274 g (39 %) of *cis*-[Co(NO₂)₂(en)₂]₂Br 14.^[11] ¹H-NMR (400 MHz, D₂O) δ : 2.52 (m, 2H, CH₂), 2.59 (m, 4H, CH₂), 2.68 (m, 2H, CH₂), 4.25 (s, 0.1H, NH₂), 4.40 (s, 0.1H, NH₂), 4.90 (s, 0.1H, NH₂), 5.25 (s, 0.1H, NH₂). ¹³C-NMR (101 MHz, D₂O) δ :

43.65; 45.37. **m.p.**: decomposes at 211 °C. ν_{\max} (cm^{-1}): 3096 (NH), 1584 (NO), 1556 (NO). λ_{\max} (ϵ): 439.0 nm ($97 \text{ M}^{-1}\text{cm}^{-1}$), 322.5 nm ($2088 \text{ M}^{-1}\text{cm}^{-1}$). **m/z** (ES) Theoretical isotope model for $\text{C}_4\text{H}_{16}\text{CoN}_6\text{O}_4$: 271.1 (100 %); 272.1 (7.4 %). Observed data: 271.1 (100 %); 272.1 (6.7 %).

5.26 Synthesis of *cis*-bis(ethylenediamine)dichlorocobalt(III) chloride (*cis*-[CoCl₂(en)₂]Cl) 15

The synthesis was performed following a procedure similar to that described in the literature.^[12] A 10 % solution of ethylenediamine (60 mL, 90 mmol) was added to a solution of CoCl₂·6H₂O (16 g, 67 mmol) in H₂O (50 mL). A stream of air was passed through the solution for 7.5 h, then left overnight. Conc. HCl (35 mL) was added and the solution was concentrated by heating to *ca.* 75 mL, with a green solid precipitating from the solution. The product was collected by filtration, washed with EtOH and ether, and dried at 110 °C until no more acid was present. The solid was dissolved in H₂O (50 mL) and evaporated to dryness to afford 6.82 g (53 %) of *cis*-[CoCl₂(en)₂]Cl 15.^[12] ¹H-NMR (400 MHz, D₂O) δ : 2.39 (m, 2H, CH₂), 2.63 (m, 4H, CH₂), 2.86 (m, 2H, CH₂), 5.19 (s, 2H, NH₂), 5.35 (s, 2H, NH₂), 5.58 (s, 2H, NH₂), 5.85 (s, 2H, NH₂). λ_{\max} (ϵ): 533.0 nm ($69 \text{ M}^{-1}\text{cm}^{-1}$), 370.5 nm ($69 \text{ M}^{-1}\text{cm}^{-1}$).

5.27 Synthesis of *cis*-(bis(ethylenediamine)dinitrocobalt(III)) chloride (*cis*-[Co(NO₂)₂(en)₂]Cl) 16

The synthesis was performed following the procedure described in the literature.^[9] 15 (2.85 g, 10 mmol) and NaNO₂ (1.5 g, 22 mmol) were dissolved in hot H₂O (60 °C, 20 mL). The mixture was stirred for 1 h at 60 °C, then cooled in an ice bath for 2 h. The product was collected by filtration and recrystallised from H₂O, to afford 0.460 g (15 %) of *cis*-[Co(NO₂)₂(en)₂]Cl 16.^[5] ¹H-NMR (400 MHz, D₂O) δ : 2.52 (m, 2H, CH₂), 2.59 (m, 4H, CH₂), 2.69 (m, 2H, CH₂), 4.25 (s, 0.1H, NH₂), 4.42 (s, 0.1H, NH₂), 5.26 (s, 0.1H, NH₂). ¹³C-NMR (101 MHz, D₂O) δ : 43.67; 45.39. **m.p.**: Decomposes at 228 °C. **m/z** (ES): Theoretical isotope model for $\text{C}_4\text{H}_{16}\text{CoN}_6\text{O}_4$: 271.1 (100 %); 272.1 (7.4 %). Observed data: 271.1 (100 %); 272.1 (7.4 %). λ_{\max} (ϵ): 437.5 nm ($202 \text{ M}^{-1}\text{cm}^{-1}$), 322.0 nm ($4140 \text{ M}^{-1}\text{cm}^{-1}$).

5.28 Synthesis of *cis*-bis[bis(ethylenediamine)dinitrocobalt(III)] tetrathionate (*cis*-[Co(NO₂)₂(en)₂]₂S₄O₆) 17

The synthesis was carried out according to a variation in the literature procedure for similar systems:^[13] a solution of Na₂S₄O₆ (0.189 g, 0.7 mmol) in H₂O (1 mL) at 50 °C was added slowly to a solution of **16** (0.306 g, 1 mmol) in H₂O (25 mL) at 50 °C. The mixture was stirred at 50 °C until a golden yellow solid precipitated. The solid was collected by filtration, washed with EtOH and ether and recrystallised from H₂O to afford 0.213 g (56 %) of *cis*-[Co(NO₂)₂(en)₂]₂S₄O₆ **17**. ¹H-NMR (400 MHz, D₂O) δ: 2.66 (m, 2H, CH₂), 2.69 (m, 4H, CH₂), 2.78 (m, 2H, CH₂). ¹³C-NMR (101 MHz, D₂O) δ: 43.62; 45.35. **m.p.**: decomposes at 239 °C. **v_{max}** (cm⁻¹): 3207 (NH), 1572 (NO), 1408 (NO). **λ_{max}** (ε): 434.8 nm (1015 M⁻¹cm⁻¹), 321.0 nm (7224 M⁻¹cm⁻¹). **m/z** (ES): Theoretical isotope model for C₄H₁₆CoN₆O₁₀S₄: 494.9 (100 %); 496.9 (20.3 %). Observed data: 495.1 (100 %); 496.0 (10.8 %). **C₈H₃₂N₁₂O₁₄Co₂S₄**: requires C 12.54, H 4.21, N 21.61; found C 12.54, H 4.21, N 21.93. **X-ray**: C₈H₃₂Co₂N₁₂O₁₄S₄, *M* = 766.56, yellow block, 0.50 × 0.45 × 0.13 mm³, monoclinic, space group *P*2₁/*a* (No. 14), *a* = 12.4425(2), *b* = 7.79690(10), *c* = 27.6488(5) Å, β = 92.3300(10)°, *V* = 2680.07(7) Å³, *Z* = 4, *D_c* = 1.900 g/cm³, *F*₀₀₀ = 1576, KappaCCD, MoKα radiation, λ = 0.71073 Å, *T* = 150(2)K, 2θ_{max} = 55.0°, 15938 reflections collected, 5959 unique (*R*_{int} = 0.0693). Final *Goof* = 1.020, *RI* = 0.0452, *wR2* = 0.1076, *R* indices based on 4704 reflections with *I* > 2σ(*I*) (refinement on *F*²), 361 parameters, 0 restraints. μ = 1.634 mm⁻¹.

5.29 Synthesis of *trans*-bis[bis(ethylenediamine)dichlorocobalt(III)] tetrathionate (*trans*-[CoCl₂(en)₂]₂S₄O₆) 18

The synthesis was performed following a procedure similar to that described in the literature for a similar system:^[13] A solution of Na₂S₄O₆ (0.675 g, 2.5 mmol) in H₂O (1 mL) at 50 °C was added slowly to a solution of **16** (1.142 g, 4 mmol) in H₂O (18 mL) at 50 °C. The mixture was stirred at 50 °C for 30min, then cooled in an ice bath and left to crystallise overnight. Green crystals were collected by filtration, washed with EtOH and ether to afford 0.156 g (11 %) of *trans*-[CoCl₂(en)₂]₂S₄O₆ **18**. ¹H-NMR (400 MHz, D₂O) δ: 2.88 (s, 8H, CH₂). ¹³C-NMR (101 MHz, D₂O) δ: 45.27. **m.p.** 207-209 °C. **v_{max}** (cm⁻¹): 3230 (NH), 1226 (SO). **λ_{max}** (ε): 617.6 nm (111 M⁻¹cm⁻¹), 368.8 nm (398 M⁻¹cm⁻¹). **m/z** (ES): Theoretical isotope model for

$C_4H_{16}Cl_2CoN_4O_6S_4$: 472.9 (100 %); 474.9 (83.1 %); 476.9 (24.4 %). Observed data: 473.0 (100 %); 475.0 (94.6 %); 477.2 (25.7 %). Theoretical isotope model for $C_4H_{16}Cl_2CoN_4$: 249.0 (100 %); 251.0 (64.2 %); 253.0 (10.8 %). Observed data: 249.0 (100 %); 251.0 (64.2 %); 253.0 (10.8 %). **X-ray**: $C_8H_{32}Cl_4Co_2N_8O_6S_4$, $M = 724.32$, green block, $0.30 \times 0.25 \times 0.10 \text{ mm}^3$, triclinic, space group $P-1$ (No. 2), $a = 9.1266(2)$, $b = 12.0312(3)$, $c = 12.6384(4) \text{ \AA}$, $\alpha = 79.7030(10)$, $\beta = 87.0570(10)$, $\gamma = 71.353(2)^\circ$, $V = 1293.70(6) \text{ \AA}^3$, $Z = 2$, $D_c = 1.859 \text{ g/cm}^3$, $F_{000} = 740$, KappaCCD, MoK α radiation, $\lambda = 0.71073 \text{ \AA}$, $T = 150(2)\text{K}$, $2\theta_{\text{max}} = 54.9^\circ$, 23057 reflections collected, 5897 unique ($R_{\text{int}} = 0.1131$). Final $GooF = 1.028$, $R_I = 0.0578$, $wR2 = 0.1080$, R indices based on 3591 reflections with $I > 2\sigma(I)$ (refinement on F^2), 295 parameters, 6 restraints. $\mu = 2.060 \text{ mm}^{-1}$.

5.30 Synthesis of *cis*-chloroamminebis(ethylenediamine)cobalt(III) dichloride (*cis*-[CoCl(NH₃)(en)₂]Cl₂) **19**

This synthesis was performed following a similar procedure to that described in the literature.^[6] NH₄Cl (3.75 g, 70 mmol) was added to a solution of [(H₂O)₂Co{(OH)₂Co(en)₂}]₂(SO₄)₂·5H₂O (2.56 g, 3.19 mmol) in H₂O (6.8 mL). The mixture was stirred at room temperature for 1 min followed by stirring at 50 °C for 5 min, and then cooled in an ice bath for 1 h without stirring. The solid was collected by filtration, washed with EtOH and ether to afford 0.44 g (46 %) of *cis*-[CoCl(NH₃)(en)₂]Cl₂ **19**.^[14] ¹H-NMR (400 MHz, D₂O) δ : 2.45 (m, 2H, CH₂), 2.66 (m, 4H, CH₂), 2.83 (m, 2H, CH₂), 3.37 (s, 0.1H, NH₃), 5.04 (s, 0.1H, NH₂), 5.18 (s, 0.1H, NH₂), 5.22 (s, 0.1H, NH₂), 5.40 (s, 0.1H, NH₂). ¹³C-NMR (101 MHz, D₂O) δ : 44.44, 44.81, 45.05, 45.17. **m.p.** 246-248 °C. ν_{max} (cm⁻¹): 3430 (NH), 3287 (NH), 3237 (NH). λ_{max} (ϵ): 538.5 nm (401 M⁻¹cm⁻¹), 340.5 nm (2101 M⁻¹cm⁻¹). **m/z** (ES): Theoretical isotope model for $C_4H_{19}Cl_2CoN_5$: 336.0 (78.3 %); 338.0 (100 %); 340.0 (47.9 %); 432.0 (10.8 %). Observed data: 336.0 (66.2 %); 338.1 (100 %); 340.1 (43.2 %); 432.0 (10.8 %).

5.31 Synthesis of *cis*-chloroamminebis(ethylenediamine)cobalt(III) tetrathionate (*cis*-[CoCl(NH₃)(en)₂]S₄O₆) **20**

A solution of Na₂S₄O₆ (0.95 g, 3.5 mmol) in H₂O (1 mL) at 50 °C was added slowly to a solution of **19** (1.00 g, 3.3 mmol) in H₂O (7 mL) at 50 °C. The mixture was stirred for 1 min at 50 °C and then for 1 h at room temperature. The solution was left

to crystallise overnight. A pink solid was collected by filtration and recrystallised from H₂O to afford 0.37 g (25 %) of *cis*-[CoCl(NH₃)(en)₂]S₄O₆ **20**. ¹H-NMR (400 MHz, D₂O) δ: 2.48 (m, 2H, CH₂), 2.70 (m, 4H, CH₂), 2.83 (m, 2H, CH₂), 3.40 (s, 0.1H, NH₃), 5.20 (s, 0.1H, NH₂), 5.26 (s, 0.1H, NH₂), 5.40 (s, 0.1H, NH₂). ¹³C-NMR (101 MHz, D₂O) δ: 44.51; 44.88; 45.10; 45.25. m.p. 185 °C. ν_{max} (cm⁻¹): 3487 (NH), 3237 (NH), 1629 (SO), 1568 (SO). λ_{max} (ε): 523.5 nm (42 M⁻¹cm⁻¹), 360.0 nm (44 M⁻¹cm⁻¹). C₄H₂₁N₅O₇ClCoS₄: requires C 10.14, H 4.47, N 14.78; found C 10.12, H 4.37, N 14.49. X-ray: C₄H₂₁ClCoN₅O₇S₄, M = 473.88, pink plate, 0.28 × 0.20 × 0.05 mm³, monoclinic, space group P2₁/n (No. 14), a = 11.9042(4), b = 9.5176(4), c = 15.2284(5) Å, β = 101.993(2)°, V = 1687.71(11) Å³, Z = 4, D_c = 1.865 g/cm³, F₀₀₀ = 976, KappaCCD, MoKα radiation, λ = 0.71073 Å, T = 150(2)K, 2θ_{max} = 54.9°, 9915 reflections collected, 3859 unique (R_{int} = 0.0895). Final GooF = 1.062, RI = 0.0509, wR2 = 0.1204, R indices based on 2981 reflections with I > 2σ(I) (refinement on F²), 209 parameters, 0 restraints. μ = 1.707 mm⁻¹.

5.32 Synthesis of bis-(ethylenediamine)oxalatocobalt(III) chloride [Co(ox)(en)₂]Cl·4H₂O **21**

The synthesis was performed following the literature procedure:^[15] 2.85 g (10 mmol) of *cis*-[CoCl₂(en)₂]Cl was added to H₂O (15 mL) and stirred at 60 °C until all material had dissolved. (NH₄)₂ox·H₂O (1.56 g, 11 mmol) was then added slowly. The mixture was stirred at 60 °C for 30min then left to crystallise. *cis*-[Co(ox)(en)₂]Cl·4H₂O was collected by filtration, washed with H₂O, EtOH and ether to afford 2.72 g (73 %) of **21**.^[15] ¹H-NMR (400 MHz, D₂O) δ: 2.60 (m, 2H, CH₂), 2.70 (m, 6H, CH₂), 5.12 (s, 1H, NH₂), 5.33 (s, 1H, NH₂). ν_{max} (cm⁻¹): 3227 (NH), 3106 (NH), 1650 (CO). λ_{max} (ε): 497.3 nm (102 M⁻¹cm⁻¹), 355.1 nm (128 M⁻¹cm⁻¹). m.p. 268-270 °C.

5.33 Synthesis of bis(bis-(ethylenediamine)oxalatocobalt(III)) tetrathionate [Co(ox)(en)₂]₂S₄O₆ **22**

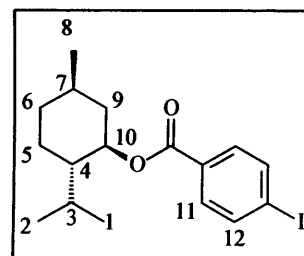
A solution of Na₂S₄O₆ (1.08 g, 4 mmol) was added slowly to a solution of **21** (1.12 g, 3 mmol) in H₂O (5 mL) at 50 °C. The mixture was stirred for 2 h and the product was collected as a pink solid by filtration. The solid was washed with EtOH and ether, then dried by suction to afford 0.856 g (75 %) of *cis*-[Co(ox)(en)₂]₂S₄O₆ **22**. ¹H-NMR (400 MHz, D₂O) δ: 2.30 (m, 2H, CH₂), 2.39 (m, 6H, CH₂). ¹³C-NMR (101

MHz, D₂O) δ : 43.42; 45.56; 167.5. **m.p.**: decomposes at 236 °C. **m/z** (ES): Theoretical isotope model for C₆H₁₆CoN₄O₁₀S₄: 490.9 (100 %); 492.9 (20.3 %). Observed data: 490.9 (100 %); 492.9 (25.7 %). ν_{\max} (cm⁻¹): 3462 (NH), 3207 (NH), 3106 (NH), 1699 (CO), 1660 (SO), 1584 (SO). λ_{\max} (ϵ): 496.4 nm (113 M⁻¹cm⁻¹), 355.0 nm (147 M⁻¹cm⁻¹). C₁₂H₃₂N₈O₁₄Co₂S₄·15/2H₂O: requires C 17.54, H 4.78, N 13.64; found C 13.24, H 4.40, N 15.36. **X-ray**: C₁₂H₄₈Co₂N₈O_{21.50}S₄, *M* = 894.68, red block, 0.30 × 0.25 × 0.10 mm³, triclinic, space group *P*-1 (No. 2), *a* = 11.7530(3), *b* = 12.5463(3), *c* = 13.2064(3) Å, α = 68.1750(10), β = 89.7030(10), γ = 73.3970(10)°, *V* = 1721.21(7) Å³, *Z* = 2, *D*_c = 1.726 g/cm³, *F*₀₀₀ = 932, KappaCCD, MoK α radiation, λ = 0.71073 Å, *T* = 150(2)K, 2 θ_{\max} = 55.2°, 30114 reflections collected, 7871 unique (*R*_{int} = 0.1149). Final *Goof* = 1.076, *RI* = 0.0565, *wR2* = 0.1300, *R* indices based on 6454 reflections with *I* > 2 σ (*I*) (refinement on *F*²), 433 parameters, 6 restraints. μ = 1.298 mm⁻¹.

5.34 Synthesis of (1*R*,2*S*,5*R*)-5-methyl-2-(1-methylethyl)cyclohexyl *p*-iodobenzoate **23**

(1*R*,2*S*,5*R*)-5-methyl-2-(1-methylethyl)cyclohexane (menthol) (7.8 g, 50 mmol) was added to a solution of *p*-iodobenzoyl chloride (13.33 g, 50 mmol) in DCM (20 mL), followed by pyridine (4.1 mL, 50 mmol). The mixture was stirred for 1 h at room temperature, then filtered and the solvent evaporated. The resultant oil was dissolved in petrol (20 mL) and washed with H₂O (3 × 10 mL). The product was collected after distillation in a Kugelrohr glass oven to obtain 14.21 g (74 %) of menthyl *p*-iodobenzoate **23**.^[16]

¹H-NMR (400 MHz, CDCl₃)^{*} δ : 0.72 (d, 3H, *H*₁, ³*J* = 7.0 Hz), 0.85 (m, 7H, *H*₂, *H*_{5eq}, *H*₈), 1.07 (m, 2H, *H*_{6ax}, *H*_{9ax}), 1.46 (m, 1H, *H*₄), 1.61 (m, 2H, *H*_{5ax}, *H*_{6eq}), 1.81 (dq, 1H, *H*₃, ³*J* = 6.5 Hz, ³*J* = 2.5 Hz), 1.92 (m, 1H, *H*_{9eq}), 4.77 (dt, 1H, *H*₁₀, ³*J* = 11.0 Hz, ³*J* = 4.5 Hz), 7.65 (d, 2H *H*₁₂, ³*J* = 8.3 Hz), 7.87 (d, 2H, *H*₁₁, ³*J* = 8.3 Hz).

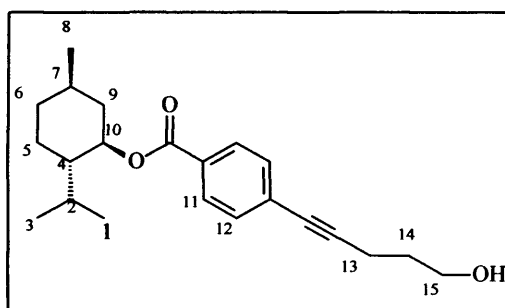


* The menthyl group has been fully assigned for compound **25** by a combination of ¹H-NMR, ¹³C-NMR, COSY, HMQC and DEPT. Compounds **23**, **24**, **26** and **27** have been assigned by their similarity to compound **25**.

5.35 Synthesis of benzoic acid-4-(4-pentyne-1-ol)-(1R,2S,5R)-5-methyl-2-(1-methylethyl)cyclohexyl ester **24**

The reaction was carried out using Schlenk techniques under an atmosphere of nitrogen. A solution of **23** (11.58 g, 30 mmol), 5-pentyne-1-ol (2.95 mL, 32 mmol) and diethylamine (5.2 mL, 50 mmol) in degassed DMF (3.9 mL, 50 mmol) was transferred to a Schlenk containing PdCl₂(CNCH₃)₂ (156 mg, 0.6 mmol), CuI (114 mg, 0.6 mmol) and PPh₃ (786 mg, 3 mmol) and stirred at room temperature for 48h. The solvent was then evaporated, and the resultant oil was dissolved in DCM (25 mL) and washed with HCl (0.1 M, 3 x 15 mL). The organic layer was dried with MgSO₄ and the solvent evaporated to

afford 9.83 g (95.6 %) of **24**. ¹H-NMR (400 MHz, CDCl₃) δ: 0.72 (d, 3H, H₁, ³J = 7.0 Hz), 0.85 (m, 7H, H₂, H_{5eq}, H₈), 1.07 (m, 2H, H_{6ax}, H_{9ax}), 1.48 (m, 1H, H₄), 1.65 (m, 2H, H_{5ax}, H_{6eq}), 1.81, (quin, 2H, H₁₄, ³J = 6.5 Hz), 1.87 (dh, 1H, H₃, ³J = 6.5 Hz,

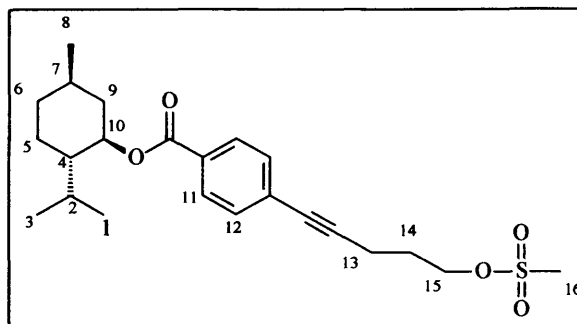


³J = 2.5 Hz), 2.04 (m, 1H, H_{9eq}), 2.50 (t, 2H, H₁₃, ³J = 6.5 Hz), 3.76 (t, 2H, H₁₅, ³J = 6.5 Hz), 4.85 (app dt, 1H, H₁₀, ³J = 11.0 Hz, ³J = 4.5 Hz), 7.41 (dd, 2H, H₁₂, ³J = 8.5 Hz, ⁴J = 1.7 Hz), 7.89 (dd, 2H, H₁₁, ³J = 8.5 Hz, ⁴J = 1.7 Hz). ¹³C-NMR (101 MHz, CDCl₃) δ: 166.06, 131.78, 129.96, 129.75, 128.89, 93.27, 80.87, 75.36, 61.71, 47.57, 41.25, 34.64, 31.80, 31.70, 26.84, 23.96, 22.42, 21.14, 16.87, 16.44. ν_{max} (cm⁻¹): 3586 (OH), 3406 (OH), 2228 (C≡C), 1713 (CO), 1671 (CO). m/z (EI/CI): 343.3 (M+H)⁺; (Accurate Mass ES): Calculated for M+H⁺: 343.2268. Measured: 343.2270. [α]_D -41.3°.

5.36 Synthesis of benzoic acid-4-(4-pentyne-1-omesyl)-(1R,2S,5R)-5-methyl-2-(1-methylethyl)cyclohexyl ester **25**

NEt₃ (2.8 mL, 20 mmol) was added to a solution of **25** (5.02 g, 14.7 mmol) in DCM (15 mL) under nitrogen. The mixture was cooled to 0 °C, a solution of mesyl chloride (1.3 mL, 17 mmol) in DCM (10 mL) was added very slowly and the mixture was stirred for 2 h at room temperature. The solution was then washed with HCl (1 M, 3 x 5mL), the organic layer dried with MgSO₄ and the solvent evaporated to afford 5.7 g (93 %) of **25**. ¹H-NMR (400 MHz, CDCl₃) δ: 0.72 (d, 3H, H₁, ³J = 7.0 Hz), 0.85 (m, 7H, H₂, H_{5eq}, H₈), 1.04 (m, 2H, H_{6ax}, H_{9ax}), 1.48 (m, 1H, H₄), 1.66 (m, 2H, H_{5ax},

H_{6eq}), 1.87 (dh, 1H, H_3 , $^3J = 6.5$ Hz, $^3J = 3$ Hz), 2.00 (quin, 2H, H_{14} , $^3J = 6.5$ Hz), 2.04 (m, 1H, H_{9eq}), 2.55 (t, 2H, H_{13} , $^3J = 6.5$ Hz), 2.97 (s, 3H, H_{16}), 4.35 (t, 2H, H_{15} , $^3J = 6.5$ Hz), 4.85 (app dt, 1H, H_{10} , $^3J = 11.0$ Hz, $^3J = 4.5$ Hz), 7.41 (dd, 2H, H_{12} , $^3J = 8.5$ Hz, $^4J = 1.5$ Hz), 7.90 (dd, 2H,

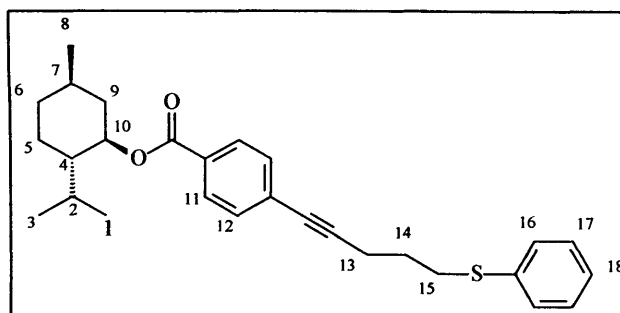


H_{11} , $^3J = 8.0$ Hz, $^4J = 1.5$ Hz). $^{13}\text{C-NMR}$ (63 MHz, CDCl_3) δ : 164.52, 130.43, 128.95, 128.42, 126.87, 89.76, 80.43, 74.01, 67.41, 46.21, 39.92, 39.43, 36.32, 33.26, 30.42, 26.97, 25.48, 22.61, 21.02, 19.74, 15.50, 14.82. ν_{max} (cm^{-1}): 2223 ($\text{C}\equiv\text{C}$), 1704 (CO), 1168 (SO) m/z (EI/CI MS): 420.3(M^+). (Accurate mass ES): 438.2309 (Calculated for $[\text{M}+\text{NH}_4]^+$), 438.2315 (Measured). $\text{C}_{23}\text{H}_{32}\text{O}_5\text{S}$ requires C 65.70, H 7.70; found C 65.62, H 7.71. m.p. 76-78 °C. $[\alpha]_{\text{D}} -48.65^\circ$.

5.37 Synthesis of benzoic acid-4-(4-pentyne-1-thiophenyl)-(1R,2S,5R)-5-methyl-2-(1-methylethyl)cyclohexyl ester 26

A solution of thiophenol (0.8 mL, 7.8 mmol) and NaOH (0.32 g, 8 mmol) in H_2O (5 mL) and EtOH (50 mL) was stirred under nitrogen for 10 min. Then a solution of **25** (3.1 g, 7.3 mmol) in EtOH (5 mL) was added very slowly. The mixture was stirred overnight, then NH_4Cl (ca 5 g) was added and the solvent evaporated. The resultant oil was dissolved in DCM (10 mL) and dried with MgSO_4 , filtered under N_2 and the solvent evaporated to afford 2.9 g (92 %) of **26**. $^1\text{H-NMR}$ (400 MHz, CDCl_3) δ : 0.71 (d, 3H, H_1 , $^3J = 7.0$ Hz), 0.84

(m, 7H, H_2 , H_{5eq} , H_8), 1.03 (m, 2H, H_{6ax} , H_{9ax}), 1.47 (m, 1H, H_4), 1.65 (m, 2H, H_{5ax} , H_{6eq}), 1.86 (dh, 1H, H_3 , $^3J = 6.5$ Hz, $^3J = 3$ Hz), 2.00 (quin, 2H, H_{14} , $^3J = 6.8$ Hz), 2.04 (m, 1H, H_{9eq}),



2.52 (t, 2H, H_{13} , $^3J = 6.8$ Hz), 3.02 (t, 2H, H_{15} , $^3J = 6.8$ Hz), 4.85 (app dt, 1H, H_{10} , $^3J = 11.0$ Hz, $^3J = 4.4$ Hz), 7.12 (t, 1H, H_{18} , $^3J = 7.0\text{Hz}$), 7.22 (m, 2H, H_{17}), 7.30 (dd, 2H, H_{16} , $^3J = 7.0$ Hz, $^4J = 1.0$ Hz), 7.36 (d, 2H, H_{12} , $^3J = 8.0$ Hz), 7.89 (d, 2H, H_{11} , $^3J = 8.5$ Hz). $^{13}\text{C-NMR}$ (63 MHz, CDCl_3) δ : 165.64, 136.15, 131.45, 129.78, 129.42,

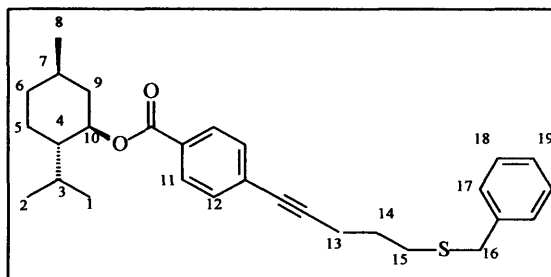
129.32, 129.09, 128.98, 128.29, 127.51, 127.17, 126.07, 92.17, 75.01, 47.27, 40.98, 34.33, 32.65, 31.47, 27.99, 26.52, 23.65, 22.08, 20.80, 18.59, 16.54. ν_{\max} (cm^{-1}): 2222 ($\text{C}\equiv\text{C}$), 1709 (CO). m/z (Accurate Mass ES): 435.2352 (Calculated for $\text{M}+\text{H}^+$), 435.2354 (Measured). $[\alpha]_{\text{D}} -37.29^\circ$.

5.38 Synthesis of benzoic acid-4-(4-pentyne-1-thiobenzyl)-(1R,2S,5R)-5-methyl-2-(1-methylethyl)cyclohexyl ester 27

A solution of benzylmercaptan (0.46 mL, 3.95 mmol) and NaOH (0.16 g, 4 mmol) in H_2O (5 mL) and EtOH (50 mL) was stirred under nitrogen for 10 min and then a solution of **25** (1.54 g, 3.66 mmol) in EtOH (5 mL) was added very slowly. The mixture was stirred overnight, then NH_4Cl (ca 5 g) was added and the solvent was evaporated. The resultant oil was purified by chromatography (eluting with a solvent gradient from 3:1 petrol:ether to 1:1) to afford 0.78 g (48 %) of **27**. $^1\text{H-NMR}$ (400 MHz, CDCl_3) δ : 0.71 (d, 3H, H_1 , $^3J =$

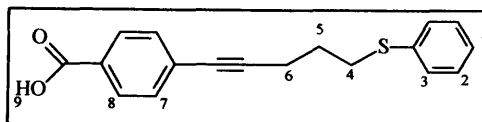
7.0 Hz), 0.84 (m, 7H, H_2 , $H_{5\text{eq}}$, H_8), 1.03 (m, 2H, $H_{6\text{ax}}$, $H_{9\text{ax}}$), 1.47 (m, 1H, H_4), 1.65 (m, 2H, $H_{5\text{ax}}$, $H_{6\text{eq}}$), 1.86 (m, 3H, H_3 , H_{14}), 2.04 (m, 1H, $H_{9\text{eq}}$), 2.52 (t, 2H, H_{13} , $^3J = 6.9$ Hz), 3.02 (t, 2H, H_{15} , $^3J = 7.2$ Hz), 3.51 (s, 2H, H_{16}),

4.85 (app dt, 1H, H_{10} , $^3J = 10.9$ Hz, $^3J = 4.4$ Hz), from 7.15 to 7.26 (m, 5H, $H_{17,18,19}$), 7.36 (dd, 2H, H_{12} , $^3J = 6.8$ Hz, $^4J = 1.5$ Hz), 7.89 (dd, 2H, H_{11} , $^3J = 6.9$ Hz, $^4J = 1.6$ Hz). Further characterisation was not obtained due to instability of the compound.



5.39 Synthesis of benzoic acid-4-(4-pentyne-1-thiophenyl) 28

Potassium tert-butoxide (0.04 g, 0.4 mmol) was added to a solution of **26** (0.183 g, 0.42 mmol) in EtOH (10 mL). The mixture was stirred at 75 °C overnight. The solvent was then evaporated and the resultant solid washed with DCM. The solid was then dissolved in EtOH and acidified with 0.1 M HCl until the solution became clear. The solution was then dried with MgSO_4 , filtered, and the solvent evaporated to afford 0.030 g (24 %) of **28**. $^1\text{H-NMR}$ (400 MHz, CDCl_3) δ : 1.88 (quin, 2H, H_5 , $^3J = 7.0$ Hz), 2.54 (t, 2H, H_6 , $^3J = 7.0$ Hz), 3.03 (t, 2H, H_4 , $^3J = 7.0$ Hz), 7.12 (t, 1H, H_1 , $^3J = 7.0$ Hz), 7.22 (t, 2H, H_2 , $^3J = 7.5$ Hz), 7.31

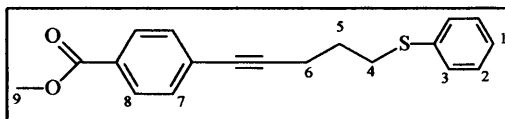


(dd, 2H, H_3 , $^3J = 8.5$ Hz, $^2J = 1.0$ Hz), 7.40 (d, 2H, H_7 , $^3J = 8.5$ Hz), 7.96 (d, 2H, H_8 , $^3J = 8.5$ Hz). $^{13}\text{C-NMR}$ (101 MHz, CDCl_3): δ 171.93, 136.45, 132.00, 130.46, 129.88, 129.70, 129.37, 128.46, 126.48, 93.40, 81.26, 33.00, 28.28, 18.95. ν_{max} (cm^{-1}): 3495 (OH), 2226 ($\text{C}\equiv\text{C}$), 1688 (CO). m/z (Accurate Mass): 297.0941 (Calculated for $\text{M}+\text{H}^+$), 297.0949 (Measured). **m.p.** 87-89 °C.

5.40 Synthesis of benzoic acid-4-(4-pentyne-1-thiophenyl)-methyl ester 29

The synthesis was performed following a procedure similar to that described in the literature^[17]. A solution of 28 (0.242 g, 0.82 mmol) in DCM (1 mL) was added to a solution of EDCI (0.314 g, 1.64 mmol) and DMAP (0.100 g, 0.82 mmol) cooled at 0 °C. The mixture was stirred for 15 min, until a white thick solution was formed. MeOH (0.5 mL) was added, the ice bath removed, and the mixture was stirred for 1 h. The product was extracted with a saturated solution of NH_4Cl in ether and the solvent evaporated to afford 0.121 g (48 %) of 29. $^1\text{H-NMR}$ (250 MHz, CDCl_3) δ :

1.87 (quin, 2H, H_5 , $^3J = 7.0$ Hz), 2.52 (t, 2H, H_6 , $^3J = 7.0$ Hz), 3.02 (t, 2H, H_4 , $^3J = 7.0$ Hz), 3.84 (s, 3H, H_9), 7.08 - 7.42 (m,



9H, $H_{1,2,3,7}$), 7.89 (dd, 2H, H_8 , $^3J = 6.7$ Hz, $^4J = 1.8$ Hz). $^{13}\text{C-NMR}$ (63 MHz, CDCl_3): δ 165.50, 135.10, 130.44, 128.38, 128.23, 127.99, 127.90, 127.47, 125.00, 91.37, 79.87, 51.10, 31.55, 26.92, 17.48. ν_{max} (cm^{-1}): 2228 ($\text{C}\equiv\text{C}$), 1716 (CO). m/z (Accurate Mass): 311.1100 (Calculated for $\text{M}+\text{H}^+$), 311.1097 (Measured). **m.p.** 47-49 °C.

5.41 Synthesis of dicobalthexacarbonyl bis(diphenylphosphino)methane ($\text{Co}_2(\text{CO})_6\text{dppm}$)

The synthesis was performed following a procedure similar to that described to literature.^[18] $\text{Co}_2(\text{CO})_8$ (11.03 g, 3 mmol) was added to a solution of dppm (1.15 g, 3 mmol) in degassed toluene (15 mL) under N_2 . The mixture was stirred overnight. The solution was filtered under N_2 using a cannula, then the solvent was evaporated to afford 1.29 g (59 %) of $\text{Co}_2(\text{CO})_6\text{dppm}$.^[19] $^{31}\text{P-NMR}$ (300 MHz, CDCl_3): δ 61.2 ppm. ν_{max} (cm^{-1}): 2042 ($\text{C}\equiv\text{O}$), 1996 ($\text{C}\equiv\text{O}$), 1980 ($\text{C}\equiv\text{O}$), 1971 ($\text{C}\equiv\text{O}$), 1790 ($\text{C}=\text{O}$).

5.42 Synthesis of dicobalt hexacarbonyl benzoic acid-4-(4-pentyne-1-thiophenyl)-(1R,2S,5R)-5-methyl-2-(1-methylethyl)cyclohexyl ester 30

$\text{Co}_2(\text{CO})_8$ (0.42 g, 1.24 mmol) was added to a solution of **26** (0.51 g, 1.12 mmol) in degassed DCM (10 mL). The mixture was stirred under nitrogen overnight. A small sample was purified by chromatography (eluting with a solvent gradient from 3:1 petrol:ether to 1:1), obtaining products **30** and **31**. **30**: Red oil. R_f 0.68. $^1\text{H-NMR}$ (400 MHz, CDCl_3) All peaks were too broad to report multiplicity or integration δ : 0.74, 0.86, 1.03, 1.13, 1.50, 1.67, 1.96, 2.04, 2.28, 3.02, 3.15, 4.87, 7.22, 7.29, 7.42, 7.92. ν_{max} (cm^{-1}): 2091 ($\text{C}=\text{O}$), 2054 ($\text{C}\equiv\text{O}$), 2029 ($\text{C}\equiv\text{O}$). m/z (MALDI): Theoretical isotope model $[\text{M}-2\text{CO}]^+$: 664.1 (100 %); 665.1 (34 %); 666.1 (7 %). Observed data: 664.1 (100 %); 665.1 (35 %); 666.1 (10 %). **31**: Maroon oil. R_f 0.48. $^1\text{H-NMR}$ (400 MHz, CDCl_3) All peaks were too broad to report multiplicity or integration δ : 0.76, 0.86, 1.03, 1.19, 1.48, 1.66, 1.92, 2.07, 2.30, 2.86, 3.03, 3.28, 4.85, 7.29, 7.36, 7.50, 7.91. ν_{max} (cm^{-1}): 2091 ($\text{C}=\text{O}$), 2065 ($\text{C}=\text{O}$), 2054 ($\text{C}\equiv\text{O}$), 2016 ($\text{C}\equiv\text{O}$), 1964 ($\text{C}\equiv\text{O}$).

5.43 Synthesis of dicobalt tetracarbonyl bis-diphenylphosphinomethane benzoic acid-4-(4-pentyne-1-thiophenyl)-(1R,2S,5R)-5-methyl-2-(1-methylethyl)cyclohexyl ester 32

$\text{Co}_2\text{CO}_6\text{dppm}$ (1.16 g, 1.6 mmol) was added to a solution of **26** (0.73 g, 1.68 mmol) in degassed toluene (10 mL). The mixture was heated at 85 °C for 1 h before being allowed to cool and then stirred overnight. The solution was filtered under N_2 using a cannula, then the solvent was evaporated to give a dark-red oil. $^1\text{H-NMR}$ (400 MHz, CDCl_3) All peaks were too broad to report multiplicity or integration δ : 0.72, 0.85, 1.03, 1.49, 1.66, 1.87, 2.53, 2.88, 3.03, 4.86, 7.23, 7.29, 7.66, 7.88. $^{31}\text{P-NMR}$ (121 MHz, CDCl_3) δ : 38.4ppm. ν_{max} (cm^{-1}): 2023 ($\text{C}\equiv\text{O}$), 1985 ($\text{C}\equiv\text{O}$), 1970 ($\text{C}\equiv\text{O}$), 1954 ($\text{C}\equiv\text{O}$), 1714 ($\text{C}=\text{O}$), 1699 ($\text{C}=\text{O}$). m/z (MALDI): Theoretical isotope model $[\text{M}-4\text{CO}]^+$: 936.2 (100 %); 937.2 (60 %); 938.2 (15 %); 939.2 (3 %). Observed data: 936.2 (100 %); 937.3 (35 %); 937.5 (15 %); 938.3 (9 %). $^{13}\text{C-NMR}$ could not be recorded due to broadening of the peaks.

5.44 Synthesis of dicobalt hexacarbonyl benzoic acid-4-(4-pentyne-1-thiophenyl)-methyl ester 35

$\text{Co}_2(\text{CO})_8$ (0.13 g, 0.39 mmol) was added to a solution of **29** (0.11 g, 0.35 mmol) in degassed DCM (5 mL) in a three-necked round bottom flask. The mixture was stirred

under nitrogen and under UV-CPL until dryness. A small sample of the residual oil was purified by chromatography (eluting with a solvent gradient from 3:1 petrol:ether to 1:1), obtaining products **35** and **35b**. **35**: $^1\text{H-NMR}$ (400 MHz, CDCl_3) All peaks were too broad to report multiplicity or integration δ : 0.82, 1.18, 1.96, 3.09, 3.82, 7.90. ν_{max} (cm^{-1}): 2090 ($\text{C}=\text{O}$), 2053 ($\text{C}=\text{O}$), 2021 ($\text{C}=\text{O}$), 1958 ($\text{C}=\text{O}$). **35b** was too unstable to report any characterisation.

5.45 Synthesis of cobalt tris-diphenylphosphinomethane-dioxide cobalt tetrachloride ($[\text{Co}(\text{dppmdo})_3](\text{CoCl}_4)$) **36**

$\text{Co}_2(\text{CO})_6\text{dppm}$ (20 mg, 2.75×10^{-2} mmol) was dissolved in CHCl_3 (1 mL). The mixture was left open to the air for 5 days, then the solid was collected by filtration to afford 30 mg (16 %) of **34** as green crystals. $^{31}\text{P-NMR}$ (121 MHz, CHCl_3) δ : 25.4ppm. ν_{max} (cm^{-1}): 1154 ($\text{P}=\text{O}$), 1124 ($\text{P}=\text{O}$). m.p.: 212 °C. X-ray: $\text{C}_{83}\text{H}_{74}\text{Cl}_{28}\text{Co}_2\text{O}_6\text{P}_6$; temperature 150(2)K; crystal system Cubic; space group P 21 3; $a=b=c=21.8970(3)$ Å, $\alpha=\beta=\gamma=90.000(0)^\circ$; final R indices [$I > 2\sigma(I)$] $R_1=0.0780$, $wR_2=0.1787$; R indices (all data) $R_1=0.0919$, $wR_2=0.1872$. m/z (MALDI): Theoretical $[\text{L}_2\text{CoCl}]^+$: 926.1 (100 %); 927.1 (56 %); 928.1 (47 %); 929.1 (20 %); 930.1 (5 %). Observed: 926.1 (100 %); 927.1 (70 %); 928.1 (54 %); 929.1 (17 %); 930.1 (5 %).

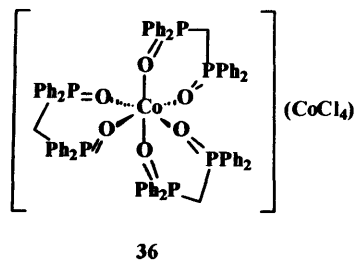
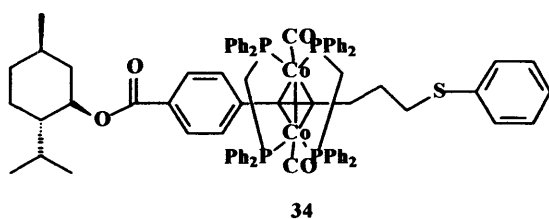
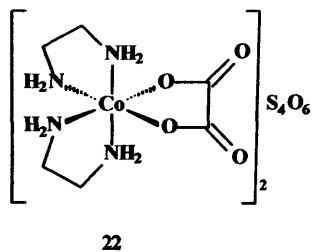
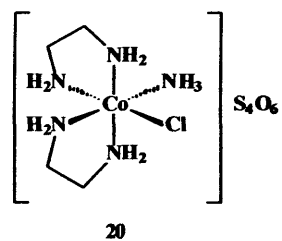
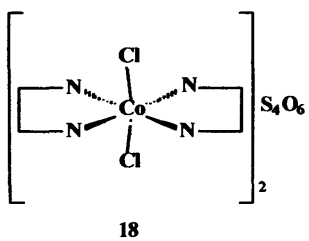
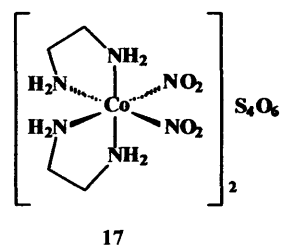
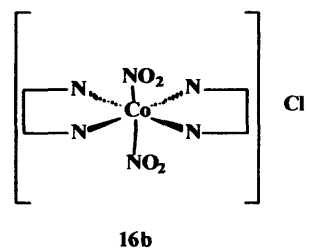
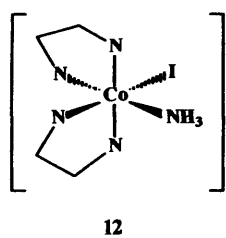
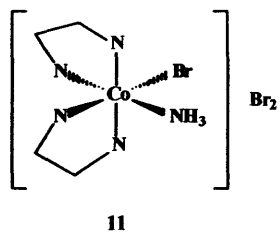
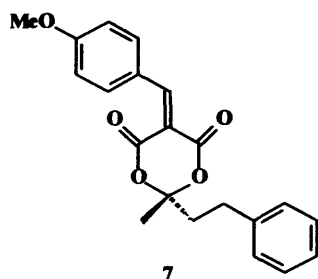
5.46 References

- [1] C. Y. K. Tan, D. F. Weaver, *Tetrahedron* **2002**, *58*, 7449.
- [2] A. G. Relenyi, D. E. Wallick, J. D. Streit, US Patent 4614671 ed., USA, **1986**, p. 5.
- [3] D. T. Mowry, *J. Am. Chem. Soc.* **1947**, *69*, 2362.
- [4] D. Parker, R. J. Taylor, *Tetrahedron* **1988**, *44*, 2241.
- [5] H. Kobayashi, K. Ohki, I. Tsujikawa, K. Osaki, N. Uryu, *Bulletin of the Chemical Society of Japan* **1976**, *49*, 1210.
- [6] K. Asakura, K. Kobayashi, Y. Mizusawa, T. Ozawa, S. Osanai, S. Yoshikawa, *Physica D: Nonlinear Phenomena* **1995**, *84*, 72.
- [7] I. Bernal, J. Cetrullo, W. G. Jackson, *Journal of Coordination Chemistry* **1993**, *28*, 89.
- [8] Y. H. Liu, F. R. Fronczek, S. F. Watkins, *Acta Crystallographica C* **1995**, *51*, 1992.

- [9] I. Bernal, *Inorganica Chimica Acta* **1985**, *96*, 99.
- [10] I. Bernal, J. Myrczek, J. Cai, *Polyhedron* **1993**, *12*, 1149.
- [11] I. Bernal, J. Cetrullo, J. Myrczek, *Materials Chemistry and Physics* **1993**, *35*, 290.
- [12] J. C. Bailar, Jr, *Inorganic Synthesis* **1946**, *2*, 222.
- [13] I. Bernal, J. Cetrullo, W. G. Jackson, *Inorg. Chem.* **1993**, *32*, 4098.
- [14] J. M. Harrowfield, B. W. Skelton, A. H. White, F. R. Wilner, *Aust. J. Chem.* **1986**, *39*, 339.
- [15] I. Bernal, J. Myrczek, J. Cetrullo, S. S. Massoud, *Journal of Coordination Chemistry* **1993**, *30*, 29.
- [16] N. Kamigata, A. Matsuhisa, H. Taka, T. Shimizu, *J. Chem. Soc. Perkin Trans. 1* **1995**, *7*, 821.
- [17] W. S. D. H. F. K. Josef Breu, *Chemistry - A European Journal* **2002**, *8*, 4454.
- [18] Y. C. Chang, J. C. Lee, F. E. Hong, *Organometallics* **2005**, *24*, 5686.
- [19] P. Hohenberg, W. Kohn, *Phys. Rev.* **1964**, *136*, B864.

APPENDIX

The appendix contains the crystal data (cif and res files) of the following compounds:





Communication

A oxygen-dependent reductive dechlorination of chloroform by (Bisdiphenylphosphinomethane)cobalthexacarbonyl $\text{Co}_2(\text{CO})_6(\text{dppm})$

Meritxell Casadesus, Michael P. Coogan *, Sarah Oakley, Elenna Davies, Li-ling Ooi

School of Chemistry, Cardiff University, Park Place, Cardiff CF10 3AT, Cymru/Wales, UK

Received 19 May 2006; received in revised form 31 May 2006; accepted 31 May 2006

Available online 10 June 2006

Abstract

The reaction of $\text{Co}_2(\mu\text{-dppm})(\text{CO})_6$ with aerated chloroform affords $[\text{Co}\{\text{Ph}_2\text{P}(\text{O})\text{CH}_2\text{P}(\text{O})\text{Ph}_2\}_3][\text{CoCl}_4]$ in low yield, and this reaction is demonstrated to be prevented under anaerobic conditions representing an unusual example of a reductive dechlorination which only takes place in the presence of oxygen.

© 2006 Elsevier B.V. All rights reserved.

Keywords: Dehalogenation; Dechlorination; Cobalt carbonyl; Dicobalthexacarbonyl; Phosphines

Dicobalthexacarbonyl alkyne complexes are of interest as they are intermediates in important carbon–carbon bond-forming reactions [1], and they are of significance in the area of molecular electronics [2]. These complexes can be stabilised by the use of bridging diphosphine ligands, and in particular there are many examples of dicobalthexacarbonyl alkyne complexes which are bridged by bis(diphenylphosphino)methane (dppm) [3]. These are usually prepared by the reaction of the bridged dicobalt hexacarbonyl complex $\text{Co}_2(\mu\text{-dppm})(\text{CO})_6$ **1** (Fig. 1) with the relevant alkyne under similar but more forcing conditions to those employed in the synthesis of the non-bridged species (e.g. small excess of cobalt species, benzene solution at reflux). While it is known [4] that dicobalt octacarbonyl reacts with chloroform, to give the tetrahedral cluster $\text{CH}(\text{Co}(\text{CO})_3)_3$, the derived alkyne complexes are typically unreactive to chloroform, and we have thus routinely recorded NMR spectra in CDCl_3 (see Fig. 2).

Equally, while dicobalt octacarbonyl is (slowly) oxidised in air, the derived alkyne complexes when phosphine

bridged are, typically, air-stable, or at least significantly more stable, and thus it is generally unnecessary to use Schlenk techniques when handling these complexes. We have, however, noted an unusual reaction between $\text{Co}_2(\mu\text{-dppm})(\text{CO})_6$ and aerated CDCl_3 . When a solution of a reaction mixture containing $\text{Co}_2(\mu\text{-dppm})(\text{CO})_6$ in CDCl_3 was left for 2 weeks the growth of a deposit of a fine microcrystalline green powder was observed. As there was no evidence of the degradation of the desired product this deposit was assumed to be derived from the (slight) excess cobalt starting material, $\text{Co}_2(\mu\text{-dppm})(\text{CO})_6$. The colour and lack of chloroform-solubility of this by-product suggested that it was an oxidation product; however, this is not the product we have previously observed upon aging of **1** which is typically the expanded cluster $\text{Co}_4(\mu\text{-dppm})_2(\text{CO})_8$ which has been previously characterised [5]. Thus, samples of $\text{Co}_2(\mu\text{-dppm})(\text{CO})_6$ were exposed to air both neat and in a variety of solvents. The characteristic green powder was observed only when $\text{Co}_2(\mu\text{-dppm})(\text{CO})_6$ was exposed to air in chloroform: in other solvents degradation was much slower and gave intractable brown solid and colourless crystals of the bis phosphine oxide derived from dppm (dppmdo) [6]. Eventually a crystal of the char-

* Corresponding author. Fax: +44 2920 874030.

E-mail address: cooganmp@cardiff.ac.uk (M.P. Coogan).

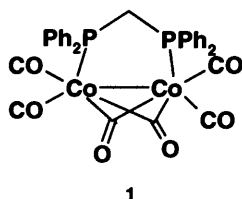


Fig. 1. Molecular structure of 1.

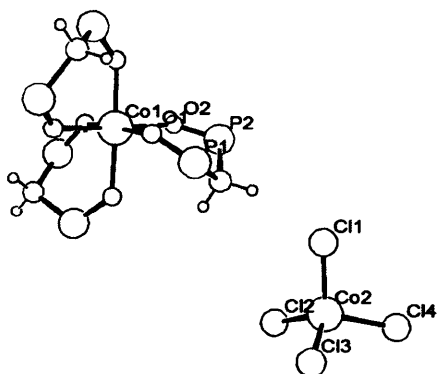
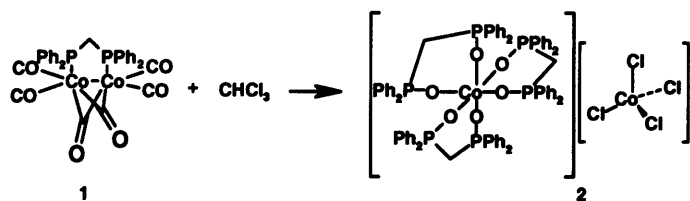


Fig. 2. ORTEP [10] view of 2 (50% probabilities) phenyl rings omitted for clarity.

acteristic green product was obtained which was suitable for single crystal X-ray diffraction studies [7], and the structure was determined to be an electrolyte consisting of a cationic cobalt complex with a single Co^{2+} ion with octahedral geometry chelated by three dppmdo ligands, $[\text{Co}(\text{dppmdo})_3]^{2+}$ and a cobalt (II) tetrachloride $[\text{CoCl}_4]^{2-}$ counterion (along with several chloroform molecules of crystallisation). This product has been previously reported from the reaction of dppmdo with cobalt chloride but has not been structurally characterised [8]. The formation of this product was entirely unexpected and there is great interest in dechlorination of organic species as they make up an important family of toxic, long-lived pollutants [9]. Therefore, both the academic interest and possible utility of a derived process led to an investigation of this reaction (see Scheme 1).

As it is known that low valent cobalt species will dechlorinate chloroform [4] it was initially assumed that the product had been formed in two steps, firstly, the reductive dechlorination of chloroform by electron transfer from the low valent Co starting material to form oxidised cobalt and chloride, followed by aerobic oxidation of free dppm



Scheme 1.

to the dioxide, all of which subsequently crystallised as the salt 2. In an attempt to observe the initial product the reaction was monitored by ^{31}P NMR. By this technique both the loss of the $\text{Co}_2(\mu\text{-dppm})(\text{CO})_6$ ($\delta_{\text{P}} 59$) and the formation of the dppmdo complex 2 ($\delta_{\text{P}} 121$) can be observed and reaction was studied under a variety of different conditions. In fact, it was found that in thoroughly degassed chloroform $\text{Co}_2(\mu\text{-dppm})(\text{CO})_6$ is stable (at ambient temperature) for periods of up to a month. Therefore, it seems that the formation of 2 requires oxygen, not only for the phosphine oxide formation, but for the dechlorination of chloroform, as this would be observed as a loss of 1 in the ^{31}P NMR. As the final product 2 slowly precipitates the ratio of ^{31}P signals for 1 and 2 were not relied on to confirm the progress of reaction, and an internal standard (Ph_3PO) was used to allow accurate monitoring of the loss of 1. It is also worth noting that no sign of the monooxide of dppm ($\delta_{\text{P}} -27, +29, J_{\text{PP}} 50$ Hz) [11] is observed in the reaction mixture. The mono-oxide is the major product in the aerobic oxidation of dppm in the absence of Co, implicating Co catalysis in the oxidation. In fact, the disappearance of the starting material signal and the appearance of the product signal are not accompanied by any signals which could be attributed to intermediate materials such as unbound dppm, new intermediate complexes or the monooxide. Clearly the failure to observe an entity is not proof of its non-existence but there must never be any appreciable concentration of any of these species in solution. It was further noted that allowing a small quantity of air into the system produces a small degree of reaction, which then stops until further air is allowed in. This finding discounts any radical-chain type mechanism for the dechlorination which could be triggered by dioxygen, as no continuing loss of 1 is observed under these conditions.

It is worth noting that the stoichiometry of the reaction requires by-products containing hydrocarbon and cobalt, as the dppm to Co ratio is greater in 2 than 1 and the dechlorination of chloroform leaves CH fragments. Unfortunately efforts to determine the composition of the byproducts are hampered by their intractable nature, and by contamination with 2.

Given the difficulties in characterising the other products, at present all that can be stated with certainty regarding the mechanism of reaction is that the starting materials are stable in the absence of oxygen, implicating a limiting initial aerobic oxidation of 1 (possibly involving loss of a carbonyl). It is possible that a reactive species produced from this oxidation then dechlorinates chloroform and is thus oxidised to the Co^{II} product. Given the lack of observation of free dppm or dppm monooxide it is likely that a Co-oxygen species then oxidises dppm, and, as dppm and the monooxide are never observed these two oxidations must be extremely rapid (faster than the disappearance of 1) and it seems likely therefore that these reactions are intramolecular, i.e. involve coordinated dppm.

In conclusion the oxygen-dependence of the reaction between chloroform and 1 has been demonstrated. Further

Table 1
Crystal data for **2**Crystal data and experimental details for **2**, green block, stable under ambient conditions collected on a Nonius KappaCCD solved using direct methods [7]

Formula	C ₈₃ H ₇₄ Cl ₂₈ Co ₂ O ₆ P ₆
<i>M</i>	2463.70
Temperature (K)	150
Crystal system	Cubic
Space group	P213
λ (Å)	0.71073
Unit cell dimensions	
<i>a</i> (Å)	21.8970(3)
<i>b</i> (Å)	21.8970(3)
<i>c</i> (Å)	21.8970(3)
α (°)	90.00
β (°)	90.00
γ (°)	90.00
<i>V</i> (Å ³)	10499.1(2)
<i>Z</i>	4
Absorption coefficient (mm ⁻¹)	1.168
Crystal size (mm ³)	0.30 × 0.40 × 0.48
θ limits (°)	3.84–26.37
Reflections collected	71743
Unique observed reflections [<i>F</i> _o > 4σ <i>F</i> _o]	7172
<i>R</i> (int)	0.1297
Goodness-of-fit on <i>F</i> ²	1.089
Final <i>R</i> indices, [<i>I</i> > 2σ(<i>I</i>)]	
<i>R</i> ₁	0.0780
<i>wR</i> ₂ (<i>F</i>) ²	0.1787
(all data)	
<i>R</i> ₁	0.0919
<i>wR</i> ₂ (<i>F</i>) ²	0.1872
Flack parameter	0.0199 (0.0350)

studies will attempt to fully explore the mechanism of the reaction and to probe the possibility of developing a catalytic version which may be of use in the dechlorination of pollutants.

We are grateful to the EPSRC Mass Spectrometry unit (Swansea) for assistance and the EPSRC for support (GR/S11480/01 Meritxell Casadesus, EP/COO7255 Sarah Oakley).

1. Experimental

[Co(dppmdo)₃][CoCl₄] **2** (see Table 1).

Co₂(CO)₈dppm (20 mg, 0.0275 mmol) was dissolved in CHCl₃ (1 mL) and the solution was left open to the air for 5 days. The solid formed was collected by filtration, washed with chloroform and dried to give **2** (16%) as green

blocks m.p.: 212 °C ³¹P (121 MHz, CDCl₃): δ 25.4 ppm; dH (400 MHz, d₆ DMSO) 7.75 (s, br, 2H) 7.40 (s, br, 3H) 4.10 (s, br, 1H) ν_{\max} 1153.9, 1123.6 cm⁻¹. M/Z. ES+ theoretical isotope pattern for [Co(dppmdo)₃]²⁺ 653.6 100% 654.1 85% 654.6 40%. Observed: 653.8 98% 654.3 100% 654.8 45%. (MALDI): Theoretical isotope pattern for [(dppmdo)₂CoCl]⁺: 926.1(100%); 927.1(56%); 928.1(47%); 929.1(20%); 930.1(5%). Observed: 926.1(100%); 927.1(70%); 928.1(54%); 929.1(17%); 930.1(5%). C₇₅H₆₆Cl₄Co₂O₆P₆·1.5 CHCl₃ requires C 54.4 H 4.03 found C 54.18 H 4.22%.

Appendix A. Supplementary material

Crystallographic data for the structural analysis have been deposited with the Cambridge Crystallography Data Centre, CCDC 607980 for compound **2**. Copies of this information may be obtained free of charge from The Director, CCDC, 12 Union Road, Cambridge CB2 1EZ, UK (Fax: +44 1223 336033; e-mail: deposit@ccdc.cam.ac.uk or www: <http://www.ccdc.cam.ac.uk>). Supplementary data associated with this article can be found, in the online version, at doi:10.1016/j.jorgchem.2006.05.053.

References

- [1] C.S. Chin, G. Won, D.S. Chong, *Acc. Chem. Res.* 35 (2002) 218; P.L. Pauson, *Tetrahedron* 41 (1985) 5855; K.M. Nicholas, *Acc. Chem. Res.* 20 (1987) 207.
- [2] M.I. Bruce, N.D. Duffy, M.G. Humphrey, *Aust. J. Chem.* 39 (1986) 159; C.J. Adams, M.I. Bruce, E. Horn, B.W. Skelton, E.R.T. Tiekink, A.H. White, *J. Chem. Soc. Dalton Trans.* (1993) 3313; P.J. Low, R. Rousseau, P. Lam, K.A. Udachin, G.D. Enright, J.S. Tse, D.D.M. Wayner, A.J. Carty, *Organometallics* 18 (1999) 3885.
- [3] Y.-C. Chang, J.-C. Lee, F.-E. Hong, *Organometallics* 24 (2005) 5686; T.J. Snaith, P.J. Low, R. Rousseau, H. Puschmann, J.A.K. Howard, *J. Chem. Soc. Dalton Trans.* (2001) 292.
- [4] G. Bor, L. Marko, B. Marko, *Chem. Ber.* 95 (1962) 333.
- [5] M.I. Bruce, A.J. Carty, B.G. Ellis, P.J. Low, B.W. Skelton, A.H. White, K.A. Udachin, N.N. Zaitseva, *Aust. J. Chem.* 54 (2001) 277.
- [6] H.-J. Christau, D. Virieux, P. Mouchet, A. Fruchier, *Eur. J. Org. Chem.* 7 (1999) 1561.
- [7] G.M. Sheldrick, *SHELXS-97, SHELXL-97*, University of Gottingen, Lower Saxony, Germany, 1997.
- [8] F. Mani, M. Bacci, *Inorg. Chim. Acta* 6 (1972) 487.
- [9] J.M. Fritsch, K. McNeill, *Inorg. Chem.* 44 (2005) 4852.
- [10] Ortep-3 for Windows: L.J. Farrugia, *J. Appl. Cryst.* 30 (1997) 565.
- [11] T.C. Blagborough, R. Davies, P. Ivison, *J. Organomet. Chem.* 467 (1994) 85.

On the spontaneous induction of chirality in the preparation of Werner's complex *cis*-[CoBr(NH₃)(en)₂]Br₂[†]

Fang Guo, Meritxell Casadesus, Eugene Y. Cheung, Michael P. Coogan* and Kenneth D. M. Harris*

Received (in Cambridge, UK) 1st February 2006, Accepted 8th March 2006

First published as an Advance Article on the web 21st March 2006

DOI: 10.1039/b601530a

The product obtained directly from the standard reaction to produce Werner's complex *cis*-[CoBr(NH₃)(en)₂]Br₂ is shown, *via* structure determination from powder X-ray diffraction data, to be a racemic crystalline phase; implications of this observation in relation to previous reports that this reaction leads to significant enantiomeric excesses are discussed.

There is considerable interest in the phenomena of chiral symmetry breaking, spontaneous resolution and chiral amplification, as one or more of these processes may have been crucial in the development of homochirality among the building blocks of life.^{1,2} A system that has been studied closely³⁻⁷ in relation to these phenomena is the reaction (Scheme 1) of [Co(H₂O)₂{(OH)₂Co(en)₂}]₂(SO₄)₂ (denoted **1**) with NH₄Br to give the chiral complex *cis*-[CoBr(NH₃)(en)₂]Br₂ (denoted **2**). This reaction is of considerable historical interest⁸ as **2** and its chlorine analogue were the first octahedral metal complexes to be resolved into Δ and Λ stereoisomers,⁹ 12 years after Werner's original prediction¹⁰ that octahedral ions of the type M(en)₂XY should exist as enantiomeric pairs. Thus, studies relating to the chirality of **2** have a direct bearing on the history of the stereochemistry of coordination compounds.

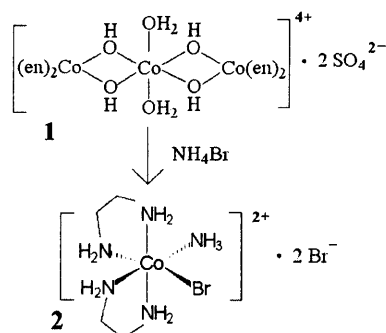
The reaction from **1** to **2** has been reported to be optimized^{3,5,6} for spontaneous resolution by variation of experimental parameters such as the rate of stirring, temperature, concentration and molar ratio of reactants, and has been shown to lead to a high enantiomeric excess (of random sense). It has also been shown that, when the reaction system is seeded with a catalytic quantity of

an optically active sample of the product, the reaction yields a high enantiomeric excess (of the same enantiomer) of the product, thus demonstrating chiral autocatalysis.⁴

Studies of spectroscopic,⁷ thermodynamic^{5,6} and kinetic⁶ properties of this reaction have provided insights into both the mechanism of the reaction and the mechanism of spontaneous resolution. Although the reaction is difficult to study directly by spectroscopic techniques, as **1** is highly insoluble in the reaction medium, the reaction is believed⁷ (on the basis of results from absorption spectroscopy) to proceed *via* an intermediate [Co(H₂O)(OH)(en)₂]. The mechanism of chiral asymmetry generation has been explained^{4,5} on the basis that the product is formed as a conglomerate crystalline phase. For a conglomerate, each individual crystal is homochiral, containing either the Δ form only or the Λ form only (and thus a racemic sample of this material would exist as a physical mixture of these homochiral crystals); clearly, it is obligatory that such crystals have a chiral space group. It is proposed that the product **2** crystallizes at an early stage of the reaction, and that the chirality of the first formed crystals is transmitted through secondary nucleation to promote further crystallization of the same chirality. When less than 50% of the product has crystallized, the enantiomeric excess can approach 100%.

As part of our interest in issues relating to chirality in crystallization processes, we have made extensive attempts to reproduce the spontaneous resolution experiments under the conditions described previously, but have consistently been unable to obtain an optically active product in spite of systematic variation of all the experimental conditions within our control (purity of reagents, solvents, temperature and concentration).¹¹ In light of this (initially surprising) observation, we have undertaken to determine the structure of the material produced directly in this reaction, employing powder X-ray diffraction (XRD) techniques (see below). In this regard, it is important to recognize that the two previous reported crystal structure determinations¹² of **2** (both from single-crystal XRD) were both carried out on samples obtained by re-crystallization of **2**, rather than studies of the solid product obtained directly in the reaction.

One of these previous structure determinations,¹³ in the chiral space group *P*2₁2₁2₁ (with one molecule in the asymmetric unit), was on a single crystal grown from a homochiral sample ((+)₅₈₉-enantiomer) of **2**, with the aim of determining the absolute configuration (Λ). This structure is here denoted phase I. The other previous structure determination¹⁴ of **2** (actually a dihydrate of **2**), on a single crystal prepared by crystallization from a racemic mixture of **2**, is a racemic structure in the achiral space group *C*2/*c*. This structure is here denoted phase II. We note that neither of



Scheme 1

School of Chemistry, Cardiff University, Park Place, Cardiff, Wales, UK CF10 3AT. E-mail: HarrisKDM@cardiff.ac.uk;

CooganMP@cardiff.ac.uk; Fax: +44-2920-874030

[†] Electronic supplementary information (ESI) available: Table of structural data. See DOI: 10.1039/b601530a

these cases involved a conglomerate crystalline phase of **2** being obtained from a racemic system.

The procedure³ for preparation of **2** (Scheme 1) involves treatment of **1** with an excess of NH_4Br in water, and precipitation of the product.¹⁵ Our powder XRD studies of the product indicate that a new solid phase of **2** is produced that is different from the previously reported structures of phases I and II discussed above. This new phase is denoted phase III, and in the present context it is clearly important to establish the structural properties of this new phase. However, as the product is obtained as a microcrystalline powder that does not contain crystals of suitable size to carry out structure determination by single-crystal XRD, alternative approaches for structural characterization are required. Fortunately, there have been significant advances in recent years in the opportunities for carrying out complete structure determination of molecular solids directly from powder XRD data,¹⁶ particularly through the development of the direct-space strategy for structure solution.^{16a} Here we have exploited the opportunity provided by these techniques in order to determine the structure of the powder sample of **2** (phase III) obtained directly from the reaction.

The powder XRD pattern^{17,18} of the sample of **2** obtained directly from the reaction was indexed using the program TREOR,¹⁹ giving the following unit cell with monoclinic metric symmetry: $a = 7.66 \text{ \AA}$, $b = 12.39 \text{ \AA}$, $c = 13.97 \text{ \AA}$, $\beta = 98.7^\circ$. The space group was assigned from systematic absences as $P2_1/n$. Unit cell and profile refinement were carried out for this unit cell and space group using the LeBail fitting procedure, leading to a good quality of fit ($R_{\text{wp}} = 8.48\%$, $R_p = 6.76\%$). With one independent formula unit $[\text{Co}(\text{C}_2\text{H}_8\text{N}_2)_2(\text{NH}_3)\text{Br}]\text{Br}_2$ in the asymmetric unit, and $Z = 4$ for space group $P2_1/n$, the calculated density is 2.202 g cm^{-3} , which lies within the anticipated density range for this material.

Structure determination was carried out directly from the powder XRD data using the direct-space genetic algorithm (GA) technique²⁰ (in the program EAGER²¹) for structure solution, followed by Rietveld refinement (using the program GSAS²²). The structural model used in the GA structure solution calculation²³ involved three independent fragments and a total of 12 structural variables.²⁴ The best structure solution was used as the starting model for Rietveld refinement, in which standard restraints were applied to bond lengths and bond angles, and were relaxed gradually as the refinement progressed. Hydrogen atoms were inserted in calculated positions. The good agreement between calculated and experimental powder XRD patterns in the final Rietveld refinement²⁵ (Fig. 1), together with the fact (see below) that the structure obtained is chemically and structurally sensible, vindicates the correctness of the structure.

The crystal structure^{26,27} is shown in Fig. 2 (fractional coordinates are given in Supplementary Information). The *cis*- $[\text{CoBr}(\text{NH}_3)(\text{en})_2]^{2+}$ complexes are arranged in chains along the *a*-axis and in chains along the *b*-axis; in each type of chain, neighbouring complexes are linked by $\text{N}\cdots\text{H}\cdots\text{Br}\cdots\text{H}\cdots\text{N}$ interactions. Along the *a*-axis, neighbouring repeat units in the chain are related by translation and the chain is relatively straight; along the *b*-axis, neighbouring repeat units in the chain are related by the 2_1 symmetry operation and the chain is helical. Within the context of the present work, however, the most important feature of the crystal structure is that it is a racemic structure in an achiral space

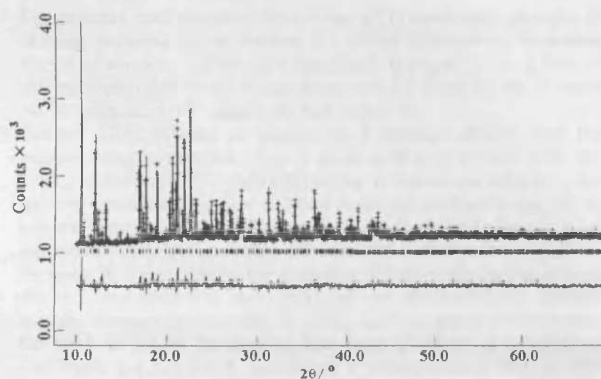


Fig. 1 Experimental (+ marks), calculated (solid line), and difference (lower line) powder XRD profiles for the final Rietveld refinement of phase III of **2**.

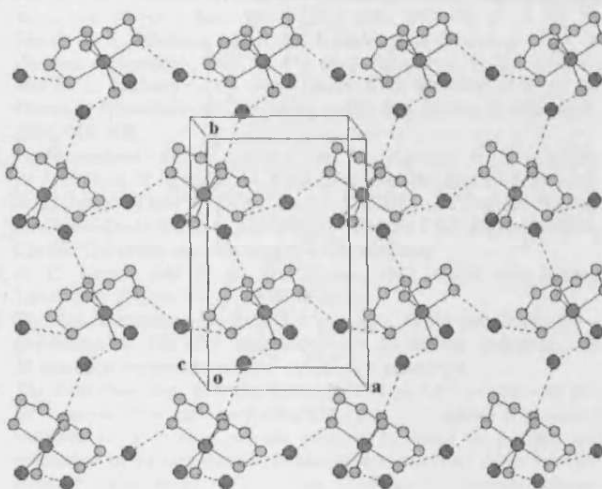


Fig. 2 Crystal structure of phase III of **2** viewed nearly along the *c*-axis, showing the straight and helical chains that run along the *a*-axis and *b*-axis respectively (Co – red; Br – green; N – blue; C – grey). Hydrogen atoms are omitted for clarity.

group ($P2_1/n$). Thus, our observation (see above) that we have never observed any enantiomeric excesses in our experiments to prepare **2** is fully explained by the fact that the structure of the product (phase III) obtained directly from the reaction in our experiments is a racemic crystalline phase.

In conclusion, our studies of the solid product obtained directly from the reaction of **1** to **2** indicate that a new racemic crystalline phase (phase III) is consistently obtained. We have thus been unable to observe the production of **2** as a conglomerate crystalline phase from the reaction under any of the wide range of experimental conditions considered in our work.^{11,28} As conglomerate crystallization is a pre-requisite for the spontaneous induction of chirality in this system, it is clear that our results are not in accord with previous reports of spontaneous resolution in the formation of **2** (recalling that, in these previous studies, no structure determination was actually carried out on the solid material obtained directly from the reaction). Although our experiments to prepare **2** have consistently yielded the racemic phase III, it would not be correct to infer that conglomerate

crystallization of **2** cannot occur, and it is certainly not our intention to cast doubt on the veracity of the previously published work. Nevertheless, our results clearly demonstrate that there is an intrinsic irreproducibility between the results obtained by different groups on this system, even when experimental procedures are followed in a manner that is ostensibly a faithful replication of previously reported procedures. These observations may reflect the types of difficulties that can often be encountered in reproducibly obtaining specific crystalline forms of a compound, as manifested *inter alia* in cases of "disappearing polymorphs".²⁹

We are grateful to EPSRC for general support to KDMH and for a research grant (GR/S11480/01) to M. P. C. Cardiff University and Universities UK are thanked for a studentship to F. G.

Notes and references

- J. L. Bada, *Nature*, 1995, **374**, 594.
- M. Avalos, R. Babiano, P. Cintas, J. L. Jimenez and J. C. Palacios, *Chem. Commun.*, 2000, 887.
- K. Asakura, K. Kobayashi, Y. Mizusawa, T. Ozawa, S. Osanai and S. Yoshikawa, *Physica D*, 1995, **84**, 72.
- K. Asakura, K. Kobayashi, Y. Mizusawa, T. Ozawa, T. Miura, A. Tanaka, Y. Kushibe and S. Osanai, *Recent Res. Dev. Pure Appl. Chem.*, 1997, **1**, 123.
- K. Asakura, D. K. Kondepudi and R. Martin, *Chirality*, 1998, **10**, 343.
- K. Asakura, A. Ikumo, K. Kurihara, S. Osanai and D. K. Kondepudi, *J. Phys. Chem. A*, 2000, **104**, 2689.
- K. Asakura, K. Inoue, S. Osanai and D. K. Kondepudi, *J. Coord. Chem.*, 1998, **46**, 159.
- A. Werner, "On the constitution and configuration of higher-order compounds", Nobel Lecture, December 11, 1913.
- A. Werner and V. King, *Berichte*, 1911, **44**, 1887.
- A. Werner and A. Vilmos, *Z. Anorg. Chem.*, 1899, **22**, 145.
- In these experiments, starting materials, solvents and reagents were used both "as supplied" and, in separate experiments, following purification using standard techniques (D. D. Perrin and W. L. F. Armarego, *Purification of Laboratory Chemicals*, Butterworth, Oxford, 1996). In order to minimize the risk of problems arising from undetected and unremovable trace impurities generated in different manufacturing processes, commercially available materials were sourced from at least two suppliers (Aldrich Chemical Company, Acros Organics or Fisher Scientific) and the preparation of **1** and the conversion from **1** to **2** were repeated with each combination of materials. The conversion from **1** to **2** was examined repeatedly at the optimum conditions from ref. 5 for spontaneous resolution, and also at the extremes of the conditions found to be successful in that work. In total, considering all different sets of conditions, the preparation of **2** was carried out *ca.* 30 times. All of the samples were tested for optical activity, but for none of the samples was optical activity observed. Powder XRD data were recorded for 5 samples; in each case, the powder XRD pattern indicated the formation of phase III.
- From a survey of the Cambridge Structural Database (Version 5.26, update August 2005).
- H. Nakagawa, S. Ohba, K. Asakura, T. Miura, A. Tanaka and S. Osanai, *Acta Crystallogr., Sect. C: Cryst. Struct. Commun.*, 1997, **53**, 216.
- I. Bernal, J. Cetrullo and W. G. Jackson, *J. Coord. Chem.*, 1993, **28**, 89.
- From the stoichiometry of the reaction from **1** to **2**, we note that the reaction must yield another (unknown) cobalt species in addition to **2**, and precipitation of **2** thus takes place from a solution containing this other cobalt species and excess NH₄Br.
- (a) K. D. M. Harris, M. Tremayne, P. Lightfoot and P. G. Bruce, *J. Am. Chem. Soc.*, 1994, **116**, 3543; (b) K. D. M. Harris, M. Tremayne and B. M. Kariuki, *Angew. Chem., Int. Ed.*, 2001, **40**, 1626; (c) *Structure Determination from Powder Diffraction Data*, ed. W. I. F. David, K. Shankland, L. B. McCusker and C. Baerlocher, OUP/IUCr, Oxford, 2002; (d) K. D. M. Harris and E. Y. Cheung, *Chem. Soc. Rev.*, 2004, **33**, 526; (e) *Z. Kristallogr.*, ed. L. B. McCusker and C. Baerlocher, 2004, **216** (12), 782.
- For structure determination, the powder XRD pattern was recorded at ambient temperature on Station 2.3 at the Synchrotron Radiation Source, Daresbury Laboratory [capillary, 0.7 mm; $\lambda = 1.3034 \text{ \AA}$ (the maximum flux at this station is between 1.1 \AA and 1.5 \AA); 2 θ range 10–70°; step size 0.02°; data collection time 7 h].
- Powder XRD patterns of samples of **2** obtained directly from the reaction often contain low-intensity peaks at $2\theta = 15.15^\circ$ and 21.82° for CuK α_1 radiation (12.79° and 18.39° in Fig. 1) that are not indexed by the unit cell determined here for **2**. These peaks are confidently assigned as impurity phases on the following basis: (i) these peaks usually have significantly different linewidths (broader) from other peaks (due to **2**) in the same 2θ region, and (ii) the intensities of these peaks relative to those due to **2** (and relative to each other) can vary substantially for different samples obtained on repeating the preparation procedure (in some cases, the peak at 12.79° is absent). The peak at 12.79° is assigned as Co(OH)Br ((a) A. Ludi, S. Locchi and Y. Iitaka, *Chimia*, 1961, **15**, 532) and the peak at 18.39° is assigned as NH₄Br ((b) H. A. Levy and S. W. Peterson, *J. Am. Chem. Soc.*, 1953, **75**, 1536), both of which are plausible impurity phases in the material recovered from the reaction.
- P.-E. Werner, L. Eriksson and M. Westdahl, *J. Appl. Crystallogr.*, 1985, **18**, 367.
- (a) B. M. Kariuki, H. Serrano-González, R. L. Johnston and K. D. M. Harris, *Chem. Phys. Lett.*, 1997, **280**, 189; (b) K. D. M. Harris, R. L. Johnston and B. M. Kariuki, *Acta Crystallogr., Sect. A: Fundam. Crystallogr.*, 1998, **54**, 632; (c) S. Habershon, K. D. M. Harris and R. L. Johnston, *J. Comput. Chem.*, 2003, **24**, 1766; (d) K. D. M. Harris, S. Habershon, E. Y. Cheung and R. L. Johnston, *Z. Kristallogr.*, 2004, **219**, 838.
- S. Habershon, G. W. Turner, B. M. Kariuki, E. Y. Cheung, A. J. Hanson, E. Tedesco, D. Albesa-Jové, M.-H. Chao, O. J. Lanning, R. L. Johnston and K. D. M. Harris, *EAGER – A Computer Program for Direct-Space Structure Solution from Powder X-ray Diffraction Data*, Cardiff University and University of Birmingham.
- A. C. Larson and R. B. Von Dreele, 1987, *GSAS*, Los Alamos Laboratory Report No. LA-UR-86-748.
- The GA calculation involved the evolution of 80 generations for a population of 100 trial structures, with 50 mating operations and 30 mutation operations carried out in each generation.
- The three fragments were the *cis*-[CoBr(NH₃)(en)]²⁺ complex and two Br⁻ anions. For the *cis*-[CoBr(NH₃)(en)]²⁺ complex, 6 structural variables $\{x, y, z, \theta, \varphi, \psi\}$ are required to define the position and orientation in the unit cell; the intramolecular geometry, taken from the structure reported in ref. 13, was fixed in the structure solution calculation. For each Br⁻ anion, 3 structural variables $\{x, y, z\}$ are required to define the position in the unit cell.
- Final Rietveld refinement: $a = 7.6704(5) \text{ \AA}$, $b = 12.4028(7) \text{ \AA}$, $c = 13.9885(10) \text{ \AA}$, $\beta = 98.726(6)^\circ$, $R_{\text{wp}} = 9.62\%$, $R_p = 7.40\%$; 3000 profile points; 110 refined variables.
- Refined Co–N distances for en ligands: 1.965 \AA , 1.978 \AA , 1.992 \AA , 1.986 \AA ; Co–N distance for NH₃ ligand: 1.976 \AA ; Co–Br distance 2.408 \AA ; N–C–C–N torsion angles for en moieties: -48.48° and -49.78° .
- Along the *a*-axis, the geometries of the N–H \cdots Br⁻ \cdots H–N interactions within the chain are (N \cdots Br distance, N–H \cdots Br angle): 3.31 \AA , 130° ; 3.32 \AA , 149° (in both cases, the N–H bonds are from NH₂ groups of the complexes). Along the *b*-axis, the geometries of the N–H \cdots Br⁻ \cdots H–N interactions within the chain are: 3.28 \AA , 169° ; 3.37 \AA , 152° (in the former, the N–H bond is from an NH₂ group; in the latter, the N–H bond is from the NH₃ group). On geometric criteria, it is reasonable to assign these contacts as N–H \cdots Br hydrogen bonds. The bromide anions in these chains and the bromide ligand in the complex are also involved in other contacts with NH₂ and NH₃ groups in neighbouring complexes, but the N \cdots Br distances are greater than 3.4 \AA and in some cases the N–H \cdots Br angles are far from linear; these contacts are more appropriately assigned as van der Waals interactions.
- In order to further explore the possibility of obtaining a conglomerate crystalline phase from a racemic sample of **2**, re-crystallization of the sample of **2** obtained directly from the reaction was carried out using a variety of solvents and under a range of different concentration conditions. The samples obtained were either phase II or phase III or mixtures of phases II and III. We found no evidence for the formation of phase I in these re-crystallization experiments.
- J. D. Dunitz and J. Bernstein, *Acc. Chem. Res.*, 1995, **28**, 193.

Synthesis of 5-alkylidene-1,3-dioxane-4,6-diones, an easily accessible family of axially chiral alkenes: preparation in non-racemic form and platinum binding studies

Meritxell Casadesus, Michael P. Coogan* and Li-Ling Ooi

Received 21st June 2006, Accepted 18th August 2006

First published as an Advance Article on the web 14th September 2006

DOI: 10.1039/b608785j

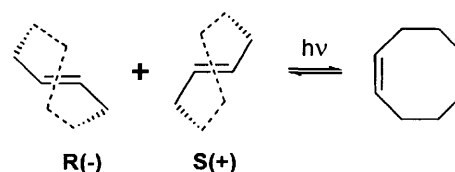
A general synthetic route to 5-alkylidene-1,3-dioxane-4,6-diones, which are a family of axially chiral alkenes, is described. Conformational issues are explored and the platinum-binding properties of these species are discussed. That these alkenes exist as stable enantiomers is established by their partial kinetic resolution upon reaction with cysteine.

Introduction

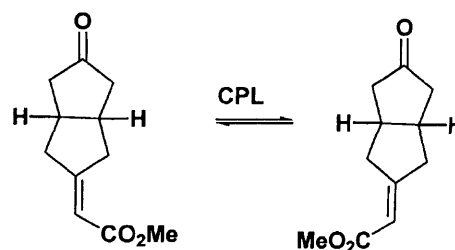
Molecules in which one of the elements of chirality involves a carbon–carbon double bond are interesting in that interconversion of enantiomers may be achieved by alkene isomerisation. Alkenes may be isomerised through many processes including irradiation with the correct frequency of electromagnetic radiation (usually u. v.) to induce diradical formation and thus lower the barrier to rotation around the carbon–carbon bond, which upon relaxation and reformation of the alkene results in isomerisation. In many cases, instead of direct excitation of the alkene, irradiation excites another group, often a carbonyl, which then transfers excitation to the alkene, generating a species in which, again, the carbon–carbon bond is formally single, allowing rotation and thus isomerisation. In chiral molecules in which interconversion of enantiomers is achieved by double bond isomerisation, this provides a path for photochemical racemisation, or, in certain cases the use of circular polarised light allows photochemical deracemisation. Circularly polarised light is intrinsically chiral, and as such the interaction with chiral molecules is diastereoisomeric, with each enantiomeric form of circularly polarised light being absorbed to a different extent by each enantiomer of the sample, with the difference being referred to as the anisotropy factor $\Delta\epsilon$. Thus, when irradiation of a racemic sample of substrate is carried out with a single enantiomer of circularly polarised light, the enantiomer of sample which has the highest extinction coefficient is racemised faster than its enantiomer, which leads to an excess of the lower absorbing enantiomer. As the $\Delta\epsilon$ values for simple molecules are small, typically $\leq 1\%$ of the absolute extinction coefficients, the enantiomeric excesses obtained in such experiments are usually very small, but they are important examples of *absolute asymmetric induction*, that is the induction of enantiomeric excesses by reactions of racemic mixtures or achiral molecules, using only the chirality of physical forces rather than chiral chemicals, and as such have implications for the origins of biological homochirality, as it has been observed that cosmic background radiation is significantly circularly polarised at many wavelengths, and thus

primordial Earth experienced non-racemic irradiation prior to the development of biological chirality.¹

The classic example of a molecule which is chiral by virtue of a double bond configuration is *trans*-cyclooctene, and this material has been shown to be capable of deracemisation by intense irradiation with circularly polarised u. v. (Scheme 1).² This is an unusual example, however, in that irradiation can cause not only interconversion of enantiomers, but also produces the (achiral) *cis*-isomer. More recently alkylidene cyclohexanes have emerged as one of the more interesting families of chiral molecules which can be racemised by photochemical isomerisation of an alkene,³ and indeed, these species have also been deracemised by irradiation with circularly polarised light (Scheme 2). Amongst other prominent molecules which have been photochemically deracemised with circularly polarised light are the crowded helical tetraaryls such as the 9,9'-oxo and thioxanthenylienes which have been studied by Feringa *et al.* (Scheme 3).⁴ The aim of the present work was to develop routes which would allow rapid access to a large and varied series of molecules which would both be capable of photochemical racemisation (and potentially deracemisation) *via* double bond isomerisation, and be crystalline, in order to allow any enantiomeric excess obtained to be enhanced by

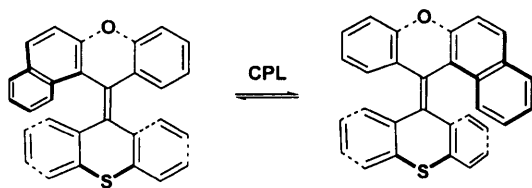


Scheme 1



Scheme 2

Department of Chemistry, Cardiff University, Park Place, Cardiff, Wales/Cymru, UK CF10 3TB. E-mail: cooganmp@cf.ac.uk; Fax: + 44 02920 874030; Tel: +44 02920 874066



Scheme 3

in situ crystallisation. A survey of the literature was made to find the simplest routes to such species, and to find which families were typically crystalline. Substituted cyclooctenes and methylene cyclohexanes both suffer from low melting points (many are liquid at ambient temperature), and the bixanthenylidenes, while typically high melting solids, are not accessible by the simple one or two step reactions which are useful if a large series of compounds is sought, therefore attention turned to developing new families of axially chiral alkenes.

Results and discussion

A consideration of the structural features required suggested that a potentially viable route to double-bond chiral compounds amenable to rapid analogue collection was the condensation of aldehydes with an activated methylene group in a prochiral ring. The direct analogues of the alkylidene cyclohexanes accessible by this route would be the condensation products of simple analogues of dimedone, which are available *via* condensations of Michael acceptors with malonate esters, however a survey of the literature in this area suggested that the precursors for the condensations (5-monosubstituted cyclohexane-1,3-diones) were best approached by routes which varied depending upon the nature of the substituent, and in many cases would require 2 or more step syntheses of the Michael acceptors, which while trivial moved away from the desired rapid access to a range of analogues. The dioxoanalogue of dimedone, Meldrum's acid, however, seemed a good candidate for studies as condensation of Meldrum's acid with aldehydes is known and high yielding and the substitution of acetone for non-symmetrical ketones in the synthesis of Meldrum's acid analogues should allow for chirality. As two of the three components in the synthesis are carbonyl compounds, a one-pot synthesis is conceivable in which malonic acid is cyclised, then condensed with the same carbonyl compound. In order to validate this approach, therefore, and to demonstrate their chirality, a study has been undertaken of 5-alkylidene-1,3-dioxane-4,6-diones.

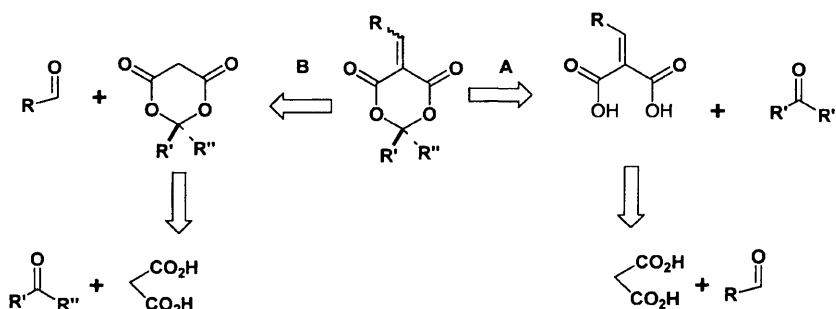
5-Alkylidene-1,3-dioxane-4,6-diones

There are a small range of examples of non-symmetrical examples of 5-alkylidene-1,3-dioxane-4,6-diones known⁵ (there are many examples of the symmetrical materials derived from Meldrum's acid), but there is no general method for their synthesis and a literature search found no mention of their chirality. Thus it was decided that a small range of alkylidene substituted non-symmetrical analogues of Meldrum's acid should be synthesised in order to assess the ease of synthesis, stability and crystallinity of these species and to allow their chirality to be confirmed.

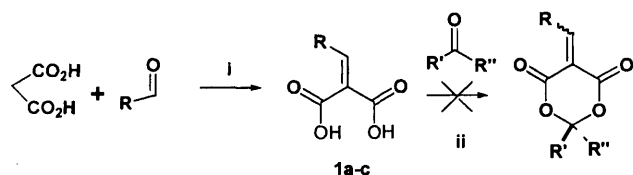
There are two obvious routes to such materials: A) the synthesis of alkylidene malonic acid derivatives, followed by cyclisation to the non-symmetrical acetals; and B) the synthesis first of cyclic malonate acetals, followed by their condensation with carbonyl compounds (Scheme 4).

The first of these routes was attempted with condensation of malonic acid with a variety of aromatic aldehydes giving the alkylidene malonic acids **1a–c** in acceptable to good yields (given the availability of the starting materials no optimisation was considered). These alkylidene malonic acids proved, however, to be reluctant to condense with aldehydes or ketones to give the desired products. A variety of reaction conditions, reagents and catalysts were screened in an attempt to obtain cyclisation, concentrating on Brønsted acids (TsOH, H₂SO₄, TFA) and standard dehydrating reagents/conditions (Dean–Stark or acetic anhydride), but in all cases the major products were either starting materials or decomposition products, with no evidence of successful cyclisation (we were able to compare crude spectra with the spectra of the desired materials obtained later to confirm this conclusion) (Scheme 5). It is possible that the lack of conformational freedom in the alkylidene malonic acids is responsible for this reluctance to cyclise. It is assumed that the ring-closing step would involve generation of an oxonium ion by acid catalysed dehydration of an intermediate hemiacetal, followed by nucleophilic attack at the sp² carbon. Although by the Baldwin-style analysis this is a 6-*endo*-trig cyclisation which is formally favoured, there may be insufficient conformational flexibility in the highly unsaturated backbone which would form the ring to allow the carboxylate to approach the sp² carbon at the Burgi–Dunitz angle.

In the light of the failure to obtain the desired species from this approach, attention turned to the initial condensation to the non-symmetrical Meldrum's acid derivatives, followed by condensation to the alkylidene species, which should suffer from no untoward stereoelectronic effects. The condensation of Meldrum's acid itself with aldehydes and ketones is well known and a huge range of



Scheme 4



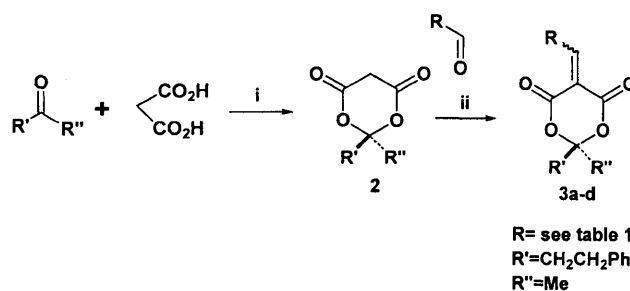
Scheme 5 (i) NH_4OAc , EtOH; (ii) various conditions.

such derivatives is known, however substituting the *gem*-dimethyl group of Meldrum's acid with a non-symmetrical substitution pattern was necessary for chiral products. The condensation of malonic acid with aromatic aldehydes has been reported to give the cyclic acetals⁶ however in the present study the reaction of equimolar ratios of aromatic aldehydes with malonic acid never gave this desired product cleanly, although a double condensation did give useful materials (see below). The major product from the reactions of aromatic aldehydes with malonic acid under the high temperature conditions recommended for the cycloacetalisation, in fact was in most cases the relevant cinnamic acid derivative. These materials are formed from the condensation used previously to give the alkylidene malonic acids, followed by thermal decarboxylation. In order to retard the Knoevenagel condensation to the alkylidene species, attention turned to the use of ketones. In order to maintain crystallinity it was felt that an aromatic substituent was desirable, and a methylene group was also likely to be useful in order that diastereotopicity could be observed in the ^1H NMR, which could confirm the chirality of the products. The attempted condensation of malonic acid with acetophenone following the literature method which had proven to be the highest yielding route to Meldrum's acid⁷ gave none of the desired product (from NMR and mass spectroscopy of the crude reaction mixtures). The literature⁸ suggested that the condensation of malonic acid with aromatic ketones gives not the 1,3-dioxane-4,6-diones but instead tends to condense *via* nucleophilic attack at the ketone, often followed by dehydration and decarboxylation to the unsaturated acid. Therefore, benzyl acetone was selected as an aliphatic ketone which has both an aromatic substituent and methylene groups, while the carbonyl group is more similar to acetone than the carbonyl of an aromatic ketone. (A range of alkylidene malonates derived from benzyl acetone have been prepared on solid supports as intermediates in solid-phase synthesis⁹ however they were not liberated from the support in this form and no comment was made on chirality.) The condensation of benzyl acetone with malonic acid was investigated under a variety of conditions, with the product mixtures varying greatly with temperature, pH and reagents. Eventually it was found that a variation of a literature⁷ procedure for Meldrum's acid provided the most reliable route to 2-methyl-2-(2-phenylethyl)-1,3-dioxane-4,5-dione **2**, whereby excess malonic acid was reacted with benzyl acetone in the presence of acetic anhydride and sulfuric acid. The excess malonic acid is easily removed by filtration of a solution of the crude reaction product in dichloromethane, and after evaporation the cyclic acetal slowly crystallises from the by-products in good yield. Interestingly this material is very susceptible to hydrolysis and must be stored under anhydrous conditions, in stark contrast to Meldrum's acid itself, which while having some hydrolytic instability is much more robust than the benzyl derivative considered here.

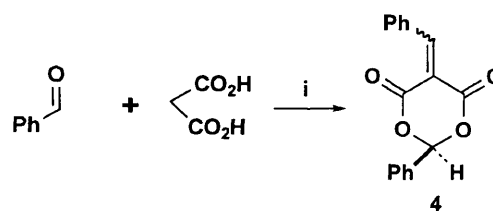
Table 1 Yields of 5-alkylidene-1,3-dioxane-4,6-diones

	R	R'	R''	Yield (%)	Mpt/°C
3a	Ph	$\text{CH}_2\text{CH}_2\text{Ph}$	H	43	107–108
3b	4- NO_2 - C_6H_4	$\text{CH}_2\text{CH}_2\text{Ph}$	H	37	146–149
3c	2- NO_2 - C_6H_4	$\text{CH}_2\text{CH}_2\text{Ph}$	H	66	89–91
3d	4-MeO- C_6H_4	$\text{CH}_2\text{CH}_2\text{Ph}$	H	66	91–93
3e	$\text{CH}(\text{CH}_3)_2$	$\text{CH}_2\text{CH}_2\text{Ph}$	H	33	79–81
4	Ph	Ph	H	21	146–148

With a robust route to a crystalline non-symmetrical Meldrum's acid derivative, **2** the Knoevenagel condensations of this material with a variety of ketones were studied. These reactions proceeded smoothly with benzaldehyde, a variety of substituted benzaldehydes (2-nitro, 4-nitro, 4-methoxy) and with isobutyraldehyde. All these products were highly crystalline and while the yields were generally better with the substituted aromatic aldehydes, even with benzaldehyde and isobutyraldehyde yields of around 50% were obtained after crystallisation of the products from the reaction mixtures (Scheme 6; Table 1). Given the few steps involved in the preparation of these species no attempt was made to optimise the yields, or even to recover more of the product than was simply delivered by crystallisation. To demonstrate that this approach could provide a one-pot route to alkylidene malonates, malonic acid and an excess of benzaldehyde were reacted under the conditions used for the synthesis of **1**, and the derived alkylidene malonate was recovered by crystallisation, albeit in a low yield (Scheme 7; Table 1). Although all of the ketone-derived species were synthesised from benzyl acetone, as these synthetic approaches work equally well for the chiral materials derived from benzyl acetone and the acetone derivatives, it seems likely that this chemistry would be applicable to derivatives of a wide range of aliphatic ketones, giving a vast scope to the species available.



Scheme 6 (i) H_2SO_4 , Ac_2O ; (ii) NH_4OAc .



Scheme 7 (i) H_2SO_4 , Ac_2O

These species proved to be considerably less susceptible to hydrolysis than the parent compound, in fact surviving prolonged exposure to water in a 2-phase system (see below). This hydrolytic stability is, presumably, the reversal of the Burgi–Dunitz angle

argument which precluded the formation of these species by cyclocondensation. In the same way that although malonic acid easily cyclo-condenses with ketones, alkylidene malonic acids seem to have insufficient conformational flexibility to allow the ring closure step to take place. It is likely that, while the methylene species is susceptible to hydrolysis, the alkylidene analogues are too rigid to allow an oxygen lone pair to align *anti* periplanar to the carbon–oxygen bond (*i.e.* *syn* periplanar with the σ^* orbital) which must be broken in hydrolysis.

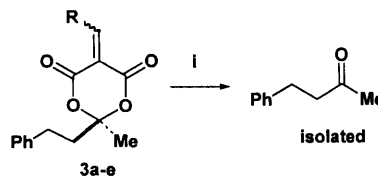
With a range of 5-alkylidene-1,3-dioxane-4,6-diones in hand which had been designed to show chirality, their ^1H NMRs were examined for evidence of diastereotopicity in the signals from the methylene groups. Rather than the simple pairs of triplets predicted by first-order coupling for the methylene groups of the 2-phenylethyl substituent, a pair of complex multiplets were observed. However, this could not be attributed to molecular chirality as the same phenomenon is observed in these signals in the precursor **2** which formally has a plane of symmetry and is thus necessarily achiral. The non-first order nature of this region of the spectrum was unexpected, and could reflect a preferred twisted conformation of the six-membered ring with a *trans* arrangement of carbonyls in which the plane of symmetry associated with the *cis* form is lost (Fig. 1). In the solid state at least, however, many analogues, and indeed Meldrum's acid itself exist in the *cis* form¹⁰ and thus the complex NMR is more likely to be the result of anisogamy, *i.e.* magnetic nonequivalence due to different coupling constants to the vicinal proton barriers in the chain.



Fig. 1 Conformers of 1,3-dioxane-1,6-diones.

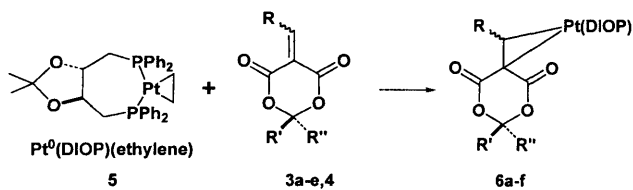
As this complex system is observed even in the achiral unsubstituted species, the use of NMR measurements to characterise molecular chirality was inappropriate. Although the molecules must necessarily exist as a pair of enantiomers, it was thought possible that they may be unstable to racemisation through an addition–elimination mechanism. The extremely polarised nature of the alkene, due to its conjugation with two carbonyls could lower the barrier to rotation, or a mechanism for racemisation could operate whereby polar solvents, or lone pairs of other molecules, act as nucleophiles in a Michael-addition–retro-Michael sequence, allowing racemisation. Given the possibility therefore that these species may not exist as stable enantiomers it was essential to investigate their stability, and as NMR was unsuitable, other methods were examined. None of the chiral HPLC columns tested (Chirocel OD, OJ) gave any separation between enantiomers, and it became apparent that GC was leading to decomposition. Mass spectra recorded at temperatures similar to the GC conditions showed that a fragmentation had occurred at high temperature (this was also observed in refluxing xylene) whereby the parent ketone (benzyl acetone) is eliminated from the ring. In the mass spectrum cationic fragments are observed correlating to the mass of the remaining portion of the molecule. In experiments, however, these fragments are lost as a mixture of decomposition products,

and only benzyl acetone is observed as a discrete product of the fragmentation (Scheme 8).



Scheme 8 (i) Xylene reflux.

As chiral stationary phase chromatography seemed unsuitable for establishing the stability of the enantiomers, attention turned to NMR chiral shift reagents. As it was expected that the esters of the alkylidene malonates would have a reasonable negative character and thus hydrogen-bonding ability, attempts were made to resolve the enantiomers with the use of the Eu-based shift reagent $\text{Eu}(\text{HFC})_3$. Although at certain ratios of shift reagent to substrate there was evidence that single peaks were becoming split, it was impossible to achieve separation between peaks which would allow a determination of the kinetic parameters for racemisation, and thus establish the stability of the new chiral system. As these chiral shift reagents seemed to be unsuitable for the molecules in question, attention turned to a different kind of chiral metal complex which has been used in *e. e.* determinations of unsaturated systems. Parker *et al.* showed¹¹ that it is possible to use the phosphorus NMR signals of homochiral platinum DIOP complexes to determine the *e. e.* of coordinated alkenes. Ethylene(DIOP) Pt^0 reacts with a wide range of alkenes with displacement of ethylene to give the alkene Pt complex. In the case of chiral alkenes, the resultant complexes exist as mixtures of diastereoisomers, which are seen as inequivalent in the ^{31}P NMR allowing the determination of the *e. e.* of the alkenes. The ^{31}P spectra are often complex, as unsymmetrically substituted alkenes lead to the ^{31}P nuclei in each molecule being inequivalent and coupling to each other, in addition to the Pt–P coupling in that fraction of the sample containing the spin-active Pt nucleus, thus giving 12 signals per diastereoisomer. Fortunately the large spectral range of ^{31}P NMR usually leads to well separated signals allowing determination of *e. e.* In the case of 5-alkylidene-1,3-dioxane-4,6-diones, the case is further complicated by the existence of two inequivalent faces of the alkene, doubling the number of isomers which can result from the complexation (Scheme 9).



Scheme 9

The reaction of 5-(4-nitrobenzylidene)-2-methyl-2-(phenylethyl)-1,3-dioxane-4,6-dione **3b** with Pt^0 (DIOP)ethylene in d_6 -benzene gave a spectrum with 32 peaks, 16 centred around 7.5 ppm and 16 symmetrically separated around the central peaks at -8 ppm and 23 ppm, assigned to the ^{195}Pt satellites (Fig. 2). By a consideration of the ratios of signal intensities, a certain degree of assignment of the signals was possible. As the sample was racemic,

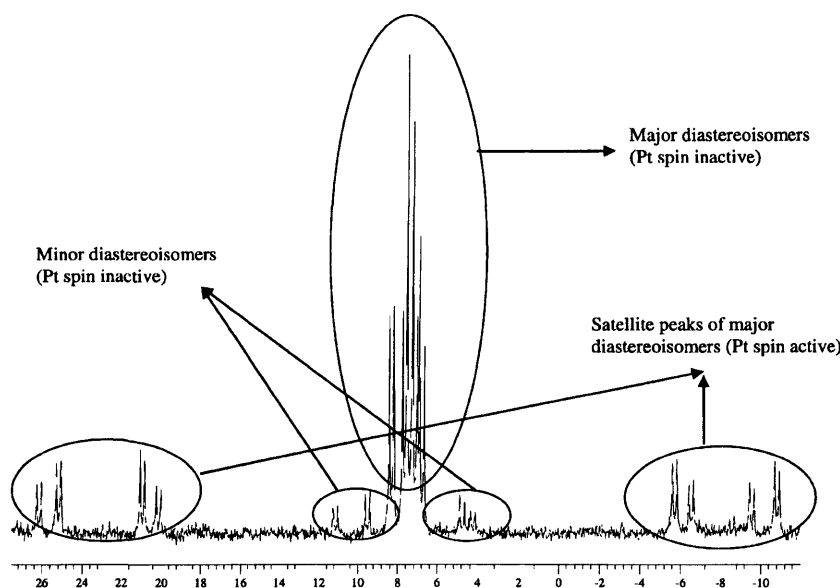


Fig. 2 ^{31}P NMR spectrum of **3b** coordinated to Pt-DIOP.

and it is common for little kinetic resolution to be observed in these complexations, it was expected that the ratio of diastereoisomers resulting from the reaction of the enantiomerically pure DIOP complex with the racemic alkene would be close to unity. However, it was expected that there could be a large degree of selectivity of which face of the alkene is complexed, as one face will experience more steric strain as a result of the conformation of the six-membered ring being distorted by the non-symmetrical substitution in the 5-position. The typical configuration of these rings is largely planar with the 5-carbon out of the plane of the ring in an envelope-type conformation.¹² One of the substituents is in a pseudo-equatorial position, far from the ring and with no role in blocking the coordination of the alkene, while the other is in a pseudoaxial position which will experience diaxial type interactions with the lone-pairs of the 1,3 oxygens, and will interact with incoming complexes to retard coordination of that face of the alkene. It is reasonable to suppose that the favoured conformation will have the larger group in the pseudoequatorial position, and thus it is likely to be the face of the alkene which is *syn* to the smaller substituent (in this case the methyl group) which is more hindered, and therefore coordination of Pt occurs predominantly on the same face as the phenethyl group. As each of the isomers thus formed should give two doublets, correlated pairs of peaks were easily assigned by their mutual J_{PP} . The remaining sets of peaks were assigned as pairs of diastereoisomers on the basis of intensities, with the isomers resulting from facial differentiation in complexation being in an approximate 10 : 1 ratio, and with these sets, the pairs of diastereoisomers reflecting the racemic nature of the sample apparently being in a 10 : 11 ratio. The assumption behind these assignments is that the relaxation times of the isomers will be similar and thus the ^{31}P line intensities can be taken as almost quantitative. In this context it would appear that there has been some slight kinetic resolution in the complex formation to give the 10 : 11 ratio, however this could be calculated for in e. e. determination on a non-racemic sample. A tentative assignment of individual ^{31}P nuclei in each complex can be made from the

Table 2 ^{31}P NMR data for the main facial isomer (minor facial isomer sidebands are too weak to accurately measure Pt-P data)

Diastereoisomer	$\delta_{\text{P}}/\text{ppm}$	$\delta_{\text{P}'}/\text{ppm}$	$J_{\text{P,P}'}/\text{Hz}$	$J_{\text{Pt,P}}/\text{Hz}$	$J_{\text{Pt,P}'}/\text{Hz}$
Major	7.12	7.62	27	4326	3228
Minor	8.28	6.77	27	4326	3231

magnitude of the value of $J_{\text{Pt,P}}$ in each case. The magnitude of $J_{\text{M,P}}$ in complexes is highly dependent on the *trans* influence, with π acidic ligands leading to low values.¹³ This effect is particularly pronounced in square planar complexes and given that one of the carbon atoms in the complex has two ester groups, it is likely to be highly π acidic and thus gives very low values for $J_{\text{P,P}}$. These assignments are summarised in Table 2.

P and P' have been determined from the magnitude of $J_{\text{Pt,P}}$ as the ^{31}P nuclei *trans* to the benzyldiene carbon and C5 of the ring respectively. The low value of J_{PP} (27 Hz compared to 59 to 72 Hz in similar complexes) is again considered more likely to be a result of the extremely electron deficient system lowering Fermi contact through the P-Pt-P system, rather than the variation in bond angles which usually explains variations in P-M-P coupling. In this case the fact that in comparison with literature examples¹² the P-M-P system is unaltered, and only the *trans* ligand varies between our systems and the literature examples militates against this line of reasoning. Other spectra were less clearly resolved than this example, with apparently only one isomer being observed in the case of **3d** and **4**. These complexes were of very low solubility and it is more likely that preferential crystallisation of one isomer led to this observation than kinetic resolution in complex formation. Conformational isomerism (hindered rotation around the C-C bond between the alkene and the 2-nitrophenyl group) is assumed to lead to the doubling of the peaks for **3c**.

In order to justify our conclusion that the phenethyl group would take up the pseudoequatorial position, thus rendering the face of the double bond *syn* to the methyl group more

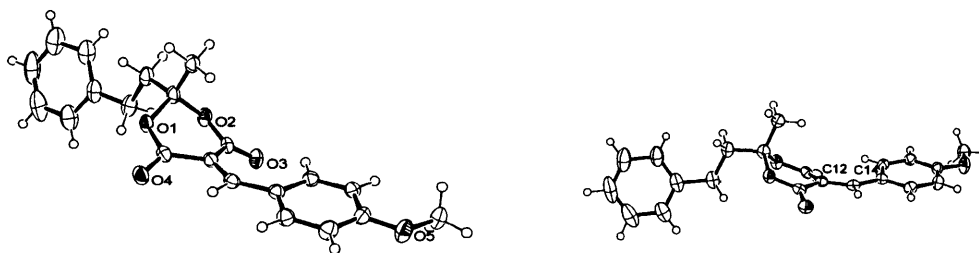
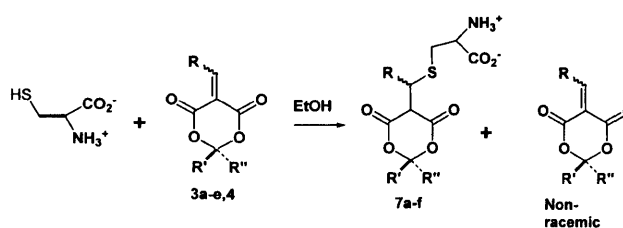


Fig. 3 ORTEP¹⁴ views (50%) of **3d** showing molecular structure, and how the methyl group sterically hinders the C12=C14 double bond.

hindered, the X-ray crystal structure of one of the compounds, **2d** the methoxyphenyl substituted example, was determined. The structure (Fig. 3) clearly shows the carbonyls in a *cis* conformation, with the envelope formed by the C-5 having the phenethyl group in a pseudoequatorial position and thus the methyl group causes severe hindrance of the *syn* face of the double bond.

Although there was now crystallographic evidence that the alkylidene malonate esters adopted necessarily chiral conformations, and the Pt⁰ complexes appeared to be capable of allowing differentiation of enantiomers by the formation of diastereoisomers in the ³¹P NMR, this is not evidence of the existence of stable enantiomers which do not easily interconvert, which would render the new family of chiral species useless. In order to investigate the stability of the enantiomers towards interconversion, a partial kinetic resolution was attempted. As the alkene of the alkylidene malonates is conjugated with two ester groups, it seemed likely to be reactive towards the addition of nucleophiles. A series of chiral nucleophiles was screened for reaction with alkylidene malonates. The only one which gave an irreversible reaction appeared to be L-cysteine. The adducts formed upon reaction of L-cysteine with a series of alkylidene malonates were insoluble in all but the most polar of organic solvents and were hydroscopic and unstable, however they were shown to be the required Michael addition products in the more easily handleable cases by NMR and mass spectrometry, although full characterisation was not achieved. A series of attempts was made to achieve kinetic resolution of the alkylidene malonates by simply reacting half an equivalent of L-cysteine in ethanol with the alkylidene malonates, then purifying the unreacted alkylidene malonate using the extreme insolubility of these compounds by evaporation of the reaction mixture followed by dissolution in chlorinated solvents and filtering off both the adducts, and any unreacted amino acid. The results of these attempts were mixed, with in some cases optical activity being observed in the alkylidene malonates, and in other cases racemic material being recovered. Attempts to standardise the procedures failed to give reproducible results, and this was assigned to the low solubility of both the reactants in ethanol, which leads to irreproducibility in the ratios of each reactant in solution due to difficult-to-control variables such as rate of stirring and particle size. Varying the solvent from alcohols gave no reaction at all, presumably as in non-polar organics the amino acid is completely insoluble. In highly polar organics the nucleophilicity of the L-cysteine may be moderated (or retro-Michael promoted) and when the reaction was attempted in a two phase system with the alkylidene malonate in an organic phase, rapidly stirred with a solution of cysteine, very little or no reaction was observed and no optical activity was observed in the unreacted

alkylidene malonates. Although these results were disappointing in that reproducible kinetic resolution was not achieved (thus no data for optical rotations are given in the experimental section), samples of optically enriched alkylidene malonates were in fact obtained for all of the species examined (Scheme 10).



Scheme 10

The optical activity could be incontrovertibly assigned to the alkylidene malonates as, along with them showing perfect spectral purity, in all cases the sign of the optical rotation observed was negative, while both L-cysteine and the adducts have positive optical rotations. The stability of these species towards racemisation was established by following the optical activity over long periods of time, at elevated temperatures and in a variety of solvents. Along with the possibility that the high degree of polarisation of the alkene could render its natural barrier to rotation (racemisation) low, the possibility exists that polar solvents may catalyse the racemisation. It was possible to demonstrate that the natural barrier to rotation is high enough for these to be considered as true atropisomers, fulfilling the Oki criteria,¹⁵ and going much further in that no loss of optical rotation was observed over many days in solution at ambient temperature. In order to demonstrate that polar solvents do not racemise these compounds by a Michael-addition-retro-Michael sequence, they were heated in acetone and ethanol with no loss of optical rotation being observed. Attempts to determine the e. e.s of the optically enriched samples using the Pt⁰ method failed, with apparently racemic spectra being recorded, presumably an indication of a very low degree of enantiomeric excess resulting from poor kinetic resolution.

Conclusion

It has been demonstrated that 5-alkylidene-1,3-dioxane-4,6-diones are an easily accessible family of axially chiral alkenes which show barriers to racemisation which allow them to be considered as stable enantiomers.

Experimental

General experimental

All starting materials and reagents were purchased from commercial suppliers and used as supplied unless otherwise stated. ^1H and ^{13}C NMR spectra were recorded on a Bruker DPX 400 MHz at 400 MHz (proton) and 160 MHz (carbon), or an APX 250 at 250 MHz and 100 MHz respectively. ^{31}P NMR were recorded on a Jeol at 121 MHz. IR spectra were recorded on a Perkin Elmer 1600 FT IR as thin films or nujol mulls; mass spectra were recorded on a VG Fisons Platform II or at the EPSRC national mass spectrometry service in Swansea (HRMS). Elemental analyses were performed by Warwick Analytical Services (University of Warwick).

Crystallographic data for **3d**: $\text{C}_{21}\text{H}_{20}\text{O}_5$, crystal system monoclinic; space group P_{21}/a ; $a = 9.6549(2)$, $b = 12.9703(3)$, $c = 14.7696(4)$ Å, $\alpha = 90$, $\beta = 108.6430(10)$, $\gamma = 90$; $Z = 4$; $T = 150(2)$ K; $\mu = 0.095$ mm $^{-1}$; $\lambda = 0.71069$ Å (MoK α); $F(000)$ 744; $3.14 < \theta < 27.48$; 20365 reflections, 3980 unique [$R(\text{int}) = 0.0826$]; $R1 = 0.0524$, $wR2 = 0.1052$ [$I > 2\sigma(I)$]; $R1 = 0.0899$, $wR2 = 0.1171$ (all data).†

3-(4-Methoxyphenyl)-2-carboxy-2-propenoic acid (1a). The synthesis of 3-(4-methoxyphenyl)-2-carboxy-2-propenoic acid (**1**) was performed following a procedure described in the literature.¹⁶ A mixture of *p*-anisaldehyde (9.0 mL, 55 mmol), malonic acid (11.44 g, 110 mmol) and ammonium acetate (0.04 g, 0.52 mmol) in ethanol (25 mL) was stirred under nitrogen at room temperature for 7 days. The solvent was then evaporated until dryness, the solid residue was dissolved in ethyl acetate, extracted then with sodium hydroxide, precipitated with hydrochloric acid and finally a solid was collected by filtration to give 5.46 g (44.7%) of **1a**.¹⁷ δH (400 MHz, CD_3OD) 3.75 (s, 3H, CH_3O), 6.85 (dd, 2H, $^3J = 7.1$ Hz, $^4J = 1.7$ Hz, Ar-H2,6), 7.45 (dd, 2H, $^3J = 7.1$ Hz, $^4J = 1.7$ Hz, Ar-H3,5), 7.55 (s, 1H, $\text{CH}=\text{C}$). Mp 207–209 °C (lit.¹⁷ 204–205 °C).

3-(4-Nitrophenyl)-2-carboxy-2-propenoic acid (1b). The synthesis of 3-(4-nitrophenyl)-2-carboxy-2-propenoic acid (**2**) was performed following a procedure similar to the one described in the literature.¹⁷ A mixture of *p*-nitrobenzaldehyde (2.02 g, 13.37 mmol), malonic acid (2.87 g, 27.57 mmol) and ammonium acetate (0.01 g, 0.13 mmol) in ethanol (25 mL) was stirred under nitrogen at room temperature for 14 days. The solvent was then evaporated until dryness, and the solid residue was dissolved in ethyl acetate. The product was extracted with sodium hydroxide, precipitated with hydrochloric acid and collected by filtration to give 1.35 g (42.6%) of **1b**.¹⁷ δH (400 MHz, CD_3OD) 7.65 (s, 1H, $\text{CH}=\text{C}$), 7.70 (d, 2H, $^3J = 8.7$ Hz, Ar-H2,6), 8.2 (d, 2H, $^3J = 8.8$ Hz, Ar-H3,5). Mp 242–244 °C.

3-(2-Nitrophenyl)-2-carboxy-2-propenoic acid (1c). The synthesis of 3-(2-nitrophenyl)-2-carboxy-2-propenoic acid (**3**) was performed following a procedure similar to that described in the literature.¹⁷ A mixture of *o*-nitrobenzaldehyde (14.70 g, 128 mmol),

malonic acid (26.62 g, 256 mmol) and ammonium acetate (0.10 g, 1.3 mmol) in ethanol (40 mL) was stirred under nitrogen at room temperature for 5 days. The solvent was evaporated until dryness and the solid residue was dissolved in ethyl acetate. The product was extracted then with sodium hydroxide, precipitated with hydrochloric acid and collected by filtration to give 1.35 g (42.6%) of **1c**.¹⁷ δH (400 MHz, CD_3OD) 7.80 (d, 1H, $^3J = 8.0$ Hz, ArH-6), 7.90 (dd, 1H, $^3J = 8.0$ Hz, $^3J = 7.0$ Hz, ArH-5), 8.00 (dd, 1H, $^3J = 8.0$ Hz, $^3J = 7.0$ Hz, Ar H-4), 8.40 (s, 1H, $\text{CH}=\text{C}$), 8.50 (d, 1H, $^3J = 8.0$ Hz, ArH-3). Mp 151–154 °C.

2-Methyl-2-(2-phenylethyl)-1,3-dioxane-4,6-dione (2). The synthesis of 2-methyl-2-(2-phenylethyl)-1,3-dioxane-4,6-dione (**2**) was performed following a similar procedure to that described in the literature.⁷ A mixture of 4-phenyl-2-butanone (45 mL, 300 mmol), malonic acid (20.8 g, 200 mmol) and sulfuric acid (0.6 mL, 12 mmol) was added to a Schlenk, under nitrogen. It was stirred for 15 min at room temperature and acetic anhydride (24 mL, 250 mmol) was then added very slowly. The mixture was stirred at room temperature for 18 hours. The solvent was evaporated until dryness, and the remaining solid was dissolved in dichloromethane, filtered, and recrystallised from ethyl acetate and petrol to give 5.39 g (11.5%) of **2**. δH (400 MHz, CDCl_3) 1.75 (s, 3H, CH_3), 2.29 (m, 2H, $\text{CH}_2\text{-CH}_2\text{-Ph}$), 2.86 (m, 2H, $\text{CH}_2\text{-CH}_2\text{-Ph}$), 3.60 (s, 2H, $\text{CH}_2(\text{CO})_2$), 7.10 (m, 3H, PhH-3,4,5), 7.25 (m, 2H, Ph-2,6). δC (101 MHz, CDCl_3): δ 26.53, 29.46, 36.64, 42.59, 107.64, 126.91, 128.69, 129.13, 140.12, 163.27. ν_{max} : 1781, 1744 cm^{-1} . Mp 85–87 °C. $\text{C}_{13}\text{H}_{14}\text{O}_4$ requires C 66.66 H 6.02 found C 65.99 H 6.04%.

5-Benzylidene-2-methyl-2-phenylethyl-1,3-dioxane-4,6-dione (3a). A mixture of **4** (0.47 g, 2 mmol), benzaldehyde (0.24 mL, 2.4 mmol) and ammonium acetate (1.5 mg, 0.002 mmol) in ethanol (10 mL) was stirred at room temperature for 18 h. A white solid was collected by filtration and washed with cold ethanol, to afford 0.276 g (43%) of **3a**. δH (400 MHz, CDCl_3) 1.75 (s, 3H, CH_3), 2.23 (m, 2H, $\text{CH}_2\text{-CH}_2\text{-Ph}$), 2.82 (m, 2H, $\text{CH}_2\text{-CH}_2\text{-Ph}$), 7.15 (m, 3H, $\text{CH}_2\text{PhH-3,4,5}$), 7.23 (app. t, 2H, $^3J = 6.5$ Hz), 7.42 (m, 2H, CHPhH-3,5), 7.51 (app. t, 1H, $^3J = 7.0$ Hz, CHPhH-4), 7.99 (app. d, 2H, $^3J = 7.72$ Hz, CHPhH-2,6), 8.39 (s, 1H, $\text{CH}=\text{C}$). δC (101 MHz, CDCl_3): δ 26.68, 29.61, 42.57, 105.97, 115.06, 126.78, 128.75, 129.08, 129.18, 132.06, 134.13, 134.22, 140.52, 158.83, 160.13, 163.72. Mp 107 °C. m/z (EI/CI MS) 173.9, 91.1, 43.2. $\text{C}_{20}\text{H}_{18}\text{O}_4$ requires C 74.52, H 5.63, N 0.00; found C 74.31, H 5.69, N 0.07%.

5-(4-Nitrobenzylidene)-2-methyl-2-(phenylethyl)-1,3-dioxane-4,6-dione (3b). A mixture of *p*-nitrobenzaldehyde (0.75 g, 5 mmol), **2** (1 g, 4.3 mmol) and ammonium acetate (0.003 g, 0.004 mmol) in ethanol (10 mL) was stirred under nitrogen at room temperature for 3 hours. A yellow solid was then collected by filtration and recrystallised from ethanol, to afford 0.59 g (37%) of **3b**. δH (400 MHz, CDCl_3) 1.75 (s, 3H, CH_3), 2.20 (m, 2H, $\text{CH}_2\text{-CH}_2\text{-Ph}$), 2.75 (m, 2H, $\text{CH}_2\text{-CH}_2\text{-Ph}$), 7.15 (m, 3H, PhH-3,4,5), 7.20 (m, 2H, Ph-H2,6), 8.00 (d, 2H, $^3J = 7.0$ Hz, ArH-2,6), 8.25 (dd, 2H, $^3J = 7.0$ Hz, $^4J = 1.8$ Hz, Ar-H3,5), 8.40 (s, 1H, $\text{CH}=\text{C}$). δC (101 MHz, CDCl_3) 26.97, 29.59, 42.66, 106.69, 118.78, 123.98, 126.91, 128.72, 129.14, 133.52, 137.80, 140.21, 149.92, 155.13,

† CCDC reference number 611771. For crystallographic data in CIF or other electronic format see DOI: 10.1039/b608785j

159.29, 162.55. Mp 146–149 °C. ν_{\max} : 1729, 1529, 1350 cm^{-1} . $\text{C}_{20}\text{H}_{17}\text{NO}_6$ requires C 65.39, H 4.66, N 3.81; found C 65.22, H 4.64, N 3.78%. m/z (EI) 367.

5-(2-Nitrobenzylidene)-2-methyl-2-(phenylethyl)-1,3-dioxane-4,6-dione (3c). A mixture of *o*-nitrobenzaldehyde (0.76 g, 5 mmol), **2** (1.0 g, 4.3 mmol) and ammonium acetate (0.003 g, 0.004 mmol) in ethanol (6 mL) was stirred under nitrogen at room temperature for 18 hours. A yellow solid was then collected by filtration and recrystallised from ethanol, to give 1.03 g (66%) of **3c**. δH (400 MHz, CDCl_3) 1.75 (s, 3H, CH_3), 2.22 (m, 2H, $\text{CH}_2\text{-CH}_2\text{-Ph}$), 2.83 (m, 2H, $\text{CH}_2\text{-CH}_2\text{-Ph}$), 7.15 (m, 3H, PhH-3,4,5), 7.24 (dd, 2H, $^3J = 7.1$ Hz, $^4J = 1.8$ Hz, PhH-2,6), 7.42 (d, 1H, $^3J = 7.7$ Hz, ArH-6), 7.60 (m, 1H, ArH-5), 7.68 (m, 1H, ArH-4), 8.24 (dd, 1H, $^3J = 8.2$ Hz, $^4J = 1.1$ Hz), 8.76 (s, 1H, $\text{CH}=\text{C}$). δC (101 MHz, CDCl_3): δ 27.02, 29.57, 42.63, 106.83, 118.04, 125.28, 126.82, 128.74, 129.08, 130.27, 130.67, 131.34, 134.25, 140.35, 146.69, 156.46, 159.36, 161.919. Mp 89–91 °C. ν_{\max} 1777, 1743, 1531, 1336 cm^{-1} . $\text{C}_{20}\text{H}_{17}\text{NO}_6$ requires C 65.39, H 4.66, N 3.81; found C 65.12, H 4.64, N 3.72%. m/z (APCI) 368 ($M + 1$), 266 ($M - 102$), 220 ($M - 148$).

5-(4-Methoxybenzylidene)-2-methyl-2-(phenylethyl)-1,3-dioxane-4,6-dione (3d). A mixture of *p*-anisaldehyde (1.12 mL, 10 mmol), **2** (2 g, 8.6 mmol) and ammonium acetate (0.006 g, 0.008 mmol) in ethanol (10 mL) was stirred under nitrogen at room temperature for 24 h. A bright yellow solid was then collected by filtration and recrystallised from ethanol, to give 2.00 g (66%) of **3d**. δH (400 MHz, CDCl_3) 1.68 (s, 3H, CH_3), 2.22 (m, 2H, $\text{CH}_2\text{-CH}_2\text{-Ph}$), 2.80 (m, 2H, $\text{CH}_2\text{-CH}_2\text{-Ph}$), 3.83 (s, 3H, OCH_3), 6.93 (dd, 2H, $^3J = 7.1$ Hz, $^4J = 1.8$ Hz, ArH-3,5), 7.18 (m, 3H, PhH-3,4,5), 7.22 (m, 2H, PhH-2,6), 8.17 (dd, 2H, $^3J = 7.1$ Hz, $^4J = 1.8$ Hz, ArH-2,6), 8.35 (s, 1H, $\text{CH}=\text{C}$). δC (101 MHz, CDCl_3) 26.52, 29.62, 42.51, 56.13, 105.54, 111.04, 114.81, 125.13, 126.70, 128.76, 129.04, 138.20, 140.69, 158.61, 160.88, 164.53, 165.14. Mp 91–93 °C. ν_{\max} : 1722 cm^{-1} . $\text{C}_{21}\text{H}_{20}\text{O}_5$ requires C 71.58, H 5.72; found C 71.41, H 5.61%. m/z (EI) 352.2.

5-Isobutylidene-2-methyl-2-(2-phenylethyl)-1,3-dioxane-4,6-dione (3e). A mixture of isobutanone (0.91 mL, 10 mmol), **2** (0.94 g, 4.00 mmol) and ammonium acetate (0.003 g, 0.004 mmol) dissolved in 10 mL of ethanol was stirred under nitrogen at room temperature for 18 hours. A white solid was collected by filtration and recrystallised from ethanol to give 0.46 g (33%) of **3e**. δH (250 MHz, CDCl_3) 1.08 (d, 3H, $^3J = 6.6$ Hz, $1/2 \times \text{CH}(\text{CH}_3)_2$), 1.11 (d, 3H, $^3J = 6.6$ Hz, $1/2 \times \text{CH}(\text{CH}_3)_2$), 1.67 (s, 3H, $\text{C}(\text{CH}_3)(2\text{-Ph-Et})$), 2.15 (m, 2H, $\text{CH}_2\text{-CH}_2\text{-Ph}$), 2.78 (m, 2H, $\text{CH}_2\text{-CH}_2\text{-Ph}$), 3.71 (dh, 1H, $J = 10.6$ Hz, 6.6 Hz, $\text{CH}(\text{CH}_3)_2$), 7.10 (m, 3H, PhH-3,4,5), 7.20 (m, 2H, PhH-2,6), 7.65 (d, 1H, $J = 10.6$ Hz, $\text{CH}=\text{C}$). δC (101 MHz, CDCl_3) 21.54, 21.86, 26.78, 29.52, 30.01, 42.57, 106.19, 116.55, 126.77, 128.71, 129.06, 140.50, 160.03, 162.55, 174.38. Mp 79–81 °C. ν_{\max} : 1731 cm^{-1} . m/z (ES) 288.2 (M). $\text{C}_{17}\text{H}_{20}\text{O}_4$ requires C 70.83, H 6.91, N 0.00; found C 70.29, H 6.97, N 0.09%.

5-Benzylidene-2-phenyl-1,3-dioxane-4,6-dione (4). A mixture of benzaldehyde (11.4 mL, 112.5 mmol), malonic acid (10.4 g, 100 mmol) and sulfuric acid (0.30 mL, 6 mmol) was stirred at 0 °C for 15 min. Acetic anhydride (12 mL, 125 mmol) was then

added very slowly and the mixture was stirred at room temperature for 18 h. A white solid was collected by filtration and it was recrystallised from ethyl acetate and petrol to obtain 2.26 g (21%) of **4**. ^1H (400 MHz, CDCl_3) 6.70 (s, 1H, sp^3CHPh), 7.40 (m, 5H, $\text{sp}^3\text{CHPhH-2-6}$), 7.50 (m, 3H, $\text{C}=\text{CHPhH-3,4,5}$), 7.95 (dd, 2H, $^3J = 8.0$ Hz, $^4J = 1.4$ Hz, $\text{C}=\text{CHPhH-2,6}$), 8.30 (s, 1H, $\text{C}=\text{CH}$). δC (101 MHz) 97.11, 116.1, 126.85, 129.30, 131.16, 131.85, 133.26, 134.11, 134.56, 159.58, 161.25, 164.55. Mp 146–148 °C. m/z (ES) 280.2 (M^+).

General procedure for deracemisation of benzylidene malonates. A mixture of the benzylidene malonate (2.18 mmol) and L-cysteine (0.132 g, 1.09 mmol) in 20 mL of ethanol was stirred at room temperature for 18 h. The solvent was then evaporated and the solid residue was dissolved in 200 mL of CH_2Cl_2 . The product was collected in the filtrate, by evaporation of the DCM, and its purity was confirmed by ^1H NMR and the optical rotation recorded in dichloromethane solution. The observed rotations were inconsistent, but when non-zero were always negative. The adducts were insoluble in dichloromethane. Examination of the insoluble fraction by NMR showed mixtures of adducts, the acids derived from hydrolysis of the dioxane ring, and other unidentified materials. Homogeneous products were never isolated and partial characterisation is listed below.

Deracemisation of 5-(4-nitrobenzylidene)-2-methyl-2-(phenylethyl)-1,3-dioxane-4,6-dione (3b). Adduct: HRMS calculated mass for $\text{C}_{23}\text{H}_{24}\text{N}_2\text{O}_8\text{S}$ [$M + \text{H}$] $^+$ 489.1326; measured mass [$M + \text{H}$] $^+$ 489.1324.

Deracemisation of 5-benzylidene-2-phenyl-1,3-dioxane-4,6-dione (4). Following the above procedure for deracemisation, a second reasonably homogeneous product was observed in the dichloromethane-insoluble material, apparently a mixture of two diastereoisomeric acids derived from hydrolysis of the adducts. Diastereoisomer A (55%): δH (400 MHz, CDCl_3) 3.20 (dd, 1H, $^2J = 10.2$ Hz, $^3J = 4.5$ Hz, CHHS), 3.36 (dd, 1H, $^2J = 10.2$ Hz, $^3J = 7.1$ Hz CHHS), 4.30 (dd, 1H, $^3J = 4.5$ Hz, $^3J = 7.0$ Hz, CHCH_2S), 7.39 (m, 3H, PhH-3,4,5), 7.51 (app. d, 2H, $^2J = 7.3$ Hz, Ph-H2,6). Diastereoisomer B (45%): δH (400 MHz, CDCl_3) 3.13 (dd, 1H, $^2J = 9.9$ Hz, $^3J = 9.0$ Hz), 3.42 (dd, 1H, $^2J = 10.0$ Hz, $^3J = 7.1$ Hz), 3.96 (dd, 1H, $^3J = 8.7$ Hz, $^3J = 7.2$ Hz), 7.39 (m, 3H), 7.58 (d, 2H, $^3J = 8.2$ Hz). HRMS calculated for $\text{C}_{20}\text{H}_{19}\text{NO}_6\text{S}$ (adduct) [$M - \text{H}$] 400.0860; measured mass [$M - \text{H}$] 400.0864.

General procedure for coordination of Pt(0)-(S)-DIOP ethene to benzylidene malonates. Pt(0)-(S)-DIOP ethene (40 mg, 0.055 mmol) was dissolved in C_6D_6 (0.7 mL). To the solution was then added an excess of benzylidene malonate and the mixture was shaken well for 2 min and the ^{31}P NMR recorded immediately. Low solubility of complexes derived from **3d**, **4** led to lack of observation of ^{195}Pt satellites. Conformational isomerism (hindered rotation around the C–C bond between the alkene and the 2-nitrophenyl group) is assumed to lead to the doubling of the peaks for **3c**.

5-Benzylidene-2-methyl-2-phenylethyl-1,3-dioxane-4,6-dione (3a). δP (121 MHz, C_6D_6) 10.22 ($J = 35.5$ Hz), 9.32 ($J = 35.5$ Hz), 8.39 ($J = 35.5$ Hz), 7.99 ($J = 32.5$ Hz), 7.24 ($J = 35.5$ Hz), 5.29 ($J = 35.5$ Hz).

5-(4-Nitrobenzylidene)-2-methyl-2-(phenylethyl)-1,3-dioxane-4,6-dione (3b). δP (121 MHz, C_6D_6) 7.12 ($J_{PP} = 27$ Hz, $J_{PIP} = 4326$ Hz), 7.62 ($J_{PP} = 27$ Hz, $J_{PIP} = 3228$ Hz), 8.28 ($J_{PP} = 27$ Hz, $J_{PIP} = 4326$ Hz), 6.77 ($J_{PP} = 27$ Hz, $J_{PIP} = 3231$ Hz). m/z (ES). Theoretical isotope model $[M + H]^+$ 1060.3 (62%), 1061.3 (100%), 1062.3 (97%), 1063.3 (42%), 1064.3 (25%), 1065.3 (10%); observed data 1060.3 (30%), 1061.3 (73%), 1062.4 (100%), 1063.5 (27%), 1064.5 (10%). Theoretical isotope model $[M + Na]^+$ 1082.2 (62%), 1083.2 (100%), 1084.2 (98%), 1085.3 (41%), 1086.3 (25%), 1087.3 (10%); observed data 1082.3 (27%), 1083.2 (85%), 1084.4 (62%), 1085.3 (20%).

5-(2-Nitrobenzylidene)-2-methyl-2-(phenylethyl)-1,3-dioxane-4,6-dione (3c). δP (121 MHz, C_6D_6) 8.52 ($J = 29.6$ Hz), 8.05 ($J = 29.6$ Hz), 7.50 ($J = 26.7$ Hz), 7.05 ($J = 29.6$ Hz), 6.80 ($J = 29.6$ Hz), 5.24 ($J = 29.6$ Hz).

5-(4-Methoxybenzylidene)-2-methyl-2-(phenylethyl)-1,3-dioxane-4,6-dione (3d). δP (121 MHz, C_6D_6) 9.72 ($J = 35.5$ Hz), 8.42 ($J = 35.5$ Hz).

5-Benzylidene-2-phenyl-1,3-dioxane-4,6-dione (4). δP (121 MHz, C_6D_6) 10.89 ($J = 32.6$ Hz), 6.84 ($J = 32.6$ Hz).

Acknowledgements

We are grateful to the EPSRC Mass Spectrometry unit (Swansea) for assistance and the EPSRC for support (GR/S11480/01) to Meritxell Casadesus. We thank Robert L. Jenkins and Robin Hicks (Cardiff University) for mass spectra and NMR assistance.

References

- 1 B. L. Feringa and R. A. van Delden, *Angew. Chem., Int. Ed.*, 1998, **38**, 3418.
- 2 Y. Inoue, H. Tsuneishi, T. Hakushi, K. Yagi, K. Awazu and H. Onuki, *Chem. Commun.*, 1996, 2627.
- 3 M. Suarez and G. B. Schuster, *J. Am. Chem. Soc.*, 1995, **117**, 6732.
- 4 N. P. M. Huck, W. F. Jager, B. De Lange and B. L. Feringa, *Science*, 1996, **273**, 1686.
- 5 Y. S. Lee, Y. S. Lee, J. Y. Lee, S. N. Kim, C.-K. Lee and H. Park, *Bioorg. Med. Chem. Lett.*, 2000, **10**, 2625; A. Michael and N. Weiner, *J. Am. Chem. Soc.*, 1936, **58**, 680; Patent: Sterling Drug Inc., GB 1147759, 1965.
- 6 W. Breitenstein, F. Marki, S. Roggo, I. Wiesenberg, J. Pfeilschifter, P. Furet and E. Beriger, *Eur. J. Med. Chem.*, 1994, **29**, 649.
- 7 A. G. Relenyi, D. E. Wallick and J. D. Streit, US Patent No. 4613671, 1986, p. 5.
- 8 E. T. McBee, Y. S. Kim and H. P. Braendlin, *J. Am. Chem. Soc.*, 1962, **84**, 3154.
- 9 X. Huang and J. Tang, *Tetrahedron*, 2003, **59**, 4851.
- 10 C. E. Pfluger and P. D. Boyle, *J. Chem. Soc., Perkin Trans. 2*, 1985, 1547.
- 11 D. Parker and R. J. Taylor, *Tetrahedron*, 1988, **44**, 2241.
- 12 A. J. Blake, H. McNab and L. C. Monahan, *J. Chem. Soc., Perkin Trans. 2*, 1991, 2003; P. V. Bernhardt, R. Koch, D. W. J. Moloney, M. Shtaiwi and C. Wentrup, *J. Chem. Soc., Perkin Trans. 2*, 2002, 515; R. M. Wilson, A. C. Hengge, A. Ataei and D. M. Ho, *J. Am. Chem. Soc.*, 1991, **113**, 7240; M.-K. Jeon and K. Kim, *J. Chem. Soc., Perkin Trans. 1*, 2000, 3107.
- 13 Joan Mason, *Multinuclear NMR*, Plenum Press, New York, 1987.
- 14 Ortep-3 for Windows: L. J. Farrugia, *J. Appl. Crystallogr.*, 1997, **30**, 565.
- 15 M. Oki, *Top. Stereochem.*, 1983, **14**, 1.
- 16 C. Y. K. Tan and D. F. Weaver, *Tetrahedron*, 2002, **58**, 7449.
- 17 D. T. Mowry, *J. Am. Chem. Soc.*, 1947, **69**, 2362.

